# TRANSITION METAL ION EXCHANGE IN ZEOLITES

by

Philip Fletcher

A Thesis Submitted for the Degree of

Doctor of Philosophy

of

The City University, London

The Department
of
Chemistry

October 1979

INDEX

LIST OF TABLES

## LIST OF FIGURES

ACKNOWLEDGEMENTS

I would like to thank British Gas for their generous sponsorship of this research project.

My sincere thanks are due to Dr R.P.Townsend for his supervision and continuous advice and encouragement throughout this project and also for his helpful criticism on the presentation of the thesis.

I would also like to thank [redacted] for the production of the X-Ray powder photographs.

Finally my thanks must go to [redacted], for her endevours in typing this thesis,and also to [redacted] for her useful contribution towards the typing of the many tables in this work.

## ABSTRACT

This work contains a study of the ion exchange characteristics of the first row transition metal ions $Cu^{2+}_{(aq)}$, $Co^{2+}_{(aq)}$, $Ni^{2+}_{(aq)}$, $Mn^{2+}_{(aq)}$ and also $Zn^{2+}_{(aq)}$ in ammonium exchanged forms of the synthetic zeolites X and Y. Also reported are investigations into the exchange of $Ag^{+}_{(aq)}$ and the amminated species $\left[Ag(NH_3)_2\right]^+$, $\left[Pt(NH_3)_4\right]^{2+}$ and $\left[Pd(NH_3)_4\right]^{2+}$ in Na-X, Na-Y and Na-MOR, and $\left[Cu(NH_3)_4\right]^{2+}$ in ammonium X and Y only.

Observed effects included sigmoidal isotherms for the exchange of aquated divalent transition metal ions but no apparent sigmoidal character to the isotherms for exchange involving amminated species. Hydrolysis and possible precipitation was observed with first row transition metal exchange in X (and to a lesser extent Y) and an irreversibility in these isotherms due to either a ternary component in the exchange or exchange into sites not accessible to the ammonium ion at 25°C.

The validity and experimental variation of the analytical techniques used was assessed and consequently the effect of experimental error upon the derived thermodynamic parameters was investigated.

Measured standard free energies and the observed selectivity trends for the systems under investigation have been rationalised using a simple dielectric theory and, in the case of silver(I) exchange, by a modified application of the dielectric theory.

## LIST OF PRINCIPLE SYMBOLS

| | |
|---|---|
| A | Ingoing Exchanging Cation |
| a | Activity |
| $A_c(max)$ | Maximum Level of Exchange |
| c | Crystal Phase |
| e | Charge on One Electron ( $1.602 \times 10^{-19} C$ ) |
| f | Zeolite Phase Activity Coefficient |
| $f_{N_\theta}$ | Normalisation Factor |
| $\Delta G^\theta$ | Standard Free Energy of Reaction |
| L | Avogadro Constant ( $6.022 \times 10^{23} mol^{-1}$ ) |
| $K_a$ | Thermodynamic Equlibrium Constant |
| $K_c$ | Kielland Quotient |
| $K_m$ | Mass Action Quotient |
| M | Metal Cation |
| m | Solution Molarity ( mol. $dm^{-3}$) |
| MOR | Synthetic Mordenite |
| N | Solution Normality (g. equiv.$dm^{-3}$) |
| $n_i$ | Number of Moles of the ith Component of any Phase |
| R | Gas Constant (8.314 J $K^{-1}$ mol.$^{-1}$) |
| r | Pauling Crystallographic Radius (nm) |
| s | Solution Phase |
| T | Absolute Temperature ( K ) |
| $T_N$ | Total Solution Normality (g. equiv. $dm^{-3}$) |
| v | Vapour Phase |
| X | Zeolite X |
| Y | Zeolite Y |
| Z | Charge on Ion |
| $\alpha$ | Zeolite Selectivity Coefficient |
| $\Gamma$ | Ratio of Solution Phase Activity Coefficients Raised to the Respective Powers |
| $\gamma_\pm$ | Mean Molal Stoichiomtric Activity Coefficient |
| $\Delta$ | Zeolite Phase Water Activity Term |
| $\epsilon$ | Local Permittivity of a Medium |
| $\mu$ | Chemical Potential |
| $\Theta$ | Percentage Mean Variance |

CHAPTER ONE INTRODUCTION

1.1. GENERAL INTRODUCTION

1.2. ZEOLITES AND THEIR STRUCTURE

1.2.1. Mordenite

1.2.2. Zeolites X and Y

1.3. THE CLASSIFICATION OF ZEOLITE STRUCTURES

1.3.1. The Structure of X and Y

1.3.2. The Structure of Mordenite

1.4. CATION SITING IN ZEOLITES

1.4.1. Breck's Classification of Ion Sites in Faujasite

1.4.2. Barrer's Classification of Ion Sites in Faujasite

1.4.3. Cation Sitings in Mordenite

1.5. THE ION EXCHANGE ISOTHERM

1.6. THERMODYNAMICS OF ION EXCHANGE

1.6.1. Determination of Solution Phase Activity Coefficients

1.6.2. Determination of Zeolite Phase Activity Coefficients

1.6.2.1. The Formalisation for Partial Exchange

1.6.3. Exchange Phase Water Activity Term

1.6.3.1. The Effect of Solution Concentration on Selectivity

1.7. CLASSIFICATION AND INTERPRETATION OF ISOTHERMS

1.8. THE DIELECTRIC THEORY

1.8.1. The Influence of Ionic Radius on Exchange Characteristics

1.8.2. The Influence of Framework Charge Density on Ion Exchange Characteristics

## 1.9. ION EXCHANGE EQUILIBRIA (REVIEW)

### 1.9.1. Alkali Metal Exchange in X and Y

### 1.9.2. Silver(I) and Thallium(I) Exchange in X and Y

### 1.9.3. Alkaline Earth Exchange in X and Y

### 1.9.4. Rare Earth Exchange in X and Y

### 1.9.5. Ammonium and Alkylammonium Ion Exchange in X and Y

### 1.9.6. Ion Exchange in Mordenite

### 1.9.7. Transition Metal Ion Exchange in X and Y

### 1.9.8. Transition Metal Ion Exchange In Mordenite

### 1.9.9. Ion Site Redistribution in Ion Exchange

## 1.1. GENERAL INTRODUCTION

During the last thirty years, the group of inorganic aluminosilicates known as zeolites, have attracted much scientific investigation due to their unique properties. Such properties include ion exchange[1-3], catalysis[4], adsorption[5,6,9], separation[133] and recovery of hydrocarbons, purification[134], drying processes and molecular sieving[7], to give just a few examples. Often highly sophisticated conceptual and mathematical models are necessary to explain the behaviour of zeolites.

Structurally the zeolites are hydrated aluminosilicates of group I or II elements and consist of infinitely extending three-dimensional networks of $AlO_4^{(-)}$ and $SiO_4$ tetrahedra linked to each other by a sharing of all the oxygens. Zeolites may be represented by the empirical formula

$$M_{2/n}O \cdot Al_2O_3 \cdot x\,SiO_2 \cdot yH_2O$$

where x is usually greater than but never less than two, n is the the valence charge of the cation. Owing to the crystalline structure of zeolites it is also possible to express them using a unit cell formula i.e.

$$M_{x/n}\ (AlO_2)_x\ (SiO_2)_y\ .ZH_2O$$

where Z is the number of intracrystalline 'zeolitic' water molecules and n the valence of the cation. The cations and water molecules are found within the zeolite framework, which is characterised by channels and voids of molecular dimensions.

Essentially, a zeolite may be regarded as a crystalline silicate having a degree of isomorphous replacement of silicon (IV) with aluminium (III) within the framework. Each isomorphous replacement leads to a charge imbalance of -1, and therefore an overall delocalised

negative charge is distributed throughout the framework. This charge is neutralised by the presence of an electrochemical equivalent of loosely bound cations that reside within the framework, both neutralising the delocalised framework charge and giving rise to ion exchange properties.

An especially important property of zeolites which arises from their open crystalline structure, is the ability to sorb guest molecules of specific dimensions into the zeolite framework voids. Molecular sieving is the term given to this property of zeolites, involving the adsorption of molecules into the intracrystalline channels being controlled by the restrictions imposed by channel and pore size[8]. This selectivity, based on molecular dimensions, can be altered by exchanging the cations originally resident in the zeolite[98] by others of different ionic radii. A change in channel size may then occur, which consequently alters molecular sieving characteristics. This modification phenomenon is exhibited by the change in sorption properties of sodium A that occurs when the sodium ions initially present are replaced with calcium(II) ions. Propane is not sorbed by sodium A but is sorbed by calcium A[48]. Similarly, the ability to undergo reversible cation exchange enables modification of the electrical fields within the zeolite crystals[49] which in turn modifies the catalytic and sorptive properties. A striking modification that can be made is the reduction to essentially zero of oxygen sorption in A that occurs if sodium ions are replaced by potassium ions[48]. Another example is seen in some early work with sodium X by Barrer[50,51] who showed that exchanging zeolites with different ions profoundly affected the forms of water and ammonia sorption isotherms through changes in observed heats of sorption.

In the past, zeolites were not utilised commercially as ion

exchangers to any significant degree. A common commercial use of inorganic ion exchangers for a long time has been that of water softening. 'Permutites', which are crystallographically amorphous aluminosilicates, were used rather than zeolites during the early post war period, although the ion exchange properties of naturally occurring zeolites such as chabazite or analcime were known at the time. Permutites remained the preferred materials until the development of polymeric organic exchange resins rendered obsolete the use of inorganic exchangers. Two factors were instrumental in this change. Firstly, both zeolites and permutites are highly susceptible to attack and decomposition by acids, whereas organic resins are much more resistant. Secondly, the rate of ion exchange is generally much greater in resins due to their more open intraparticulate structure. Consequently the rate of exchange in large polymeric resin beads is comparable with that in much smaller inorganic exchange particles thus allowing a more rapid 'through-put' of solution in an ion exchange column. Polymeric resins became the now preferred materials.

In recent years, the use of zeolites as ion exchangers has been revived due to increasing concern over the disposal of waste effluents and their polluting effects on the environment. In this case, where large scale removal of polutants is involved, the high cost of polymeric resins makes the use of low-cost naturally occurring zeolites, or in some cases synthetic zeolites[10], commercially viable. Investigations[11,14,15,16] have been made into the use of zeolites X and Y and clinoptilolite for the removal of ammonia and ammonium ion from effluents in lakes.

Another interesting new use of zeolites involves their addition as builders to detergents in place of sodium polyphosphate salts as water softeners. Investigations have shown that synthetic zeolites, especially

A and X, are suitable substitutes.[12,13]

In recent years an increasingly serious problem has been the storage of radioactive isotopes. Radioisotopes are frequently removed from an effluent using an ion exchanger. Due to their thermal stability and resistance to high energy radiation, zeolites are found to be superior to polymeric resins which usually degrade at temperatures exceeding 200°C [19]. Zeolites have therefore been used for this extraction process and investigations have involved synthetic mordenite[17,18] chabazite and zeolite A.[20]

Zeolites generally occur or are synthesised as aluminosilicates of group I or group II elements, in particular sodium, potassium, magnesium calcium and barium. The systematic investigation of transition metal exchanged zeolites dates back little more than 10 years. It is in this field of transition metal zeolites that many important commercial developments are at present taking place. Zeolites are becoming increasingly important as catalysts especially in hydrocracking[135] and isomerisation[136] reactions. Transition metals or noble metals dispersed on zeolites act as hydrogenation-dehydrogenation components of the "bi functional" catalysts[21] which are used in reforming reactions.

The development of microcalorimetric bead techniques[22] as a means of detecting and quantitatively estimating the presence of flammable gases in the atmosphere, which first involved alumina beads supporting noble metal catalysts[23,24], is now using transition metal exchanged zeolites as catalysts[4]. This change is occurring due to the observed poisoning of conventional beads by chemicals such as lead compounds and silicone oils, both of which are found in the industrial environment.

Early studies using zeolite X exchanged with first row transition metals[4] and the precious metals rhodium, iridium, platinum and palladium[24] showed firstly that zeolites have higher resistance to poisoning than conventional catalysts, possibly due to a molecular sieving effect, and secondly that copper, platinum and palladium exchanged forms of X were in fact highly active catalysts. Recent work[25] has described the initial results of a study of methane oxidation using transition metal exchanged mordenite. These results emphasised the high catalytic potential of platinum, palladium and copper zeolites. The 'activity' of copper exchanged zeolites has, in particular, been given extensive consideration recently[137,138].

The study of ion exchange characteristics of zeolites has attracted a great deal of interest, deservedly so as zeolites are seen to be rapidly finding new applications in the field of catalysis and ion exchange. Detailed surveys of the kinetics[28], thermodynamics of cation exchange[53] and cation location[45,52] in crystal structures have been carried out. This is partly because their regular crystalline structure and framework rigidity make them useful model systems on which to base theoretic developments.

A major part of the work on ion exchange has been concerned with exchange involving the alkali or alkaline earth cations, in both synthetic[26,27,28,29,30] and natural zeolites[119], even though there is much interest in transition metal and noble metal exchanged zeolites as catalysts, and in the use of zeolites to scavenge transition metals from effluents. This relative neglect (until more recently) of transition metal exchange is partly due to the difficulties encountered in examining the ion exchange characteristics of transition metals. They tend to

precipitate as basic salts from alkali or even weakly acidic solutions[31] and, on the other hand, transition metal salt solutions themselves may be sufficiently acidic to decompose or dealuminate a zeolite. Because of these factors careful control over ion exchange conditions must be exercised in order to obtain truly reversible ion exchange.

## 1.2. Zeolites and their Structure.

A zeolite has been defined by Smith[52] as being "a crystalline aluminosilicate with a tetrahedral framework structure enclosing cavities occupied by cations and water molecules, both of which have enough freedom of movement to permit cation exchange and reversible dehydration". The name "zeolite" will be used here in this narrow sense, although it should be noted that there are other natural and synthetic crystalline aluminosilicates that possess 3-dimensional framework structures with ion exchange properties, and which may contain guest molecules or salts irreversibly occluded in the interstices of the framework lattice, yet are not normally classified as zeolites. These are called "felspathoids" and should not be confused with zeolites as defined by Smith[52]. Although the dividing classification line between zeolites and felspathoids is somewhat diffuse, (for example cancrinite or sodalite), the main characteristic considered is the presence and size of channels and voids within the structure.

### 1.2.1. Mordenite

Natural mordenite is a highly siliceous zeolite which takes its name from the locality of Morden in Nova Scotia, where it occurs naturally and in large proportions, in the volcanic rock in the area[32]. It was known as early as 1864 and is frequently found in sedimentary deposits in the

U.S.S.R. and the U.S.A..

Synthetic sodium mordenite is supplied by the Norton company under the trade name of Zeolon. The oxide formula is observed to vary slightly through different batches but a typical silicon to aluminum ratio is 5:1, giving the typical oxide formula as

$$Na_2O.\ Al_2O_3.\ 10SiO_2.\ 6H_2O$$

An interesting feature of synthetic mordenite is the existence of at least two forms of mordenite having the same morphological characteristics[42] yet different adsorption properties. The so-called "small port" mordenite can readily sorb small molecules such as oxygen or nitrogen, but slightly larger molecules such as methane are only slowly sorbed. The second form of mordenite ("large port") can sorb molecules as large as benzene or cyclohexane[33]. One possible explanation for this[33] is that small port mordenite contains extraneous amorphous matter within the structure consequently affecting the sorption properties.

### 1.2.2. Zeolites X and Y.

These two zeolites are synthetic, and isostructural with the mineral faujasite, which occurs naturally. Both X and Y are of especial interest because of the exceptionally large dimensions of the three dimensional interconnecting network of cavities that make up their structure. Mordenite, by contrast, has smaller channel sizes of much lower connectivity. Synthetic zeolite Na-Y differs from Na-X by the degree of isomorphous substitution of aluminium within the framework, leading to two zeolites with the same aluminosilicate backbone, but having slightly

different unit cell dimensions and quite different ion site distributions. The silicon to aluminium ratio is known to vary more than does that of mordenite[34].

for zeolite X Si/Al = 1 to 1.5

for zeolite Y Si/Al = 1.5 to 3

Typical oxide formulae are

X $Na_{86}(AlO_2)_{86}\ (SiO_2)_{106}\ 264H_2O$

Y $Na_{56}(AlO_2)_{56}\ (SiO_2)_{136}\ 250H_2O$

## 1.3. CLASSIFICATION OF ZEOLITE STRUCTURES

Zeolites are classified[34,35] into seven groups based on their framework topology. The structural classification by Meier[36] is based on the repeated occurrence of subunits, which are specific arrangements of (Si or Al)$O_4$ tetrahedra within the structure of the framework. These subunits called "secondary building units" (SBU) are shown in Figure 1.1. (The positions of the tetrahedral silicons or aluminiums are denoted by O, and oxygen atoms lie near the connecting solid lines which are not intended to indicate chemical bonds).

Breck[48] uses a classification which is based on the seven SBU's, where zeolites are categorised in terms of the secondary building unit that comprises the framework. However, other structural blocks, chains and sheets of tetrahedra exist which allow inter-relationships between the tetrahedra to be more readily exhibited than by the use of S.B.U. Thus, most zeolites can be classified in terms of linked polyhedra built up from combinations of some of the secondary building units or from

chain layer structures[37] based on the secondary building units.

Figure 1.1

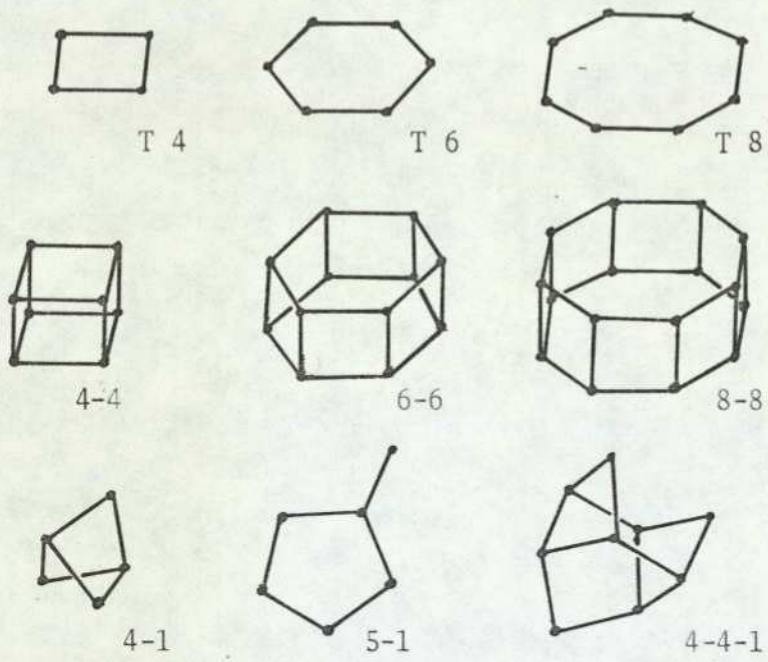


SECONDARY BUILDING UNITS

These finite units can contain up to 16 tetrahedral atoms per unit. The unit cells of framework silicates, based on the secondary building units, contain an integral number of SBU's. Many of the frameworks encountered can be built up from several different SBU's.

Examples of relevant polyhedral voids are:-

Figure 1.2.

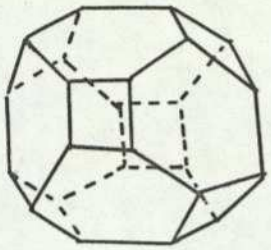

β cage (14-hedron type I)
Truncated Octahedron

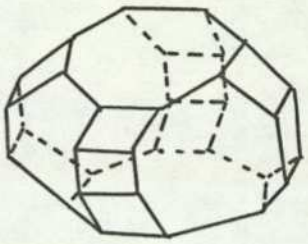

γ cage (18-hedron)

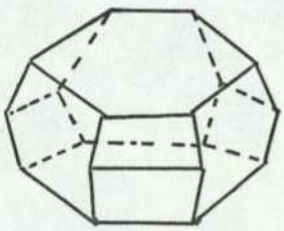

ε cage (11-hedron)

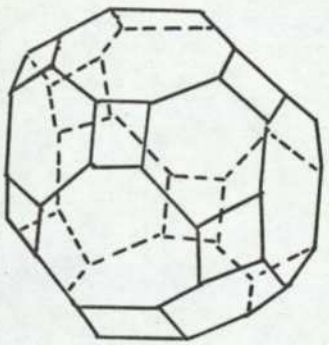

α cage (26-hedron type I)
Truncated Cuboctahedron

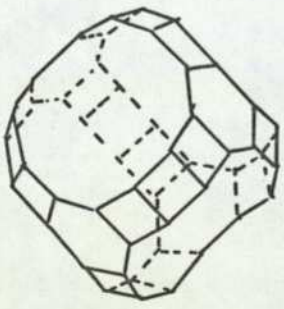

26-hedron type II

### 1.3.1. Structure of X and Y

The aluminosilicate framework of these two zeolites can be described in terms of linked distorted truncated octahedra (sodalite units) joined in tetrahedral coordination through 6-oxygen windows. Each link involves two 6-oxygen windows, one from each sodalite unit, to give hexagonal prisms containing 12 $(Si,Al)O_4$ tetrahedra. Alternatively, the structure can be described purely in terms of linked hexagonal prisms (6-6 units). The topological arrangement of the linked sodalite units is such that the synthetic faujasites can be considered to have two independent though interconnecting three dimensionsl metworks of cavities. One network consists of 26-hedra type II[38] (Figure 1.2) sometimes called "supercages". These voids are created by the tetrahedral linking of the sodalite units and are themselves linked by sharing of 12-oxygen windows. These 12-oxygen windows have free dimensions of about 0.74 nm. The other network is the linking of the sodalite units via the hexagonal prisms, which have 6-oxygen windows of free dimension 0.25 nm.

A simple diagrammatic way of describing the zeolite cavities in X and Y is as follows:

Figure 1.3.

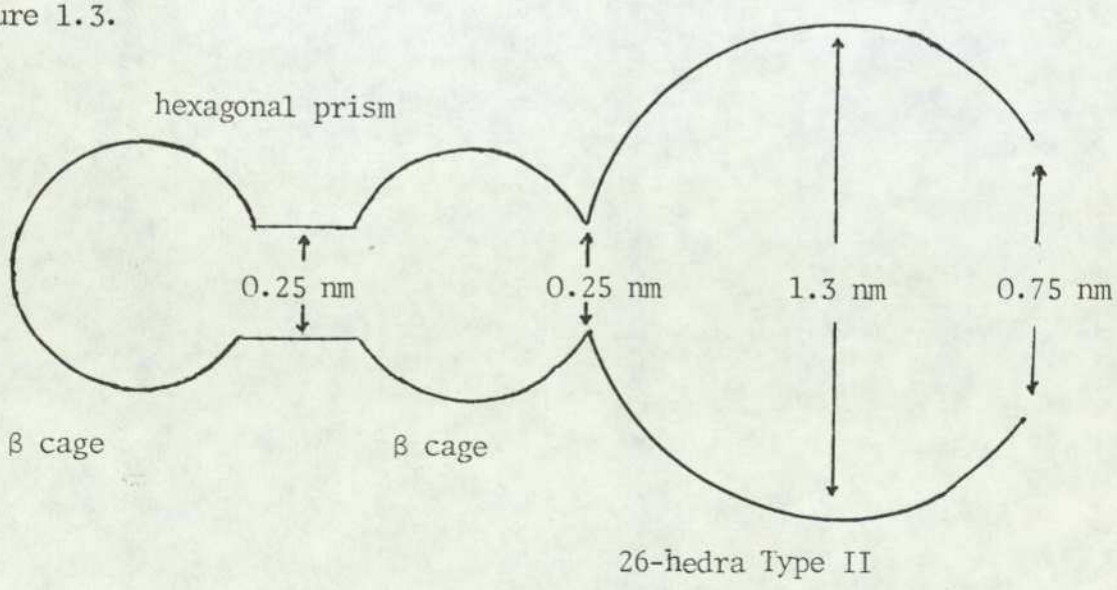

This indicates the relationship between the main channels (i.e. the 26-hedra type II cages) and the sodalite units. For an ion to penetrate the sodalite units or hexagonal prism it must pass through a 'window' of 0.25 nm diameter.

Figure 1.4.

The Faujasite Structure

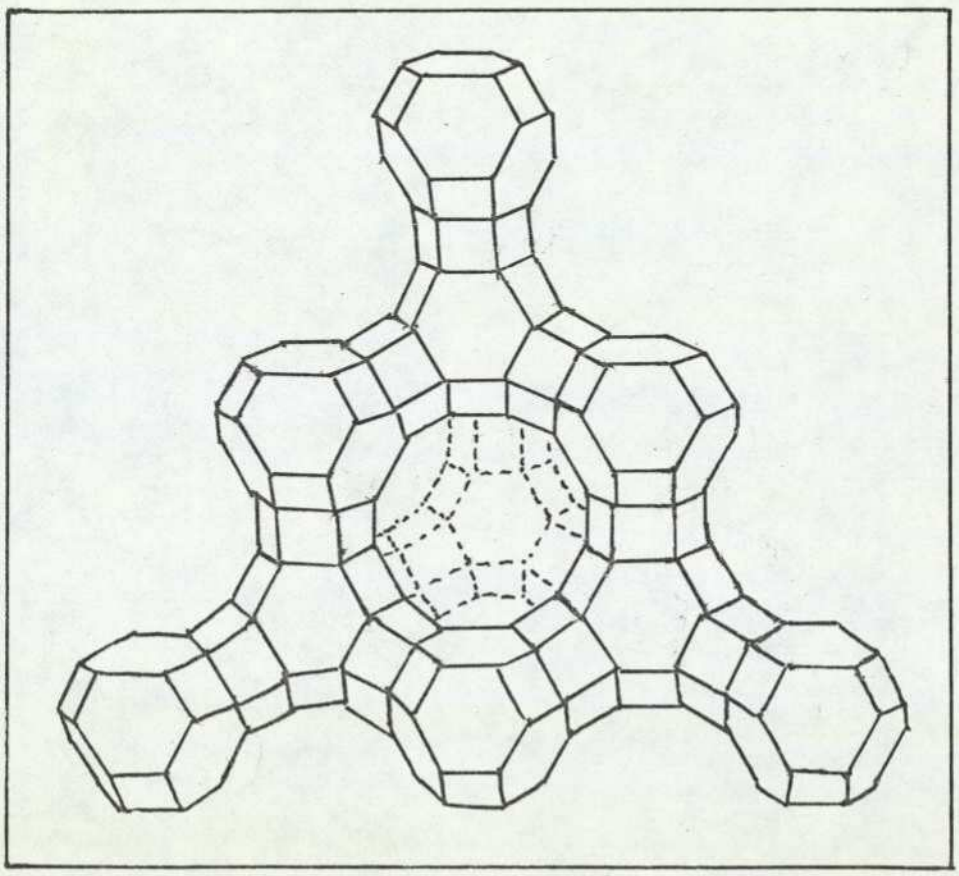

The Proposed Structure of Faujasite Showing the Linking of the Sodalite Cages via the Hexagonal Prisms

Figure 1.5 The Mordenite Structure

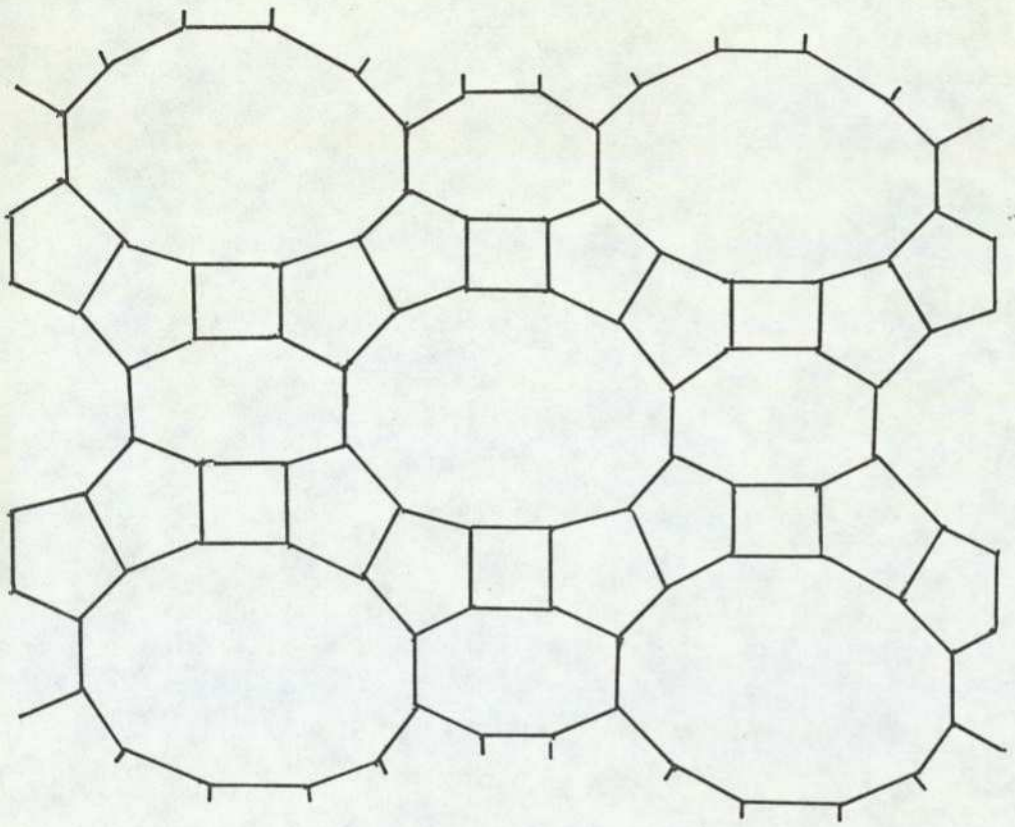

The main channels of mordenite, based on the 5-ring chain

### 1.3.2. The Structure of Mordenite[39,40]

Mordenite can be classified in terms of linked chain structures rather than through the construction of linked truncated polyhedra (c.f. faujasite). The basic secondary building unit of mordenite is the $(Si\ Al)_8O_{16}$ [41] unit involving the linking of the eight silicon or aluminium atoms to form a framework of four five membered rings (fig.1.5) Sets of these chains lie parallel to each other and are linked by shared oxygens. This leads to the construction of open channels in the c-direction (Figure 1.6) which are lined on both sides by 'side-pockets' and directed along the b-direction (Figure 1.6). These side pockets belonging to adjacent channels, are staggered by being displaced with respect to each other. A pocket in one channel is linked to each of two pockets in an adjacent channel by the sharing of distorted 8-oxygen windows of free dimension ~0.28 nm.

The main feature of the mordenite structure is, however, the large eliptical main channels of free dimension 0.67 x 0.70 nm giving access to side pockets via oxygen windows of 0.39 nm free diameter.

## 1.4. CATION SITINGS WITHIN THE ZEOLITE FRAMEWORK.

Complex zeolitic structures often provide more than one kind of site for the exchangeable cations. This is well demonstrated by the family of aluminosilicates having the faujasite structure.

Ion sites are a function of both aluminosilicate structure and position of the tetrahedrally coordinated oxygens. The number of electro-chemical equivalents necessary to neutralise the negative framework charge may be less than the total number of available cation sites. In

MORDENITE

b - direction

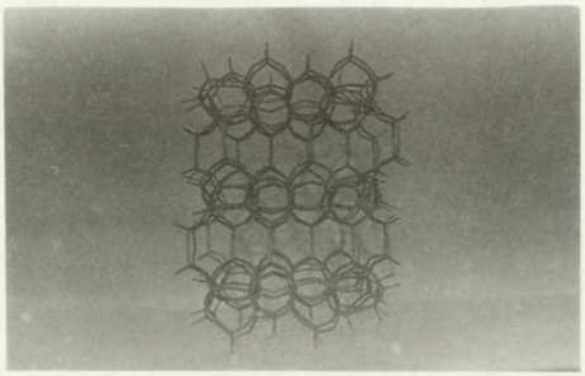

c - direction

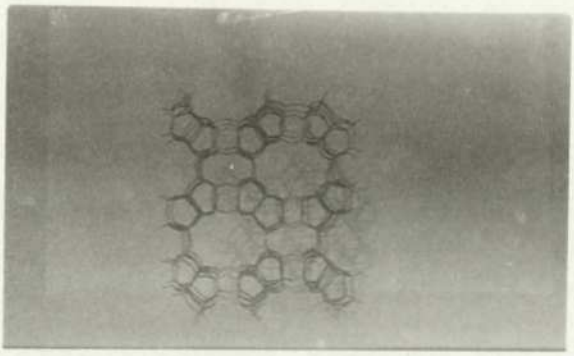

a - direction

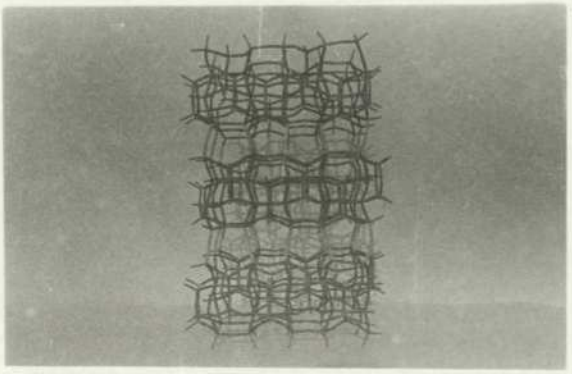

Figure 1.6

consequence when the cations distribute themselves among the sites in such a way as to minimise the free energy of the system there may be only partial or even zero occupancy of some of the site sets available. The parameters controlling cation distribution throughout the available sites are complex and involve such properties of the cation species as ionic charge, ionic radii, hydration energy and electronic structures. Properties of the zeolite which may effect the cation distribution are the water content, temperature and especially the framework charge. Consequently the data obtained for ion site distributions for different samples and by different authors are not always in agreement. These variations may reflect fundamental differences in the histories and morphology of the samples as well as the Si/Al ratio.

In faujasite-type zeolites and in mordenite , the available ion sites and known subsequent degrees of occupancy for different ions have been conveniently summarised by Breck[43] and Barrer[44] respectively. Both these discussions emphasise different approaches and inconsistencies between authors. Examples of ion site distributions in hydrated zeolites are given in table 1.1 and figure 1.7.

### 1.4.1. Breck's classification of cation sites in faujasite.

In the literature, different authors use different nomenclatures. Breck's classification is widely employed, and is as follows.

Site I - A 16 fold site located in the centre of the hexagonal prism;

Site I' - Inside the sodalite cage adjacent to a six-oxygen window leading to a hexagonal prism;

Site II' - Inside the sodalite cage adjacent to six-oxygen window leading to a supercage.

Site II - Adjacent to the single six-oxygen window but outside the

sodalite cage and therefore inside the 26 hedra type II.

Site III - Positioned closed to the wall of the large cavities next to the 4-rings.

Site IV - In the 12-oxygen rings between the large cavities.

### 1.4.2. Barrer's classification[44] of available cation sites in faujasite.

Barrer's classification, based on work by Smith[45]; is slightly different to that of Breck.

Site I - In centre of hexagonal prisms (16 per unit cell).

Site I' - In the sodalite units, adjacent to six oxygen windows leading to the hexagonal prisms. (32 per unit cell).

Site U - Centre of sodalite cages (8 per unit cell).

Site II - In the plane of the six-oxygen windows linking the sodalite cages and 26-hedra type II cages (32 per unit cell).

Site II' - Near site II but inside sodalite cages.

Site II* - Near site II but inside the 26-hedron (32 per unit cell)

Site III - against the 4-rings on the walls of the 26 hedron type II cage. (48 per unit cell).

Site IV - In the centre of 26-hedron type II cages. (8 per unit cell).

Site V - In the 12-oxygen rings of the 26-hedron type II cages. (16 per unit cell).

Summarizing table 1.1 , it is seen that early X-ray studies[81] on hydrated sodium X containing 80 sodium ions per unit cell show 16 sodium ions are located in the hexagonal prisms (S I) and the remainder are located in the 8 - supercage units within the unit cell. Within the large cages, 32 are located near the 6-oxygen rings connecting the

The Projection of AL + Si Atoms In The Faujasite Structure

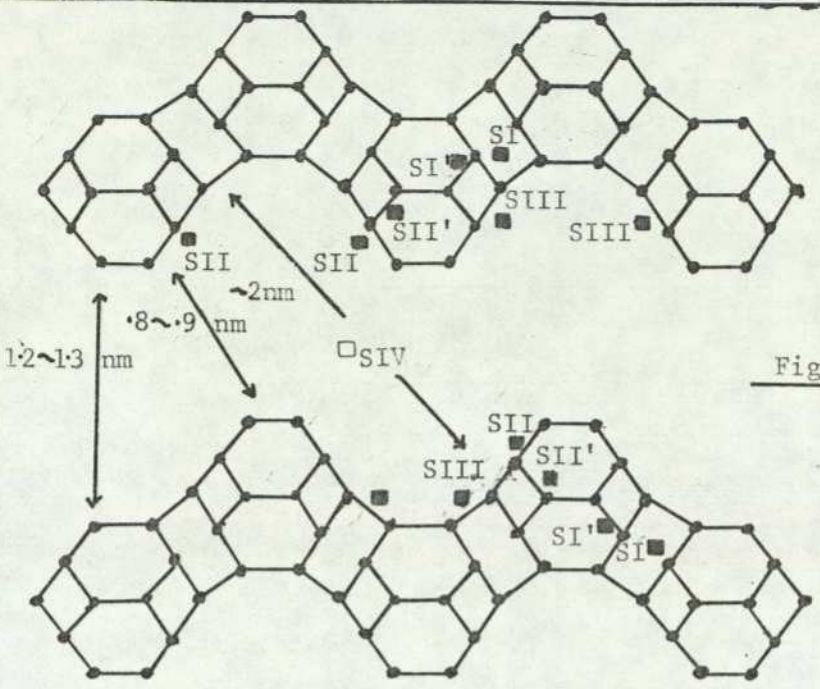


Figure 1.7

The free dimensions of the structure are shown and also the position of the cation sites are indicated(■)

Table 1.1

Cation Sitings in Hydrated Faujasite Type Zeolites

| Zeolite | Al per unit cell | Sites I | I' | II' | II | II* | V |
|---|---|---|---|---|---|---|---|
| Na,Ca faujasite | 57.6 | | 16 Na,Ca | 32 $H_2O$ | 11 $H_2O$ | | |
| Ca faujasite | | | 9.7 Ca | 11.5 Ca | | 32 $H_2O$ | 2.2 Ca |
| La faujasite | 59 | 3.3 La | 28 $H_2O$ | | | 14 $H_2O$ | 10.3 La |
| La-X | 86.8 | | 12 La | 32 $H_2O$ | 17 La | | 4 La |
| Na-X | | 9 Na | 8 Na 11 $H_2O$ | 26 $H_2O$ | 24 Na 8 $H_2O$ | | |
| K-Y | 48.2 | | 13.6 K | | 17.8 K | | |
| K-Y | 54.7 | 1.3 K | 13.3 K | | | 20 K | |
| K-X | 86.5 | 8.9 K | 7.2 K | | 23.2 K | | |

sodalite units and the supercages (SII sites). The remainder could not be located by X-ray and were believed to be hydrated. However, X-ray analysis by Olsen[100] indicated that there were only 9 sodium ions in the SI position, 8 in the SI' and 24 sodium ions in the SII position. Little evidence[100] was found for the presence of specific sitings of sodium ions in the supercage structure other than those in site II.

Recent X-ray data by Beagley, Dwyer and Ibrahim[46] gave site distributions for sodium ion in the supercages of hydrated zeolite X. Their data served to confirm that of previous workers[100]. A summary as given by them is presented in table 1.2.

Table 1.2

Summary of Sodium Ions and Water molecules in a Unit Cell of Hydrated Na-X

| Site | Broussard and Shoemaker[81] | Olson[100] | Olson * | Hseu[147] | Beagley[46] Dwyer and Ibrahim |
|---|---|---|---|---|---|
| I | 16 $Na^+$ | 9 $Na^+$ | 9 $Na^+$ | 9 $Na^+$ | 9 $Na^+$ |
| I' | - | 8 $Na^+$<br>12 $H_2O$ | 8 $Na^+$<br>12 $H_2O$ | 11 $Na^+$<br>12 $H_2O$ | 8 $Na^+$ |
| II' | - | 26 $H_2O$ | 26 $H_2O$ | 32 $H_2O$ | 25 $H_2O$ |
| II | 32 $Na^+$ | 24 $Na^+$ | 24 $Na^+$<br>8 $H_2O$ | 22 $Na^+$ | 22 $Na^+$ |
| II* | - | 8 $H_2O$ | - | 6 $H_2O$ | - |
| III | - | | 31 $Na^+$ and/or $H_2O$ | 20 $Na^+$ | 32 $Na^+$ |
| IV | - | | | | 3 $Na^+$ |
| V | - | | | | 7 $Na^+$ |

*re-interpretation by Beagley, Dwyer and Ibrahim based on a different number of water molecules per unit cell to that originaly assumed by Olson.

Cation positions in hydrated sodium Y were reported by Marti, Soria and Cano[47] in 1976, and a comparison of their results with previously published cation positions in natural dehydrated type Y was made. They found the following cation positions (Table 1.3) and deduced that the differences between the dehydrated natural zeolite and their sample arose from the thermal history of the natural zeolite, which caused a cation migration to occur in the sodalite units.

Table 1.3

Sodium Ions and Water Molecules in a Hydrated Na-Y

| Atom or Molecule | Number of Ions per Unit Cell |
|---|---|
| Si, Al | 192 |
| Na S(I) | 3.27 |
| Na S(I') | 11.92 |
| $H_2O$ S(II') | 7.83 |
| Na S(II) | 1.16 |
| Na S(III) | 34.47 |

An important difference between Na-X and Na-Y (Tables 1.2 and 1.3) is that sodium ions in the supercages of sodium Y are confined to the S(III) sites whereas in sodium X the supercage ions are resident in S(III), S(IV) and S(V) sites.

### 1.4.3. Ion Sitings in Mordenite.

Little data is available for the cation site distributions in hydrated mordenite or for the location of water molecules within the framework. It appears that in Na-MOR there are two site sets. 50% of the sodium ions are resident in the main channels being located in the 8-oxygen windows[39] with the remainder in the side pockets.

## 1.5. THE ION EXCHANGE ISOTHERM

For a binary ion exchange system the equilibrium may be written as

$$Z_B A^{ZA+}_{(s)} + Z_A B^{ZB+}_{(c)} \rightleftharpoons Z_B A^{ZA+}_{(c)} + Z_A B^{ZB+}_{(s)} \qquad 1.100$$

where $Z_A$ and $Z_B$ are the respective charges on ions A and B, and the subscripts (s) and (c) refer to solution and crystal phases respectively.

Experimentally, ion exchange isotherms are obtained by equilibrating solutions of constant total solution normality, but having varying proportions of the two exchanging cations, with known sample weights of the homoionic zeolite of interest. The equilibrium composition of both crystal and solution phase are generally determined by analysis of the equilibrated solutions but occasionally direct analyses of the zeolite are undertaken.

By convention the ion exchange equilibrium is characterised by an isothermal plot of concentration of one exchanging ion in solution against the concentration of that same ion in the crystal phase as constant pressure and total solution normality. Usually the isotherm is plotted in terms of the equivalent fraction of the entering ion (i.e. ion A in

equation 1.100) in solution ($A_s$) against that in the zeolite ($A_c$).

For binary ion exchange

$$A_s = \frac{Z_A m_A}{Z_A m_A + Z_B m_B} \qquad 1.110$$

where m is solution molarity (i.e. mol $dm^{-3}$).

$A_c$ may be similarly expressed in terms of the molality of the ion in the crystal solution, but is much more conveniently expressed as

$$A_c = \frac{N_A}{N_A + N_B} \qquad 1.120$$

where $N_A$.. is the number of gram equivalents of ions A or B in the zeolite phase respectively. $(N_A + N_B)$ is therefore the total ion exchange capacity of the sample. The ion exchange capacity is usually expressed in gram equivalents per hectogram (i.e. g equiv. per 100g).

It must be noted that the specific exchange capacity is a function of the exchange cation composition due to the variation of zeolitic water content with varying cation composition, and also because of the different atomic or molecular weights of the exchangeable cations. In aqueous media the relevant exchange capacity is that of the hydrated zeolite.

In ion exchange equilibrium experiments the total solution normality ($T_N$) must be kept constant since the selectivity of the zeolite for the ingoing ion is not only a function of $A_c$ but also total normality. This

is particularly important in the case of hetrovalent ion exchange, as is explained in section 1.6.3.1. For binary ion exchange conditions

$$T_N = Z_A m_A + Z_B m_B$$

hence

$$m_A = \frac{A_S . T_N}{Z_A} \qquad 1.130$$

Also for binary exchange

$$B_S = 1 - A_S \quad \text{and} \quad B_C = 1 - A_C$$

then

$$m_B = \frac{(1 - A_S)\ T_N}{Z_B} \qquad 1.140$$

Thus the conventional isotherm plot adequately defines the equilibrium conditions at specified temperature and total normality for binary exchange only.

## 1.6. THERMODYNAMICS OF ION EXCHANGE

An adequate model for the rigorous thermodynamic treatment of the ion exchange reaction was formulated by Gaines and Thomas[53] for ion exchange in clay minerals. This treatment not only takes into account exchange of ions between the solution and exchanger but also considers possible changes in both the quantity of solvent guest molecules within, and salt imbibition by, the exchanger. Two cases were investigated.

Their first case considered both the exchange of cations and the sorption of solvent from solution, but neglected salt imbibition. Their second case considered the exchanger phase with all three phenomena occurring. It is acceptable in practice to use the model corresponding to the first case, because experimental evidence[54] has shown that

imbibition of salts by zeolites from solution is insignificant except in the case of high salt solution concentrations ( $\sim$ 1 mol $dm^{-3}$).

Implicit in the Gaines and Thomas treatment is the understanding that the exchanger phase comprises the wet solid. This is because the exchanger imbibes water and the degree of imbibition can be different for different ion exchanged forms. This definition also eliminates a complicating term which would arise, namely the free energy of hydration of each homoionic form.

The Gaines and Thomas treatment involves consideration of three phases. These are the vapour, solution and exchanger. The standard states are defined, in terms of water, as follows. Thus each standard state is chosen so that the activity of water is the same in each phase. The chemical potential of the water in the solution phase $\mu_w(S)$ is then equal to the standard chemical potential $\mu_w^\theta(S)$ when the solution phase is pure solvent and the activity of water in the solution phase $a_w(S)=1$ Then

$$\mu_w^\theta(C) = \mu_w^\theta(S) = \mu_w^\theta(V) \qquad 1.150$$

where the subscript (V) indicates the vapour phase. Considering the standard state for the exchanger we see that imbibed water must also be involved. Thus we chose the standard states of the exchanger as being the homoionic solids in equilibrium with an infinitely dilute solution of the relevant ion. Then considering the ion $A^{ZA+}$, $A_c = a_A(C) = f_A = 1$ in the standard state, where $a_A(C)$ is the activity of the ion in the crystal phase and $f_A$ is the activity coeficient of ion $A^{ZA+}$ in association with its equivalent of zeolite. The standard states for the ions in the solution phase are defined in terms of the hypothetical ideal molal solutions of the salts. Thus, considering ion $A^{ZA+}$, $m_A=a_A(s)=\gamma_A=1$ in the standard state, where $a_A(S)$ is the activity of the ion in solution

and $\gamma_A$ is the individual ion activity coefficient in solution.

For a binary exchange reaction of the type exhibited by equation 1.100 the thermodynamic equilibrium constant is

$$K_a = \frac{a_A^{ZB}(C) \cdot a_B^{ZA}(S)}{a_A^{ZB}(S) \cdot a_B^{ZA}(C)} \qquad 1.160$$

where $a_A^{ZB}(C)$ .... etc. are the respective activities of the ions A and B in their respective solution (S) or crystal (C) phases. By expressing activities in terms of concentration and their corresponding activity coefficients we have

$$K_a = \frac{A_c^{ZB} \cdot f_A^{ZB} \cdot m_B^{ZA} \cdot \gamma_B^{ZA}}{B_c^{ZA} \cdot f_B^{ZA} \cdot m_A^{ZB} \cdot \gamma_A^{ZB}} \qquad 1.170$$

Where $A_c$ and $B_c$ refer to the equivalent fractions of ions A and B in the zeolite phase. The functions $m_A$ and $m_B$ are the molalities (mol $kg^{-1}$) of the ions in solution, $\gamma_A$ and $\gamma_B$ are the solution phase single ion activity coefficients and $f_A$, $f_B$ the activity coefficients for ions $A^{ZA+}$ and $B^{ZB+}$ in association with their equivalent of exchanger framework.

For the thermodynamics of ion exchange in zeolites it is convenient to define a selectivity quotient $\alpha'$ at any particular equilibrium position on the isotherm.

$$\alpha' = \frac{A_c \cdot B_s}{B_c \cdot A_s} \qquad 1.180$$

A more convenient form of selectivity coefficient in terms of

molarities is

$$\alpha = \frac{A_c \cdot m_B}{B_c \cdot m_A} \qquad 1.190$$

from which it is clear that

$$\alpha = \frac{Z_A}{Z_B}\,\alpha' \qquad 1.200$$

and only in the case of uni-univalent exchange does $\alpha = \alpha'$

For the equilibrium shown in (1.100) a mass action quotient can be defined

$$K_m = \frac{A_C^{ZB} \cdot m_B^{ZA}}{B_C^{ZA} \cdot m_a^{ZB}} \qquad 1.210$$

This should not be confused with the selectivity coefficient $\alpha$. Both of these coefficients are experimentally determined from the ion exchange isotherm but are only identical in the case of uni-univalent exchange. From equations (1.70) and (1.210) it can be seen that $K_m$ and $K_a$ are related by

$$K_a = \frac{K_m \, f_A^{ZB} \cdot \gamma_B^{ZA}}{f_B^{ZA} \cdot \gamma_A^{ZB}} \qquad 1.220$$

At this stage we can introduce a third quotient $K_c$ which includes the solution activity correction. For historical reasons[55] this is called the Kielland quotient

$$K_c = K_m \, \Gamma \qquad 1.230$$

where $$\Gamma = \gamma_B^{ZA} \Big/ \gamma_A^{ZB}$$

Thus from equation (1.170) and (1.230)

$$K_a = K_c \, f_A^{ZB} \Big/ f_B^{ZA} \qquad 1.240$$

The standard free energy of ion exchange per equivalent of exchange $\Delta G^{\ominus}$ is given by

$$\Delta G^{\ominus} = \frac{-RT}{Z_A Z_B} \ln K_a \qquad 1.250$$

Thus the determination of $\Delta G^{\ominus}$ from empirical isotherm data involves two procedures. Firstly the solution activity correction must be applied, which gives $K_c$, and secondly the evaluation of the zeolite phase activity coefficients to give $K_a$ must be undertaken.

### 1.6.1 Determination of Solution Phase Activity Coefficients.

Empirical data on the mean molal stoichiometric activity coefficients for various salts are given in the literature[56]. An expression for the mean molal stoichiometric activity coefficients may be derived using a modified Debye-Huckel approach[57] (Section 3.5.2.1); however the values of single ion activity coefficients cannot be separately determined, since ions in solution must be accompanied by an equivalent number of ions of opposite charge. Fortunately, however, the ratio of single ion activity coefficients raised to their respective powers can be determined from the experimentally measured mean molal stoichiometric activity coefficients $\gamma_{\pm(AX)}$ and $\gamma_{\pm(BX)}$, where the subscripts AX and BX refer to the salts (i.e. X is the common anion). Implicit therefore in this determination is the understanding that in a binary mixture of salts AX and BX the anion X associated with ion A is indistinguishable from that associated with ion B.

The relation between $\gamma_{\pm(AX)}$ and the individual ion activity coefficients $\gamma_A$ and $\gamma_X$ is[58]

$$\ln \gamma_{\pm(AX)} = \frac{1}{Z_A + Z_X} \left[ Z_X \ln \gamma_A + Z_A \ln \gamma_X \right] \qquad 1.260$$

Similarly

$$\ln \gamma_{\pm(BX)} = \frac{1}{Z_B+Z_X}\left[Z_X \ln\gamma_B + Z_B \ln\gamma_X\right] \qquad 1.270$$

Multiplying (1.260) throughout by $\frac{Z_B(Z_A+Z_X)}{Z_X}$ and (1.270) by $\frac{Z_A(Z_B+Z_X)}{Z_X}$ yields respectively

$$\left(\frac{Z_B(Z_A+Z_X)}{Z_X}\right) \ln \gamma_{\pm(AX)} = Z_B \ln \gamma_A + \left(\frac{Z_A.Z_B}{Z_X}\right) \ln \gamma_X \qquad 1.280$$

and

$$\left(\frac{Z_A(Z_B+Z_X)}{Z_X}\right) \ln \gamma_{\pm(BX)} = Z_A \ln \gamma_B + \left(\frac{Z_A.Z_B}{Z_X}\right) \ln \gamma_X \qquad 1.290$$

Subtracting (1.280) from (1.290) gives

$$\ln \frac{\gamma_B^{ZA}}{\gamma_A^{ZB}} = \frac{1}{Z_X}\left\{Z_A(Z_B+Z_X)\ln \gamma_{\pm(BX)} - Z_B(Z_A+Z_X)\ln \gamma_{\pm(AX)}\right\} \qquad 1.300$$

This expression does not however correspond to the experimental situation, as it yields $\Gamma$ in terms of the mean molal stoichiometric activity coefficients for a given molality in terms of the pure salt solutions. What is required is an expression in terms of activity coefficients of AX and BX in mixed solution.

Glueckauf [59] derived expressions for this situation. $\gamma_{\pm\,AX}^{(BX)}$ and $\gamma_{\pm\,BX}^{(AX)}$, where the superscripts refer to the presence of the co-member of a binary salt solution, are expressed in terms of the pure salt activity coefficients by the following equations

$$\log \gamma_{\pm AX}^{(BX)} = \log \gamma_{\pm(AX)} - \frac{m_B}{4I}\left[k_1 \log \gamma_{\pm(AX)} - k_2 \log \gamma_{\pm(BX)} - \frac{k_3}{1+I^{-1/2}}\right] \qquad 1.310$$

and

$$\log \gamma_{\pm BX}^{(AX)} = \log \gamma_{\pm(BX)} - \frac{m_B}{4I}\left[k_4 \log \gamma_{\pm(BX)} - k_5 \log \gamma_{\pm(AX)} - \frac{k_6}{1+I^{-1/2}}\right] \qquad 1.320$$

where

$$k_1 = Z_B (2Z_B - Z_A + Z_X)$$

$$k_2 = Z_A (Z_B + Z_X)^2 (Z_A + Z_X)^{-1}$$

$$k_3 = \tfrac{1}{2} Z_A Z_B Z_X (Z_A - Z_B)^2 (Z_A + Z_X)^{-1}$$

$$k_4 = Z_A (2Z_A - Z_B + Z_X)$$

$$k_5 = Z_B (Z_A + Z_X)^2 (Z_B + Z_X)^{-1}$$

$$k_6 = \tfrac{1}{2} Z_A Z_B Z_X (Z_B - Z_A)^2 (Z_B + Z_X)^{-1}$$

and I is the ionic strength of the solution.

The proceedure is therefore to determine $\gamma_{\pm AX}^{(BX)}$ and $\gamma_{\pm BX}^{(AX)}$ in terms of $\gamma_{\pm(AX)}$ and $\gamma_{\pm(BX)}$ over the range of ionic strength covered by the isotherm solutions. Then by analogy with equation (1.300),

$$\ln \Gamma = \frac{1}{Z_X}\left[Z_A(Z_B+Z_X) \ln \gamma_{\pm BX}^{(AX)} - Z_B(Z_A+Z_X) \ln \gamma_{\pm AX}^{(BX)}\right] \qquad 1.330$$

## 1.6.2. Determination of the Zeolite Phase Activity Coefficients

In the rigorous treatment proposed by Gaines and Thomas[53], for the three phase system to be at equilibrium it must be true that

$$\mu_w(V) = \mu_w(S) = \mu_w(C) = \mu_w^{\ominus}(C) + RT \ln a_w(C) \qquad 1.340$$

where $a_w(C)$ is the activity of water in the exchanger. Similarly

$$\mu_A(S) = \mu_A(C) = \mu_A^{\ominus}(C) + RT \ln a_A(C) = \mu_A^{\ominus}(C) + RT \ln A_c f_A \qquad 1.350$$

and

$$\mu_B(S) = \mu_B(C) = \mu_B^{\ominus}(C) + RT \ln a_B(C) = \mu_B^{\ominus}(C) + RT \ln B_c f_B \qquad 1.360$$

The Gibbs-Duhem equation is

$$\sum_i n_i \, d\mu_i = 0 \qquad 1.370$$

where $n_i$ is the number of moles of the ith component of a particular phase. This can be applied to the exchanger phase with three assumptions being made:

(1) The summation includes all the components in the exchanger which affect the equilibrium.

(2) Salt imbibition can be ignored.

(3) The total number of exchange sites in the exchanger phase is invariant.

Combining equations (1.340) (1.350) (1.360) and (1.370)

$$n_w RT \, d\ln a_w(C) + n_A RT \, d\ln A_c f_A + n_B RT \, d\ln B_c f_B = 0 \qquad 1.380$$

The RT terms cancel and multiplying throughout by $\frac{Z_A Z_B}{Z_A n_A + Z_B n_B}$ puts the equation in terms of equivalent fractions of ions in the zeolite.

Then

$$\left(\frac{n_w Z_A Z_B}{Z_A n_A + Z_B n_B}\right) d\ln a_w(C) + \left(\frac{n_A Z_A}{Z_A n_A + Z_B n_B}\right) Z_B \, d\ln A_c f_A +$$

$$\left(\frac{n_A Z_B}{Z_A n_A + Z_B n_B}\right) Z_A \, d\ln B_c f_B = 0 \qquad 1.390$$

If $A_c + B_c = 1$ then a consideration of the terms in the brackets shows the denominator equals 1 and the second and third terms in brackets reduce to the equivalent fractions of the ions in the zeolite.

Then

$$n_w . Z_A . Z_B . d\ln a_w(C) + Z_B . A_c . d\ln A_c f_A + Z_A . B_c . d\ln B_c f_B = 0 \qquad 1.400$$

Simplifying and separating the logarithmic terms

$$n_w . Z_A . Z_B . d\ln a_w(C) + Z_B . dA_c + Z_A . dB_c + A_c . d\ln f_A + B_c . d\ln f_B = 0 \qquad 1.410$$

By taking the logarithm of equation (1.240) we introduce

$$\ln K_a = \ln K_c + \ln f_A^{ZB} - \ln f_B^{ZA} \qquad 1.420$$

Hence $$d\ln K_c + d\ln f_A^{ZB} - d\ln f_B^{ZA} = 0 \qquad 1.430$$

On combining 1.430 with 1.410 explicit expressions for $f_A$ and $f_B$ can be derived by elimination of either $f_A$ or $f_B$.

$$d\ln f_A^{ZB} = (Z_B - Z_A)\, dB_c - B_c d\ln K_c - n_w Z_A Z_B\, d\ln a_w(C) \qquad 1.440$$

$$d\ln f_B^{ZA} = (Z_B - Z_A)\, dA_c + A_c d\ln K_c - n_w Z_A Z_B\, d\ln a_w(C) \qquad 1.450$$

These explicit expressions can be evaluated by integrating between the standard states and a value of $A_c$. For a zeolite exchanger phase it is assumed that the water activity term is negligible, an assumption that has been examined and validated[60]. For the case of $f_A$ the integration is between $f_A^{ZB} = A_c = 1$ and $f_A^{ZB}$ at $A_c$. If the water activity term is ignored then $f_A^{ZB} = 1$ at $A_c = 1$ even when the concentration of ions in the solution phase is not zero. The integration path is now simplified[139] and becomes

$$\int_{f_A=A_c=1}^{f_A(A_c)} d\ln f_A^{ZB} = (Z_B - Z_A) \int_1^{A_c} dB_c - \int_{K_c(A_c=1)}^{K_c(A_c)} (1-A_c)\, d\ln K_c \qquad 1.460$$

or

$$\ln f_A^{ZB} = (Z_B - Z_A) B_c - \int_{K_c(A_c=1)}^{K_c(A_c)} (1-A_c)\, d\ln K_c \qquad 1.470$$

This integral can be transformed[145] since

$$\ln K_c = \ln K_c^{(A_c)} + \left(\frac{\partial \ln K_c}{\partial A_c}\right) dA_c \qquad 1.480$$

where $\ln K_c^{(A_c)}$ is the value of $\ln K_c$ at $A_c$.

Then
$$\ln f_A^{ZB} = (Z_B - Z_A)B_c - \ln K_c^{(A_c)} + A_c \ln K_c^{(A_c)} + \int_{A_c}^{1} \ln K_c \, dA_c \qquad 1.490$$

and
$$\ln f_B^{ZA} = -(Z_B - Z_A)A_c + A_c \ln K_c^{(A_c)} - \int_{0}^{A_c} \ln K_c \, dA_c \qquad 1.495$$

Finally substitution of 1.490 and 1.495 into 1.240 gives

$$\ln K_a = (Z_B - Z_A) + \int_{0}^{A_c} \ln K_c \, dA_c \qquad 1.500$$

This equation entails calculation of the thermodynamic equilibrium constant by integration of the plot of $\ln K_c$ against $A_c$, from terms taken or derived from the experimental isotherm.

### 1.6.2.1. Formalisation for Partial Ion Exchange

For cases of partial ion exchange, Sherry[70,82] and Barrer, Rees and Shamsuzzoha[74] normalised their isotherms by expressing the exchange in terms of the exchangeable cations only. This requires multiplication of the experimentally derived values of $A_c$ by a normalising factor $f_N$, where

$$f_N = {}^{1}/_{A_c\,(max)} \qquad 1.501$$

and $A_c(max)$ is the value of $A_c$ corresponding to the maximum level of ion exchange. Then

$$A_c^N = A_c f_N \qquad 1.502$$

and also

$$B_c^N = 1 - A_c^N \qquad 1.503$$

This procedure implies that those ions with which the counter ion $A^{ZA+}$ does not exchange may be regarded as part of the zeolite lattice, and not involved in ion exchange. The standard states used for deter-

mination of $\Delta G^{\ominus}$ by application of Gaines and Thomas treatment[53] remain the same (Section 1.6) but the total exchange capacity now corresponds to the maximum level of exchange attainable by $A^{ZA+}$ rather that that attainable by the outgoing cation $B^{ZB+}$. The Gaines and Thomas expression for $K_a$ then becomes

$$\ln K_a = (Z_B - Z_A) + \int_0^1 \ln K_c^N \, dA_c^N \qquad 1.504$$

where $K_c^N$ is the normalised Kielland quotient.

Vansant and Uytterhoeven[140] criticized this approach on two grounds. Firstly they stated that the normalisation procedure assumed that the unexchanged fraction of ions had no influence on the exchange equilibrium. Secondly they considered that the normalisation procedure made no allowance for $A_c$ (max) being a function of temperature. They therefore formulated a new procedure for the determination of $K_a$ involving an integration of the un-normalised Kielland plot between $A_c$(max) and a value representing the fully exchanged form. Since this standard state (i.e. $A_c = 1$) cannot be physically achieved the means of accomplishing, and the physical significance of this final integration step is ambiguous.

In their reply, Barrer, Klinowski and Sherry[95] raise this problem of ambiguity, pointing out the mathematical and conceptual errors in the procedure proposed by Vansant and Uytterhoeven. Barrer, Klinowski and Sherry then presented a rigorous justification of the original normalisation procedure.

### 1.6.3. The Exchanger Phase Water Activity Term.

In the general application of the Gaines and Thomas treatment it is

usual to ignore the water activity terms. If this assumption is unjustified the integration procedure (equation 1.500) may yield values for $\Delta G^{\ominus}$ that are substantially in error. This possible source of error lies fundamentally in the definition of the zeolite phase standard states being each homoionic solid in equilibrium with an infinitely dilute solution of the relevant ion[53]. Actual ion exchange experiments are carried out at a total solution normality $T_N$ leading to a possibility of the zeolite undergoing substantial osmotic swelling in transition from the infinitely dilute solution to solution strength $T_N$. The activity of the water in the zeolites under those conditions would then deviate from unity and similarly the zeolite phase activity coefficients $f_A$ and $f_B$, even though the zeolite is still in its homoionic form. If the approximation is made that the volume of an exchange equivalent is negligible compared with the molar volume of vapour[53], the Gaines and Thomas expression for $K_a$ becomes[60].

$$\ln K_a = (Z_B - Z_A) + \int_0^1 \ln K_c \, dA_c + \Delta \qquad 1.505$$

where

$$\Delta = -Z_B Z_A \left[ \int_1^{a_w(a)} n_w^A \, d\ln a_w + \int_{a_w(a)}^{a_w(b)} n_w^{AB} d\ln a_w - \int_1^{a_w(b)} n_w^B \, d\ln a_w \right] \qquad 1.506$$

On application of the mean value theorem[60] equation 1.506 becomes

$$\Delta = -Z_A Z_B \left[ \bar{n}_w^A \, d\ln a_w(a) + \bar{n}_w^{AB} \ln\left(\frac{a_w(b)}{a_w(a)}\right) - \bar{n}_w^B \ln a_w(b) \right] \qquad 1.507$$

where $n_w^{-A}$ and $n_w^{-B}$ are the mean water contents of the homoionic A and B forms of zeolite in transition from the infinitely dilute solution to $T_N$ (water activities are respectively $a_w(a)$ and $a_w(b)$ and $n_w^{-AB}$ is the mean water content in passing from homoionic A to homoinic B zeolite). If exchange reations are carried out in dilute solutions then Raoults law applies and $\ln \frac{a_w(b)}{a_w(a)} \longrightarrow 0$. hence equation (1.507) reduces to

$$\Delta = -Z_A Z_B \left[ \bar{n}_w^A - \bar{n}_w^B \right] \ln a_w \qquad 1.508$$

Using equations (1.506) to (1.508), Barrer and Klinowski[60] calculated values of $\Delta$ for exchanges in zeolite A[63]. They found that the term was never significant itself but the values of the first and third integrals in equation (1.506) could be large but of opposite sign and similar magnitude. Thus for the determination of $K_a$ it was concluded[60] that the $\Delta$ term could be omitted.

1.6.3.1. Effect of Solution Concentration on Selectivity.

Barrer and Klinowski[60] have shown that whilst the values of the solid phase ion activity coefficients may change markedly with external solution concentration, the ratio $f_A^{Z_B} / f_B^{Z_A}$ remains nearly constant. Thus it is possible to predict changes in isotherm shape with change in total solution normality providing an experimental isotherm has been obtained at one value of the total normality $T_N$.

This is explained as follows. The complete Gaines and Thomas treatment[53] gives for the activity coefficients of ions A and B in exchanger phase the following expressions

$$\ln f_A^{ZB} = -(Z_A - Z_B)B_c - B_c \ln K_c^{(A_c)} + A_c \ln K_c^{(A_c)} + \int_{A_c}^{1} \ln K_c \, dA_c$$
$$- Z_A Z_B \left[ \int_1^{a_w(a)} n_w^A \, d\ln a_w^A + \int_{a_w(a)}^{a_w(A_c)} n_w^{AB} \, d\ln a_w \right] \qquad 1.510$$

and

$$\ln f_B^{ZA} = -(Z_B - Z_A)A_c + A_c \ln K_c^{(A_c)} - \int_0^{A_c} \ln K_c \, dA_c + Z_A \cdot Z_B \left[ \int_{a_w(a)}^{a_w(b)} n_w^{AB} \, d\ln a_w \right.$$
$$\left. - \int_1^{a_w(b)} n_w^B \, d\ln a_w \right] \qquad 1.520$$

Barrer and Klinowski[60] showed that the contents of the square brackets are significant and therefore as the external solution concentration is changed and the equilibrium activity of the water changes then so do the values of $f_A$ and $f_B$. A given value of $A_c$ can thus correspond to different

values of $f_A$ and $f_B$ depending on the external solution concentration. However, combining (1.510) and (1.520)

$$\ln\left[\frac{f_A^{ZB}}{f_B^{ZA}}\right] = (Z_B - Z_A) - \ln K_c^{(A_c)} + \int_0^1 \ln K_c \, dA_c + \Delta \qquad 1.530$$

where $\Delta$ was defined previously (Section 1.6.3).

or (using equation (1.505))

$$\ln\left[\frac{f_A^{ZB}}{f_B^{ZA}}\right] = \ln K_a - \ln K_c^{(A_c)} + \Delta \qquad 1.540$$

The two factors which can affect $\ln\left[\frac{f_A^{ZA}}{f_B^{ZA}}\right]$ are the water activity term and salt imbibition. It has been shown that $\Delta$ is small and the salt imbibition at low salt concentrations is insignificant[54]. Therefore $f_A^{ZB} / f_B^{ZA}$ is independent of external solution concentration.

Therefore[60]

$$\frac{m_B^{ZA}}{m_A^{ZB}} \Gamma = \frac{B_s^Z \cdot \Gamma}{A_s^{ZB} \cdot Q} = \frac{K_c \, B_c^{ZA} \, f_B^{ZA}}{A_c^{ZB} \, f_A^{ZB}} \qquad 1.550$$

where

$$Q = Z_B^{ZA} \Big/ \left\{ Z_A^{ZB} (T_N)^{(Z_A - Z_B)} \right\} \qquad 1.560$$

Thus if $A_s$ is known for a given value of $A_c$ at a known total normality $T_N$, $A_s$ may be predicted for any $T_N$ value providing that $\Gamma$ is known at that new solution concentration.

In the case of $Z_A = Z_B$ Q in the quotient (1.550) is unity and thus $A_c$ can vary with $T_N$ only in so far as $\Gamma$ varies. In the conventional range of concentrations used for ion exchange $\Gamma$ varies little hence it is fair to say that for $Z_A = Z_B$ the observed selectivity is independent of the total solution normality. In the cases where $Z_A \neq Z_B$ for a given value of $A_c$ at two normalities $T_{N(1)}$ and $T_{N(2)}$ the equality is[60]

$$\frac{A_s^{ZB}(1)\ Q(1)}{(1-A_s(1))^{ZA}\ \Gamma(1)} = \frac{A_s^{ZB}(2)\ Q(2)}{(1-A_s(2))^{ZA}\ \Gamma(1)} = \text{Constant} \qquad 1.570$$

Two important points are to be noted from this result. Firstly with increasing dilution the exchanger displays increasing selectivity for the cation of higher valency. Secondly, it was observed that[60] the shape of the isotherm could change markedly with total normality so that a sigmoidal isotherm could lose its inflexion point as $T_N$ is changed, and the converse. This makes clear the difference between selectivity and thermodynamic affinity and shows that the thermodynamic affinity cannot be predicted from the shape of the isotherm, and also that to infer the presence of one or more ion sites participating in ion exchange from the sigmoid shape of an isotherm is not generally justified.

To further emphasise the difficulties inherent in interpreting sigmoidal isotherms in terms of a multi-site exchange process Barrer and Klinowski[61] undertook a further theoretical treatment of ion exchange in a multi-site exchanger using an extension of Kielland's treatment[55]. Their conclusion was that "we cannot clearly decide how many groups of sites contribute to the exchange by examination of plots if the numbers of sites is greater than one".

## 1.7. CLASSIFICATION AND INTERPRETATION OF ISOTHERMS

### Basic Definitions and Concepts.

Definitions of selectivity were given earlier in this chapter (Section 1.6)

$$\alpha' = \frac{A_C B_S}{A_S B_C} \qquad 1.180$$

$\alpha'$ may be determined at any value of $A_c$ by consideration of the exchange isotherm. A typical example is given below which is representative of exchange of potassium into sodium $X^{63}$ at a total solution normality of 0.1 g equiv $dm^{-3}$ and at a temperature of 298K.

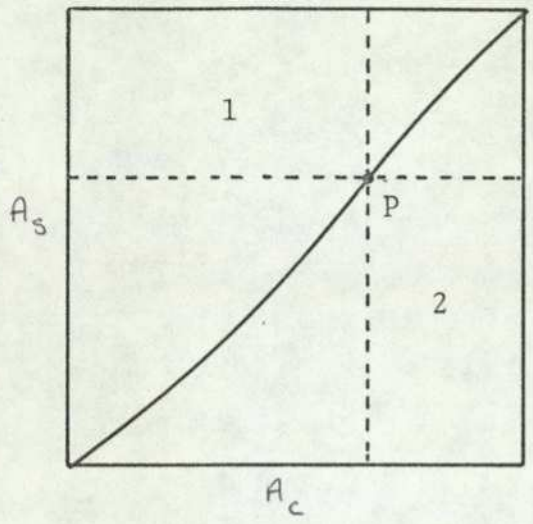


Thus for any point P

$$\alpha' = \frac{\text{Area 1}}{\text{Area 2}}$$

The following conditions then pertain:-

| | |
|---|---|
| $\alpha' > 1$ | Zeolite selective for $A^{ZA+}$ |
| $\alpha' = 1$ | Zeolite shows no preference |
| $\alpha' < 1$ | Zeolite selective for $B^{ZB+}$ |

A second selectivity coefficient was also defined earlier (1.190)

$$\alpha = \frac{A_c \, m_B}{B_c \, m_A}$$

where

$$\alpha = \frac{Z_A}{Z_B} \alpha' \qquad (1.200)$$

Thus for $Z_A = Z_B$ $\alpha = \alpha'$ , but if $Z_A \neq Z_B$ then the following conditions are now relevant

| | | |
|---|---|---|
| $\alpha > Z_A/Z_B$ | : | Zeolite selective for $A^{ZA+}$ |
| $\alpha = Z_A/Z_B$ | : | Zeolite shows no preference |
| $\alpha < Z_A/Z_B$ | : | Zeolite selective for $B^{ZB+}$ |

Various types of isotherms have been encountered and the tendency is for the isotherms to fall into distinct categories. This does not imply, however, that the interpretation is simple[60,61].

The types may be classified as follows:

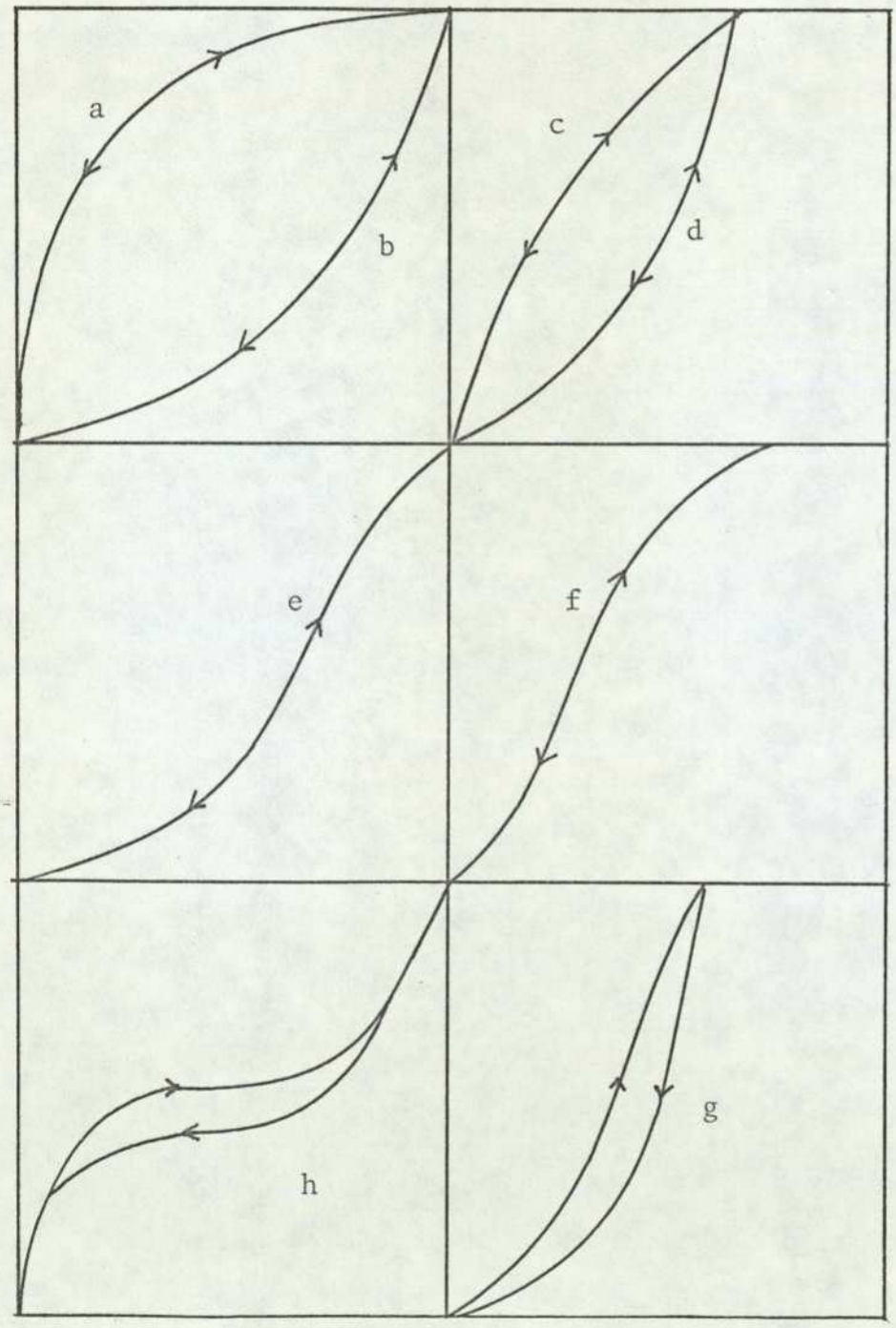

Types a and b show isotherms exhibiting preference for the outgoing ion and the ingoing ion respectively (see equations 1.180 and 1.190).

(a) $Li \rightleftharpoons Na\text{-}A^{(6)}$

$Li \rightleftharpoons Na\text{-}X^{(64)}$

(b) $Ag \rightleftharpoons Na\text{-}X^{(64)}$

$Tl \rightleftharpoons Na\text{-}X^{(64)}$

Types c and d show similar characteristics to a and b but terminate at a level of ion exchange below the maximum capacity for the outgoing cation. The reasons for partial exchange are complex, and not fully understood. Explanations in terms of exclusion from ion sites in terms of framework channel size and size of crystal cation radii (i.e. ion sieve effects) have been proposed[62]. Also volume steric effects can occur. Here, the available zeolitic channel void is filled before complete replacement of the original resident cation is achieved. This is really only possible in the case of exchange with very large ions such as alkylammonium ions[66] or large metal ion complexes[78]. Ion sieve effects are observed when the ions themselves have radii which should not cause their exclusion from the zeolite channels. These ions are often strongly hydrated[30] and it is this factor which may cause their exclusion from certain sites. In many cases[66,67], however, partial ion exchange has been observed where volume steric effects are unlikely and the maximum level of exchange does not correspond to that which would be expected if total removal of the 'available' cations were completed. It is evident that partial exchange is not simply explained by steric considerations alone[90]. An example of type d isotherm is $Rb \rightleftharpoons Na\ X$ exchange[62] whereas type c is seen in first row transition metal exchange in mordenite[65].

Types e and f are sigmoidal isotherms and have for uni-univalent exchange been explained in terms of differences in selectivity by different ion sites for the ingoing ion[64]. As is shown by Barrer and Klinowski[60] and explained in Section 1.6.3.1.this simple interpretation cannot be applied to heterovalent ion exchange. Partial ion exchange has also involved sigmoidal isotherms, for first row transition metals in sodium X and Y[68,69]. Also sigmoidal isotherms, terminating at 100%, have been observed for Ca and Ba in X and Y[82].

Types g and h are isotherms showing irreversibility and hence "hysteresis loops". Type g was observed by Barrer and Townsend[78] for the exchange of amminated zinc in ammonium Phillipsite. Type h was observed in the case of Ag $\rightleftharpoons$ Na and Li $\rightleftharpoons$ Ag exchange in basic cancrinite[71]. These isotherms are characteristic of exchange systems in which recrystallisation of the zeolite phase occurs during exchange. If the zeolite framework can recrystallise easily then the plateau region where the two crystal phases co-exist will also exhibit reversibility[72]. The hysteresis loop arises when the growth of the new phase is hindered by an energy barrier arising from strain and interfacial free energy contributions[73]. An interesting, and unusual example of type h is the uni-divalent exchange involving strontium and sodium in X, as discussed by Sherry[99]. It was observed that a time dependent hysteresis effect occurred at 25°C. In the composition region of the hysteresis loops the zeolite separates into two solid phases, one strontium-rich with an expanded lattice, and the other strontium-deficient with a contracted lattice.

## 1.8. DIELECTRIC THEORY

It has been shown[74,75,76] that ion exchange affinities may be rationalised in terms of dielectric theory. The reversible work W

necessary to create a charge Ze on a sphere of radius r embedded in a medium of permittivity $\varepsilon$ is[77]

$$W = \frac{Z^2.e^2}{8\pi r\varepsilon} \qquad 1.580$$

e is the charge of one electron ($1.602 \times 10^{-18}$ A S), $\varepsilon = \varepsilon_r.\varepsilon_0$ where $\varepsilon_r$ is the relative permittivity (formerly called the "dielectric constant"), and $\varepsilon_0$ is the permittivity of free space being equal to ($8.854 \times 10^{-12}$ $A^2S^4$ $kg^{-1}m^{-3}$)

The Helmholtz free energy of charge formation may be equated to the reversible work function and since for a condensed phase reaction

$(PV) \rightarrow 0$

Then $G \approx F$

and $W = G \approx F$ 1.590

where G is the Gibbs free energy of charge formation.

In the case of an ion exchange reaction of the type

$$Z_B A^{ZA+}_{(s)} + Z_A B^{ZB+}_{(c)} \rightleftharpoons Z_B A^{ZA+}_{(c)} + Z_A B^{ZB+}_{(s)} \qquad 1.100$$

$$\Delta G = \left[Z_B G_A(c) + Z_A G_B(s)\right] - \left[Z_B G_A(s) + Z_A G_B(c)\right] \qquad 1.600$$

If the values of G in the equation refer to the work of charge formation of the individual ions $A^{ZA+}$ and $B^{ZB+}$ in their standard states in both the crystal and solution phases then $\Delta G$ is a standard free energy change. The standard free energy for 1 equivalent of exchange $\Delta G$ is related to the standard free energy change for a two ion system by

$$\Delta G^{\ominus} = \frac{L.\Delta G}{Z_A Z_B} \qquad 1.610$$

where L is the Avogadro constant. Substituting (1.610) into (1.600) and simplifying we have

$$\Delta G^{\ominus} = \frac{L.e^2}{8\pi}\left\{\frac{Z_B}{r_B}\left[\frac{1}{\varepsilon_B(S)} - \frac{1}{\varepsilon_B(C)}\right] + \frac{Z_A}{r_A}\left[\frac{1}{\varepsilon_A(C)} - \frac{1}{\varepsilon_A(S)}\right]\right\} \qquad 1.620$$

It can be shown that dielectric theory can explain certain ion exchange phenomena in terms of simple parameters. Examples are given in the following sections.

### 1.8.1. The Influence of Ionic Radius and Charge on Ion Exchange Characteristics.

Barrer, Rees and Shamsuzzoha [74] used dielectric theory to explain uni-divalent exchange between the solution and crystal phases. They provided a semi-quantitative explanation for the affinity sequence for the Ca-Na, Sr-Na, Ba-Na exchanges in X.

Assuming

1) $\varepsilon_A(C) \sim \varepsilon_B(C) = \varepsilon_c$

2) $\varepsilon_A(S) \sim \varepsilon_B(S) = \varepsilon_s$

Then for uni-divalent exchange with the divalent ion $A^{2+}$ as the ingoing ion

$$\Delta G^{\ominus} = \frac{L.e^2}{8\pi}\left[\left(\frac{2}{r_A} - \frac{1}{r_B}\right)\left(\frac{1}{\varepsilon_c} - \frac{1}{\varepsilon_s}\right)\right] \qquad 1.630$$

It has been shown that for all experimentally determined values [74]

$$\varepsilon_c < \varepsilon_s$$

so it follows that

$$\left(\frac{1}{\varepsilon_c} - \frac{1}{\varepsilon_s}\right) > 0 \qquad 1.635$$

Then the condition for $\Delta G^{\ominus}$ to be negative (i.e. for the zeolite to have an affinity for ion $A^{2+}$ over $B^{+}$) is

$$\left(\frac{2}{r_A} - \frac{1}{r_B}\right) < 0 \qquad 1.640$$

or $r_A > 2r_B$

Thus the radius of the divalent incoming ion should be at least twice that of the univalent ion for the above condition to be fulfilled.

Barrer and Townsend[78] used this theory to rationalise the thermodynamic affinity sequence for the exchange of $Cu^{2+}$, $Co^{2+}$, $Ni^{2+}$, $Mn^{2+}$ and $Zn^{2+}$ in synthetic ammonium mordenite. They made use of the condition (1.620) simplified to

$$\Delta G^{\ominus} = \frac{L.e^2}{8.\pi}\left[\left(\frac{2}{r_M} - \frac{1}{r_{NH_4}}\right)\left(\frac{1}{\varepsilon_c} - \frac{1}{\varepsilon_s}\right)\right] \qquad 1.650$$

where $r_M$ is the Pauling radius of the metal ion and $r_{NH_4}$ the radius of the ammonium ion.

The major assumption was that the term $\left(\frac{1}{\varepsilon_c} - \frac{1}{\varepsilon_s}\right)$ did not change significantly for the different transition metal ions. They predicted a thermodynamic affinity sequence using this theory which fitted their calculated affinity sequence with the exception of the hydrated copper(II) ion. This deviation was explained in terms of the distorted structure of the hydrated copper ion in solution due to the Jahn-Teller effect.[144] In a further study[78] they observed a greater selectivity for amminated transition metal ions compared with the hydrated species, and this was also rationalised in terms of dielectric theory.

### 1.8.2. Influence of Framework Charge Density on Ion Exchange Characteristics.

Uni-univalent and uni-divalent exchange behaviour on aqueous solution and two isostructural zeolites which differ in charge density was considered recently by Barrer and Klinowski[75]. Previous observations which led to the general conclusion that "the ion of larger

crystallographic radius is preferred by the zeolite of lower charge density over the entire range of exchanger composition" were justified by the dielectric approach.

The equilibrium may be considered in terms of the uni-univalent solid state reaction.

$$A^+_{(hc)} + B^+_{(1c)} \rightleftharpoons A^+_{(1c)} + B^+_{(hc)}$$

where $A^+$ and $B^+$ are the two exchanging cations and the subscripts (1c) and (hc) refer to the two crystal phases which were of low and high charge density respectively. In addition, $r_A$ was defined as being greater than $r_B$. Then by rearrangement of equation (1.620)

$$\Delta G^\Theta = \frac{L.e^2}{8\pi}\left[\frac{1}{r_A\varepsilon_A(1c)} + \frac{1}{r_B\varepsilon_B(hc)} - \frac{1}{r_A\varepsilon_A(hc)} - \frac{1}{r_B\varepsilon_B(1c)}\right] \qquad 1.660$$

Then by rearranging 1.660

$$\Delta G^\Theta = \frac{L.e^2}{8\pi}\ \frac{r_A\varepsilon_A(1c)\varepsilon_A(hc)\ \varepsilon_B(1c)-\varepsilon_B(hc)\ -r_B\varepsilon_B(1c)\varepsilon_B(hc)\ \varepsilon_A(1c)-\varepsilon_A(hc)}{r_Ar_B\varepsilon_A(1c)\varepsilon_A(hc)\varepsilon_B(1c)\varepsilon_B(hc)} \qquad 1.670$$

Considerations of charge density then lead to the conclusion

$$\varepsilon_A(1c) < \varepsilon_A(hc)$$

$$\varepsilon_B(1c) < \varepsilon_B(hc)$$

Thus for $\Delta G^\Theta > 0$

$$\frac{r_B}{r_A} > \frac{\varepsilon_A(1c)\varepsilon_A(hc)[\varepsilon_B(hc)-\varepsilon_B(1c)]}{\varepsilon_B(1c)\varepsilon_B(hc)[\varepsilon_A(hc)-\varepsilon_A(1c)]} \qquad 1.680$$

Barrer and Klinowski[75] stated that $r_A > r_B$ thus it would be expected that

$$\varepsilon_A(1c) > \varepsilon_B(1c)$$

and

$$\varepsilon_A(hc) > \varepsilon_B(hc)$$

therefore

$$\frac{\varepsilon_A(hc)}{\varepsilon_B(hc)} \approx \frac{\varepsilon_A(lc)}{\varepsilon_B(lc)} = k \sim 1$$

Thus equation (1.680) reduces to

$$\frac{r_B}{r_A} > k > 1$$

and it follows then that since $r_A > r_B$, "$\Delta G^o$ for uni-univalent solid-solid exchange should be negative when in a pair of isostructural zeolites the larger cation enters the zeolite of lower framework charge"[75].

## 1.9. ION EXCHANGE EQUILIBRIA.

### 1.9.1. Alkali Metal Ion Exchange in X and Y.

Investigations of ion exchange equilibria in the synthetic zeolites Na-X and Na-Y were performed by Sherry[70], Barrer and Rees[79,76,74] and more recently by Lai and Rees[80]. The two early studies were essentially in agreement, showing that alkali metal cations with large crystal radii such as $Cs^+$ and $Rb^+$ and also $NH_4^+$ [66] cannot completely replace all of the sodiums in Na-X and Na-Y. The study of Na-Y in these two reports showed clearly that 16 $Na^+$ ions per unit cell cannot be exchanged by $Cs^+$ and $Rb^+$; the isotherm terminated at about 68% replacement of $Na^+$ from a sample of Na-Y having 50 $Na^+$ per unit cell. This corresponds to 16 per unit cell resident in the sodalite units[81,47]. Lai and Rees[80] replaced 43 $Na^+$ ions out of a total of 68 using either $Rb^+$ or $Cs^+$. It is important to note that the sample of Y used in that work[80] had a higher Al/Si ratio than those used by Barrer[79,76,74] and Sherry[70]. $Cs^+$ and $Rb^+$ exchange in zeolite X is not as well understood. It would be expected that a sample of zeolite Na-X having 85 cations, with 16 resident in the sodalite units and hexagonal prisms, would give an isotherm terminating

at ~ 82% sodium replacement, corresponding to the 16 Na being unexchanged. However, isotherms shown by Barrer et al[74] and Sherry[70] clearly do not terminate at this point. Sherry extrapolated his isotherm to 82% but later[1] changed his opinion, agreeing with the general conclusion that approximately 65% of the sodium ions can be replaced by $Cs^+$ and $Rb^+$ in zeolite X. This corresponds to replacement of only 53 of the 85 sodium ions initially present.

The overall behaviour of alkali metals in zeolites X and Y was conveniently interpreted by Sherry[70]. In zeolite X, Sherry categorised ion exchange in terms of three distinct cation sites:

(1) 37 cations per unit cell which cannot be located by X-ray and are assumed to be present in the large cages in hydrated form.

(2) 32 cations per unit cell located near the 6-ring tetrahedra connecting the 26 hedra type II cages and the sodalite units;

(3) 16 cations resident in the small cages (i.e. sodalite units and hexagonal prisms.).

It was assumed that at low levels of ion exchange for the ingoing ion, the exchange process was confined to the large cages only. In this case a selectivity series Cs > Rb > K > Na > Li was observed in both X and Y. This series showed a trend in which the selectivity of the negatively charged framework for the metal ion decreases with increasing hydration energy of the ingoing cation. Overall, therefore, the process was interpreted as being ion exchange with mobile hydrated ions in the first type of exchange site, and is consistent with the expected trend based on hydration energies. (It has been estimated[70] that there are 3 water

molecules per ion in the main cages in faugesite. If 32 ions are co-ordinated to framework lattice oxygens in X, then effectively each of the remaining 37 ions are hydrated by coordination with no more that 6 water molecules each. For alkali metals it is assumed that the smaller the ion the greater the hydration layer, hence ion exchange from full hydration in solution to a situation with a maximum of 6 waters per ion in the zeolite would be essentially an endothermic process (assuming a negative value of $\Delta H$ of hydration) and would lead to a more positive value for the free energy of exchange for the system. However, it is important to stress that the overall effect of enthalpy of hydration on the free energy of the system must involve changes in hydration of both exchanging cations). At higher levels of exchange (above 50%) the selectivity trend observed was Na > K > Rb > Cs > Li in X, and Cs > Rb > K > Na > Li in Y.

The trend in zeolite X was interpreted by assuming that the ions in the second type of exchange site were now undergoing exchange. This would involve interaction with the zeolite lattice and consequently a partial stripping of the hydration shell around the cation. Ion selectivity would therefore be expected to decrease with increasing ionic size, as the smaller the ion, the stronger would be the interaction with the oxygen atoms involved in the SII sites. The actual selectivity series is a net one, i.e. the result of the opposing effects of this coulombic interaction of the ion with the lattice, and the energy necessary to partially dehydrate the ion.

The observed trend in zeolite Y[70] above 50% exchange was Na > K > Rb > Cs > Li, and is consistent with exchange involving only the mobile hydrated ions. Hence it was concluded that all the ions in the large

cages of Y were hydrated and not present in SII sites.

Ion exchange at higher levels of exchange in both zeolites was assumed to involve the third type of exchange sites (i.e. those within the small cages) and a selectivity sequence of Na> K >Li was observed, which is consistent with high coulombic attractions between the framework lattice and the ion and also the opposing effect of partial dehydration.

1.9.2 Silver and Thallium Exchange in X and Y.

Ion exchange isotherms by Sherry[70] in X and Y for the $Tl^+$ and $Ag^+$ aquo ions have indicated very high selectivities. Comparison with other univalent cations gives the following selectivity trends:

Ag > Tl > Cs > Rb > K > Na > Li for X below 50% exchange;

Ag > Tl > K > Rb > Cs > Li for X above 50% exchange;

Tl > Ag > Cs > Rb > $NH_4$ > K > Na > Li for Y below 68%;.

In both zeolites, the silver ions exchange to 100% whereas $Tl^+$ exchanges completely in X, but only to 68% in Y. This corresponds to 16 $Na^+$ ions per unit cell left unexchanged in the small cages, implying that $Tl^+$ can penetrate the 6 oxygen windows linking the 26 type II hedra cages and the sodalite units in X, but not in Y. Sherry[70] interpreted this observation in terms of a very slow rate of exchange in the lattice structure of Y compared with X. Barrer, Davies and Rees[76] argued that the inability to remove the $Na^+$ ions from the sodalite units in Y by exchange with $Tl^+$ was due to an unfavourable equilibrium. They stated that the the higher framework charge of X would result in the SI sites (in the

presence of $Tl^+$) being of lower energy than in Y due to greater interaction with the highly polarisable $Tl^+$ ion. However, Sherry[2] reported that 100% exchange of $Na^+$ with $Tl^+$ in Y could be obtained at 100°C using a thallium solution containing 0.1 g equiv. $dm^{-3}$. The resulting isotherm exhibited preference for the $Tl^+$ ion over the complete range of $Tl^+$ loading. This indicated that the inability to remove sodium ions from the β-cages at 25°C was due to a slow rate of diffusion of $Tl^+$ through the 6 ring oxygen windows.

The very high selectivity for $Ag^+$ and $Tl^+$ can be attributed to the high polarisability of $Ag^+$ and $Tl^+$ compared with $Na^+$ and hence to a stronger binding by these ions to framework lattice. This is consistent with the fact that selectivity in Y for $Ag^+$ and $Tl^+$ is less than in X[70] corresponding to the lower framework charge density and hence lower energy of interaction due to the induced polarisation of the ions.

### 1.9.3. Alkaline Earth Ion Exchange In X and Y

The study of alkaline earth exchange was undertaken by several workers during the late 1960's and early 1970's. Barrer, Rees and Shamsuzzoha[74] obtained a thermodynamic affinity sequence of $Li^+ < Na^+ < Ca^{2+} < K^+ < Sr^{2+} < Ba^{2+} < Rb^+$ in zeolite X at 25°C and 0.1 g equiv $dm^{-3}$ total solution normality. This was consistent with the sequence obtained by Sherry[82]. Both sets of workers observed that the $Ca^{2+}$ - $Na^+$ exchange in X had an initial fast step then a slow step. Sherry showed that at the end of 24 hours, exchange at 25°C proceeded to 82-85% replacement of sodium by calcium, whereas 100% replacement was not achieved in less than four days. Replacement of 82% of the $Na^+$ ions corresponds to ion exchange within the large cages only, hence it was concluded

that the slow step involves exchange of the $Ca^{2+}$ with $Na^{+}$ ions in the small cages and, as with alkali-alkali metal exchange, involved stripping off the solvation shells to allow passage of the ions through the 6-oxygen windows.

Ion exchange of $Ba^{2+}$ with sodium in X at 25°C[83] has been reported to terminate at a level of exchange corresponding to complete exchange within the large cages (i.e. 82%) whereas Barrer et al[74] reported a maximum level of only 74% exchange at the same solution normality for zeolites of similar composition. It has been concluded that ion size and hydration energies contribute to the maximum level of exchange. Sherry[83] obtained Ba - Na - X isotherms at 5°C, 25°C and 50°C at a solution strength of 0.1 g equiv. $dm^{-3}$, and observed that at 50°C complete replacement of $Na^{+}$ with Ba could be effected. As in the case of Ca-Na exchange, the isotherm was sigmoidal.

In more recent work involving $Ca^{2+}$ exchange by Mortier, Costenoble and Uytterhoeven[84], the level of exchange was shown to be dependent on the nature of the outgoing cation for zeolites under the same exchange conditions. 68% exchange was obtained for $Ca^{2+}$ in Na-Y compared to 90% in K-Y.

### 1.9.4. Rare Earth Exchange in X and Y.

Sherry[83] in 1969 reported exchange of rare earth cations in Na-X and Na-Y. Exchange of $La^{3+}$ showed similarities to that of $Ba^{2+}$, in that the 16 $Na^{+}$ ions within the small cages did not exchange. However, complete exchange of $Na^{+}$ occurred at 100°C over a period of 13 days. This again was interpreted as a temperature dependent diffusion of $La^{3+}$ through the 6-oxygen windows into the small cages, involving a partial

stripping of the hydration layers on the ions.

### 1.9.5. Ammonium and Alkyl Ammonium Exchange in X and Y.

A study of the ion exchange characteristics of the ammonium ion and some of its alkyl derivatives in zeolites Na-X and Na-Y has been performed by Theng et al[66]. The exchanges were accomplished at 25°C using a total solution normality of 0.1 g equiv. $dm^{-3}$. None of the ions could effect a complete replacement of the $Na^+$ ions in the zeolites, and it was assumed that for steric reasons exchange was confined to the large cavities. The maximum levels of exchange were, however, consistently below the values expected for complete removal of $Na^+$ ions from even the large sites, and below the limit imposed by the volume requirements of the particular entering ions. Maximum exchange levels decreased with increase in molecular weight and polarizability of the ingoing cation.

The effect of framework selectivity for the cation in determining the maximum level of ion exchange was shown to be important by the observation that for a given alkylammonium ion, the maximum limit of exchange obtained decreased with an increase in the selectivity of the zeolite for the outgoing cation. It was suggested that the ion exchange process involved a re-distribution of the exchangeable cations over the different crystallographic sites, which is governed by the nature and affinity of the entering alkylammonium ions and those ions initially present. They[66] concluded that electrostatic interactions were involved and the alkylammonium ions should interact less with the framework charges as the length and the number of alkyl groups increased. The electrostatic parameter which was correlated with maximum exchange capacity was the polarisability, and hence this factor would be expected to be more important

in X than in Y.

### 1.9.6. Ion Exchange in Mordenite

The most important features of cation exchange in mordenite are demonstrated by the exchange of the alkali metals into sodium or ammonium mordenite. A study of these phenomena was made in 1974 by Barrer and Klinowski[85]. Either the sodium or ammonium exchanged forms of mordenite were used to determine the exchange characteristics of the ion pairs $Na^+ \rightleftharpoons Cs^+$, $NH_4^+ \rightleftharpoons K^+$, $NH_4^+ \rightleftharpoons Na^+$, $NH_4^+ \rightleftharpoons Li^+$, $2NH_4^+ \rightleftharpoons Ca^{2+}$, $2NH_4 \rightleftharpoons Sr^{2+}$ and $2NH_4 \rightleftharpoons Ba^{2+}$. Equilibria were normally measured at 25°C, and at a constant solution normally of 0.05 g equiv. $dm^{-3}$. Alkali metal exchange showed no ion-sieve effects and thus gave 100% replacement of the initial ions (i.e. $K^+$, $Cs^+$ $Li^+$ and also $NH_4^+$) reflecting the relatively open nature of the mordenite structure. The thermodynamic affinity sequence was Cs > K > Na > Li, and conformed to the rule that the larger, less-highly solvated ions are preferred in the zeolite phase. This order of selectivity can also be justified by dielectric theory[74,75,78].

The exchange studies[85] on $Ca^{2+}$, $Sr^{2+}$ and $Ba^{2+}$ showed that none of these metals could completely replace all of the sodiums. Maximum levels of exchange were 60%, 62%, and 84% respectively. This difficulty of access to the side pockets cannot be explained in terms of crystallographic radii and was therefore considered to be associated with the strong hydrating tendencies of the alkaline earth ions. The ion exchange for the equilibrium $2NH_4^+ \rightleftharpoons Ba^{2+}$ gave an isotherm indicating 100% exchange by extrapolation and was treated accordingly for the calculation of $\Delta G^\ominus$, which was found to be 5.1 kJ $(g\ eq)^{-1}$. A positive value would be predicted by consideration of ionic radii[87]

### 1.9.7 Transition Metal Ion Exchange in X and Y

Many of the features common to the behaviour of alkaline earth metal ion exchange in X and Y are observed in the case of transition metal exchange, such as sigmoidal isotherms, incomplete exchange, and temperature dependent equilibria.

Transition metal ions have small ionic radii compared with the larger alkali or alkaline earth metals. Therefore complete access to the sites within the sodalite units or hexagonal prisms would be expected. However, the combination of high charge and small radius gives them a high charge density, and consequently higher hydration energies than are observed with alkali metals or alkaline earths. The partial exchange observed is often attributed[65,68] to the large hydrated radius[86] of the ions, inhibiting diffusion through the 6-oxygen windows into small cages. In consequence hydration energies should be an important factor in equilibrium transition metal ion exchange. Other factors must also be considered. For example an early publication by Maes and Cremers[96] showed that the ion exchange reaction of the synthetic zeolites Na-X and Na-Y with $Co^{2+}$, $Zn^{2+}$ and $Ni^{2+}$ aquo ions was non stoichiometric due to hydrolytic sodium loss. This loss was greater in sodium X ($\sim$ 5 ions per unit cell) than in sodium Y. This hydrolysis explanation is consistent with results of later work by Marti, Soria and Cano[97] where considerable hydrolysis was observed with the exchange of Cu(II) aquo ions into sodium Y prior to cation location determination using E.S.R.

The studies on transition metal exchange have been devoted to exchange with the sodium form of the zeolites, and have produced diverse results and interpretations, even more so than in the exchange of alkaline earths where some inconsistency between different workers data is

observed.

Early work by Gallei, Eisenbach and Ahmed[93] involved the characterisation of the ion exchange properties of $Mn^{2+}$, $Co^{2+}$ and $Ni^{2+}$ aquo species in Na-X and Na-Y at 25°C and total solution normality of 0.1 g equiv. $dm^{-3}$. Their sample of Na-Y contained a high aluminium content and they calculated that the ion-exchangeable component sited in the main channels was 76% of total cation content. This was based on the assumption that 16 Na ions were resident in the sodalite cages and hexagonal prisms. Sigmoidal isotherms showing high selectivity for the divalent cation were observed for exchange into both X and Y. The maximum level of exchange in Y was found to be in the sequence Ni < Co < Mn (72%, 74% and 78% respectively). In zeolite X the maximum levels of exchange for all three metal ions was considered to be slightly below 82%, and their extrapolation to this value gave highly sigmoidal isotherms. Their interpretation of the sigmoidal isotherms was that ion exchange was confined to the supercages and involved two sets of sites, each having different selectivities for the ingoing cation. They characterised the equilibria by developing a mathematical model to calculate equilibrium constants for each of the two site groups within the exchangeable component of the zeolite phase. It is important to note that reversibility of these systems was not confirmed.

Gal and Radovanov[69] examined exchange of $Ni^{2+}$, $Co^{2+}$, $Zn^{2+}$ and $Cd^{2+}$ in Na-X at 5°C, 25°C and 45°C, again using a total solution normality of 0.1 g equiv. $dm^{-3}$. They exhaustively exchanged samples with solutions of 1 g equiv. $dm^{-3}$ and obtained maximum exchange levels for Ni, Co, Zn and Cd of 71.7%, 75.4%, 76.5% and 97.5% respectively. Their total zeolite phase analysis indicated that hydrolysis even at such high

concentration of metal ion was small being noticeable in the case of Na-X and Co-X only. In their discussion, a correlation was assumed to exist between the decreasing extent of ion exchange and decreasing ion radii of the exchanging cations. These values of radii were not, however, the Pauling crystallographic radii usually quoted. The conventional Pauling radii do not give such a trend. (Table 1.4)

Table 1.4

Extent of Transition Metal Exchange[69]

| Cation | Extent of Exchange/% | Radii[69] /nm | Radii[87] (Pauling) /nm |
|---|---|---|---|
| Ni | 71 | 0.069 | 0.072 |
| Co | 75.4 | 0.072 | 0.074 |
| Zn | 76.5 | 0.074 | 0.074 |
| Cd | 97.5 | 0.097 | 0.097 |

Their isotherms were sigmoidal and selective for the divalent ion and showed no apparent change in selectivity, or in level of maximal ion exchange as the temperature was raised. The thermodynamic parameters obtained at 298K were

| | Cd | Zn | Co | Ni |
|---|---|---|---|---|
| $\Delta G^{\theta}$/ kJ equiv$^{-1}$ | -4.13 | -2.32 | -1.31 | -2.09 |
| $\Delta H^{\theta}$/kJ equiv$^{-1}$ | 11.6 | 9.0 | 5.9 | 6.5 |
| $\Delta S^{\theta}$/JK$^{-1}$ equiv$^{-1}$ | 53 | 38 | 24 | 29 |

indicating an increase in $\Delta G^{\ominus}$ with decrease in size of the hydrated divalent cation. They concluded that exchange characteristics were a complicated function of the available crystallographic sites, ion sizes, extents of ion hydration and solution phase complexation of the ion.

However, this work is in direct conflict with that of Maes and Cremers[68] who investigated ion exchange of $Co^{2+}$, $Ni^{2+}$, $Cu^{2+}$ and $Zn^{2+}$ in Na-X and Na-Y at 25°C, but using a more dilute solution normality of 0.01 g equiv. $dm^{-3}$. Their results gave highly selective sigmoidal isotherms for all the ions except $Ni^{2+}$ at temperatures of 5°C, 25°C and 45°C. The maximum levels of exchange and selectivities exhibited a temperature dependence, both functions increasing with increasing temperature. The maximum levels of exchange were in the order Ni < Co < Zn for both X and Y at 25°C. Full exchange for zinc and cobalt were affected at 45°C but nickel exhibited very little temperature dependence as regards the maximal exchange level. The copper isotherm in X indicated 100% ion exchange at 25°C whereas the actual level of ion exchange was ~ 83% indicating a considerable amount of hydrolysis (exchange of $H_3O^+$).

Table 1.5

Maximum Levels of Exchange as Reported by Maes and Cremers[68]

| Analytical Method | T/°C | Metal Ion | | | |
|---|---|---|---|---|---|
| | | Cu | Zn | Co | Ni |
| 1 | X 5 | | 0.85±0.01 | 0.76±0.01 | 0.68±0.02 |
| 1 | X 25 | | 0.90±0.01 | 0.855±0.01 | 0.70±0.02 |
| 1 | X 45 | | | 0.99 0.01 | 0.90 0.02 |
| 1 | Y 5 | | 0.80±0.01 | 0.74±0.01 | 0.70±0.02 |
| 1 | Y 25 | | 0.945±0.01 | 0.80±0.01 | 0.70±0.02 |
| 1 | Y 45 | | | 0.98±0.02 | 0.71±0.02 |
| 2 | X 25 | 0.83±0.02 | | | |
| 2 | X 45 | | 1.00±0.01 | | 0.925±0.02 |
| 2 | Y 25 | 0.086±0.01 | | | |
| 2 | Y 45 | | | | 0.73±0.02 |

Maximum levels of exchange are expressed in equivalent fraction of the ingoing ion

Analytical methods

1 Radio Tracer Methods
2 Atomic Absorption Spectrophotometry

These values are generally higher than those reported in other investigations[87,68] and above the value of 82% expected for complete exchange within the supercages. Nickel appears to be the only ion giving consistent results between different sets of workers. Reversibility was only confirmed by Maes and Cremers[68] for $Co^{2+}_{(aquo)}$ in X. The selectivity trends observed show that for low levels of ion exchange the series were

X; $Zn > Cu >> Co \sim Ni$

and Y; $Cu > Zn > Ni \sim Co$

The systems exhibited a selectivity reversal at higher levels of transition metal ion exchange, which was characterised by a considerable decrease in the value of the selectivity quotient. Zeolite Y showed a preference for $Ni^{2+}$ throughout the isotherm.

Table 1.6

Standard Free Energies for First Row Transition Metal Exchange In Zeolites Na-X and Na-Y as Reported by Maes and Cremers[68]

| Metal Ion | T/$^oC$ | $\Delta G^\theta$/ kJ equiv$^{-1}$ | |
|---|---|---|---|
| | | X | Y |
| Co(II) | 5 | -0.24 | +0.94 |
| | 25 | +0.31 | +1.26 |
| | 45 | - | - |
| Zn(II) | 5 | -0.96 | +1.25 |
| | 25 | -0.51 | - |
| | 45 | -0.88 | - |
| Ni(II) | 5 | -1.34 | +0.23 |
| | 25 | -2.31 | -0.19 |
| | 25 | -2.05 | +1.05 |

If ion exchange is not confined to the supercages, then passage through the 6-oxygen windows into the sodalite cages must involve stripping, or partial removal, of the hydration shell around the metal ions. This is obviously not the only important parameter, as $Cu^{2+}$ and $Ni^{2+}$ have similar standard free energies of hydration[87] and yet show strikingly different maximum exchange levels. Maes and Cremers[86] compared the direct coordination of cation to framework with "inner sphere" complex formation and the interposition of water between ion and framework in the zeolite with "outer sphere" coordination. Their conclusion was that the relative concentration of inner sphere complexes increases in the order Ni < Mn < Co < Zn < Cu < Cd. Thus the increase in efficiency of charge neutralisation from nickel to copper is the same trend as observed in the maximum levels of ion exchange. The difficulty of obtaining a maximum exchanged form is therefore suggested to be related to the coordinating ability of the metal ion, and to the type of coordination involved in both the large and small cages. It was concluded[86] that nickel exchange was confined to the large cages.

In a more recent publication, Lai and Rees[80] examined ion exchange equilibria of $Co^{2+}$ in Na-X and Na-Y, $Zn^{2+}$ in Na-X and $Cu^{2+}$ in Na-Y. The $Al_2O_3/SiO_2$ ratio in their sample of Y was higher than that which had been used in previous work. The equilibria were studied at 25°C and total solution normality 0.1 g equiv. $dm^{-3}$. Maximum levels of exchange again varied from those obtained by other workers. The indications were that 16 ions per unit cell were left un-exchanged by copper and zinc in both zeolites and the limits for $Co^{2+}$ exchange in sodium X and Y are approximately 70% in both cases. These values for copper and zinc are closer to the values that would be expected for complete exchange into the main channels, but again the inconsistencies observed

in levels by different workers must be considered. Lai and Rees[80] did not observe de-cationation occurring with ion exchange of copper into X as was observed by Maes and Cremers[68], and interestingly obtained the same maximum exchange level.

The possibility of site redistribution of original ions within the zeolite on introduction of an exchanging cation was suggested by Lai and Rees[80] by introducing the concept that sodium ions may be "crowded" into small sites by introduction of large hydrated species into the super-cages. There does appear to be a correlation between a high population of sodalite cages, reflected by a lowering of the maximum exchange levels, and the increased water structuring properties of the transition metals.

### 1.9.8. Transition Metal Ion Exchange in Mordenite

Recent investigations by Barrer and Townsend, involved the determination of the ion exchange characteristics of the first row transition metals $Mn^{2+}$, $Co^{2+}$, $Ni^{2+}$, $Cu^{2+}$ and $Zn^{2+}$ in the ammonium form of synthetic mordenite[65]. The study was further extended to the amminated species[78] $\left[Zn(NH_3)_4\right]^{2+}$, $\left[Co(NH_3)_6\right]^{3+}$ and $\left[Cu(NH_3)_4\right]^{2+}$ in the same zeolite. Ion exchange isotherms were constructed at 25°C ahd at a total solution normality of 0.08 g equiv. $dm^{-3}$ in a pH range of 4 - 6 for aquated species, and ~ 10 for the amminated ions.

First row transition metal aquo species exhibited ion sieving effects terminating in all cases at maximum exchange levels of ~ 50% total capacity. This implied that exchange was confined to the main channels of the zeolite structure, and reflected the greater water structuring properties of transition metal ions compared with alkaline earths,

which exchange to much higher levels[85]. Changes in pH, effected by changing the anion of the transition metal ion, had no significant effect upon the equilibria involving aquated species. Reversibility was thoroughly tested throughout and it was shown that heating the exchanged samples caused diffusion of transition metals into side-pocket sites which were not normally accessible to the hydrated species at ambient temperatures. Isotherms indicated that in all cases the ammonium ion was preferred over the divalent ions. The values of free energy of exchange calculated were as follows.

Table 1.7

Values of the Standard Free Energy(kJ (g equiv$^{-1}$)) as Reported by Barrer and Townsend[65]

| Entering Ion | | | | | | | |
|---|---|---|---|---|---|---|---|
| Mn(II) | +0.099 | +3.858 | -0.301 | -0.080 | -0.324 | -0.281 | 0.000 |
| Co(II) | +0.661 | +4.420 | -0.020 | +0.201 | -0.430 | 0.000 | +0.281 |
| Ni(II) | +0.748 | +4.507 | +0.023 | +0.244 | 0.000 | +0.043 | +0.324 |
| Cu(II) | +0.260 | +4.019 | -0.221 | 0.000 | -0.244 | -0.201 | +0.080 |
| Zn(II) | +0.701 | +4.460 | 0.000 | +0.211 | -0.023 | +0.020 | +0.301 |
| $NH_4$ | -3.754 | 0.000 | -4.460 | -4.019 | -4.507 | -4.420 | -3.858 |
| Na | 0.000 | +3.754 | -0.701 | -0.260 | -0.748 | -0.661 | -0.099 |
| | Na | $NH_4$ | Zn(II) | Cu(II) | Ni(II) | Co(II) | Mn(II) |

Leaving Ion

Standard free energies were measured for the exchamge of transition metals with ammonium in mordenite, other standard free energies were calculated via the triangle rule

These calculations show that even for exchange with the smaller sodium ion, the transition metal ions are not preferred.

The observed trend in affinity was

$$Mn > Cu > Co > Zn > Ni$$

This trend was rationalised using dielectric theory[78] in terms of the Pauling crystallographic radii of the exchanging cations. Barrer and Townsend[65] pointed out that the trend in selectivity mirrored the trend in standard free energy (i.e. affinity) throughout most of the isotherm range. At very dilute concentration of transition metal ion, however, changes in the order of the selectivity trend were observed, indicating the danger of predicting trends in selectivity from trends in $\Delta G^{\theta}$ .

Work extended to amminated species[78] where the same maximum exchange limits of ~50% as that seen with the aquated species was observed for all the exchanging complexed ions. The isotherms were highly rectangular, showing a preference for the amminated transition metals over the ammonium ion in all cases, and much higher selectivities than those observed for the aquated transition metal ions were found. This high selectivity for amminated species was also rationalised by dielectric theory, assuming that a much higher selectivity implied a higher value of $\Delta G^{\theta}$. Since, by dielectric theory, $\Delta G^{\theta}$ is expected to be a function of ionic radii (see Section 1.8. ) the $\Delta G^{\theta}$ would be expected to become larger and more negative with the larger ionic radii of the complexed cations. Thermodynamic and selectivity data as presented by previous workers are compared in Table (1.8).

Table 1.8

Comparisons of Thermodynamic Affinity Sequences for Transition Metal Ions in Different Zeolites[141]

| Authors | Reference | Zeolite | T/$^{o}_{C}$ | Affinity Sequence |
|---|---|---|---|---|
| Gal et al. | 69 | Na-A | 25 | Ni < Co < Zn |
| " | 157 | Na-X | 25 | Co < Ni < Zn < Cd |
| Nikashina et al. | 158 | Na-A | - | Ni < Co < Zn < Cu |
| " | 158 | Na-X | - | Ni < Co ∿ Zn < Cu |
| Barrer and Townsend | 65 | $NH_4$-MOR | | Ni < Zn ∿ Co < Cu |
| Maes and Cremers | 68 | Na-X | 25 | Co < Zn < Cu < Ni† |
| " | 68 | Na-Y | 5 | Zn < Co < Ni |

The most common trend observed is

Ni < Co < Zn < Cu

Maes and Cremers[68] obtained as the thermodynamic sequence (†) but also described the overall selectivities of zeolite X and Y as increasing in the order Ni < Co < Zn < Cu where this order was qualitatively deduced from "the ease of exchange in both zeolites" as seen in "the maximum exchange capacities" observed[65]. This order is similar to the affinity sequences obtained by other workers with various zeolites[88,89,69,65]. The different affinity sequence observed by Maes and Cremers could arise from the lack of data points throughout the whole isotherm range, especially in the range Ac = 0.8 ⟶ 1. This ambiguity, associated with the Kielland plot in this region, gives rise to ambiguity in the estimation of the integral $\int_0^1 \ln K_c \, dA_c$ and hence underlines the importance of obtaining data points over the whole range of the isotherm.

### 1.9.9. Site Redistribution on Ion Exchange

Re-distribution of the original ions in a zeolite, upon ion exchange, leading to a new ion site distribution having the lowest free energy attainable for a given ratio of exchangeable cations, is one hypothesis accounting for observed limited exchange levels which are inconsistent with experimental cation location studies on homoionic zeolites. This is a statistically justifiable procedure[90] and a recent review by Cremers[3] gave collected evidence for this. A mechanism for redistribution was suggested by Vansant and Uytterhoeven[66] for the work on alkylammonium exchange on X and Y, where a correlation between the increasing size of incoming cation and the decreasing exchange limit was observed. Further work, however, by Mortier et al[91] on the cation sitings in alkylammonium and ammonium exchanged forms of potassium K-Y led to the conclusion that ion redistribution alone could not account for partial exchange. They stated that a sample of K-Y was exhaustively exchanged with $NH_4^+$ ions, and observed that although ammonium ions resided in the large cavities there was still a substantial amount of potassium resident in the SII sites in the main channels. Site redistribution was shown to occur to a considerable extent with the alkylammonium ions. As the exchanging ions became more bulky the level of intracrystalline water decreased and the maximum exchange level decreased whilst the potassium occupancy of the sites I and I' increased. The $K^+$ population of SII decreased with increasing exchange for the incoming cation, showing a trend in which the decrease is less as the size of the entering ions increased. It appears that for bulky ions exchange is confined to replacement of the hydrated potassium ions that are not bound to any crystallographic sites within the zeolite. As ion exchange of $NH_4^+$ occurred, removal of both inorganic cation and intracrystalline

zeolitic water appeared to occur simultaneously. Vansant[66] suggested that the exchange limit was reached when a further introduction of organic ions would require removal of the first hydration layer of the inorganic cation already present. This did not seem to apply to slightly smaller ions such as $NH_3Me^+$ or $NH_4^+$. Similarly, Mortier, Costenoble and Uytterhoeven[84] have shown that the maximum levels of calcium exchange in Y at room temperature depend on the nature of the outgoing cation. Using the same experimental conditions for both potassium and sodium Y gave 68% exchange in Na-Y and 90% in K-Y for calcium. X-ray data revealed that in Na-Y, exchange was limited to the supercages and no evidence of $Ca^{2+}$ population of SI' or SI was found. Calcium exchanged zeolite prepared from the potassium form gave a different ion distribution and also indicated $Ca^{2+}$ present in the SI' sites. The authors point out that for calcium to displace sodium in the sodalite cages it must displace a stable Na-hydrate structure and form a hydrate structure itself by coordinating to 3 oxygen and three water molecules, within the β-cage. This stable hydrate structure is not found in the potassium-exchanged form and therefore exchange of calcium into the sodalite cages in K-Y is more feasible than in the case of Na-Y. Similarly, recent work on $Ce^{3+}$ exchange[92] into Na-Y has indicated that as progressively more $Ce^{3+}$ is introduced into the zeolite and the $Ce^{3+}$ population of SI' is increased, then the sodium population of SI' increases at the expense of the SI sites. These data indicate that in general the relative occupancies of the various sites are dependent on both exchanging cations. In addition, Sherry, reviewing the situation[2] stated that the migration of ions into sites inaccessible to the incoming ions could be temperature dependent and hence account for the temperature dependent maximum exchange levels. It should also be noted that the hydration level of the zeolite and relative hydration energies of the exchanging cations are

also critical factors in determining the maximum levels of exchange and the relative site populations.

One feature common to equilibrium studies in zeolites is the general inconsistency of both selectivity trends and maximum exchange levels of different complementary studies. These inconsistencies can often arise from the preparation history of the samples and also be a function of the $Al_2O_3/SiO_2$ ratio, but they may in some cases reflect the practical methods used in obtaining equilibrium data. One notable inconsistency is that of ammonium exchange in sodium X. Theng, Vansent and Uytterhoeven[66] show an isotherm terminating at 60% exchange whereas Lai and Rees[80], using similar conditions obtain a 100% exchange level. These inconsistencies show the need for further studies of ion exchange equilibria in synthetic zeolites, and it is the object of this project to contribute towards the understanding and elucidation of ion exchange mechanisms by consideration of transition metal exchange in sodium and ammonium synthetic zeolites.

CHAPTER TWO EXPERIMENTAL

2.1. INTRODUCTION

2.1.1. Preparation of $Ag(NH_3)_2^+$

2.1.2. Preparation of $Cu(NH_3)_4^{2+}$

2.2. PRELIMINARY CONCEPTS AND PROCEDURES

2.3. SOLUTION STABILITY

2.4. ANALYTICAL PROCEDURES

2.4.1. Solution Analyses

2.4.1.1. Zinc(II) by EDTA
2.4.1.2. Cobalt(II) by EDTA
2.4.1.3. Nickel(II) by EDTA Back Titration
2.4.1.4. Manganese(II) by EDTA
2.4.1.5. Copper(II) by Sodium Thiosulphate Titration
2.4.1.6. Silver(I) by Sodium Chloride Titration
2.4.1.7. Silver(I) by EDTA
2.4.1.8. Uranium by EDTA
2.4.1.9. Vanadium by Potassium Permanganate
2.4.1.10 Atomic Absorption Techniques
2.4.1.11 Trace Quantities of Zinc and Manganese

2.4.2. Zeolite Phase Analyses

2.4.2.1. $SiO_2$ ($K_2CO_3/Na_2Co_3$ fusion).
2.4.2.2. $SiO_2$ (HF)
2.4.2.3. Water content
2.4.2.4. Ammonium Ion and Ammonia
2.4.2.5. Aluminium (Gravimetric)
2.4.2.6. Aluminium (Atomic Absorption)
2.4.2.7. Sodium
2.4.2.8. Extraction of Transition Metals from Zeolites
2.4.2.9. Determination of Transition Metals
2.4.2.10 Determination of Zinc in Zeolites
2.4.2.11 Platinum and Palladium
2.4.2.12 Silver and Ruthenium

2.5. PREPARATION AND ANALYSES OF AMMONIUM ZEOLITES

2.6. ION EXCHANGE TESTS

2.7. KINETIC TESTS

2.8. ION EXCHANGE INVOLVING $Ru(NH_3)_6^{3+}$

2.9. ION EXCHANGE EXPERIMENTS

2.9.1. Reverse Isotherm Points

2.9.1.1. Method 1

2.9.1.2. Method 2

2.10. ION EXCHANGE OF COPPER(II)

2.10.1. The Ion Exchange of Uranyl Ions

2.11. ADDITIONAL REVERSIBILITY TESTS

2.12. X-RAY ANALYSES

## 2.1. Introduction

The ion exchange characteristics of three synthetic zeolites were examined at 25°C. These were X, Y and mordenite (MOR). One sample of synthetic zeolite X (molecular sieve 13X) was supplied by B.D.H. (lot no. 1730230) and at a later date a further sample of synthetic X (SK20) was supplied by Union Carbide. Two samples of synthetic zeolite Y were obtained from Union Carbide. Only one sample of large-port synthetic mordenite was examined; this was provided by Norton, U.S.A. All samples were supplied in the sodium form. Washing with 0.1 mol $dm^{-3}$ sodium chloride solution was initially executed to ensure that the zeolites used were in their homoionic sodium forms.

Ion exchange experiments were carried out using the chloride and nitrate salts of Co(II), Ni(II), Mn(II), Cu(II), $UO_2^{2+}$, $VO^{2+}$, Ag(I) and $NH_4^+$, all supplied by B.D.H. and of AnalaR grade. In addition, the uranyl acetate used was AnalaR grade but uranyl formate and oxalate were bench reagent grade. 99.9998% pure zinc was supplied by Koch Light Laboratories. Complexed precious metal ions were supplied by Johnson-Matthey Limited, in the form of tetrammineplatinum(II) chloride $Pt(NH_3)_4Cl_2$ and tetramminepalladium(II) chloride $Pd(NH_3)_4Cl_2$.

Differential thermal and thermogravimetric analyses were performed on samples of the $Pd(NH_3)_4Cl_2$ and $Pt(NH_3)_4Cl_2$ salts using a Mettler thermoanalyser model 2. This enabled an estimation of the purity of the samples. Results showed that the platinum complex contained enough water to be in the hemihydrate form whereas the palladium complex contained only 4% w/w water. In addition, for both metal complexes, oxygen uptake occurred on

heating, giving rise to the compounds $PdO_x$ and $PtO_x$, where $x \sim \frac{1}{2}$ and was dependent upon rate of heating.

Ion exchange experiments were attempted with acid salts of the oxovanadium ion $VO^{2+}$. The oxalate, propionate and butyrate salts of oxovanadium(IV) were prepared by methods outlined in the literature[101,102]. It was suggested in the literature[102] that oxovanadium(IV) oxalate was an ionic species (i.e. $VO^{2+}(C_2O_4)^{2-}$) hence it was hoped that this salt could be used for exchange experiments. The preparative method for $VO(C_2O_4).2H_2O$ involved reacting stoichiometric amounts of vanadium pentoxide and oxalic acid at 100°C in an aqueous media. Contrary to reported observations[102] it was not found possible to recrystallise the oxalate from water efficiently. Instead, it was necessary to obtain the product by evaporation to dryness. The final product was reported to be $VO(C_2O_4).2H_2O$. Analyses by atomic absorption spectroscopy for vanadium content and by potassium permanganate titration[103] for oxalate content (with subsequent corrections for VO(IV) oxidation) were performed. These data (Table 2.1) indicated a higher water content than was expected[102].

### 2.1.1. Preparation of the Silver(I) Diammine ion $Ag(NH_3)_2^+$

The dissolution of either silver chloride or silver nitrate in dilute aqueous ammonia gives rise to the formation of the silver diammine cation[105]. It was found that the nitrate salt dissolved faster to give a stable solution of lower pH (pH ~10) than that observed for the chloride salt (pH ~ 12), and consequently all exchange experiments were confined to using diamminesilver(I) nitrate solutions.

The preparative method employed was to dissolve 16.8 g of AnalaR silver nitrate in approximately 250 $cm^3$ of water, then add dropwise 10%

w/v aqueous ammonia solution until the initially formed brown precipitate of silver oxide completely re-dissolved. The resulting solution was diluted to 500 $cm^3$ with dilute aqueous ammonia (pH ~ 10) giving rise to a solution containing 0.2 g equiv. $dm^{-3}$ of the silver salt. Ion exchange equilibria were then performed using solutions of half this strength.

### 2.1.2. Preparation of Amminated Copper.

65 g of copper chloride (1 g equiv) were dissolved in 500 $cm^3$ of distilled water. To this solution was added 1:1 aqueous ammonia solution until the initially formed blue precipitate redissolved, and the pH was approximately 10.5. This solution was then made up to 1000 $cm^3$ with dilute ammonia (pH 10.5), and was used in this form for all ion exchange experiments and equilibria involving the diaquotetramminecopper(II) ion. Ion exchange equilibria were constructed at pH 10.5±0.3.

## 2.2. PRELIMINARY CONCEPTS AND PROCEDURES

Transition metals are prone to precipitate as basic salts from alkaline or even weakly acid solutions, hence simple solution stability tests were performed in order to determine the limits within which transition metal salts would be suitable for ion exchange. Many transition metals exhibit in solution a sufficiently low pH to decompose or dealuminate a zeolite[108] and thus measurements of pH values of various equilibrium solutions were undertaken.

The ammonium form of all three zeolites was chosen for use for three reasons:

(1) The presence of ammonium chloride is known to suppress precipitation of basic transition metal salts[104].

(2) Ammonium zeolite imparts a less alkaline reaction to solution than does the corresponding alkali metal form.

(3) Ion exchange was performed with certain amminated transition metals in dilute ammonia solution. The presence of ammonia in solution gives rise to the equilibrium

$$NH_3 + H_2O \rightleftharpoons NH_4^+ + OH^-$$

In this situation the use of zeolites in the sodium form would result in ternary ion exchange systems. Kinetic plots were also constructed, firstly to assess the time necessary for complete equilibration, and secondly to determine whether or not a pseudo-equilibrium was actually obtained (i.e. whether after the initial fast exchange, a much slower exchange of ions into smaller side pockets within the zeolite occurred, giving rise to time equilibrium not effectively being obtained).

## 2.3. SOLUTION STABILITY

To determine the suitability of a particular metal ion species for ion exchange, the limits within which precipitation of basic salts occurred were determined for certain ions, and also the natural pH of all the transition metal ion solutions employed were determined (table 2.2 ) Limits of precipitation were determined by preparing solutions of constant normality for each transition metal ion (0.1 g equiv. $dm^{-3}$) but containing varying proportions of metal ion and ammonium ion. Since solution stability measurements had been previously determined for the first row transition metal ion and ammonium mixtures[65], tests in this present work were confined to vanadyl(IV) oxalate, vanadyl(IV) sulphate uranyl(VI) nitrate and uranyl(VI) acetate. 25 $cm^3$ aliquots of each solution were taken and titrated against dilute ammonia. The values of pH at which precipitates appeared and disappeared were noted (table 2.3).

Table 2.1 Analysis of Oxovanadium(IV) Oxalate

| Component | %w/v | Theoretical % based on $VO(C_2O_4)$ |
|---|---|---|
| V | 25.59 | 26.69 |
| $C_2O_4$ | 44.12 | 46.07 |
| $O_2$ | 8.03* | 8.44 |
| $H_2O$ | 22.26 | 18.8 |

* Oxygen coordinated to the vanadium atom (value estimated by diference)

Table 2.2 pH Values of Transition Metal Salt Solutions

| Metal Salt | Concentration/ mol $dm^{-3}$ | pH |
|---|---|---|
| $CuCl_2$ | 0.05 | 4.25 |
| $Cu(NO_3)_2$ | " | 3.68 |
| $CoCl_2$ | " | 4.45 |
| $NiCl_2$ | " | 4.48 |
| $UO_2(H_2CO)_2$ | | 3.3 |
| $Zn(NO_3)_2$ | " | 5.7 |
| $Cu(NH_3)_4Cl_2$ | " | 10.5 |
| $MnCl_2$ | " | 4.85 |
| $UO_2(NO_3)_2$ | " | 2.1 |
| $UO_2(NO_3)_2$ | 0.005 | 2.4 |
| $UO_2(H_2CO)_2$ | " | 4.2 |
| $UO_2(CH_3CO)_2$ | 0.05 | 4.3 |
| $VOSO_4$ | 0.005 | 3.25 |
| $VOC_2O_4$ | " | 4.05 |
| $Pt(NH_3)_4$ | 0.025 | 6.45 |
| $Pd(NH_3)_4$ | " | 7.8 |
| $Ag(NH_3)_2$ | 0.05 | 10.5 |
| $AgNO_3$ | " | 4.6 |
| $NH_4Cl$ | 1.0 | 4.2 |

Table 2.3 Values of the pH at which Precipitation first Occurs for Various Equilibrium Solutions

| Equivalent Fraction of Transition Metal Ion plus the pH at Which Precipitation Occurs | | | | | | | |
|---|---|---|---|---|---|---|---|
| $UO_2(CH_3CO)_2$ | pH | $UO_2(H_2CO)_2$ | pH | $UO_2(NO_3)_2$ | pH | $VO(C_2O_4)$ | |
| 1.0 | 6 | 1.0 | 6 | 1.0 | 4.0 | 1.0 | |
| 0.9 | 6 | 0.9 | 7.1 | 0.8 | 4.08 | 0.7 | |
| 0.8 | 6 | 0.8 | 8 | 0.6 | 4.1 | 0.5 | Stable to |
| 0.7 | | 0.7 | 9.5 | 0.4 | 4.2 | 0.3 | pH > 11 |
| 0.6 | Intrinsicaly | 0.6 | Stable To | 0.2 | 4.2 | 0.2 | |
| 0.3 | Unstable | 0.4 | pH > 11 | 0.1 | | 0.1 | |
| 0.2 | | 0.2 | | | | | |
| 0.1 | | 0.1 | | | | | |

From these data and those previously determined[65], it was concluded that all the first row transition metal ion solutions could be employed at a constant total normality 0.1g equiv. $dm^{-3}$; however observations should be made to determine if copper(II) precipitated within the zeolite matrix, as it was observed that copper precipitated at a much lower pH than those observed with the other metal ions tested.

All samples of uranyl nitrate were found to be stable to about pH 4.2 Uranyl acetate solutions containing an equivalent fraction of uranyl ion < 0.8 showed intrinsic instability (i.e. without increasing the natural pH's of the solutions at all by adding ammonia).

Measurements of the pH's of solutions[65] of the first row transition metal ions Co(II), Ni(II), Mn(II) (table 2.2) exhibited values in the region 4.5. This was a suitable range for ion exchange reactions to be examined without suspicion of decomposition of the zeolite framework. Cu(II) solutions were in the pH region 3.5, and therefore prolonged exposure of zeolite X to this pH would be bound to result in dealumination. All uranyl nitrate solutions tested (table 2.2) had pH values in the region of 2.3 and were therefore considered unsuitable. Uranyl acetate solutions were around pH 4.5, which was acceptable. Uranyl formate solutions showed pH's in the region of 4, and it was decided that 0.01 g equiv. $dm^{-3}$ solutions should be suitable, however, further observations revealed that the formate solutions were unstable to sunlight.

The preliminary conclusion on uranyl exchange was that organic acid salts were preferable to mineral acid salts. Exchange with uranyl formate would be possible if adequate precautions were taken to avoid exposure to sunlight. Uranyl acetate solutions may be used if, in all cases, the

equivalent fraction of the uranyl ion exceeds 0.8.

Stability and pH tests on vanadyl oxalate and vanadyl sulphate (table 2.2) indicated that vanadyl sulphate solutions of between 0.01 g equiv. $dm^{-3}$ and 0.1 g equiv. $dm^{-3}$ are intrinsically unstable due to the associated phenomena of hydrolysis and precipitation occurring. In addition the solutions had pH values of ~ 3.5, which was too acidic for use with zeolitesX and Y. Oxovanadium(IV) oxalate exhibited slightly higher solution pH's, but solution instability was observed at both the natural pH of the solutions and at elevated values of pH. Solutions containing oxovanadium(IV) propionate or butyrate (0.1 or 0.01 g equiv. $dm^{-3}$) were observed to precipitate a green flocculent substance at their natural pH over a period of 24 hours, and were therefore also rejected as unsuitable.

Solutions of aquo silver nitrate (0.1 g equiv. $dm^{-3}$) were found to be stable within the pH region 0-5.8. Addition of dilute ammonia solution to such a solution of silver(I) gave rise to a brown precipitate of silver oxide above pH 5.8, which redissolved at a pH > 9.8 due to the formation of the complex $\left[Ag(NH_3)_2\right]^+$ [127]. Likewise, any reduction in the pH of an ammoniacal solution of the silver ammine to below pH 9.8 gave a precipitate of $Ag_2O$.

Addition of 0.2 g samples of either Na-X or Na-Y to 50 $cm^3$ solution aliquots of either $\left[(Ag(NH_3)_2\right]^+$ or $Ag^+(aq)$ ions (0.1 g equiv.$dm^{-3}$), followed by subsequent equilibration at 25°C, did not give rise to an apparent precipitation of brown silver oxide in either the zeolite or solution phases.

Solutions containing 0.05 g equiv.$dm^{-3}$ of the ammonia complexes of either platinum or palladium showed complete stability over all elevated ranges of pH.

On the basis of the foregoing evidence, it was considered justifiable to attempt kinetic tests and ion exchange experiments with Cu(II) (nitrate), Ni(II), Co(II), Zn(II), Mn(II), $UO_2$(VI) (acetate or formate), Ag(I), $\left[Ag(NH_3)_2\right]^+$, $\left[Cu(NH_3)_4\right]^{2+}$, $\left[Pt(NH_3)_4\right]^{2+}$, $\left[Pd(NH_3)_4\right]^{2+}$ and $VO^{2+}$ (oxalate) with ammonium as the counter ion in all cases. Excluded were any other oxovanadium species. The amminated $Pt^{106}$, $Pd^{107}$ and Ag complexes showed intrinsic stability at high pH but all ion exchange experiments were performed at the natural pH of the aqueous salt solutions. Solutions containing 0.1 g equiv.$dm^{-3}$ $Ag(NH_3)_2^+$ showed signs of precipitating brown silver oxide at pH < 9.8. The analytical techniques used for these ion exchange experiments and also for the zeolite analyses are described in the next section (2.4) and a more detailed discussion of their application follows later (section 2.9).

## 2.4. ANALYTICAL PROCEDURES

Due to the varying types of analytical procedures applied this section is divided into two main sections. (Solution analysis and zeolite phase analysis).

### 2.4.1. Solution Analyses

Titrimetric - Usually titrimetric analyses were employed for the determination of large quantities of transition metal ions in isotherm solutions. The following described techniques (sections 2.4.1.1. to 2.4.1.8) generally involve 10 $cm^3$ aliquots of metal ion solutions of

0.1 g equiv. $dm^{-3}$ total concentration.

2.4.1.1. Zinc by EDTA[110].

An aliquot of zinc solution was pipetted into a conical flask and made up to a volume of 100 $cm^3$ with distilled water. The solution was made just alkaline by the addition of one or more drops of 1:1 aqueous ammonia solution. 10 $cm^3$ of 10% aqueous ammonium acetate were added and at this point the solution was checked for clarity, and that the pH remained above 7. The solution was then titrated against standard EDTA in the presence of 5 drops of Eriochrome Black T indicator until a sharp colour change of red to blue was observed.

This titration is best performed using 10$cm^3$ aliquots of 0.1 g equiv. $dm^{-3}$ zinc solution and approximately 0.1 g equiv. $dm^{-3}$ EDTA. A sharp end point is not observed with solutions as dilute as 0.02 g equiv.$dm^{-3}$. EDTA, and the titration appears very sensitive to pH at all concentrations.

(1 mole EDTA ≡ 1 mole $Zn^{2+}$)

2.4.1.2. Cobalt by EDTA

The method suggested by Vogel[111] was found to be adequate.

To an aliquot of cobalt solution was added 6 drops of 2% xylenol orange indicator and about 50 $cm^3$ of distilled water. Dilute sulphuric acid was added dropwise until the solution turned yellow (about 1 or 2 drops).

Powdered hexammine was added until a deep red colour was formed. This solution was then heated to 50°C and titrated against standard EDTA

until a colour change of red to yellow was observed.

The end-point was not sharp, and addition of the EDTA was made slowly with shaking near the end-point. This method is adequate using cobalt and EDTA solutions of ~0.1 g equiv. $dm^{-3}$ and also works for more dilute solutions, down to 0.02 g equiv. $dm^{-3}$.

2.4.1.3. Nickel by Back-Titration.

The methods[112,113] in Vogel were found unsuitable due to poor colour changes at the end-point. A variation of one of these methods[112] was used.

To an aliquot of nickel solution was added a volume of standard EDTA known to be in excess of the nickel solution, followed by about 50 $cm^3$ of distilled water. To the solution was added a few drops of 1:1 aqueous ammonia and 10 $cm^2$ of 10% ammonium acetate solution. The resulting solution was titrated against standard zinc solution in the presence of 5 drops of Eriochrome Black T indicator until a colour change of blue to red was observed. A blank titration using an equivalent volume of the same EDTA as previously used with no nickel present was also performed. The difference in volumes of zinc used gave the amount of nickel present.

This method can be used for dilute solutions of 0.02 g equiv. $dm^{-3}$ as well as for more concentrated solutions.

2.4.1.4. Manganese by EDTA[114]

An aliquot of Mn(II) solution was made up to a volume of 50 $cm^3$ with distilled water. 5 $cm^3$ of 10% hydroxylammonium chloride (which

prevents formation of manganese oxide[115]) and 10 $cm^3$ of 30% aqueous triethanolamine were added. This solution was made alkaline by the addition of 25 $cm^3$ of 880 ammonia and then titrated against standard EDTA in the presence of 5 drops of 0.5% thymolphthalexone indicator until a colour change of blue to colourless (or very pale pink) was observed.

(1 mole EDTA ≡ 1 mole $Mn^{2+}$ )

This method is not suitable for dilute solutions.

2.4.1.5. Copper(II) by Sodium Thiosulphate Titration[116]

To an aliquot of Cu(II) solution was added 2 $cm^3$ of 50% potassium iodide solution, and the volume was adjusted to about 50 $cm^3$. This solution, which contained a yellow suspension of iodine was titrated against standard sodium thiosulphate until the yellow colour almost disappeared. At this point 10 $cm^3$ of 10% ammonium thiocyanate were added to convert any precipitated Cu(I) to copper thiocyanate and thus liberate any iodine adsorbed on the precipitate. The yellow colour returned and 1 $cm^3$ of fresh starch suspension was added. Titration was continued until a colour change of dark blue to colourless or pale pink was observed.

(1 mole Cu(II) ≡ 1 mole $S_2O_3^{2-}$ )

This titration is suitable for solutions of 0.1 g equiv. $dm^{-3}$ but not for dilute solutions ( < 0.02 g equiv. $dm^{-3}$).

For analyses of $\left[Cu(NH_3)_4\right]^{2+}$ solutions this method was used with the modification that the first step involved dropwise addition of dilute acetic acid to the copper solution to remove the complexed ammonias from the ions. This was evidenced by a colour change from dark blue to pale

blue.

2.4.1.6. Silver by Sodium Chloride Back-Titration.

The method in the literature for titration of sodium chloride into silver solutions using an adsorption indicator[117] failed to give a sharp enough end-point. For an accurate standardisation of several different silver solutions it was important to titrate a standard solution from a burette into an unknown sample rather than have the unknown in the burette. Hence a variation on the usual sodium chloride/silver titration[117] using fluorescene adsorption indicator was developed.

To an aliquot of silver solution was added a volume of standard sodium chloride solution known to be in excess of the silver equivalent. This was then titrated against standard silver chloride solution in the presence of 10 drops of 2% fluorescene indicator until a permanent pink colour developed in the silver chloride precipitate.

This method was found to be applicable for solutions of 0.1 g.equiv. $dm^{-3}$ concentration, but no sharp end-point was observed for dilute solutions.

2.4.1.7. Silver by EDTA.

A method in the literature[118] described how silver could be determined in alkaline media by the addition of a small quantity of potassium nickel cyanide ($K_2Ni(CN)_4$) to a silver solution. This gives rise to the equilibrium

$$2Ag^+ + Ni(CN)_4^{2-} \rightleftharpoons 2\,Ag(CN)_2^- + Ni^{2+}$$

The liberated nickel is then determined with standard EDTA using murexide indicator.

The use of murexide indicator did not give rise to a sharp end-point and the following method was developed.

To a known aliquot of silver solution was added dilute ammonia dropwise until the silver oxide which had initially precipitated had redisolved. About 0.2 g of $K_2Ni(CN)_4$ were added, followed by a volume of standard EDTA which was known to be in excess of the nickel, then 10 $cm^3$ of 10% ammonium acetate solution. This was titrated against standard zinc solution in the presence of 5 drops of Eriochrome Black T indicator until a colour change of blue to red occurred.

This method was the most commonly used one for analyses of silver isotherm solutions.

2.4.1.8. Uranium by Back-Titration

To an aliquot of uranyl(VI) solution was added a known and excess volume of standard EDTA. This solution was adjusted to a pH of between 3 and 4 with an acetic acid/sodium acetate buffer. To the solution was added excess ascorbic acid (0.5g) and the solution was boiled for 10 - 15 minutes until a colour change from yellow to green was observed (due to the formation of U(VIII) ). The solution was cooled and to it was added 6 drops of xylenol orange indicator. Powdered hexammine was next added until the solution had a pH of ~5, and the excess EDTA was titrated against standard zinc until a colour change of yellow to red was observed.

This titration was found to be suitable for solutions with concentrations ranging from 0.01 to 0.1 g equiv. $dm^{-3}$. A better end-point was, however, obtained for solutions of higher strength if, after boiling with ascorbic acid the solution was first cooled and then buffered to just above pH 7 with ammonia and ammonium acetate. Zinc solutions were standardised against EDTA in the presence of 5 drops of Eriochrome Black T indicator with a colour change of blue to red.

2.4.1.9. Vanadium(IV) by Potassium Permanganate.

To an aliquot of vanadium(IV) solution was added excess concentrated sulphuric acid (ca 10 $cm^3$) and the solution was made up to a volume of 100 $cm^3$. The solution was heated to 60°C and titrated against standard potassium permanganate solution until the first permanent pink tinge was observed.

$$(5V(IV) \equiv 1MnO_4^- )$$

In this titration it was important to keep the temperature of the solution at 60°C. The titration could be carried out with vanadium and permanganate solutions of 0.1 g equiv. $dm^{-3}$, but solutions much less concentrated than this gave a very poor end-point.

2.4.1.10. Atomic Absorption Techniques.

For solution analyses of platinum and palladium, and for all the 1st row transition metals in very dilute conditions, it was necessary to use atomic absorption techniques. This involved diluting the solution to be analysed to a concentration within the linear working range for the particular metal. Then comparisons of the strength of absorption of the solution with that of a standard of known concentration. Interference

Table 2.4 Working Conditions for Atomic Absorption Spectrometer

| Element | Flame Type | $\lambda$/nm | Region of Linearity of Responce/ppm | Strength of Absorption | | Interferences |
|---|---|---|---|---|---|---|
| | | | | ppm | Abs Units | |
| Co | Air-Acetylene | 240.7 | 0 5 | 5 | 0.15 | - |
| Cu | " | 324.8 | 0 5 | 5 | 0.25 | - |
| Ni | " | 232.0 | 0 5 | 5 | 0.15 | - |
| Zn | " | 213.9 | 0 1 | 0.5 | 0.12 | - |
| Mn | " | 279.5 | 0 3 | 2 | 0.16 | - |
| Pt | " | 247.6 | 0 75 | 50 | 0.11 | - |
| Pd | " | 247.6 | 0 15 | 10 | 0.18 | - |
| Ag | " | 328.1 | 0 4 | 4 | 0.3 | - |
| Al | Nitrous Oxide-Acetylene | 309.27 | 0 50 | 50 | 0.22 | Ionisation, controlled by addition of KCl |
| Na | Air-Acetylene | 295 | 0 1 | 0.8 | 0.23 | - |
| Ru | " | 349.5 | 0 50 | 35 | 0.3 | - |
| Fe | " | 248.3 | 0 5 | 5 | 0.18 | - |

from the presence of other ions is often observed. Working conditions are expressed in table 2.4.

All atomic absorption methods were employed using a Perkin Elmer 360 Atomic Absorption Spectrometer.

2.4.1.11. Determination of Trace Quantities of Zinc and Manganese.

Zinc[120].

Zinc was satisfactorily analysed using "zincon" O- 2( (2-hydroxy-5-sulphenylazo)benzylidine)hydrozino benzoic acid in the presence of a pH 9 buffer solution.

Zincon solution consisted of 0.13 g of the compound dissolved in 3 $cm^3$ of 10% sodium hydroxide solution and diluted to 100 $cm^3$.

pH 9 buffer consisted of 50 $cm^3$ of 0.025 mol $dm^{-3}$ sodium tetraborate mixed with 4.6 $cm^3$ of 0.1 mol $dm^{-3}$ hydrochloric acid[132].

Buffer and zincon solutions were mixed in the volume ratio 5:2 respectively.

Aliquots of zinc were pipetted into volumetric flasks and a quantity of the buffer/zincon solution proportional to the flask volume, was added(14 $cm^3$ of buffer/zincon per 50 $cm^3$ of final solution volume). Solutions were made up to the mark and read against a reagent blank on an EEL absorptiometer using the 607 filter. Comparison was with standard zinc solutions, linearity of response of the absorptiometer was over the range 0 - 2ppm.

Manganese[121]

A method developed by Townsend[122] was used for determination of trace quantities of manganese.

Aliquots of manganese solution were pipetted into a 50 $cm^3$ volumetric flask with 10 $cm^3$ of distilled water, and immediately 1 $cm^3$ of fresh formaldoxime hydrochloride in a 1:1 ethanol : water solution was added. After shaking, 1 $cm^3$ of 4% sodium hydroxide was added and the solution diluted to 50 $cm^3$. The solutions were read against a reagent blank on the EEL absorptiometer using the 602 filter and compared with standard manganese solutions. Linearity of response was observed between 0 - 2 ppm. Resulting solutions were stable for less than one hour.

2.4.2. Zeolite Analysis.

2.4.2.1. $SiO_2$ Method (1) ($Na_2CO_3/K_2CO_3$ fusion).

This method is applicable only to the ammonium and sodium exchanged forms of the zeolites. It has been observed[125] that if this method is applied to transition metal exchanged zeolites, considerable diffusion of transition metals into the platinum crucible occurs.

An aliquot of zeolite (usually about 0.2g) was weighed into a platinum crucible and intimately mixed with five times its own weight of a potassium carbonate/sodium carbonate fusion mixture (the fusion mixture contained molar ratios of the two carbonates). The crucible was partially covered and heated, slowly at first, to 1000°C using a Meker burner. This temperature was sustained for 20 minutes. The crucible was allowed

to cool below red heat and then carefully immersed in about 50 $cm^3$ of water in a porcelain dish. The dish was covered with a clock glass and to it was added 60 $cm^3$ of concentrated HCl. When effervescence ceased the dish was warmed on a steam bath for one hour at which point 1 $cm^3$ of concentrated sulphuric acid was added and then the resultant mixture was evaporated to complete dryness. A further 50 $cm^3$ of 1:1 HCl were next added plus a few drops of sulphuric acid and the resultant suspension was again evaporated to complete dryness. Finally 50 $cm^3$ of 5% HCl were added and the mixture was digested on the steam bath for 10 or 15 minutes, then filtered hot through a no. 42 Whatman ashless filter paper. The filtrate was washed with hot dilute HCl, then water, and the wet filter paper was ignited slowly to 1000°C in a preweighed platinum crucible to constant weight. This gave the direct weight of the $SiO_2$ content of the zeolite. The filtrate and washings were retained for analysis for aluminium (section 2.4.2.5) iron (section 2.4.1.10) and other elements.

### 2.4.2.2. $SiO_2$ Method (ii) (using hydrofluoric acid)

A sample of zeolite was weighed into a platinum crucible and heated to constant weight at 1000°C on a Meker burner. After cooling in a desicator, the ignited weight was noted and the residue was treated twice as follows. Each time a few drops of water plus 2 drops of concentrated sulphuric acid and about 3 $cm^3$ of 48% hydrofluoric acid was added, and the solution was evaporated to dryness. The residue was next heated to constant weight and the difference between the initial and final ignited weights was taken as the weight of $SiO_2$. (A slightly different procedure was followed with transition metal zeolites; see section 2.4.2.8).

2.4.2.3. Water Content of Zeolites.

The water content was calculated from the weight loss observed after ignition to constant weight of a previously untreated zeolite sample which had been equilibrated over saturated ammonium chloride solution in a desiccator. A correction had to be made for the ammonium and/or ammonia content of the zeolites (section 2.4.2.4.)

The probable mechanism for thermal decomposition of the zeolites is as follows[109].

The zeolite can be expressed generally as $(NH_4)_n(AlO_2)_n\ (SiO_2)_m\ XH_2O$. On heating, the initial weight loss involves primarily the intracrystalline zeolitic water. Further heating to a higher temperature results in loss of ammonia leaving the hydrogen zeolite (i.e. $(H)_n\ (AlO_2)_n\ (SiO_2)_m$ At higher temperatures this hydrogen is then lost together with further oxygen by means of a dehydroxylation reaction. This leaves $Al_2O_3$ and $SiO_2$. The total weight loss on heating can then be expressed as a loss of $(NH_4)_2O$ plus $H_2O$. With ammonia in the zeolite determined as $(NH_4)_2O$ the subtraction of this weight from the total weight loss gives the water content. This mechanism has been substantiated for decomposition of ammonium mordenite[109] but thermogravimetric analyses for $NH_4$-X and $NH_4$-Y (Appendix IV) indicate that the second and third stages (i.e. removal of ammonia and dehydroxylation respectively) may occur simultaneously.

2.4.2.4. Ammonia and Ammonium Ion.

A known weight of zeolite was added to the flask of a Kjeldahl apparatus along with glass beads (to assist boiling) and about 100 $cm^3$ of

water. After connecting the apparatus up, 50 $cm^3$ of ~20% sodium hydroxide were added and the suspension was boiled for about 45 minutes. The liberated ammonia was trapped into a flask containing a known volume of standard hydrochloric acid. This was subsequently re-standardised with standard sodium tetraborate solution using methyl red indicator.

This method gave both the ammonium ion content of the zeolite and also the quantity of any complexed ammonia associated with the exchanged transition metal ion that may have been present. The quantity of each was determined where possible from a prior knowledge of extent of exchange of other cations present in the crystal.

2.4.2.5. Aluminium.

A known aliquot of filtrate from the fusion method used for $SiO_2$ determination (section 2.4.2.1.), was pipetted into a 600 $cm^3$ beaker and just neutralised with 1:1 ammonia solution. 4 $cm^3$ of 1:1 HCl were added. The solution was then made up to 200 $cm^3$, warmed, and an excess of 5% 8-hydroxyquinoline solution was added. The solution was next warmed to 50°C and 40 $cm^3$ of 40% ammonium acetate were added slowly with stirring. The suspension was heated to 70°C (and no higher) on a steam bath, and maintained at this temperature for 10 minutes. The resulting precipitate was allowed to settle and the solution checked for colour. If it was not yellow more oxine (i.e. 8-hydroxyquinoline) was added, but a large excess of oxine was avoided. After cooling the suspension was filtered through a preweighed P4 sintered crucible and washed with hot water. Finally the precipitate was dried at 140°C for two hours, cooled and weighed. For determination of aluminium content, the stoichiometry was assumed to be $Al(C_9H_6ON)_3$. If applicable a correction was made for

presence of iron assuming a formula $Fe(C_9H_6ON)_3$ (see section 2.4.1.10).

2.4.2.6. Aluminium by Atomic Absorption.

When aluminium had to be determined in the presence of transition metals (which was often the situation during the analyses of transition metal exchanged zeolites), analyses for aluminium was made by atomic absorption spectroscopy (section 2.4.1.10).

2.4.2.7. Sodium in Zeolites

Approximately 0.2 g of zeolite were added to a preweighed platinum crucible and the hydrofluoric acid treatment was applied (section 2.4.2.2). Care was taken to at no stage heat the crucible excessively as this renders the final residue partially insoluble. Upon removal of $SiO_2$ the crucible and contents were placed in a beaker containing 100 $cm^3$ of 10% hydrochloric acid and digested on a steam bath for 1 hour. The resulting solution was then diluted to 250 $cm^3$ and analysed for sodium content by flame photometry.

2.4.2.8. Determination of the Transition Metal Ions in Zeolites.

Samples of exhaustively exchanged transition metal zeolites were subjected to either or both of the following treatments.

(i) A 0.2g sample was treated directly with a 10 $cm^3$ volume of 48% hydrofluoric acid solution, in a platinum crucible, and evaporated to dryness, avoiding heating to constant weight. The process was repeated, and the platinum crucible and contents were placed in a 250 $cm^3$ beaker with 50 to 100 $cm^3$ of 1:1 HCl and digested for 45 minutes. The result-

ing solution was diluted to 250 $cm^3$ and analysed for metal ion content.

(ii) A 0.2g sample of zeolite was treated directly with 50 $cm^3$ of aqua regia and heated on a steam bath for 24 hours. The resulting mixture was filtered and the solution diluted to 250 $cm^3$.

2.4.2.9. Transition Metal Analysis

Both methods of dissolving the zeolite (section 2.4.2.8) were found to give consistent results for X and Y. Aliquots of the sample solution were diluted to achieve a metal ion content of about 5 ppm before analysis by standard atomic absorption techniques (section 2.4.1.10).

2.4.2.10. $Zn^{2+}$ in X and Y

The upper limit of linear response of the atomic absorption spectrometer to this metal ion was 1 ppm. This limit was considered marginally too low for accurate analyses to be achieved and an alternative method was adopted, involving a gravimetric determination of zinc using sodium quinaldinate[126].

An aliquot of sample solution was pipetted into a 600 $cm^3$ beaker and just neutralised with 1:1 ammonia. 1 $cm^3$ of concentrated nitric acid was added and the solution was boiled in order to oxidise any iron present to Fe(III). 20 $cm^3$ of 20% sodium tartrate solution were then added to the boiling solution in order to complex the Fe(III). The solution was cooled and just neutralised, then one excess drop of 1:1 ammonia was added. The solution was diluted to 150 $cm^3$ and heated to 50°C. 10 $cm^3$ of sodium quinaldinate were added with stirring and digested at 50°C for 1 hour. The precipitate was filtered through a pre-

weighed sintered glass crucible, washed with hot water and dried at 110°C. The precipitate was weighed as

$$Zn\ (C_{10}H_6O_2N)_2 \cdot H_2O$$

2.4.2.11. Platinum and Palladium in Zeolites.

The conventional method of analysis for transition metals in the zeolite phase, involving the analysis of zeolite residues after hydrofluoric acid treatment by atomic absorption spectrometry, gave inconsistent results for platinum and palladium, possibly due to an incomplete uptake of the metal by hydrochloric acid. The methods involving either fusion with $Na_2CO_3/K_2CO_3$ (section 2.4.2.1) or direct dissolution in aqua regia (using a porcelain crucible) gave rise to only partial uptake of precious metal possibly because of formation of insoluble precious metal silicates[125]. Consequently these methods were not employed.

The following methods were therefore used.

(A) The assumption was made that stoichiometric exchange of $\left[Pt(NH_3)_4\right]^{2+}$ or $\left[Pd(NH_3)_4\right]^{2+}$ with either $NH_4^+$ or $Na^+$ in the zeolite phase was achieved. Hence, with a prior knowledge of the exchange capacity and the ammonium content before and after exchange with the relevant previous metal ion ($NH_4$ determined as in section 2.4.2.4), it was possible to estimate the Pt or Pd content of the zeolite.

(B) This method involved heating the precious metal exchanged zeolite to constant weight followed by determination of the silica content by HF treatment (Section 2.4.2.2.). The resulting residue was analysed for sodium content by the method explained previously (section

2.4.2.7). The weight of residue left after the hydrofluoric acid treatment was assumed to be composed of $Al_2O_3$, $Na_2O$ and either PdO[131] or PtO respectively. Consequently having a prior knowledge of the $Na_2O$ and $Al_2O_3$ contents (by inference from the $SiO_2$ content) the precious metal component could be determined.

The platinum content of the zeolite was determined as PtO rather than $Pt^{131}$ as it was observed that on heating a sample of $Pt(NH_3)_4Cl_2$ on a thermogravimetric analyser oxygen uptake occurred. It was assumed that heating $\left[Pt(NH_3)_4\right]^{2+}$ in the zeolite phase would result in a similar uptake of oxygen.

The two estimations for platinum metal content (methods A and B) gave results consistant to within 3% of each other.

2.4.2.12. Silver and Ruthenium in the Zeolite Phase

Attempts to dissolve silver and ruthenium stoichiometrically from the zeolite phase by methods (i) and (ii) (section 2.4.2.8), followed by subsequent analysis using atomic absorption techniques, gave inconsistant results. The maximum levels of ion exchange in these systems was determined by exhaustive exchange of 0.2g samples of the sodium zeolite with 0.1g equiv. $dm^{-3}$ solutions of the particular metal ion, followed by subsequent analyses of the resulting solution for sodium content by flame photometer.

This method was also applied to determination of maximum levels of exchange of both the platinum and palladium complexes in sodium zeolites.

## 2.5. Preparation and Analyses of $NH_4$ Zeolites.

The ammonium exchanged forms of zeolites X, Y and MOR were prepared by taking a 20g sample of the sodium zeolite and equilibrating it with a volume of 1 g equiv. $dm^{-3}$ aqueous ammonium chloride solution that was sufficient to ensure an approximately five times excess of ammonium ion over the total exchange capacity of the zeolite. The solution was changed daily for a fresh aliquot each time over a period of 7 days. The final three equilibrations were performed at 70°C. The zeolites were subsequently washed briefly with four 100 $cm^3$ aliquots of distilled water then dried at 60°C, and left in a dessicator over a saturated solution of aqueous sodium chloride for ten days to allow maximum uptake of water to occur. Each zeolite was analysed for ammonium, water, sodium, silica, aluminium and iron content by the methods described in section 2.4. 40 g samples of each zeolite were made by this method. Analysis results are shown in Table 4.1.

These data show that 100% ion exchange of $NH_4^+$ in mordenite was obtained. 73% exchange in synthetic X and 92% replacement of $Na^+$ by $NH_4^+$ occurred in synthetic Y.

An attempt to obtain 100% ion exchange in X and Y was made by employing three different methods.

(1) 10g samples of the partially ammonium exchanged zeolites were boiled with 25 $cm^3$ of 1 mol $dm^{-3}$ aqueous ammonium chloride for 30 minutes. The zeolites were briefly washed and the process repeated twice. Analyses for $Na^+$ and $NH_4^+$ content are shown in table 4.3.

(2) 0.5 g samples of the partially exchanged zeolites were heated

under vacuum at temperatures of 125°C and 175°C for 1 hour in order to allow jump diffusion of sodium ions from within the sodalite units into the main channels to occur. It was intended then to wash the zeolites with ammonium chloride solution and remove the sodium ions from the main sites. Analysis for ammonium content directly after the heating process showed that for both zeolites, despite the relatively low temperatures, approximately 25% and 35% of the ammonium content was removed at 125°C and 175°C respectively.

(3) 0.3g samples of the partially exchanged ammonium X were placed in sealed glass ampoules with 50 $cm^3$ quantities of 1 mol $dm^{-3}$ aqueous ammonium chloride solution and heated to 150°C in an oven for 1½ hours. The zeolite was subsequently washed and analysed for sodium and ammonium content. Results (table 4.3) showed 96% replacement of sodium ions from zeolite X although a considerable portion of this replacement was by hydronium ion.

None of the 3 procedures employed gave 100% ammonium ion exchange in either zeolite. Method (3) would possibly give 100% removal of sodium ions if repeated several times but the 'scaling up' process necessary for use of 40 g samples of zeolite would require impractical volumes of solution. In addition, hydrolysis and dealumination problems vitiate this method.

It was decided that ion exchange experiments would be performed on the samples of X and Y that had been initially exchanged to levels of 73% and 92% respectively. At a later date, further samples of synthetic sodium zeolites X and Y were obtained. These new samples of X and Y were used for the determination of ion exchange equilibria involving

$[Pt(NH_3)_4]^{2+}$, $[Pd(NH_3)_4]^{2+}$, $Ag^+(aq)$, $[Ag(NH_3)_2]^+$, $[Ru(NH_3)_6]^{3+}$ and $NH_4^+$ in the sodium forms. The ion exchange equilibria studied are summarised in table 2.8.

## 2.6. Ion Exchange Tests.

Initial simple semi-empirical tests were performed to determine whether or not ion exchange appeared feasible in a particular case. These tests involved observing the colour of a 0.2g sample of zeolite after it had been exposed to a 50 $cm^3$ sample of a solution of metal ion of concentration 0.1 g equiv. $dm^{-3}$. The observations were as follows.

Table 2.5. Transition Metal Exchanged Zeolites

| Metal Ion | Zeolite Colour | | |
|---|---|---|---|
| | X | Y | MOR |
| Cu(II) (chloride) | green | green | - |
| Cu(II) (nitrate) | blue | blue | - |
| $Cu(NH_3)_4^{2+}$ | deep blue | deep blue | |
| Co(II) | pink | pink | - |
| Ni(II) | green | pale green | - |
| $UO_2^{2+}$ (acetate) | yellow | yellow | yellow |
| $UO_2$ (formate) | yellow | yellow | yellow |
| $VO^{2+}$ (sulphate) | black solution | green | green |
| $VO^{2+}$ (oxalate) | black solution | green | green |
| $Pd(NH_3)_4^{2+}$ | pale yellow | white | white |

This colour test obviously could not be applied to exchange involv-

ing the Ag, $Zn^{2+}$, $Mn^{2+}$ or $\left[Pt(NH_3)_4\right]^{2+}$ ions, which are colourless or near-colourless. Other preliminary tests involved analyses of the original and corresponding equilibrated solutions after mixing and equilibrating a metal ion solution with a zeolite. Methods are described in detail in section 2.4.2. Any drop in metal ion solution concentration implied either that ion exchange had occurred or alternatively that precipitation of basic salts had taken place. Next, each of the resultant zeolites were separated from its solution by centrifugation and then washed 3 times with water. The zeolites were then re-equilibrated with 50 $cm^3$ aliquots of a 0.2 g equiv. $dm^{-3}$ solution of ammonium chloride for a period of four days. The resulting solutions were analysed for metal ion content by atomic absorption spectroscopy (section 2.4.1.10) except for the uranyl ion which was determined by EDTA titration (section 2.4.1.8). Results in table 2.6. express the number of mequiv. $g^{-1}$ output from the zeolite.

Table 2.6. Reversibility Tests

| Metal Ion | X mequiv. $g^{-1}$ | Y mequiv. $g^{-1}$ | MDR mequiv. $g^{-1}$ |
|---|---|---|---|
| Cu(II) (chloride) | 0.317 | 0.99 | - |
| Cu(II) (nitrate) | 2.24 | 1.81 | - |
| $Cu(NH_3)_4^{2+}$ | 1.8 | 1.73 | - |
| Co(II) | 1.96 | 1.54 | - |
| Ni(II) | 1.74 | 1.31 | - |
| $UO_2^{2+}$ (acetate) | 1.34 | 1.04 | 0.71 |
| $UO_2^{2+}$ (formate) | 1.46 | 1.13 | 0.83 |
| $VO^{2+}$ (sulphate) | - | - | - |
| $VO^{2+}$ (oxalate) | 0.086 | 0.06 | 0.04 |
| $Pt(NH_3)_4^{2+}$ | 0.696 | 0.48 | 0.37 |

These results indicated that the first row transition metal ions and complexed platinum(II), copper(II), and silver(I) did exchange and were at least to some extent reversible. Little trace of $VO^{2+}$ ion could be observed in the reverse ion exchanged solution when either vanadyl oxalate or sulphate were employed. Similarly, the recovered copper content was low and the level of recovered uranyl ion from the formate solution was considerably lower than that seen for the other first row transition metals This gave grounds for suspicion of precipitation of basic salts or hydroxide from copper, uranyl (formate) and all vanadyl solutions.

2.6.1. Further Tests on Vanadium.

The literature[123] indicated that green oxovanadium hydroxide was the most likely species to be precipitated (i.e. $VO(OH)_2$). An ESR spectra was taken at liquid nitrogen temperatures of a sample of oxovanadium (IV) mordenite prepared by equilibration with a solution of vanadyl oxalate (figure 2.1). The observed signal was strong and characteristic of V(IV)[124] and indicated the presence of a V(IV) species in the zeolite.

To determine whether, as expected, the vanadium content was a precipitate or not, solutions of 0.1 g equiv. $dm^{-3}$ oxovanadium(IV) sulphate and oxylate were stabalised with a few drops of concentrated hydrochloric acid. This lowered the pH to ~3. 50 $cm^3$ samples of these solutions were equilibrated with 0.2g samples of zeolites X, Y and MOR, and examined.

(1) $VO(SO_4)$. Oxovanadium sulphate solution in contact with zeolite X turned black, whereas exchange of the same solution with either Y or MOR gave rise to blue zeolites within 10 to 15 minutes. On continuing the equilibration zeolite Y started to turn green after about 30

minutes whereas mordenite remained blue for over 5 hours. Neither Y or mordenite could be stabilised in the blue form in the dry state.

(2) $VO(C_2O_4)$. Contacting zeolite X with vanadyl oxalate solution caused both zeolite and solution phases to turn black, as with vanadyl sulphate exchanges involving X. Zeolites Y and MOR remained indefinitely colourless. ESR spectra of these two zeolites gave no indication that any uptake of vanadium had occurred.

In conclusion, the indications are that with vanadyl(IV) sulphate solution (acid stabilised) ion exchange of $VO^{2+}$ ion did occur, along with exchange of $H_3O^+$. This continual removal of acid from the solution led eventually to instability, with consequent precipitation of $VO(OH)_2$ in the zeolite. With acid stabilised solutions of oxovanadium(IV) oxalate, although precipitation was avoided in Y and mordenite, no ion exchange occurred; this indicates that the sample of oxalate used was a neutral complex, and not an ionic salt, as indicated in the literature[102].

## 2.7. KINETIC TESTS.

A kinetic test for each metal salt was effected by equilibrating two aliquots of 0.05 mol $dm^3$ solutions with samples of zeolite in the proportions of 0.1g of zeolite to 50 $cm^3$ of solution for $NH_4$-X and $NH_4$-Y, and 0.1g of zeolite to 25 $cm^3$ for $NH_4$-MDR. Samples A contained 0.4g and sample B contained 0.2g of zeolite. The mixtures were constantly agitated at 25°C and at known time intervals 2 $cm^3$ samples of the homogenous suspension were withdrawn, centrifuged and analysed by atomic absorption spectroscopy. Sample A was analysed over a period of one to four days, whilst sample B was analysed over a period of three days to one month.

Two equilibrium mixtures were used because it was found to be difficult to withdraw more than a few homogenous samples of suspension from the mixture without causing a significant disturbance of the equilibrium position. The use of two samples each containing large volumes of solution, minimised the total removal of suspension from either sample to almost negligible percentage proportions.

The kinetic data are shown in Appendix II (An example is graphically represented in Figure 2.2) indicating that all systems involving hydrated and amminated transition metals including silver, platinum(II) and palladium(III), in X and Y attained approximately 95% of the final equilibrium uptake of transition metal within one hour at 25°C. Complete equilibrium was achieved over a period of < 24 hours, after which time no further changes could be observed. A further examination involved repeating the exchanges of cobalt(II) and nickel(II) into X, but in these cases the samples were shaken 'violently'. Analysis showed that complete equilibrium was attained within one hour in these cases, indicating that the previously observed uptake over 24 hours was probably a function of interparticulate diffusion rather than a slow intraparticulate diffusion process (i.e. a diffusion and redistribution of ions into other site sets within the zeolite framework). Kinetic tests involving mordenite required, in all cases, about three days for complete equilibrium to be obtained, a phenomenon previously observed[65].

## 2.8. ION EXCHANGE TESTS INVOLVING $Ru(NH_3)_6^{3+}$

Conventional isotherm solutions (section 2.9.) were constructed for the hexammineruthenium(III)-sodium exchanges. 50 $cm^3$ aliquots of these solutions were contacted with 0.2g samples of Na-X. Na-Y and Na-MOR.

It was observed that over a period of ~ 5 days these suspensions all exhibited a colour change from the original pink shade through a deep red to a final deep blue colour, with the formation of a blue precipitate on the inside of the equilibration bottles. The original solutions (not in contact with any zeolite) were observed to follow this same colour change and precipitation over a period of 6 weeks. It has been observed previously that addition of aqueous alkali to solutions of $Ru(NH_3)_6\ Cl_3$ gives rise to a blue precipitate of unknown stoichiometry[160].

It is therefore suggested that the presence of sodium in solutions containing $\left[Ru(NH_3)_6\right]^{3+}$ gives rise to an alkaline reaction with the aqueous medium, thus causing precipitation of the blue compound. It would be expected that the presence of the alkaline zeolitic environment would enhance the precipitation.

Exchange of hexammineruthenium(III) with ammonium zeolites led to a similar precipitation problem but over a longer period of time (~10 days) which is consistent with the much lower alkaline reaction of the ammonium ion with the aqueous medium compared to the sodium ion.

## 2.9. ION EXCHANGE EXPERIMENTS

Ion exchange isotherms were constructed for each transition metal ion species using one of three slightly differing methods. Method 1 (the most commonly employed method) was employed to determine the ion exchange equilibria of all transition metal species into either sodium or ammonium zeolites. Method 2 was used for the measurement of the $NH_4$-Na exchange in Zeolites X and Y. Method 3 was used for the analysis of ion exchange equilibrations involving $Pt(NH_3)_4^{2+}$ in sodium

zeolites.

Method 1 - This procedure involved the preparation of 12 isotherm solutions of constant total normality. This concentration was 0.1 g equiv. $dm^{-3}$ for all the first row transition metals and also silver and 0.05 g equiv. $dm^{-3}$ for solutions involving the platinum and palladium tetrammine cations. $50cm^3$ aliquots of these solutions were added to sets of plastic bottles, each of which contained 0.2g of either the sodium or ammonium form of the appropriate zeolite, and the sealed bottles were agitated for 7 to 10 days at $25^oC$. The solutions and zeolites were then separated by centrifuging at 4000 rpm for 10 minutes, and the solution concentrations were determined by the methods outlined in sections 2.4.1.1 to 2.4.1.11. The corresponding original solution concentrations were also determined at the same time and values of $A_c$ and $A_s$ were calculated from these data. Data points outside the limits obtained using the above procedure were also obtained by varying the solution to zeolite ratio. This gave data in the areas $A_s \rightarrow 0$ and $A_s \rightarrow 1$. A typical set of isotherm solutions are shown in Table 2.7.

The analytical methods applied to solution phase determinations of transition metal ion exchange in the zeolites are summarised in table 2.9

Each analytical determination was carried out in duplicate and where necessary isotherm points themselves were duplicated.

Method 2 - This involved the construction of an isotherm as outlined for method 1. The analytical procedure, however, was different. After equilibration, the resulting solutions were separated and analysed for ammonium content by the kjeldahl method as described in section 2.4.2.4.

Table 2.7. Ion Exchange Isotherm Solutions

| $M^{2+}$/Eq fraction | Vol/$cm^3$ | wt zeolite/g. |
|---|---|---|
| 1.0 | 75 | 0.1 |
| 1.0 | 50 | 0.1 |
| 1.0 | 50 | 0.2 |
| 0.9 | 50 | 0.2 |
| 0.8 | 50 | 0.2 |
| 0.7 | 50 | 0.2 |
| 0.6 | 50 | 0.2 |
| 0.5 | 50 | 0.2 |
| 0.4 | 50 | 0.2 |
| 0.3 | 50 | 0.2 |
| 0.2 | 50 | 0.2 |
| 0.1 | 50 | 0.2 |
| 0.05 | 50 | 0.2 |
| 0.05 | 25 | 0.2 |
| 0.05 | 25 | 0.4 |

Method 3 (used for tetrammineplatinum/sodium isotherms)

This method involved analysis of the sodium ion component of the equilibrium solutions rather than the tetrammineplatinum(II) concentration. Analyses for sodium were by flame photometry.

Certain equilibria were found to be of a ternary nature, involving transition metal, ammonium and sodium from within the zeolite. The sodium contents of solution were determined in these cases by direct analyses of the equilibrated transition metal ion solutions using flame photometry, due allowance being made for interference from other ions

present in solution. These data, together with a prior knowledge of the original sodium content of the ammonium exchanged zeolite, enabled the sodium content of the crystal phase to be determined at any particular value of equivalent fraction of transition metal ion in solution.

Tetramminepalladium/Sodium Isotherms

Isotherms for these systems were constructed by the conventional method. Analysis of the resulting solutions was again by flame photometry for the sodium content for those solutions where the equivalent fraction of complexed palladium in solution was >0.6 (i.e. where the difference in the sodium content of the original and final solutions was large ) and by atomic absorption spectroscopy for palladium over the rest of the isotherm.

2.9.1. Reverse Isotherm Points.

Before any equilibrium thermodynamic procedures could justifiably be applied to any experimental isotherm data it was necessary to establish that true reversible equilibrium conditions existed over the whole isotherm. Two methods of establishing reversibility were employed. (A third conventional method which involved applying the procedure described in section 2.9. in reverse with the original zeolite now being the maximally ion exchanged transition metal zeolite, was not applied due to evidence in the literature[65] suggesting that redistribution of metal ions within the zeolite occurred on drying. This redistribution of ions would cause irreversibility).

2.9.1.1. Method 1.

Known weights of ammonium zeolite were equilibrated with known vol-

umes of a given metal/ammonium ion solution, as described in section 2.9. After analysis, this yielded a forward isotherm point. The centrifugate, taken for analysis was removed in such a way as to ensure that no zeolite was transferred or lost in the process. All the zeolite was then washed twice using 50 $cm^3$ aliquots of distilled water in the case of first row transition metals and very dilute ammonia solution in the case of exchanges involving the $Cu(NH_3)_4^{2+}$ or $Ag(NH_3)_2^{+}$ ions. The zeolite was then re-equilibrated with a new metal/ammonium solution containing a lower proportion of metal ion than that employed for the forward equilibration. After equilibration, the mixture was centrifuged again and the solution and corresponding original solution were analysed. The reverse equilibrium position was calculated from these data.

2.9.1.2. Method 2.

This method involved construction of a forward isotherm point with a high value of $A_c$. The solution plus zeolite was centrifuged and exactly 25 $cm^3$ of centrifugate were removed for analysis, thus enabling determination of the forward isotherm point. To the remaining mixture was added an exactly known volume of fresh solution of the same total solution normality as before, but containing a higher concentration of the original outgoing cation (either Na or $NH_4$) and therefore a proportionally lower concentration of the transition metal ions than was used in the original isotherm solution. After a second equilibration, analysis of this resulting solution, together with prior knowledge of both the degree of exchange for the transition metal after the forward equilibration and the transition metal solution concentration at this original equilibrium, enabled reverse isotherm points to be calculated.

### 2.9.2. Preparation of Transition Metal Zeolites

Samples of exhaustively exchanged transition metal X and Y were prepared by equilibration of 3g samples of ammonium zeolite with 250 $cm^3$ volumes of the relevant metal ion solution (0.2g equiv. $dm^{-3}$) for a period of 24 hours. The samples were centrifuged and re-equilibrated with a further 250 $cm^3$ of solution. This re-exchange process was repeated a total of four times. Samples of transition metal exchanged mordenites were prepared by extending each equilibration time to 3 days.

After equilibration the zeolites were separated from the aqueous solutions, washed and dried at 50°C overnight. The zeolites were placed in a desiccator over saturated sodium chloride for a minimum period of 1 week to allow absorption of intracrystalline water to reach equilibrium.

Subsequent analyses of the zeolites were then performed by the methods described in section 2.4.

## 2.10. ION EXCHANGE OF Cu(II)

Initially, an ion exchange isotherm was constructed for the copper(II) aquo ion using copper(II)chloride solutions. It was observed that the maximum extent of ion exchange exceeded the maximum exchange capacity (figure 4.29) and that the isotherm was not reversible. All samples of copper(II) X and Y were green which indicated precipitation of basic copper chloride rather than, or in addition to, exchange of the blue aquo ion. It was assumed that precipitation had occurred in these systems and consequently all further ion exchange with copper(II) was confined to solutions of the copper nitrate salt. Copper nitrate solutions exhibited no greater stability towards pH[65] than copper chloride solutions but it

was observed that all copper zeolites prepared with the nitrate solutions were blue. (see also section 4.1.3.)

### 2.10.1. The Ion Exchange of Uranyl Ions

Isotherm solutions containing uranyl formate plus ammonium ion were observed to be intrinsically stable in the absence of sunlight and to so some extent stable at elevated values of pH (Section 2.3.) Attempts were made to construct an isotherm (section 2.9.), for exchange with ammonium X using uranyl formate solutions. Analyses involved back-titration with EDTA (section 2.4.1.8.). Inconsistent results were obtained using these methods, possibly due to the inherent inaccuracies of the analytical techniques, but also probably due to the occurrence of precipitation of basic uranyl salts.

Isotherm solutions containing uranyl acetate and the ammonium ion were found to be unstable, again leading to the precipitation of basic uranyl salts. (Table 2.3.). Consequently all attempts to obtain a reversible exchange isotherm for the uranyl ion were abandoned.

## 2.11. REVERSIBILITY TESTS

An additional check on reversibility, in addition to those described in section 2.9.1., was employed in some cases. This involved initial exhaustive exchange of 0.2g samples of the $NH_4$/Na zeolites with aqueous transition metal ion solutions (0.1 g equiv. $dm^{-3}$), followed by washing with distilled water and exhaustive re-exchange with an ammonium chloride solution (0.5 mol $dm^{-3}$). The total volume of ammonium ion solution used for the reverse exchanges was collected and analysed for total transition metal ion content by atomic absorption techniques (section 2.4.1.10) The

resulting zeolite sample was then similarly re-exchanged with a dilute solution of sodium chloride solution (0.5 mol $dm^{-3}$) in order to determine whether or not any apparently irreversibly held transition metal ions could be dislodged by using sodium rather than ammonium ion. Results are expressed in table 4.21.

## 2.12 X-RAY ANALYSIS

In order to check that the crystallinity of the samples had been retained throughout the exchange procedure, samples of the original material and final product were examined by X-ray powder diffraction. Apparent retention of crystallinity was confirmed in all cases.

Table 2.8. Ion Exchange Equilibria

| Equilibria | Zeolite* |
|---|---|
| $Cu^{2+} \rightleftharpoons NH_4^+$ | $NH_4$ X, $NH_4$ Y |
| $Co^{2+} \rightleftharpoons NH_4^+$ | $NH_4$ X, $NH_4$ Y |
| $Zn^{2+} \rightleftharpoons NH_4^+$ | $NH_4$ X, $NH_4$ Y |
| $Ni^{2+} \rightleftharpoons NH_4^+$ | $NH_4$ X, $NH_4$ Y |
| $MN^{2+} \rightleftharpoons NH_4^+$ | $NH_4$ X, $NH_4$ Y |
| $Cu(NH_3)_4^{2+} \rightleftharpoons NH_4^+$ | $NH_4$ X, $NH_4$ Y |
| $Ag^+ \rightleftharpoons Na^+$ | Na X, Na Y, Na MOR |
| $Ag(NH_3)_2^+ \rightleftharpoons Na^+$ | Na X, Na Y, Na MOR |
| $Ag(NH_3)_2^+ \rightleftharpoons NH_4^+$ | $NH_4$ MOR |
| $Pd(NH_3)_4^{2+} \rightleftharpoons Na$ | Na X, Na Y, Na MOR |
| $Pt(NH_3)_4^{2+} \rightleftharpoons Na$ | Na X, Na Y, Na MOR |

* All equilibrium studies using the ammonium exchanged zeolites X or Y involved partially exchanged ammonium/sodium zeolites prepared at 70°C (Analysis Table 4.1). Exchange studies using pure sodium X or Y involved use of different zeolite samples to those employed elsewhere; (Analysis Table 4.4). Studies using mordenite involved the same zeolite sample fully exchanged with either sodium or ammonium ion as the starting material.

Table 2.9. Analytical Methods Applied to Isotherm Determinations

| Exchanging Ion | Method/Section | |
|---|---|---|
| Cu | 2.4.1.5. | (dilute solutions 2.4.1.10) |
| Co | 2.4.1.2. | (dilute solutions 2.4.1.10) |
| Zn | 2.4.1.1. | (dilute solutions 2.4.1.11) |
| Mn | 2.4.1.4. | (dilute solutions 2.4.1.11) |
| Ni | 2.4.1.3. | (dilute solutions 2.4.1.10) |
| Ag | 2.4.1.7. | (dilute solutions 2.4.1.10) |
| $Ag(NH_3)_2$ | 2.4.1.7. | (dilute solutions 2.4.1.10) |
| $Cu(NH_3)_4$ | 2.4.1.5. | (dilute solutions 2.4.1.10) |
| $Pt(NH_3)_4$ | Na by flame photometer | |
| $Pd(NH_3)_4$ | 2.4.1.10 | |
| $NH_4$ | $NH_4$ by Kjeldahl method | |

ESR Spectrum of Oxovanadium (IV) Mordenite

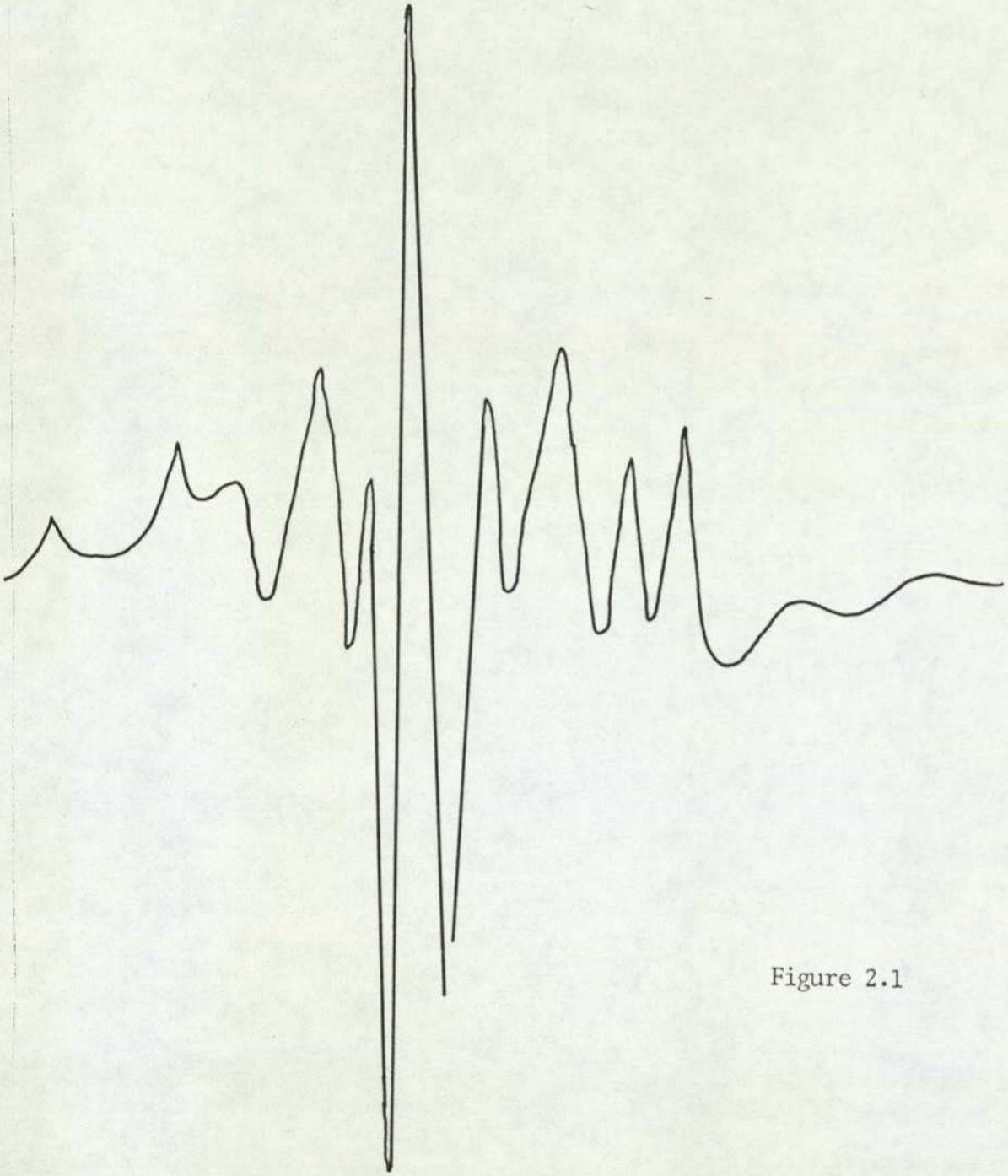

Figure 2.1

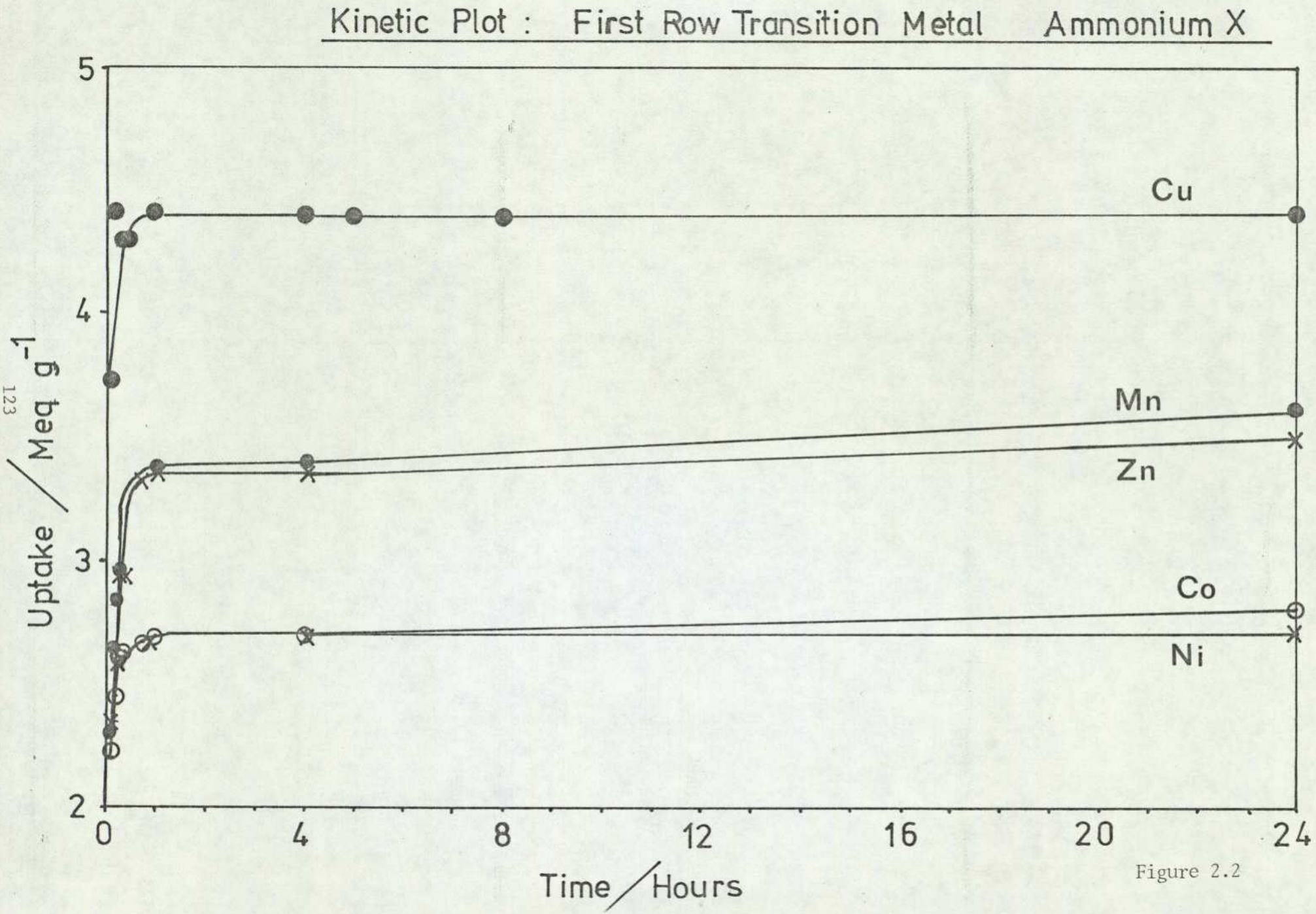
Kinetic Plot : First Row Transition Metal Ammonium X
Uptake / Meq g$^{-1}$
Time / Hours
Cu
Mn
Zn
Co
Ni
5
4
3
2
0
4
8
12
16
20
24

Figure 2.2

## CHAPTER THREE EXPERIMENTAL ERROR AND VALIDITY OF THEORETICAL TREATMENT

## 3.1. ACCURACY OF EXPERIMENTAL TECHNIQUES

The analyses of both zeolite and solution phases involved using both gravimetric and titrimetric techniques (chapter 2). The factors affecting the accuracy of these techniques can be broadly classified under two headings:

(i) Restriction of the limits of detection due to the sensitivity and calibration of analytical apparatus and the consequent reproducibility obtained in use.

(ii) Fluctuations in estimations due to the inherent sensitivity of the chemical techniques.

These contributions to the experimental error (i and ii) cannot be directly resolved but the total experimental error can be determined by the statistical variation of the observed results, and is expressed in this thesis by the percentage mean variance $\Theta$ where

$$\Theta = \frac{\sum_i |x_i - \bar{x}|}{n_i} \times \frac{100}{\bar{x}}$$

$\bar{x}$ is the mean value of $x_i$ and

$$\bar{x} = \sum x_i / n_i$$

where $n_i$ is the number of observed readings.

## 3.2. MEASUREMENT OF EXPERIMENTAL ERROR

### 3.2.1. Accuracy of Zeolite Phase Determinations

The experimental error due to the accuracy and sensitivity of the analytical balance is small being $< 0.5\%$ for a typical sample weighing 0.2 g. Hence it is appropriate to express the accuracy of the analytical

procedures applied to the zeolite phase by tabulating the component and the mean percentage variation observed on an average set of analysis results for each zeolite.

Table 3.1.

| | X | | Y | | MOR | |
|---|---|---|---|---|---|---|
| | θ | Average Number of Analyses | θ | Average Number of Analyses | θ | Average Number of Analyses |
| $SiO_2$ | 1.01 | 6 | 0.79 | 6 | 0.57 | 4 |
| $Al_2O_3$ | 0.73 | 4 | 0.98 | 4 | 1.09 | 8 |
| $(NH_4)_2O$ | 0.28 | 4 | 0.25 | 4 | - | 4 |
| MO | 0.93 | 2 | 1.13 | 2 | 1.28 | 4 |
| $Na_2O$ | 1.25 | 4 | 1.14 | 4 | 1.37 | 4 |
| $H_2O$ | 1.20 | 6 | 1.18 | 6 | 1.39 | 4 |
| $Fe_2O_3$ | 0.74 | 1 | 0.61 | 1 | 0.81 | 1 |

These data represent the observed experimental errors obtained for all analysed components of a 0.2g zeolite sample. The least accurate determinations are in all cases those for sodium, water and silica. In the case of sodium, this is not surprising, as the graduated scale on the flame photometer gives only an accuracy of $\pm$ 1 in 100. The accuracy of determination of silica content is dependent upon the accuracy of the initial determination of the water content (section 2.4.2.2.), consequently any errors in water determination (possibly due to the inhomogeneity of the sample), would create a corresponding error in the silica determination. The general trends of table 3.1. show greater error in determination when the percentage of a component is low. This is consistent with use of a constant weight of sample being used for analysis.

### 3.2.2. Solution Phase Analyses.

This section deals with the experimental error observed in the determination of the components of the isotherm equilibrium solutions and consequently the inferred concentrations in the zeolite phase.

#### 3.2.2.1. Colorimetric Analyses.

The major cause of experimental errors observed during the use of colorimetric determinations may be ascribed to the calibration scale on the absorptiometer, which would not allow readings to be taken with an uncertainty $\pm$ 1%. An example experimental error arising in this manner is seen in the determination of copper(II) as copper tetrammine when concentrations of the metal were low (see section 2.4.1.11), and the required result was derived from a difference between two small readings (table 3.2.).

Table 3.2. Absorbance Readings For Isotherm Solutions

| | Initial Solution | Final Solution | Difference | % Error |
|---|---|---|---|---|
| X | 19.5 $\pm$ 0.5 | 10.5 $\pm$ 0.5 | 9.0 $\pm$ 1 | $\pm$ 11 |
| | 19.5 $\pm$ 0.1 | 7.5 $\pm$ 0.5 | 12 $\pm$ 1 | $\pm$ 8.3 |
| Y | 19.5 $\pm$ 0.1 | 2.5 $\pm$ 0.5 | 17.0 $\pm$ 1 | $\pm$ 6 |
| | 19.5 $\pm$ 0.1 | 1.0 $\pm$ 0.5 | 18.5 $\pm$ 1 | $\pm$ 5.5 |

This shows a possible error of between 5 and 10% in the copper concentration in the zeolite phase (obtained by the difference between initial and final solution phase concentrations). The percentage error in the final solution concentration (i.e. the equivalent fraction of the

Table 3.3 The Cobalt $\rightleftarrows$ Ammonium Isotherm in Zeolite X

| | Equilibria | | Analysis | | | | |
|---|---|---|---|---|---|---|---|
| Solution / g.equiv.dm$^{-3}$ | wt.Zeolite/g | volume solution /cm$^3$ | volume /cm$^3$ | EDTA(initial) /cm$^3$ | EDTA(final) /cm$^3$ | Difference | $\theta$ |
| 0.1 | 0.2 | 50 | 10 | 1.30 ±0.01 | 10.25±0.01 | 1.05 ±0.02 | 1.9 |
| 0.09 | 0.2 | 50 | 10 | 10.05 ±0.005 | 8.98±0.01 | 1.07 ±0.015 | 1.4 |
| 0.08 | 0.2 | 50 | 10 | 9.08 ±0.01 | 8.08±0.01 | 1.0 ±0.02 | 2.0 |
| 0.07 | 0.2 | 50 | 10 | 7.88 ±0.015 | 6.96±0.005 | 0.92 ±0.02 | 2.17 |
| 0.06 | 0.2 | 50 | 10 | 6.78 ±0.00 | 5.92±0.01 | 0.86 ±0.01 | 1.16 |
| 0.05 | 0.2 | 50 | 10 | 5.835±0.01 | 5.0 ±0.01 | 0.82 ±0.02 | 2.43 |
| 0.04 | 0.2 | 50 | 10 | 4.405±0.01 | 3.72±0.00 | 0.68 ±0.01 | 1.47 |
| 0.03 | 0.2 | 50 | 20 | 6.785±0.005 | 5.33±0.01 | 1.45 ±0.015 | 1.05 |
| 0.02 | 0.2 | 50 | 20 | 5.46 ±0.01 | 4.1 ±0.01 | 1.36 ±0.02 | 1.47 |
| 0.01 | 0.2 | 50 | 20 | 2.34 ±0.02 | 1.17±0.01 | 1.17 ±0.03 | 2.56 |
| 0.005 | 0.2 | 50 | 20 | 1.175±0.00 | 0.4 ±0.005 | 0.775±0.005 | 0.64 |
| 0.1 | 0.2 | 100 | 10 | 11.3 ±0.01 | 10.58±0.02 | 0.7 ±0.03 | 4.28 |
| 0.1 | 0.2 | 200 | 10 | 11.3 ±0.01 | 10.82±0.01 | 0.46 ±0.02 | 4.35 |
| 0.1 | 0.1 | 200 | 10 | 11.3 ±0.01 | 11.06±0.01 | 0.21 ±0.02 | 9.52 |

metal ion in solution) could vary between 5 and 50%.

### 3.2.2.2. Atomic Absorption Techniques

The experimental error observed when this method was applied to the determination of the transition metal ions in the isotherm solution phase is dealt with in section 3.4.

### 3.2.2.3. Titrimetric Determinations.

In general, titrimetric methods were employed for analysis involving the solution phase and the accuracy of these determinations was governed by both the limit of calibration of the burette used and the accuracy of pipetting procedures. Zeolite phase metal ion concentrations were usually determined by analysing both the initial and equilibrated solutions and inferring the solid phase content by difference. The uptake of metal ion by the zeolite is governed by several factors including the ion exchange capacity of the exchanger, the amount used and also the selectivity. For zeolites X and Y, equilibrations were usually made using about 0.2g of zeolite; with mordenite, larger aliquots of about 0.3g were necessary. Analyses were performed on 10 or 20 $cm^3$ aliquots of the solutions using 0.1 g equiv. $dm^{-3}$ titre, using a 10 $cm^3$ "grade A" burette graduated in units of 0.02 $cm^3$. Titrations were performed until consistent results to within approximately 0.02 $\sim$ 0.03 $cm^3$ were obtained and the mean of all the values was taken. A typical set of titration figures is shown in table 3.3. This table shows that as one progresses through a set of equilibrium solution data the experimental error stays reasonably consistent ($\sim\pm$ 0.01 $cm^3$). However, when the difference between the concentrations of the initial and final solutions becomes small the percentage mean variance on the difference (last column in table 3.3.) in-

creases consdierably. This is particularly noticeable in the region $A_s \rightarrow 1$, where the result required is a small difference between two large titres and it in consequence becomes very difficult to determine accurately. Thus (table 3.3.) analyses of 10 $cm^3$ samples out of a total solution volume of 200 $cm^3$ result in errors approaching $\pm$ 10%. Direct analysis of all 200 $cm^3$ of a sample would, however, result in impractically large volumes of titre being used. Thus a limit to the accurate determination of the metal ion content in the zeolite phase $A_c$ is observed.

This problem may be partially solved by using small volumes of equilibration solution together with a reduction in the mass of zeolite used. This leads to solutions that may be analysed with greater accuracy but a greater error in determination of the mass of the zeolite sample now arises. Similar problems can occur in the region $A_s \rightarrow 0$ when the zeolite is not selective for the entering ion (i.e. $A_c \rightarrow 0$ also). Under these conditions, not only are the total concentrations, but also the differences between initial and final solution concentrations are tending to zero. These problems can be partially compensated for by analysing larger proportions of the total equilibrium solution (i.e. 20 or 25 $cm^3$ instead of 10 $cm^3$).

## 3.3. REVERSIBILITY

(i) Conventional Method - The most commonly employed method for obtaining reverse points for a particular exchange isotherm was to prepare the exhaustively exchanged zeolite, then after washing and drying this sample, to use it to construct the reverse isotherm. Previous work[65] has shown that the thermal drying process may lead to a redistribution of the ions within the zeolite phase, which is then reflected in the reverse isotherm by it not being coincident with the forward iso-

therm. In this thesis it is later proposed that the removal of any guest molecule present within the zeolite at the time of equilibrium, even at ambient temperatures by vacuum techniques, can lead to a redistribution of ions or a migration of ions into sites inaccessible to the ingoing ion at ambient temperatures. Hence the older conventional method was not used as a means of proving reversibility in any of the work reported here.

(ii) "Wet Methods for Testing Reversibility - Two methods for determining reverse points using wet samples have been employed (section 2.9.1.)

(a) A method employed by Barrer and Townsend[65] involved firstly the determination of a forward isotherm point by conventional means. Upon equilibrium being reached all the zeolite sample was then separated from the supernatant liquid by centrifuging. The whole sample was washed and re-equilibrated with the reverse exchange solution, which contained a higher proportion of the original outgoing cation. Upon equilibrium being reached this solution was analysed and hence a reverse isotherm point was determined.

One possible problem with the above method is that the washing of the zeolite sample after determination of the forward point could lead to the sample being in contact with a more dilute solution of the exchanging cations for a sufficiently long time for a re-equilibration to occur. Hence fast separation techniques were used in this work to minimise errors arising from this source. However, the effect of washing may not be very important for theoretical reasons. If we consider the equilibrium

$$A^{+}_{(s)} + B^{+}_{(c)} \rightleftharpoons A^{+}_{(c)} + B^{+}_{(s)}$$

then the thermodynamic equilibrium constant

$$K_a = \frac{a_A(C) \cdot a_B(S)}{a_A(S) \cdot a_B(C)}$$

Where $a_A(C)$, $a_B(S)$ etc. refer to the activities of ions A and B in crystal and solution phase. Upon washing the zeolite sample, dilution of the solution phase component leads to the concentrations of $A^+$ and $B^+$ in solution being reduced by the same degree. Therefore, assuming that the activity coefficient ratio of the two ions does not vary considerably upon dilution, it is reasonable to assume that the ratio $a_B(S)/a_A(S)$ does not vary considerably either, and hence the equilibrium position would be retained. This is not the case for uni-divalent exchange, however, since the equilibrium constant in this case is

$$K_a = \frac{a_A(C) \cdot a_B(S)^2}{a_A(S) \cdot a_B(C)^2}$$

consequently the function $a_B(S)^2/a_A(S)$, having a squared term, would not be expected to remain constant upon dilution and the equilibrium position would then be expected to change. This is a point referred to recently in a discussion between Rees and Klinowski[148] where Klinowski pointed out that this effect "is a simple consequence of the fact that the isotherms are normally expressed in terms of equivalent fractions rather than molalities." Barrer and Klinowski gave a quantitative treatment of this effect[60].

A second factor to consider is the rate at which equilibrium is attained. For zeolite X and Y equilibrium in the main channels is reached within a few minutes, hence if re-equilibration after washing is an important factor, almost instantaneous separation procedures between zeolite and solution would be required. Since it has been observed that conven-

tional centrifuging and fast filtration techniques produce reversible isotherms it may be assumed that re-equilibration upon dilution is not an important factor.

(b) A second "wet" method was developed to accommodate for any possible re-equilibration upon dilution that may take place, and also to minimise any problems occurring due to hydrolysis or loss of sample through continual washing.

This involved determining a forward isotherm point at a high value of $A_c$ in the conventional way, followed by high velocity centrifuging, then removal of exactly 25 $cm^3$ of the solution for analysis. The removed solution was replaced by a known volume of another solution of the same total normality but containing an accurately known but larger preparation of the outgoing cation than the original solution. The resulting mixture was re-equilibrated and upon attaining equilibrium the solution was separated and analysed. These data together with a prior knowledge of the degree of exchange obtained after the first equilibration enabled reverse isotherm points to be calculated (section 2.9.1.).

In all cases except the exchanges involving platinum and palladium (where method (a) was not used), this second method of determining reversibility gave similar results to method (a), indicating the effectiveness of the first method, and the negligible effect that washing has on the zeolite sample prior to reverse exchange.

## 3.4. EXPERIMENTAL ERROR FOR Pt and Pd SYSTEMS

(i) Platinum - Isotherms were determined for the $Pt(NH_3)_4^{2+} \rightleftharpoons Na^+$

exchange by determination of the difference in the sodium content of the initial and finally equilibrated solutions. Flame photometer techniques were employed in this determination, resulting in an initial error of ± 1% due to calibration limitations inherent in the flame photometer galvanometer. Upon equilibrium being reached, the sodium content in solution may increase by anything up to 100% for solutions containing initially high concentrations of $Pt(NH_3)_4^{2+}$ and low concentrations of $Na^+$ ions. Hence in these cases this difference between initial and final solutions may be easily and accurately determined to within ± 2%. However, with isotherm solutions which contain initially high concentrations of sodium the situation is different. For the determination of equilibria in the region $A_c \rightarrow 0$, very small percentage changes in the sodium content in solution occur upon equilibration. This results in the determination of values of equivalent fraction of $Pt(NH_3)_4^{2+}$ in the zeolite phase to only be reliable within ± 10 to 25% in this region. Thus the accuracy by which the selectivity quotient may be determined in these cases was poor.

(ii) Palladium - Isotherm points were constructed using both the flame photometer and the atomic absorption spectrometer as analysis tools. The flame photometer analysis allowed determination of sodium changes to within approximately ± 4% in the region where $Pd(NH_3)_{4(S)}^{2+} > 0.6$. The use of atomic absorption spectormetry gave a similar error for the determination of palladium in the crystal phase in the region where $Pd(NH_3)_4^{2+} < 0.6$. In addition, the determination of solution phase palladium concentrations in the region where $Pd(NH_3)_{4(S)}^{2+} < 0.05$ resulted in an error approximating to ± 30% as $Pd(NH_3)_{4(S)}^{2+} \rightarrow 0$. In consequence of these errors, the calculated values of selectivity quotient should be interpreted with caution.

## 3.5. COMPUTER ANALYSIS OF RESULTS

A computer program (CABIEZ) was developed for the application of thermodynamic procedures (section 1.6.) to those ion exchange isotherms which exhibited binary ion exchange characteristics. The program can be divided into four sections.

(a) A least squares treatment for fitting a polynomial equation to experimental isothermdata.

(b) Graph plotting techniques

(c) The thermodynamic treatment of isotherm data.

(d) The integration of the Kielland plot.

### 3.5.1. Least Squares Treatment.

The experimental isotherms contained approximately 20 points depicting equilibrium positions within the range $0 < A_s < 1$. For the Gaines and Thomas treatment[53] isotherm data are required over the whole of this range, and also a value for the maximum level of ion exchange is required in order to calculate the normalisation factor $f_N$ (section 1.6.2.1.). Smoothing the isotherm data by eye may be a subjective approach and it was considered justifiable to best-fit a polynomial equation by the method of least squares[127]. The equation took the form

$$y = A_o + A_1x + A_2x^2 + A_3x^3 + \ldots\ldots\ldots A_nx^n$$

where y represents $A_c$ and x represents $A_s$

To each isotherm a set of polynomial equations were fitted, with the

order of equation n varying between 2 and 6. Choice of the appropriate polynomial equation was based on the observed smoothness of fit and the value of standard deviation of the sum of residuals between the observed value of y and the predicted value of y using the polynomial equation. This standard deviation was expressed by the following equation

$$R = \sqrt{\left(\frac{(y_{obs} - y_{calc})^2}{(N - m - 1)}\right)}$$

where

N = Number of points and m = order of Polynomial.

The program used calculated the R factor for a series of polynomials and selected the best polynomial on the basis of the lowest value of R. An aid to the choice of polynomial equation was given by utilizing in addition a graph-plotting routine, which gave a visual output for each polynomial equation fit and also the experimental data points from which the polynomial was derived. This additional check was a useful safeguard, as it was observed that when high order polynomial equations were fitted to data points corresponding to either the isotherm or the Kielland plot, low values for the R factor were often observed, yet the actual polynomial was a wavy line through the data points. Such a fit is definitely not consistent with that expected for an experimental isotherm. On the other hand, there is no intrinsic reason per se why a Kielland plot should not show several maxima and minima.

The best-fitting techniques used to model the exchange isotherms functioned adequately for isotherms approaching linearity and for isotherms exhibiting low selectivity for the incoming ion, as depicted in figures 3.1. , 3.2. and 3.3. . Figure 3.1., for example, shows a second order polynomial equation fitted to the experimental data obtain-

ed for the exchange involving $Ag(NH_3)_2^+$ and $Na^+$ ions in X. Here the data are unambiguous and the best fitting polynomial adequately 'allows' for those experimental data points that do not appear to be consistent with the general shape of the isotherm. In the case of isotherms of rectangular shape, or those with a greater experimental scatter of data points, fits were generally not satisfactory. Examples of these poorer fits are shown in figures 3.4. and 3.5. . Figure 3.4. in particular depicts a highly rectangular isotherm, where, at high levels of ion exchange, there is an observed fluctuation around a level of ion exchange of 98% as $A_s$ is increased to unity. The curve shows that the lack of constraint of the polynomial equation between these data points causes the polynomial to bend and curve to accommodate for these fluctuations in data.

A second problem which occurs when polynomial equations are best-fitted to highly rectangular isotherms arises from part of the mathematical procedure used, which involves minimising the square of the absolute differnce between the y-coordinate of the experimental point and the predicted value of the y-coordinate. Compensation for this difference is adjusted over the whole range of the isotherm to give overall the best fit, but this means that the percentage variation at low values of y can often differ from the original value by as much as 100%. Highly selective isotherms, when large changes in $A_c$ take place for only small changes in $A_s$ at low values of $A_s$, often result in the polynomial equation plotting the mean position of the values of $A_c$ rather than the actual trend observed. This effect is seen in figure 3.6. and 3.7. . Figure 3.7. shows a rectangular isotherm, and the best fitting polynomial equation that was obtained for these data. Figure 3.6. shows the same isotherm, but experimental points obtained at low values of $A_c$ have been removed, and the resulting best-fitting polynomial equation is very different. Figure

3.7. shows, in fact, that in reality the introduction of points at low values of $A_c$ tends simply to pull the whole isotherm towards $A_c \rightarrow 0$ rather than a better mapping of the true isotherm shape. Thus the best - fitting of polynomial equations to highly rectangular isotherms is not a justifiable procedure and often results in a best-fitting curve which in no way reflects the original experimental data. To compensate for this the computer program used had written into it the facility to replace some of the 'corrected' data points (predicted by the best fitting polynomial equation) with their original data points and use these data to calculate the normalised selectivity quotient.

If the polynomial equation chosen by the computer on the basis of R values was accepted, then the corrected values of y (representing $A_c$) were used for the thermodynamic procedures along with the original values of $A_s$. The normalisation factor was the calculated value of y at x = 1, as predicted using the chosen polynomial. As a further refinement, a facility for statistically weighting the isotherm data pairs $A_c=A_s=0$ and $A_c(max), A_s=1$ was incorporated in order to force the best-fitting polynomial through these points.

Normalisation of the isotherm[95] was effected by dividing each value of $A_c$ by the maximum level of ion exchange. The thermodynamic procedures described in section 1.6, were then applied to each isotherm point in turn. In the computer program, the thermodynamic procedure was divided into two sections: firstly, the calculation of solution phase activity coefficients, and secondly, the calculation of zeolite phase activity coefficients.

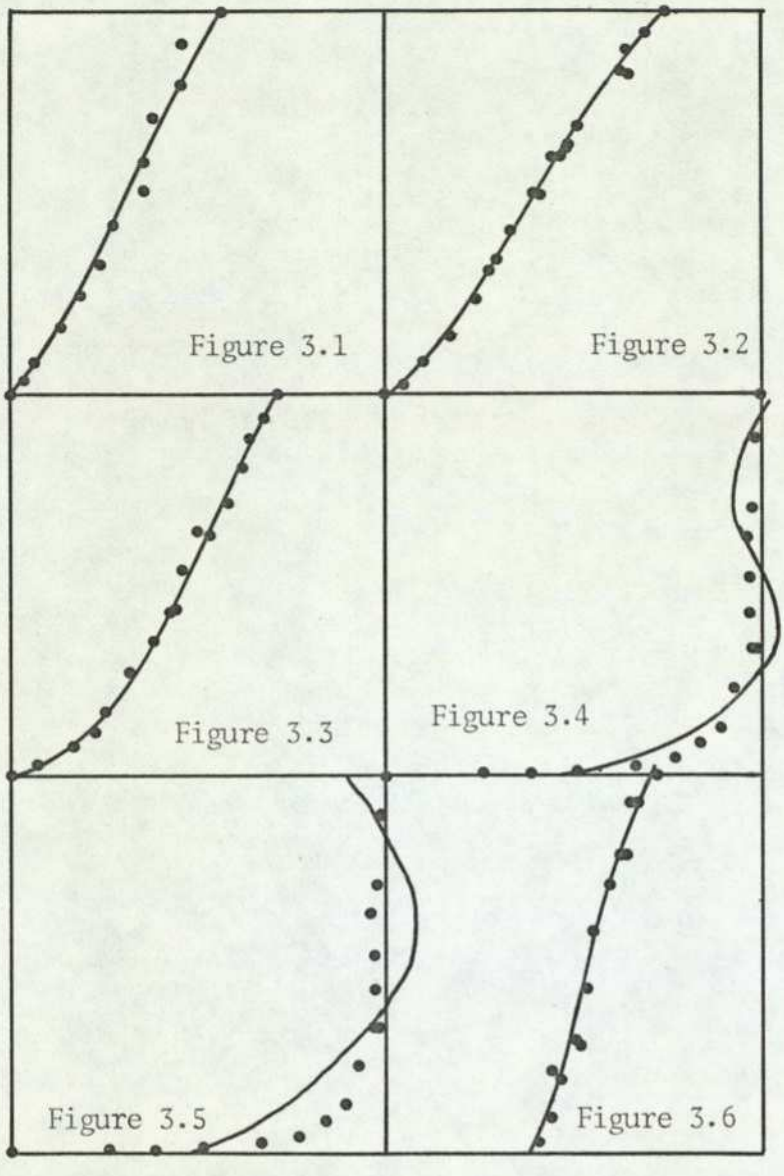

Figure 3.1

Figure 3.2

Figure 3.3

Figure 3.4

Figure 3.5

Figure 3.6

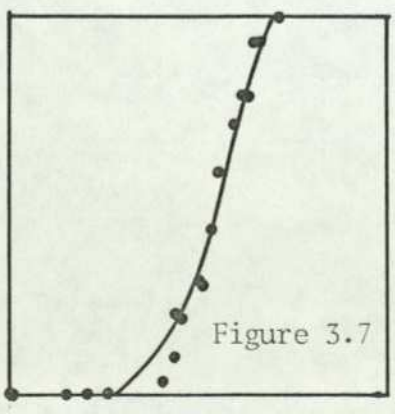

Figure 3.7

### 3.5.2. The Thermodynamic Treatment

For each value of $A_s$ the value of the concentration of each ion in solution was calculated (mol $dm^{-3}$) and thence from this the total ionic strength of solution was determined. Using this value of ionic strength the values of the mean molal stoichiometric activity coefficients for each component salt were calculated using a modified Debye-Huckel expression[128]. The calculation of the constants in this equation is described in section 3.5.2.1.

#### 3.5.2.1. The Calculation of $\Gamma$

The values of the activity coefficient ration $\Gamma$ are determined using the method of Glueckauf[59] (section 1.6.1.). Glueckauf's equations involve the calculation of the mean molal stoichiometric activity coefficients for each salt in a binary salt mixture over a range of values of the ionic strength of the solution. The calculation of these activity coefficients involves using values of the mean molal stoichiometric activity coefficients $\gamma_{\pm}$ for the pure salts at the same ionic strength; these values are given in the literature. However the data in the literature were often for the wrong range of ionic strength, in which case it was necessary to predict values of $\gamma_{\pm}$ by extrapolation or interpolation. The extrapolation method involved using a modified Debye-Huckel[128] equation to fit the literature data, and then predict values of the mean molal activity coefficient at the required ionic strengths:

$$\log \gamma_{\pm} = \frac{-A \left|Z_A Z_B\right| \sqrt{I}}{1 + B.a.\sqrt{I}} + b.I \qquad 3.100$$

where A and B are functions dependent on the absolute temperature and permittivity of the medium as follows[128]:

$$A = \sqrt{\frac{2\pi N}{1000}} \cdot \frac{e^2}{2.303\ k^{3/2}} \cdot \frac{1}{(\varepsilon T)^{3/2}}$$

$$B = \left( \frac{8\pi e^2 N}{1000\ k} \right)^{\frac{1}{2}} \cdot \frac{1}{(\varepsilon T)^{1/2}}$$

values $A = 0.5115\ mol^{-\frac{1}{2}}\ dm^{3/2}\ K^{3/2}$

$B = 3.291 \times 10^{-9}\ cm^{-1}\ mol^{-3/2}\ dm^{3/2}\ K^{1/2}$

The parameters a and b are dependent on the properties of both the salt and the supporting medium, a is often termed the "radius of the ionic atmosphere" surrounding the particular ion and b is a coefficient introduced to compensate for interactions arising at higher concentrations

To predict values of $\gamma_\pm$, literature values of $\gamma_\pm$ at two values of the ionic strength were substituted into equation 3.100, and the equations were then solved for a and b simultaneously. The following procedure was followed in calculating a and b.

For two values of $\gamma_\pm$ with their corresponding values of ionic strength I, the simultaneous equations to be solved are:

$$P = \frac{Q}{1 + R.a} + S.b \qquad 3.110$$

$P = \log \gamma_\pm(1)$

$Q = -A.Z_A.Z_B.\sqrt{I}(1)$

$R = B.\sqrt{I}(1)$

$S = I(1)$

$$T = \frac{U}{1 + V.a} + W.b \qquad 3.120$$

$T = \log \gamma_\pm(2)$

$U = -A.Z_A.Z_B\sqrt{I}(2)$

$V = B.\sqrt{I}(2)$

$W = I(2)$

Multiplying 3.110 by W/S

$$\frac{PW}{S} = \frac{Q(W/S)}{1 + R.a} + W.b \qquad 3.130$$

Rearranging 3.120

$$W.b = T - U/(1+V.a) \qquad 3.140$$

Substituting 3.140 into 3.130

$$\frac{PW}{S} = \frac{Q(W/S)}{1 + R.a} + T - U/(1+V.a) \qquad 3.140$$

Multiplying through by $(1 + Ra)(1 + Va)$

$$\frac{PW}{S}(1+R.a)(1+V.a) = \frac{QW}{S}(1+V.a) + T(1+R.a)(1+V.a) - U(1+R.a) \qquad 3.160$$

expanding the term $(1 + Ra)(1 + Va)$

$$1 + R.a + V.a + RV.a^2 \qquad 3.170$$

Rearranging 3.160

$$\left(\frac{PW}{S} - T\right)(1+ R.a)(1+ V.a) - \frac{QW}{S}(1+ V.a) + U(1+ R.a) = 0 \qquad 3.180$$

Substituting 3.170 into 3.180

$$\left(\frac{PW}{S} - T\right)(1 + R.a + RV.a^2) - \frac{QW}{S}(1 + V.a) + U(1 + R.a) \qquad 3.190$$

Expanding 3.190

$$\frac{PW}{S} - T + R.a\left(\frac{PW}{S} - T\right) + V.a\left(\frac{PW}{S} - T\right) - \frac{QW}{S} - \frac{VQW.a}{S} + RV.a^2\left(\frac{PW}{S} - T\right)$$

$$+ U + RU.a = 0 \qquad 3.200$$

Collecting $a^2$ terms

$$RV\left(\frac{PW}{S} - T\right)a^2$$

Collecting a terms

$$(R+V)\left(\frac{PW}{S} - T\right) - \frac{QWV}{S} + RU\ a$$

Collecting constants

$$\frac{PW}{S} - T - \frac{QW}{S} + U$$

These values can then be substituted into the general equation for the solution of simultaneous equations i.e.

$$X = \frac{-B \pm \sqrt{(B^2 - 4.A.C)}}{2.A}$$

where

$$A = RV\left(\frac{PW}{S} - T\right)$$

$$B = (R + V)\left(\frac{PW}{S} - T\right) - \frac{QWV}{S} + RU$$

$$C = \frac{PW}{S} - T - \frac{QW}{S} + U$$

X = the value of 'a' in equation 3.100.

Two values of X are produced by this procedure. One value is observed to be negative, the other positive. Due to the physical significance of the parameter a [128] the positive value of X is chosen and substituted into either equation 3.110 or 3.120 to obtain a value for b .

A computer program (Appendix III), designed to follow this procedure was used to calculate a and b for several sets of values of $\gamma_{\pm}$ and I. The averages of all the calculated calues of a and b were taken as the best representation of the relationship between $\gamma_{\pm}$ and I.

It was observed that a and b varied by up to $\pm$ 5% when different pairs of values of $\gamma_{\pm}$ and I were employed. However, the parameter b invariably compensates for any changes in a. The validity of using these mean values of a and b to calculate values of $\gamma_{\pm}$ by extrapolation was checked by first back-calculating $\gamma_{\pm}$ for values of I at which experimentally obtained values of $\gamma_{\pm}$ were available in the literature. These

checks produced values for $\gamma_{\pm}$ differing from experimentally derived values by $<0.5\%$ in most cases, exept for values of activity coefficients at high ionic strength, where deviation was still observed to be less than 2.5%.

These activity coefficients, calculated from the Debye Huckel model being the mean molal activity coefficients of the pure salts, consequently required correction, using Glueckauf's expressions[59,65] (Section 1.6.1 ) to give values for the mean molal stoichiometric activity coefficients of the salts in mixed solutions. These corrected values, were subsequently substituted into equation 1.330, resulting in a calculation of $\Gamma$ (the ratio of the single ion activity coefficients raised to the powers of the charges on the respective ions ). The value of $\Gamma$ and the corresponding value of $K_m$ (the mass action quotient, equation 1.210) were then substituted into equation 1.230 to give the corresponding value of $K_c$ (the Kielland coefficient). Both decadic and natural logarithms of these values were taken.

The above procedure was performed on all isotherm points exept for points where either $A_c$ or $A_s$ equalled zero, because use of such data points would have involved taking logarithms of zero (equation 1.230)

The computer output at this stage gave values of $K_c$, selectivity quotients for both normalised and unnormalised isotherm points, and also corresponding values of solution concentration, ionic strength, the solution phase activity coefficient ratio $\Gamma$ , $\log_{10}K_c$ and $\ln K_c$.

3.5.2.1.1 Glueckauf's Expressions

Glueckauf's model[59] is used to calculate the value of the activity coefficient of one salt in the presence of a second salt (both salts sharing a common anion). In essence, Glueckauf's method corrects the observed value of $\gamma_{\pm(AX)}$ for a pure salt solution at a given value of I for the effects arising from the presence of salt BX, which also has a value $\gamma_{\pm(BX)}$ in pure BX solution at the same value of I. It was observed that the values of $\Gamma$ calculated by this method for a uni-univalent binary mixture usually deviated from unity by less than 3% (see table 3.4.), and are virtually independent of the total solution concentration. The situation was not found to be the same for uni-divalent binary mixtures where, as exhibited by tables 3.5. and 3.6., the ratio $\Gamma$ is dependent on the nature of the ions involved and can vary considerably with changes in the ratio of the concentrations of the two exchanging cations. $\Gamma$ for uni-divalent mixtures was generally found to be in the region of 1.5.

In a recent report by Rees[129], the validity of Glueckauf's method was questioned. Rees produced experimental values of $\Gamma$, as measured for $Ca^{2+}/Na^{+}$ systems using ion selective electrodes. These data showed that Glueckauf's method predicted approximately the same values as those determined using ion selective electrodes but the degree of divergence in $\Gamma$ over a given range of cation ratios was greater using the ion selective electrodes. As yet no ion selective electrodes are available for use with transition metals.

The measured mass action quotient

$$K_m = \frac{A_c^{ZB} \cdot m_B^{ZA}}{B_c^{ZA} \cdot m_A^{ZB}}$$

is related to the normalised Kielland quotient by $K_c = K_m \times \Gamma$ . As is shown (Table 3.6) $\Gamma$ shows values for transition metal- ammonium solutions of up to $\sim$ 1.7 which means that the solution phase correction of $K_m$ can be as great as 70% for these systems. For a uni-univalent binary mixture having a common anion of unit charge

$$\Gamma = \frac{\gamma^2_{\pm(BX)}}{\gamma^2_{\pm(AX)}} \qquad 3.220$$

for uni-divalent binary mixtures

$$\Gamma = \frac{\gamma^4_{\pm(BX)}}{\gamma^3_{\pm(AX)}} \qquad 3.230$$

In this case if $\gamma_{\pm(AX)} << \gamma_{\pm(BX)}$ then $\Gamma$ will increase to a value greater than unity.

e.g.

$\gamma_{\pm(AX)} = 0.6 \quad \gamma_{\pm(BX)} = 0.8 \qquad \Gamma = 1.9$

$\gamma_{\pm(AX)} = 0.4 \quad \gamma_{\pm(BX)} = 0.8 \qquad \Gamma = 6.4$

$\gamma_{\pm(AX)} = 0.3 \quad \gamma_{\pm(BX)} = 0.8 \qquad \Gamma = 15$

We can see that for low values of $\gamma_{\pm(AC)}$ which are often observed for transition metal salts[130] the resultant value of $\Gamma$ will have a dramatic effect upon the value of $K_c$ with respect to $K_m$.

This can cause very serious errors in the calculated value of $\Delta G^{\ominus}$. Figure 3.8. shows how a model system can vary due to changes in $\Gamma$. As $\Gamma$ increases, this invariably leads to increases in the value of $\ln K_c$.

Tables 3.4,3.5 and 3.6 Values of Γ Calculated for Mixtures of Cations

Table 3.4 Univalent Cations- Total Solution Normality 0.1 g equiv. $dm^{-3}$

| Solution | Γ |
|---|---|
| $AgNO_3/NaNO_3$ | 1.012 |
| KCl/NaCl | 1.039 |
| $NH_4Cl/NaCl$ | 1.015 |
| CsCl/NaCl | 1.031 |

Table 3.5 Divalent Cations- Total Solution Normality 0.1 g equiv. $dm^{-3}$
(Transition metal and sodium chloride solutions)

| Ional Strength /mol $dm^{-3}$ | Metal Ions - Γ | | | | | |
|---|---|---|---|---|---|---|
| | Co(II) | Cu(II) | Mn(II) | Ni(II) | Zn(II) | Zn(II)* |
| 0.1500 | 1.736 | 1.721 | 1.755 | 1.732 | 1.707 | 1.629 |
| 0.1462 | 1.725 | 1.711 | 1.744 | 1.726 | 1.695 | 1.619 |
| 0.1412 | 1.710 | 1.696 | 1.729 | 1.711 | 1.679 | 1.604 |
| 0.1312 | 1.680 | 1.665 | 1.699 | 1.681 | 1.647 | 1.574 |
| 0.1212 | 1.648 | 1.634 | 1.667 | 1.649 | 1.613 | 1.543 |
| 0.1113 | 1.615 | 1.602 | 1.634 | 1.616 | 1.578 | 1.511 |
| 0.1062 | 1.600 | 1.584 | 1.617 | 1.599 | 1.560 | 1.494 |

Table 3.6 Divalent Cations- Total Solution Normality 0.1 g equiv. $dm^{-3}$
(Transition metal and ammonium chloride solutions)

| Ional Strength /mol $dm^{-3}$ | Metal Ions - Γ | | | | |
|---|---|---|---|---|---|
| | Co(II) | Cu(II)* | Mn(II) | Ni(II) | Zn(II)* |
| 0.1500 | 1.694 | 1.611 | 1.713 | 1.695 | 1.558 |
| 0.1462 | 1.683 | 1.599 | 1.702 | 1.684 | 1.547 |
| 0.1412 | 1.668 | 1.585 | 1.687 | 1.670 | 1.532 |
| 0.1312 | 1.638 | 1.554 | 1.657 | 1.639 | 1.501 |
| 0.1212 | 1.607 | 1.522 | 1.625 | 1.608 | 1.469 |
| 0.1113 | 1.574 | 1.489 | 1.593 | 1.575 | 1.435 |
| 0.1062 | 1.557 | 1.471 | 1.576 | 1.558 | 1.481 |
| 0.1012 | 1.540 | 1.454 | 1.558 | 1.542 | 1.400 |

*Nitrate Salts Used

Figure 3.8 Kielland Plots

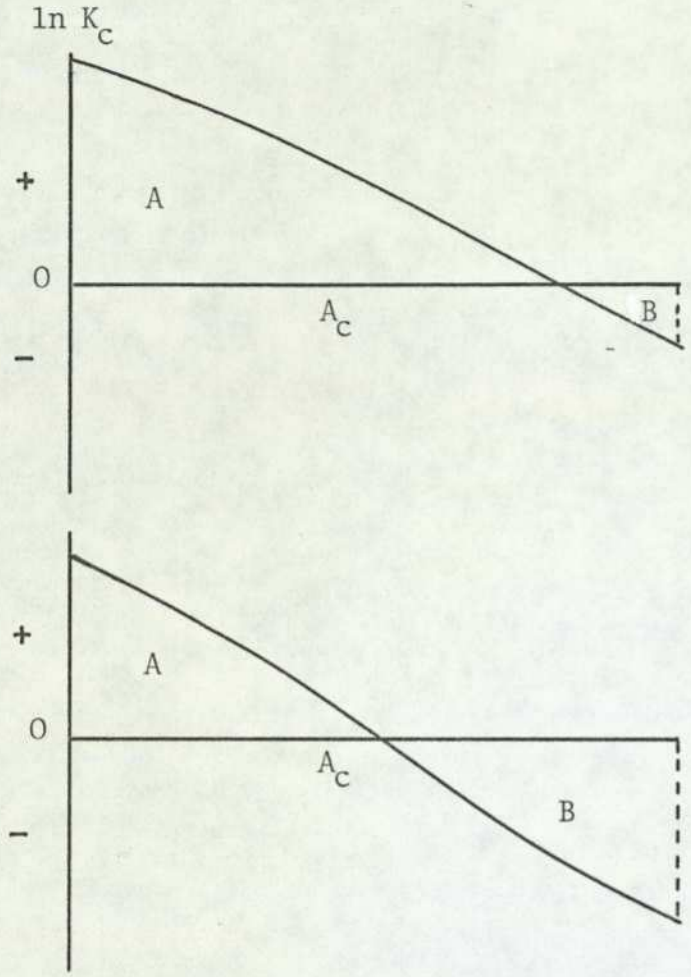


$$\Delta G^{\theta} = f\left(\text{Area A - Area B}\right)$$

In figure 3.8., changing $\ln K_c$ can lead to an almost infinite increase in the estimation of the area beneath the curve, reflecting a more positive value for $K_a$ and hence a more negative $\Delta G^{\ominus}$ value. This shows not only the importance of correctly determining $\Gamma$, but also the dangers in interpreting trends in affinity from trends in the selectivity quotient

3.5.2.2. The Calculation of Zeolite Phase Activity Coefficients

The next stage in the computer procedure, was to 'best-fit' polynomial equations to the values of $A_c$ with their corresponding values of

$\ln K_c$, deriving an equation of the form

$$\ln K_c = A_o + A_1 A_c + A_2 A_c^2 + A_3 A_c^3 + \ldots\ldots A_n A_c^n$$

The criteria on which the choice of which polynomial equation were made were those used in the choice of polynomial equation for isotherm data (section 3.5.1.) . By analytically integrating the derived equation 3.10 and following procedures of Gaines and Thomas[53] (section 1.6.2) values of zeolite phase activity coefficients at their corresponding values of $A_c$ were calculated, and also, using equations 1.500 and 1.250, values for the equilibrium constant $K_a$ and the standard Gibbs free energy per gram equivalent of exchange $\Delta G^{\ominus}$ were calculated.

## 3.6. THE EFFECT OF EXPERIMENTAL ERROR ON THE DERIVED THERMODYNAMIC DATA.

### 3.6.1. The Thermodynamic Functions $\ln K_c$, $f_A$ and $f_B$.

These three functions are highly dependent on the observable selectivity quotient throughout the range $0 < A_c < 1$. Thus these derived functions can be critically dependent on the treatment of data prior to the construction of the Kielland plot. This pre-treatment involves both the normalisation and the curve-fitting procedures.

#### 3.6.1.1. Effect of the Normalisation Factor

Various systems were systematically analysed using the computer program (CABIEZ section 3.5.) by altering the value of $A_c$(max) within the range $\pm$ 0.02 of the observed value. These systems were $Ni^{2+} \rightleftharpoons NH_4^+$ exchange in mordenite, and the $NH_4^+ \rightleftharpoons Na^+$ exchanges in X and Y. The data

Table 3.7 Values of $\Delta G^{\theta}$ and $K_a$ obtained by varying $A_c$(max)

| System | $\Delta G^{\theta}$/kJ(g equiv)$^{-1}$ | $K_a$ | $A_c$(max) |
|---|---|---|---|
| Ammonium and Sodium Exchange in X | -0.444 | 1.197 | 0.715 |
| | -0.3777 | 1.165 | 0.72 |
| | -0.243 | 1.103 | 0.73* |
| | -0.174 | 1.073 | 0.735 |
| | -0.107 | 1.044 | 0.74 |
| Ammonium and Sodium Exchange in Y | -2.405 | 2.649 | 0.69 |
| | -2.23 | 2.469 | 0.70 |
| | -0.206 | 2.303 | 0.71 |
| | -1.997 | 2.245 | 0.714* |
| | -1.889 | 2.150 | 0.72 |
| | -1.80 | 2.077 | 0.725 |
| Nickel(II)[143] and Ammonium Exchange in MOR | 4.254 | 0.0319 | 0.40 |
| | 4.365 | 0.0291 | 0.405 |
| | 4.579 | 0.0244 | 0.416* |
| | 4.496 | 0.0262 | 0.416† |
| | 4.665 | 0.0228 | 0.42 |
| | 4.767 | 0.0210 | 0.425 |

* Data chosen as correct by using $A_c$(max) as determined by best-fitting polynomial equation(CABIEZ)

† Normalised Data as used by Townsend [143] (i.e a different curve fitting procedure to *)

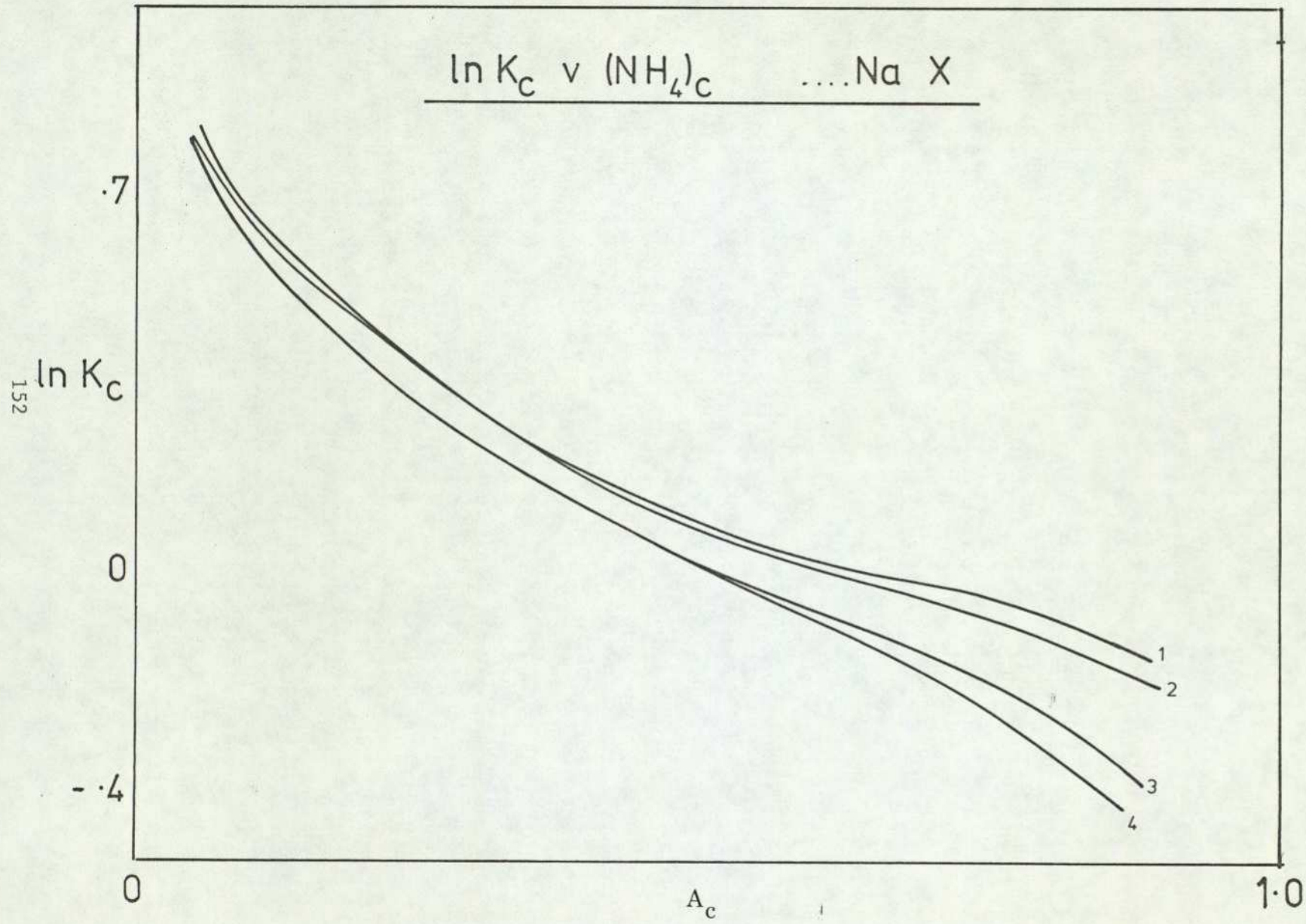


| N° | $A_c$ max |
|---|---|
| 1 | 0·715 |
| 2 | 0·72 |
| 3 | 0·735 |
| 4 | 0·74 |

Figure 3.9

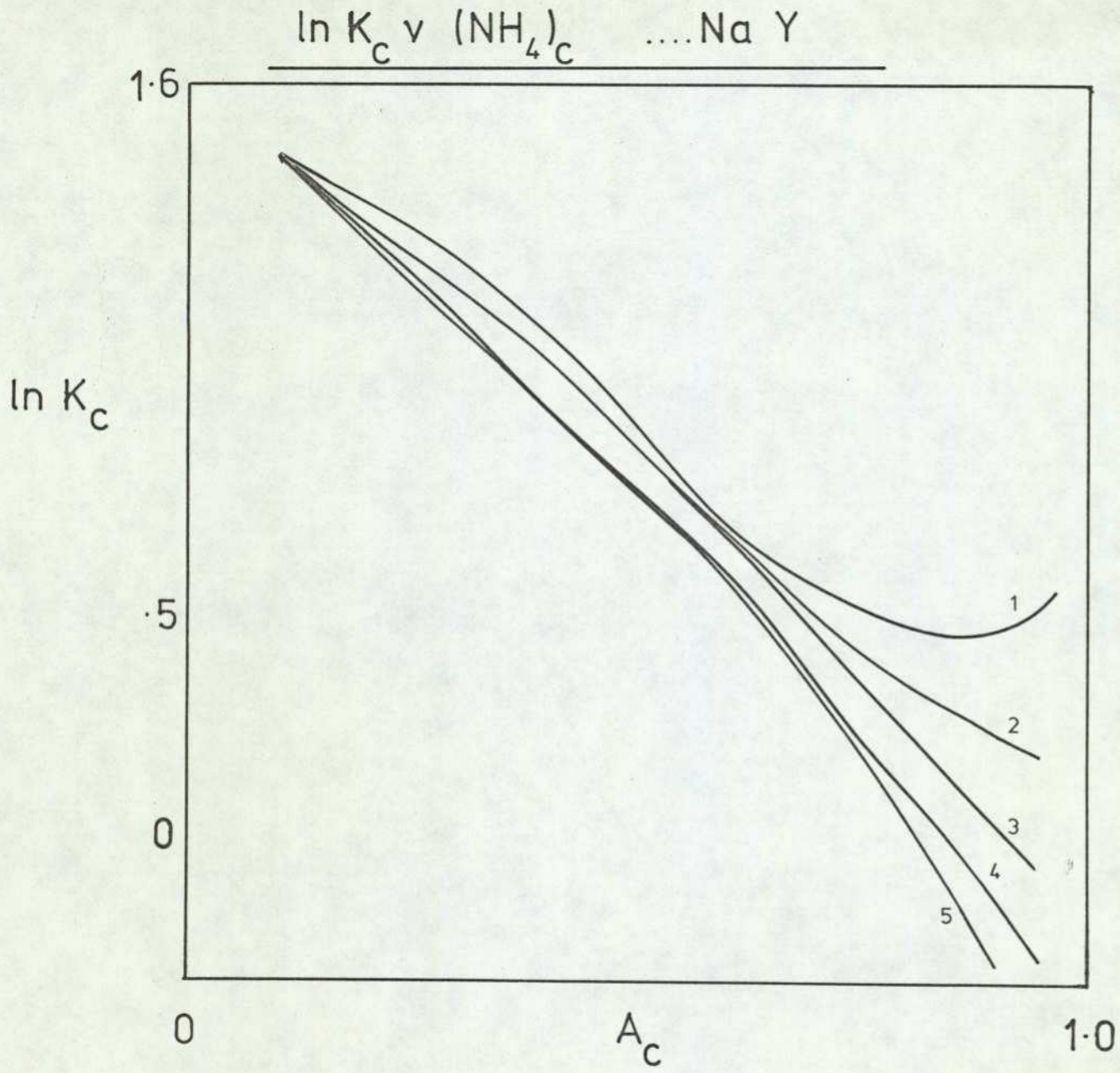


| N° | $A_c$ max |
|---|---|
| 1 | 0·69 |
| 2 | 0·70 |
| 3 | 0·71 |
| 4 | 0·72 |
| 5 | 0·725 |

Figure 3.10

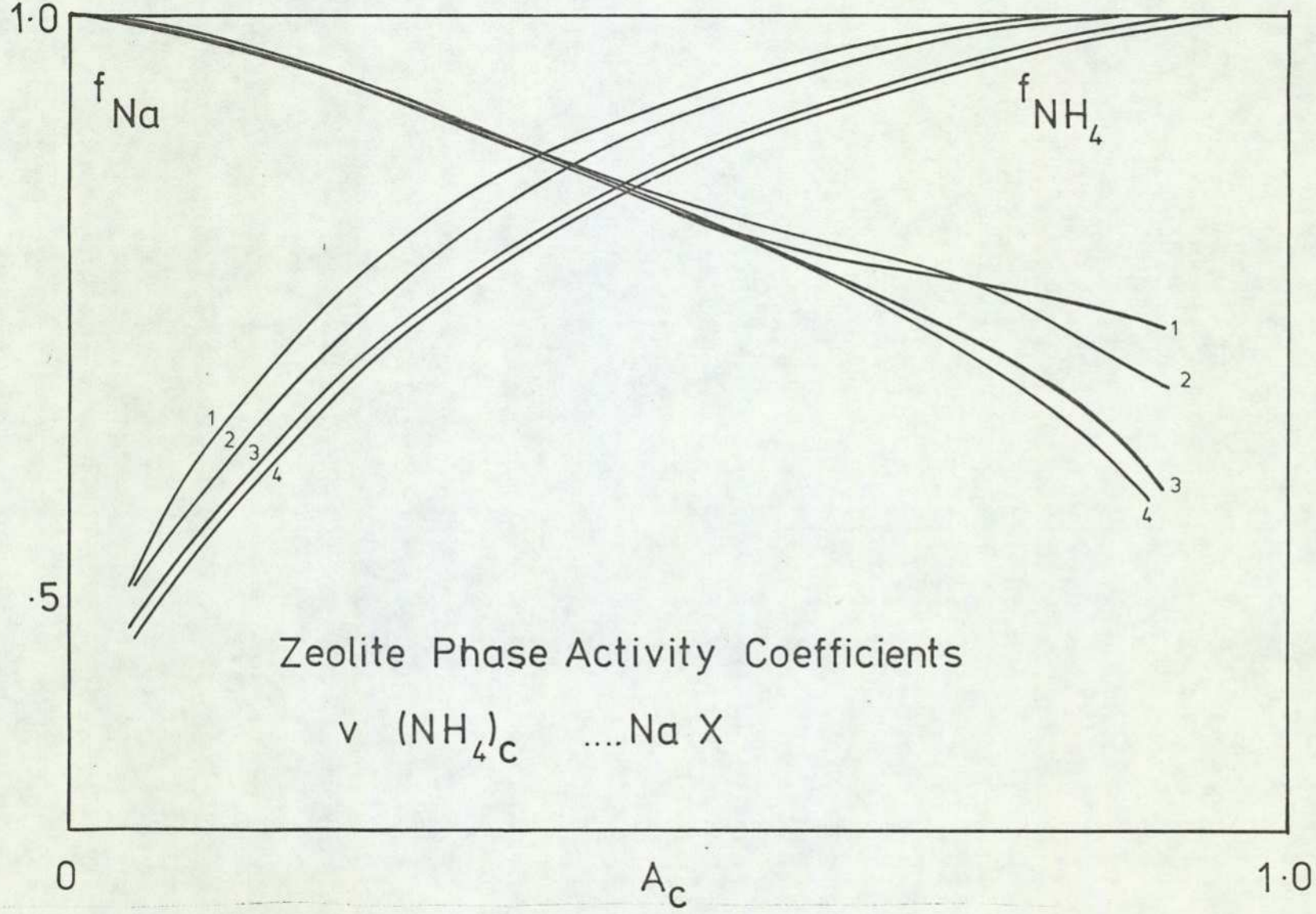


| N° | $A_c$ max |
|---|---|
| 1 | 0·715 |
| 2 | 0·72 |
| 3 | 0·735 |
| 4 | 0·74 |

Figure 3.11

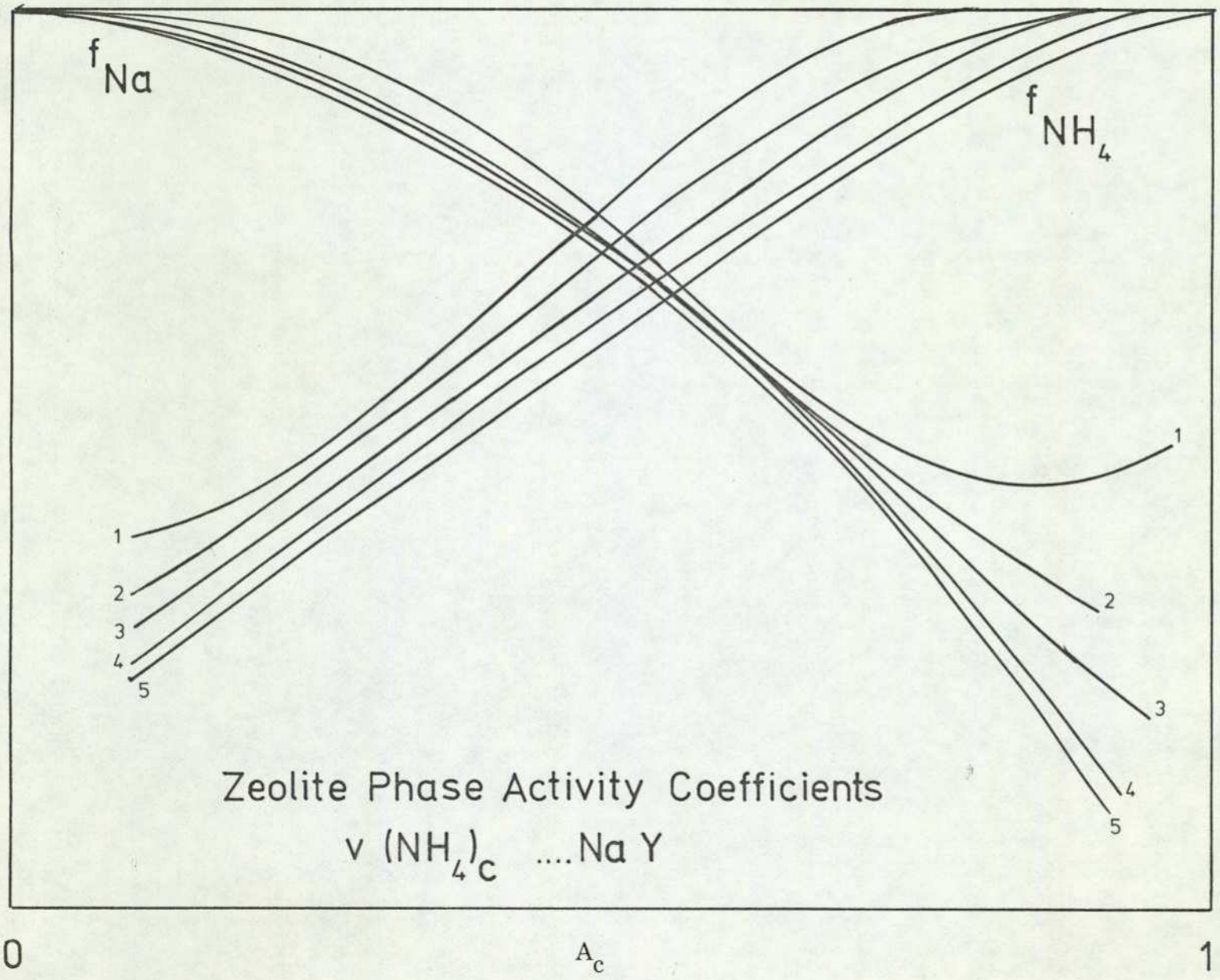


| N° | $A_c$ max |
|---|---|
| 1 | 0·69 |
| 2 | 0·70 |
| 3 | 0·71 |
| 4 | 0·72 |
| 5 | 0·725 |

Figure 3.12

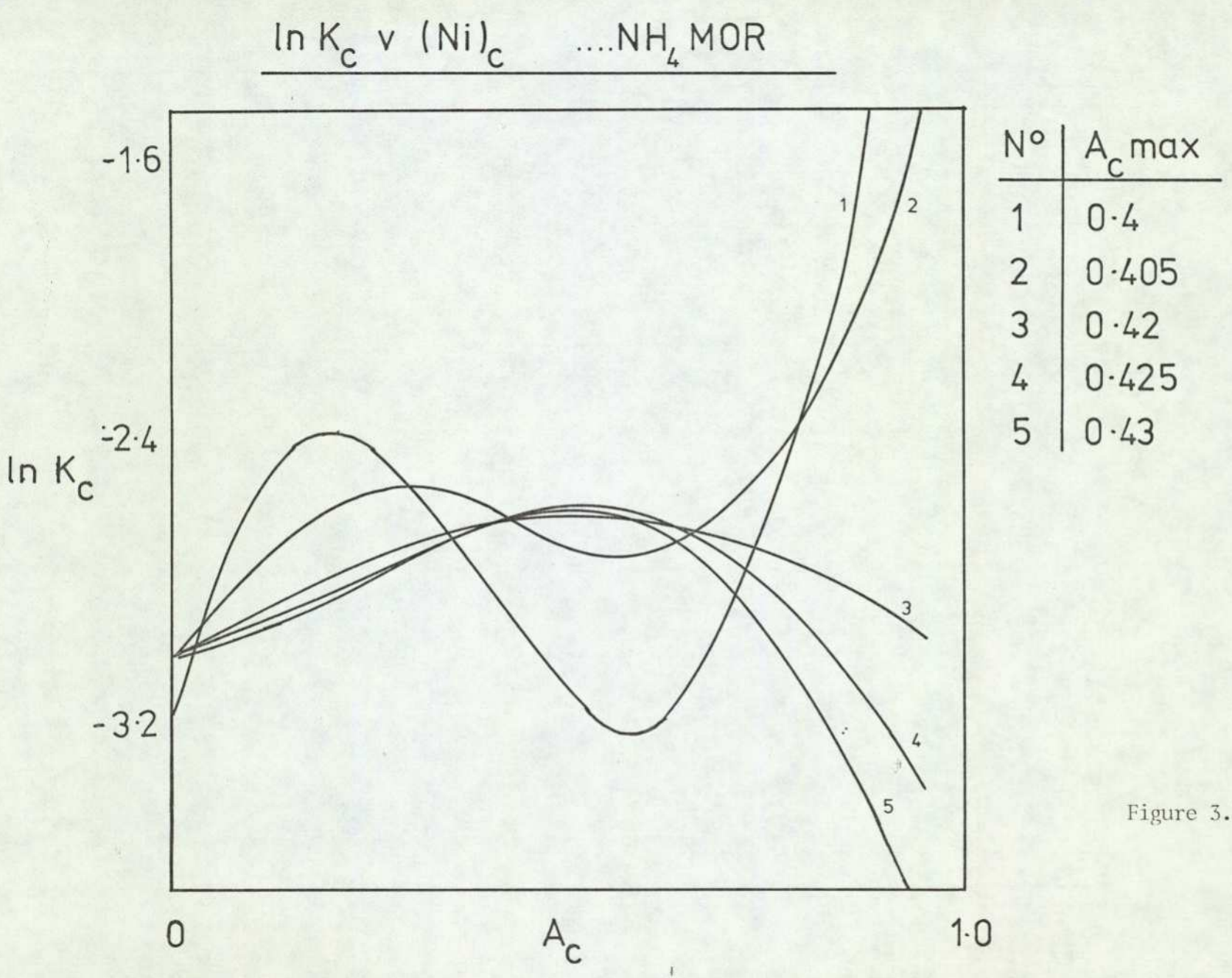
ln $K_c$ v $(Ni)_c$ ....$NH_4$ MOR
-1·6
-2·4
-3·2
ln $K_c$
0
$A_c$
1·0
1
2
3
4
5
N° | $A_c$ max
1 | 0·4
2 | 0·405
3 | 0·42
4 | 0·425
5 | 0·43

Figure 3.13

Zeolite Phase Activity Coefficients v $Ni_{(c)}$...$NH_4$ MOR

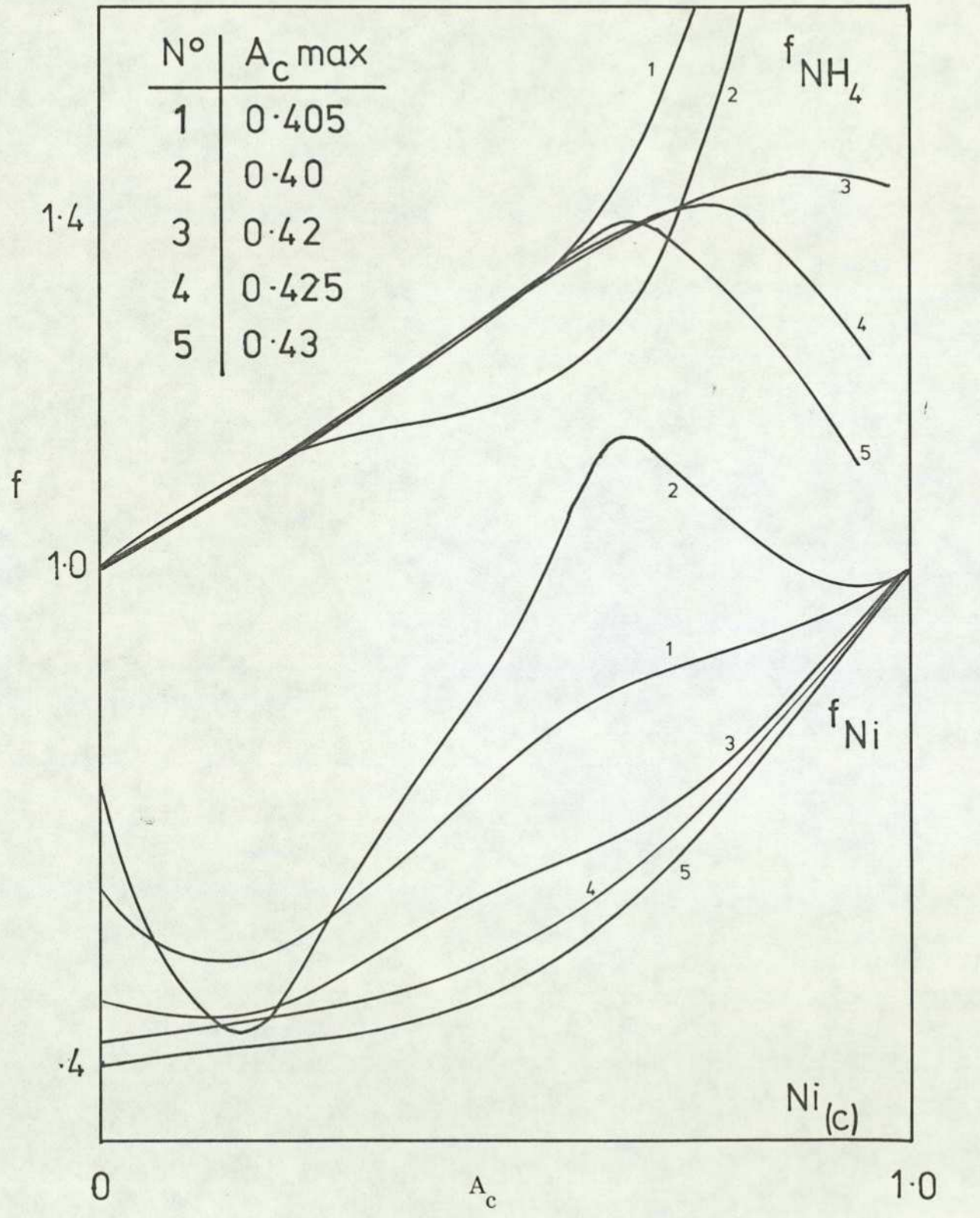


Figure 3.14

for the mordenite system is published elsewhere[65]. Values of $\Delta G^{\ominus}$ and $K_a$ as a function of $A_c(max)$ are given in table 3.7. Kielland plots and plots of $f_A$ and $f_B$ against $A_c$ corresponding to the data in table (3.7.) are given in figures (3.9.) to (3.14.).

3.6.1.1.1. The Systems $NH_4 \rightleftharpoons Na$ in X and Y.

Kielland plots for both X and Y, figures (3.9) and (3.10.) exhibit changes in the values of $\ln K_c$ at given values of $A_c$ if $A_c(max)$ is varied. The most dramatic changes occur in the region $A_c \rightarrow A_c(max)$; in this region $B_c$ is, of course, tending to zero. The variation in Kielland plots with $A_c(max)$ tends to be less marked in the region $0.5 > A_c > 0$. for both zeolite systems. In addition, the effect of varying $A_c(max)$ seems to be more marked in Y than in X. It should be noted, however, that there is a much greater "statistical spread" of data points and hence more ambiguity about the position of the Kielland plots for the $NH_4 \rightleftharpoons Na$/Y system than with X.

Thus the greater variability of the Kielland plots in Y may in part reflect the way the polynomial equations used to "fit" the data accommodated for the ambiguity in the data.

The divergence of the Kielland plots can be simply rationalised by considering the functions involved.

$$K_m = \frac{A_c^{ZB} \cdot m_B^{ZA}}{B_c^{ZA} \cdot m_A^{ZB}}$$

where $K_m$ is the mass action quotient, for the given solution concentrations $m_A$ and $m_B$. In this case $Z_A = Z_B = 1$.

Now since

$$K_c = K_m \cdot \Gamma \qquad 1.230$$

and because the solution phase components do not change with $A_c(max)$, changes in $A_c(max)$ can only affect $K_c$ through $A_c$ and $B_c$. However, very small changes in $A_c(max)$ can markedly change $K_m$ as is demonstrated in the following arguement.

Figure 3.15

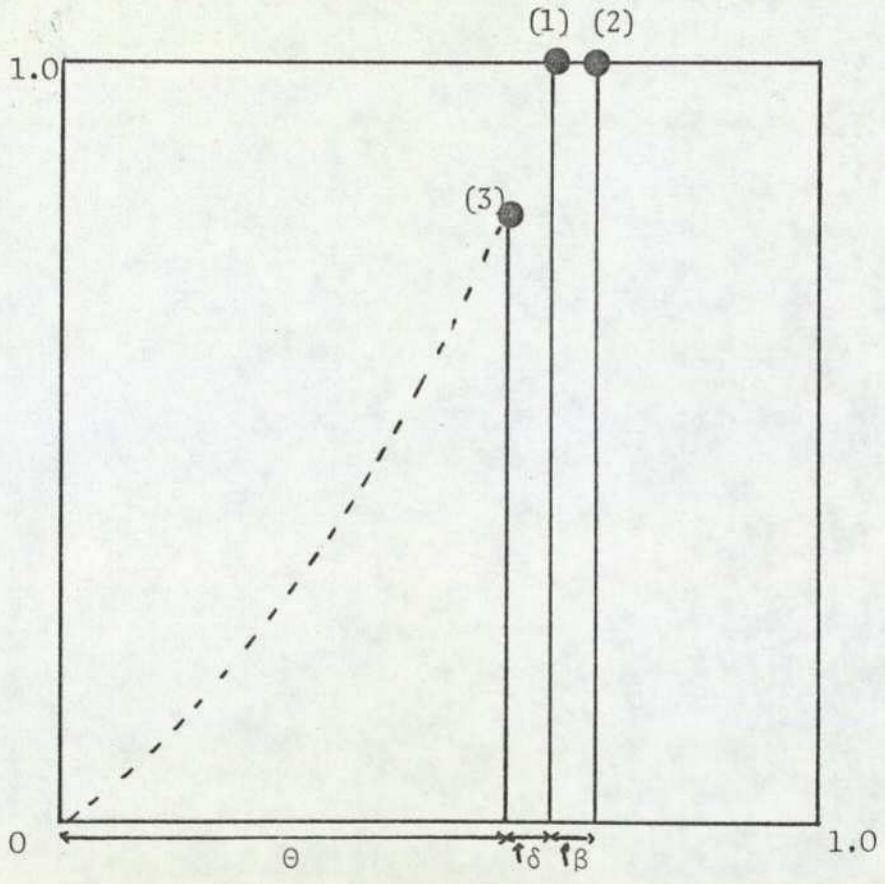


Consider an experimental isotherm point, depicted by point (3) on the above hypothetical isotherm (figure 3.15), and let the limits of

uncertainty in $A_c(max)$ be delineated by points (1) and (2). Then

$$A_c(1) = \frac{\Theta}{\Theta + \delta} \qquad \text{and} \qquad A_c(2) = \frac{\Theta}{\Theta + \delta + \beta}$$

If in this case the uncertainty in $A_c(max)$ is small then $(\Theta + \delta + \beta) \rightarrow (\Theta + \delta)$ and the two values of $A_c$ are similar, and $A_c$ varies only slightly with any change in $A_c(max)$. However,

$$B_c(1) = \frac{\delta}{\delta + \Theta} \qquad \text{and} \qquad B_c(2) = \frac{\delta + \beta}{\delta + \Theta + \beta}$$

and if $\beta$ and $\delta$ are both small and of the same order of magnitude (which is the case in a real system when $A_c \rightarrow A_c(max)$), the values of $B_c$ can vary enormously. It is possible to reach the situation where the change in $B_c$ brought about by a small change in $A_c(max)$ is greater than the original value of $B_c(1)$. Then it follows that $K_m$ and also $K_c$ will change very markedly. The main point is, however, that any decrease in the value of $A_c(max)$ will lead to an overall decrease in the values of $B_c$ and an increase in the corresponding $K_c$. This effect is most marked in the region $A_c \rightarrow A_c(max)$.

Changes in the values of $f_A$ and $f_B$ (figures (3.11.) and (3.12.) follow a similar pattern to that observed for $K_c$ (figures (3.9.) and (3.10). This is expected due to the fact that these functions are calculated from the best-fitting polynomial equation used to smooth the points of the Kielland plot.

Values of $f_A$ vary more than $f_B$ for different values of $A_c(max)$ over the whole range of $A_c$ values, except when $A_c \rightarrow A_c(max)$, where $f_B$ shows very large fluctuations. In general $f_A$ and $f_B$ increase as $A_c(max)$ is decreased.

The variations in $f_A$ and $f_B$ can also be rationalised, by consideration of the following equations

$$\ln f_A^{ZB} = \underbrace{(Z_B - Z_A)B_c}_{1} \underbrace{- \ln K_c + A_c \ln K_c}_{2} + \underbrace{\int_{A_c}^{A_c = A_c(max)=1} \ln K_c dA_c}_{3} \qquad 3.240$$

For uni-univalent exchange term (1) of the equation is zero. Also, as explained above, values of $\ln K_c$ become more positive as the value of $A_c(max)$ is reduced. Hence, term (2) of the equation becomes more negative as the value of $A_c(max)$ is reduced, since it must be true that $\ln K_c > A_c \ln K_c$. In contrast, term (3) of equation (3.240) must show an overall increase in its value as $\ln K_c$ becomes more positive (i.e. $A_c(max)$ decreases). The important point is that in this term the integration involves the whole Kielland plot from $A_c \rightarrow A_c(max)$ and will result in a large increase in the value of the integral at low values of $A_c$, hence we observe the increases in $f_A$, with decreasing $A_c(max)$, are not restricted to the region $A_c \rightarrow A_c(max)$.

$$\ln f_B^{ZA} = \underbrace{-(Z_B - Z_A)A_c}_{1} \underbrace{+ A_c \ln K_c}_{2} \underbrace{- \int_0^{A_c} \ln K_c dA_c}_{3} \qquad 3.250$$

Term (1) of this relationship will show a very slight decrease in its value as $A_c$ increases slightly with decreasing $A_c(max)$. Term (2) should reflect an overall increase in its value as both $A_c$ and $\ln K_c$ increase with decreasing $A_c(max)$. Term (3) will show a decrease in its value as the value of the integral becomes more positive with decreasing $A_c(max)$. The overall effect appears to be dominance by term (2) over term (3) (figures (3.11) and 3.12) as shown by a general increase in the value of $f_B$ with increasing $\ln K_c$. It is important to note that both terms (2) and (3) will only significantly change when the value of $A_c$ is such that

there is a large change in $\ln K_c$ (upon changing $A_c(max)$) and consequently these terms are only significant in the region $A_c \rightarrow A_c(max)$.

### 3.6.1.1.2. $Ni^{2+} \rightleftharpoons NH_4$ Exchange in Mordenite.

Dramatic changes are observed in this Kielland plot upon varying $A_c(max)$ (figure (3.13)). Changes occur throughout the whole range of $A_c$, but they are especially noticeable in the region where $A_c \rightarrow 1$. This can be explained by the same considerations as were given to the $NH_4^+ \rightleftharpoons Na^+$ exchange in X and Y above (section 3.6.1.1.). However, a significant difference is that in uni-divalent exchange the Kielland quotient is a function of $B_c^2$. Consequently any changes in $B_c$ cause greater changes in $\ln K_c$ than those observed in uni-univalent exchange. Large changes are also observed at low values of $A_c$, and again these changes are much greater than those observed for the simple uni-univalent systems. These may reflect the high sensitivity of the function $\ln K_c$ has for changes in $A_c$ and may also reflect the way the polynomial expression accommodates for data having a high 'spread' due to experimental variation in the isotherm points. As with the Kielland plot, the values of $f_A$ and $f_B$ similarly vary very markedly as $A_c \rightarrow A_c(max)$. At low levels of $A_c$, values of $f_B$ are far less dependent on changes in $A_c(max)$ than are values of $f_A$, behaviour which can again be rationalised by the same approach as used in section 3.6.1.1.1.

### 3.6.1.1.3. Trends in $\Delta G^\ominus$ and $K_a$

Figures (3.9.), (3.10.) and (3.13.) show that reducing $A_c(max)$ to the lower limit of uncertainty leads to an overall increase in $K_c$. Then

the function $\int_0^1 \ln K_c \, dA_c$ must become more positive, and this gives a larger value for the true thermodynamic equilibrium constant $K_a$ and hence a more negative value for the standard free energy. This trend is seen with all systems (table 3.7.)

The Kielland plot for the $NH_4^+ \rightleftharpoons Na^+/X$ system (figure 3.10.) shows that shifts from positive values at low $A_c$ through to negative values as $A_c \rightarrow A_c(max)$. When this is the case, any error in the calculation of $\ln K_c$ as a function of $A_c$ can have very large effects on the final computed value of $\Delta G^\ominus$. This is because in these cases the function $\int_0^1 \ln K_c dA_c$ is a summation of a positive and negative area, and these two areas are of comparable magnitude. Thus $\int_0^1 \ln K_c dA_c \sim 0$, and $K_a$ approaches unity. In the $NH_4^+ \rightleftharpoons Na^+/X$ system $K_a \sim 1.1 \pm 0.8$ for the range of $A_c(max)$ values chosen (i.e. a change of $\pm$ 8%). However, because $K_a \sim 1$, the effect of varying $K_a$ by only $\pm$ 8% results in a change in $\Delta G^\ominus$ of $\pm$ 200%. In contrast the Kielland plot for $NH_4 \rightleftharpoons Na/Y$ gives positive values for $\ln K_c$ over the whole range of $0 < A_c < 1$. Again, the variation in $\ln K_c$ as $A_c(max)$ is changed is $\sim \pm$ 8%, but because the integral is no longer a sum of two values of opposite sign and similar magnitude, this system shows a much smaller change in $\Delta G^\ominus$ (approximately 2.1 $\pm$ 0.3 kJ g equiv.$^{-1}$). The $Ni^{2+} \rightleftharpoons NH_4^+$ exchange in mordenite however shows a more marked change; $K_a$ increases by $\sim$50% when $A_c(max)$ is varied by about 6%. Owing to the low value of $K_a$ in this case, and the logarithmic dependence of $\Delta G^\ominus$ on $K_a$, the change in $\Delta G^\ominus$ is, however, only 10%.

These data demonstrate the marked dependence of $\Delta G^\ominus$ on the value of $K_a$ and emphasise the importance of accurately determining $A_c(max)$, and the dangers inherent in uncritically comparing $\Delta G^\ominus$ values obtained

from complementary studies by different workers. It should be noted that the variation of $A_c$(max) involved in this survey is larger than should be observed under experimental conditions. Certainly, the highest and lowest values of $A_c$(max) used in this exercise would not be consistent with the shapes of the experimental isotherms. It does however, point out the critical nature of the correct determination of the maximum level of ion exchange, and the consequent need for care in interpretation and use of the functions $K_c$, $f_A$ and $f_B$.

3.6.1.2. The Curve-Fitting Procedure.

A second and possibly no less significant cause of error is the curve-fitting procedure applied to the isotherm and its effect upon the derived thermodynamic functions. This effect was shown by an analysis of data on the $Ni^{2+} \rightleftharpoons NH_4^+$ exchange in mordenite as found in a previous study[65]. Two curve-fitting procedures were followed.

Method 1. - This method was employed by Barrer and Townsend[65] to smooth the original isotherm data, and involved best fitting a polynomial equation of the form $y = A_0 + A_1x + A_2x^2 + ..A_nx^n$, and assigning $y = A_s$ and $x = A_c$.

Method 2. - This involved best-fitting the polynomial equation as in method 1, but reversing the assignments. The smoothed and corrected data were analysed by CABIEZ using the same level of $A_c$(max), equal to 0.416 for each case. The difference in the derived thermodynamic functions for both cases is indicated in table 3.7., and figure (3.16). The kielland plots for the two cases vary considerably and it would be expected that the values of $f_A$ and $f_B$ would vary similarly.

However, both $\Delta G^{\ominus}$ and $K_a$ change little with the change in curve-fitting procedure. The implication is that the overall shape of the Kielland plot is not the most important factor in the determination of $\Delta G^{\ominus}$, but rather it is its position with respect to the zero axis that matters. Why the two curve-fitting procedures give different results is less obviously rationalised than the effect of varying $A_c(max)$, but it is obviously of some consequence if it is desired to interpret or make use of the functions $f_A$ and $f_B$.

The experimental data expressed in chapter 4 is interpreted within the constraints imposed by the observable experimental variation as exhibited in this chapter.

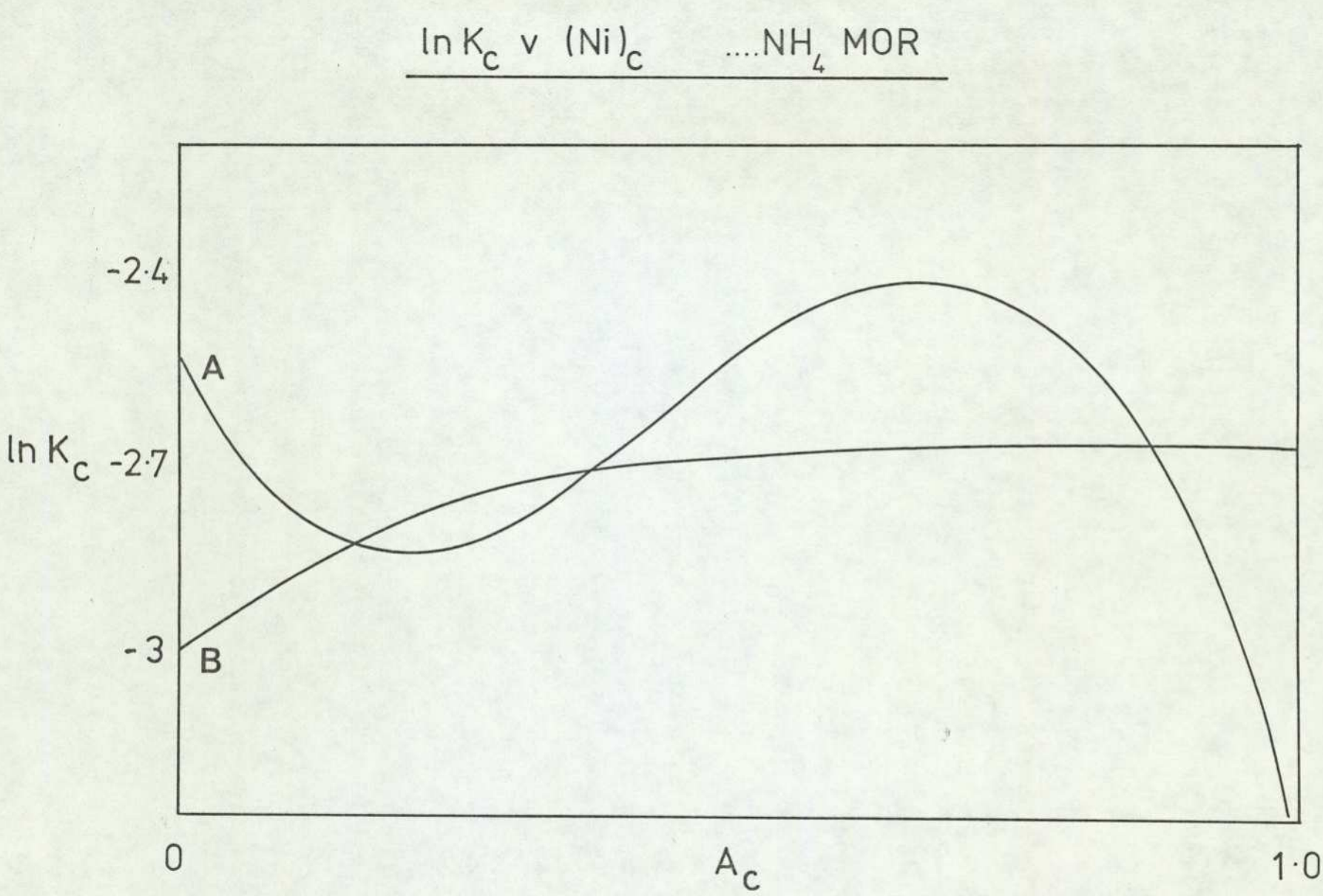


Figure 3.16

CHAPTER FOUR RESULTS

4.1. ANALYSES OF ZEOLITES

4.1.1. Ammonium Exchange Zeolites (Exchanged at 70°C)

4.1.2. Sodium Zeolites

4.1.3. Transition Metal Exchange Zeolites

4.1.4. Platinum and Palladium Zeolites

4.2. ION EXCHANGE ISOTHERMS

4.3. ISOTHERMS AND DERIVED DATA

4.3.1. Uni-Univalent Exchange

4.3.2. Uni-Divalent Exchange

4.4. FURTHER REVERSIBILITY TESTS ON TRANSITION METAL EXCHANGE IN X AND Y

4.5. ION SITE REDISTRIBUTION

4.6. X RAY DATA

RESULTS

Ion exchange and analytical data are detailed under three headings in this chapter: the composition of maximally exchanged zeolites, the exchange isotherms and the derived thermodynamic data.

## 4.1. (1) Analyses of Zeolites

Complete chemical analyses were performed on the ammonium exchanged forms of the sodium zeolites X, Y and MOR after repeated exchanges at 70°C. These data are detailed in table 4.1. After subsequent transition metal ion exchange using the ammonium zeolites (or in the case of exchange with $\left[Pt(NH_3)_4\right]^{2+}$, $\left[Pd(NH_3)_4\right]^{2+}$, $\left[Ag(NH_3)_2\right]^{+}$ and $Ag^{+}$, the sodium zeolites) the analytical procedures described in section 2.4. were used to analyse the following cationic forms.

| X | Y | MOR |
|---|---|---|
| Cu | Cu | Ag |
| Zn | Ni | $Ag(NH_3)_2$ |
| Mn | Zn | $Pd(NH_3)_4$ |
| Ni | Mn | $Pt(NH_3)_4$ |
| Co | Co | |
| Ag | Ag | |
| $Ag(NH_3)_2$ | $Ag(NH_3)_2$ | |
| $Pd(NH_3)_4$ | $Pd(NH_3)_4$ | |
| $Pt(NH_3)_4$ | $Pt(NH_3)_4$ | |

These data are shown in tables 4.6. to 4.14 inclusive

Experiments with the cations $[Pt(NH_3)_4]^{2+}$; $[Pd(NH_3)_4]^{2+}$; $Ag^+$ and $[Ag(NH_3)_2]^+$ were carried out using different batches of zeolites X and Y to those used for exchange of the first row transition metal ions. Due to incomplete exchange of sodium ion with ammonium ions in those zeolites at 25°C (figures 4.1. and 4.2.), ion exchange experiments with the platinum, palladium and silver ions were performed using the sodium exchanged form of the zeolites X and Y and also MOR. Analyses for the maximally exchanged forms of these transition metal zeolites are shown in tables 4.11 to 4.14 inclusive. Determinations of the water contents of $Pt(NH_3)_4$ and $Pd(NH_3)_4$ exchanged forms of X and Y and MOR were not carried out due to the very limited quantity of precious metal exchanged zeolite that was available for destructive chemical analyses.

4.1.1. Analysis of Ammonium Exchanged Zeolites (Exchanged at 70°C)

The analytical data are expressed below as an oxide formula. (See also table 4.1. overleaf).

$NH_4$/Na X

$0.251\ Na_2O.\ 0.723(NH_4)_2O.\ Al_2O_3\ .\ 2.67SiO_2\ .\ 5.57H_2O$

$NH_4$/Na Y

$0.0832(Na_2O).\ 0.942(NH_4)_2O.\ Al_2O_3\ .\ 4.772(SiO_2).\ 0.092(Fe_2O_3).\ 6.942(H_2O)$

$NH_4$ MOR

$0.006\ Na_2O.\ 0.972Na_2O.\ Al_2O_3.\ 11.16SiO_2.\ 6.791H_2O$

Table 4.1. shows that incomplete exchange of sodium by ammonium ion occurred in zeolites X and Y. The ion exchange capacities of all three zeolites and their levels of ion exchange with respect to ammonium ion are detailed in table 4.2.

Table 4.1 Analyses of Ammonium Exchanged Zeolites

| Zeolite | X | | Y | | MDR | |
|---|---|---|---|---|---|---|
| Component | % | mol/100g | % | mol/100g | % | mol/100g |
| $SiO_2$ | 38.41 | 0.6402 | 50.57 | 0.8428 | 71.45 | 1.191 |
| $Al_2O_3$ | 24.42 | 0.2394 | 18.102 | 0.1766 | 10.89 | 0.1067 |
| $Fe_2O_3$ | 0.08 | 0.0005 | 0.26 | 0.00163 | 0.09 | 0.0005 |
| $NH_4$ | 6.22 | 0.3455 | 5.88 | 0.3266 | 3.76 | 0.2061 |
| $(NH_4)_2O$ | 8.99 | 0.1728 | 8.49 | 0.1633 | 5.39 | 0.1037 |
| Na | 2.86 | 0.120 | 0.68 | 0.03 | 0.029 | 0.00126 |
| $Na_2O$ | 3.85 | 0.0628 | 0.916 | 0.0147 | 0.037 | 0.00063 |
| $H_2O$ | 24.02 | 1.334 | 22.067 | 1.226 | 12.32 | 0.7247 |
| Total | 99.75% | | 100.59% | | 100.15% | |

Exchange Levels and capactites of Ammonium Exchanged Zeolites

| Zeolite | $NH_4$-X | $NH_4$-Y | $NH_4$-MOR |
|---|---|---|---|
| Ion Exchange Capacity/meq $g^{-1}$ | 4.79 | 3.53 | 2.134 |
| Maximum level of ion exchange w.r.t. $NH_4^+$ | 0.723 | 0.9246 | 0.972 |

These data (tables 4.1. and 4.2.) show the usual inconsistencies inherent in the experimental techniques used. Reasonable consistency for the

ammonium and sodium components of all three zeolites is obtained. There is a slight variation between the sum of the total number of equivalents of ammonium plus sodium amd the number of equivalents of aluminium per unit cell for all three zeolites. It may be that a small amount of ion exchanged hydronium ion was present in the sample of $X^{96}$, though this could not be more than 2.5% of the total exchange capacity. Zeolite Y shows a slightly higher value for the total exchangeable component than the zeolite exchange capacity; however, the deviations are within experimental error in all cases.

Table 4.3 Exchangeable components of $NH_4$-X prepared by various methods

| Preperative conditions | $NH_{4(c)}$ | $Na_{(c)}$ | Estimated $H_3O^+_{(c)}$ |
|---|---|---|---|
| Section 2.5. Method 1 | 0.832 | 0.151 | 0.026 |
| Section 2.5. Method 2 | 0.856 | 0.043 | 0.101 |

### 4.1.2. Analysis of the Sodium Zeolites

These analyses (table 4.4.) show the chemical composition of the second batch of sodium zeolite samples used. In addition, the sodium exchanged form of mordenite which was analysed previously in the ammonium form (table 4.1.), is included. The data in table 4.4. are expressed below as oxide formulae.

Na X

$0.9987(Na_2O).\ Al_2O_3\ .\ 2.533\ SiO_2.\ 5.93SiO_2$

NaY

$0.988(Na_2O).\ 2.97\times10^{-3}(Fe_2O_3).\ Al_2O_3.\ 4.294(SiO_2).\ 7.89H_2O$

Na MDR

$1.01(Na_2O).\ 5.38\times10^{-3}(Fe_2O_3).Al_2O_3.\ 11.028(SiO_2).\ 6.93H_2O$

Table 4.4 Analyses of Sodium Zeolites

| Zeolite | X | | Y | | MDR | |
|---|---|---|---|---|---|---|
| Component | % | mol/100g | % | mol/100g | % | mol/100g |
| $SiO_2$ | 36.01 | 0.600 | 45.43 | 0.7572 | 69.56 | 1.159 |
| $Al_2O_3$ | 24.17 | 0.2369 | 18.171 | 0.1782 | 10.72 | 0.1051 |
| $Fe_2O_3$ | 0.00 | | 0.084 | $3.28\times10^{-4}$ | 0.09 | $5.66\times10^{-4}$ |
| Na | 10.88 | 0.4732 | 8.18 | 0.3556 | 4.88 | 0.2339 |
| $Na_2O$ | 14.66 | 0.2366 | 11.04 | 0.1778 | 6.58 | 0.1061 |
| $H_2O$ | 25.34 | 1.4077 | 25.31 | 1.406 | 13.12 | 0.7288 |
| Total | 100.21% | | 99.95% | | 99.98% | |

Table 4.5 Ion Exchange Capacities

| Zeolite | Capacity/meq.$g^{-1}$ | $SiO_2/Al_2O_3$ |
|---|---|---|
| Na X | 4.74 | 2.533 |
| Na Y | 3.56 | 4.249 |
| Na MDR | 2.104 | 11.028 |

These results (tables 4.4. and 4.5.) show reasonable correlation between the $Al_2O_3$ and $Na_2O$ components in all cases. Mordenite appears to have a slightly higher number of equivalents of sodium than aluminium per unit cell but the $SiO_2$:$Al_2O_3$ ratio is consistent with that obtained for analyses of $NH_4$-MOR.

### 4.1.3. Analysis of 1st Row Transition Metal Exchanged Zeolites (Initially $NH_4$(Na-X and -Y).

Total analyses of the transition metal exchanged zeolites were performed using methods described previously (section 2.4.2.). It was assumed that in all cases substantial dealumination did not occur, and consequently the $Al_2O_3$ component was determined by assuming that the $SiO_2/Al_2O_3$ ratio remained unchanged on exchange.

Table 4.6 Analyses of Transition Metal Exchanged Y.

| Exchanged form | Co Y | | Ni Y | | Cu Y | |
|---|---|---|---|---|---|---|
| Compnent | % w/w | mol/100g | % w/w | mol/100g | % w/w | mol/100g |
| $SiO_2$ | 46.39 | 0.7732 | 46.82 | 0.7803 | 46.21 | 0.7702 |
| $Al_2O_3$ | 16.613 | 0.1483 | 16.75 | 0.1642 | 16.54 | 0.1622 |
| $Fe_2O_3$ | 0.25 | 0.00157 | 0.25 | 0.00157 | 0.25 | 0.00157 |
| MO | 7.58 | 0.1010 | 8.496 | 0.1133 | 9.39 | 0.1183 |
| $(NH_4)_2O$ | 1.72 | 0.0331 | 1.936 | 0.0372 | 0.00 | 0.000 |
| $Na_2O$ | 0.679 | 0.0109 | 0.798 | 0.0130 | 0.00 | 0.000 |
| $H_2O$ | 27.25 | 1.514 | 25.13 | 1.396 | 27.86 | 1.5478 |
| Total | 100.48 % | | 100.15% | | 100.25% | |

Table 4.7 Analyses of Transition Metal Exchanged Y

| Exchanged form | Zn Y | | Mn Y | |
|---|---|---|---|---|
| Component | % w/w | mol/100g | % w/w | mol/100g |
| $SiO_2$ | 45.64 | 0.7606 | 49.31 | 0.8215 |
| $Al_2O_3$ | 16.48 | 0.1620 | 17.64 | 0.1729 |
| $Fe_2O_3$ | 0.25 | 0.00157 | 0.25 | 0.00157 |
| MO | 10.27 | 0.1267 | 9.29 | 0.1297 |
| $(NH_4)_2O$ | 1.41 | 0.0271 | 1.646 | 0.0315 |
| $Na_2O$ | 0.710 | 0.0113 | 0.738 | 0.0119 |
| $H_2O$ | 25.91 | 1.439 | 21.454 | 1.1918 |
| Total | 100.67% | | 100.33% | |

Table 4.8 Analyses of Transition Metal Exchanged X

| Exchanged form | Co X | | Ni X | | Cu X | |
|---|---|---|---|---|---|---|
| Component | % w/w | mol/100g | % w/w | mol/100g | % w/w | mol/100g |
| $SiO_2$ | 35.32 | 0.5886 | 34.00 | 0.582 | 33.55 | 0.5592 |
| $Al_2O_3$ | 22.45 | 0.2200 | 22.158 | 0.2172 | 21.33 | 0.2091 |
| $Fe_2O_3$ | 0.07 | 0.0004 | 0.07 | 0.0004 | 0.07 | 0.0004 |
| MO | 12.38 | 0.1650 | 11.56 | 0.162 | 13.11 | 0.1652 |
| $(NH_4)_2O$ | 0.98 | 0.0188 | 1.9 | 0.0367 | 0.00 | 0.0000 |
| $Na_2O$ | 1.10 | 0.0177 | 2.19 | 0.0353 | 0.00 | 0.0000 |
| $H_2O$ | 28.29 | 1.571 | 27.33 | 1.516 | 31.96 | 1.7756 |
| Total | 100.05% | | 100.108% | | 100.02% | |

Table 4.9 Analyses of Transition Metal Exchanged X

| Exchanged form | Mn X | | Zn X | |
|---|---|---|---|---|
| Component | % w/w | mol/100g | % w/w | mol/100g |
| $SiO_2$ | 36.02 | 0.602 | 34.33 | 0.5722 |
| $Al_2O_3$ | 22.90 | 0.2245 | 21.8 | 0.2137 |
| $Fe_2O_3$ | 0.07 | 0.0004 | 0.07 | 0.0004 |
| MO | 12.98 | 0.1828 | 14.22 | 0.1746 |
| $(NH_4)_2O$ | 1.25 | 0.024 | 1.47 | 0.0282 |
| $Na_2O$ | 0.73 | 0.0118 | 0.703 | 0.0113 |
| $H_2O$ | 26.02 | 1.446 | 27.64 | 1.535 |
| Total | 99.97 % | | 100.23 % | |

Table 4.10 Analyses of Amminated Copper(II) Exchanged Zeolites

| Exchanged form | $Cu(NH_3)_4$ X | | $Cu(NH_3)_4$ Y | |
|---|---|---|---|---|
| Component | % w/w | mol/100g | % w/w | mol/100g |
| $SiO_2$ | 35.22 | 0.587 | 45.53 | 0.7588 |
| $Al_2O_3$ | 22.39 | 0.2195 | 16.29 | 0.1597 |
| $Fe_2O_3$ | 0.07 | | 0.25 | 0.00157 |
| CuO | 10.21 | 0.1275 | 9.28 | 0.1168 |
| $(NH_4)_2O$ | 1.812 | 0.0348 | 1.495 | 0.0287 |
| $NH_3$ | 3.58 | 0.21 | 4.17 | 0.245 |
| $Na_2O$ | 3.40 | 0.0548 | 0.887 | 0.0143 |
| $H_2O$ | 22.99 | 1.174 | 22.28 | 1.114 |
| Total | 99.62% | | 100.19% | |

Table 4.11. Analyses of Silver Exchanged Zeolites

| Exchanged form | Ag X | | Ag Y | | Ag MOR | |
|---|---|---|---|---|---|---|
| Component | % w/w | mol/100g | % w/w | mol/100g | % w/w | mol/100g |
| $SiO_2$ | 25.43 | 0.4238 | 33.58 | 0.5597 | 59.62 | 0.9936 |
| $Al_2O_3$ | 17.08 | 0.1675 | 13.44 | 0.1317 | 9.21 | 0.0903 |
| $Fe_2O_3$ | 0.00 | 0.00 | 0.08 | $5.12z10^{-4}$ | 0.08 | $5.12x10^{-4}$ |
| $Ag_2O$ | 38.83 | 0.1676 | 30.53 | 0.1317 | 18.63 | 0.0803 |
| $Na_2O$ | 0.00 | 0.00 | 0.00 | 0.00 | 0.615 | 0.0099 |
| $H_2O$ | 18.62 | 1.0344 | 22.43 | 1.246 | 11.91 | 0.6616 |
| Total | 99.96 | | 100.08 | | 100.06 | |

Table 4.12 Analyses of Silver Diammine Exchanged Zeolites

| Exchanged form | $Ag(NH_3)_2$ X | | $Ag(NH_3)_2$ Y | | $Ag(NH_3)_2$MOR | |
|---|---|---|---|---|---|---|
| Component | % w/w | mol/100g | % w/w | mol/100g | % w/w | mol/100g |
| $SiO_2$ | 30.55 | 0.5092 | 39.25 | 0.6538 | 62.37 | 1.0395 |
| $Al_2O_3$ | 20.36 | 0.1996 | 15.69 | 0.1538 | 9.63 | 0.0942 |
| $Fe_2O_3$ | 0.00 | 0.00 | 0.08 | $5.12x10^{-4}$ | 0.08 | $5.12x10^{-4}$ |
| $Ag_2O$ | 26.415 | 0.1139 | 19.62 | 0.0845 | 16.34 | 0.0707 |
| $NH_3$ | 3.97 | 0.2335 | 5.25 | 0.309 | 2.34 | 0.1376 |
| $Na_2O$ | 5.35 | 0.0863 | 4.28 | 0.0690 | 1.46 | 0.0235 |
| $H_2O$ | 13.59 | 0.755 | 15.94 | 0.8839 | 7.84 | 0.4344 |
| Total | 100.06 | | 100.12 | | 100.07 | |

The analytical data for the first row transition metals in both $NH_4$-X and $NH_4$-Y indicate slight annomalies in some cases. Ion exchange of hydrated copper(II) into both zeolites indicated complete removal of the sodium amd ammonium content of the zeolite without obtaining 100% occupancy of the zeolite with copper ions.

The same situation arose, to a lesser extent, in the exchange of cobalt(II) into $NH_4$-X. In this case $3.08 \times 10^{-1}$ g equiv. $hg^{-1}$ of ammonium and $0.9 \times 10^{-1}$ g equiv. $hg^{-1}$ of sodium are removed upon exchanging with the $Co(H_2O)_6^{2+}$ ion, yet only $3.65 \times 10^{-1}$ g equiv. $hg^{-1}$ of cobalt (II) are found in the zeolite. This is equivalent to 83% of the original sodium and ammonium ions being removed and replaced by only 76% cobalt(II). A reverse effect is noticed with exchange of nickel(II) into X, where the ingoing nickel component appears to exceed the total sodium and ammonium component being removed. This is seen in that the total number of moles of ion exchangeable component per 100 g of zeolite was somewhat greater than the number of moles per 100g of $Al_2O_3$ (table 4.8.).

The exchange isotherm for manganese(II) in Y (figure 4.13) shows a marked change in selectivity at high manganese loadings, resulting in a marked inflexion in the isotherm. Slight irreversibility was observed in this region, and it was suspected that precipitation of manganese basic salts may have occurred. However, the analytical data (table 4.7.) indicates good agreement between the manganese exchanged into the zeolite and the sodium and ammonium replaced.

In the case of ion exchange of zinc(II) in both faujasite type zeolites the indications are that slightly more zinc has been introdu-

ced into the zeolite than would be expected on the basis of the quantity of sodium and ammonium removed. However, these data are verging on the limits of experimental error and it may be justifiable to conclude that within the limits of experimental detection, in all cases except Cu-X, Cu-Y, Ni-X and Co-X genuine ion exchange occurred.

Exchanging transition metals into $NH_4$-Y resulted in the remaining sodium in the zeolite being reduced in all cases except copper by about 15%. Since the residual sodium was only $\sim$ 7% of the total exchange capacity, this was equivalent to only $\sim$1% of the total ion exchange capacity of the zeolite. Thus for most cases the sodium involvement in the ion exchange process was nearly negligible. When zeolites were exchanged using copper as the chloride salt, substantial excess values of copper in the zeolite over that expected in terms of the alumina content was seen, indicating precipitation of basic copper chloride salts into the faujasite framework.

It is probable that in the cases of cobalt(II) exchange in X and for copper exchange in both X and Y, that hydronium exchange has occurred to some extent also, a phenomenon previously observed with zeolites X and Y[96]. Both these ions impose a more highly acidic reaction with the aqueous medium[65] than do either manganese or zinc.

With nickel exchange in X the situation is different. Precipitation of the basic salt has occurred during the preparative procedure (section 2.9.2.). The nickel salts used import a similar acidity to aqueous solutions as do the cobalt salts[65], consequently it may also be justifiable to suspect that simultaneous exchange of hydroxonium ions occurred into X and possibly Y when exchanging with nickel.

The analytical results for $Ag(NH_3)_2^+$ exchanged zeolites (table 4.12) show exchange of the amminated silver ion was accompanied by more ammonia being found in the zeolite than would be expected on the basis of the silver content. This may be explained by the washign process used prior to the zeolite analyses, which involved washing the zeolite with dilute ammonia solution (pH $\geq$10). In earlier attempts, washing with distilled water was found to cause the silver ammine ions to lose ammonia molecules, leading to the precipitation of brown silver oxide in the zeolite lattice in the case of all three zeolites. The washing and drying process later adopted, using ammonia solution, led to ammonia being sorbed as guest molecules within the zeolite.

Due to the maximum levels of exchange for silver aquo and silver ammine zeolites (tables 4.11 and 4.12) being estimated by analysing the number of moles of sodium removed, it was not possible to determine whether or not hydrolysis (in the case of $Ag^+(aq)$ or exchange of ammonium ions (in the case of $Ag(NH_3)_2^+$ ) had occurred. However, the maximum levels of exchange were in all cases, consistent with the shapes of the isotherms (determined by uptake of silver ions). Consequently it may be concluded that exchange of $H_3O^+$ of $NH_4^+$ was insignificant in these cases.

One noticeable feature of the analysis results for $Ag^+(aq)$ in the three zeolites was the decrease in the water content that occurred when sodium was replaced with silver ions. This effect is more marked in X than in Y due to the lower quantity of silver ions in the Y zeolite.

Table 4.10 shows that the exchanged copper ions in both X and Y had lower $Cu:NH_3$ ratios than would be expected. The results correspond

to the following stoichiometries:

X $Cu(NH_3)_{1.61}^{2+}$

Y $Cu(NH_3)_{2.11}^{2+}$

It was observed that upon equilibrating the dried copper ammine exchanged zeolites over saturated sodium chloride solutions both zeolites turned green over a period of around 15 days. This is undoubtedly explained by a gradual loss of complexed ammonia into the vapour phase above the zeolites, viz:

$$Cu(NH_3)_4 + xH_2O_{(v)} \rightleftharpoons Cu(NH_3)_{4-x}(H_2O)_x + NH_{3(v)}$$

This argument is substantiated by earlier observations [78] involving ion exchange of $Cu(NH_3)_4^{2+}$ into ammonium mordenite where a much lower ammonia loss was reported when the zeolite was equilibrated over saturated ammonium chloride solution. The existence of the ammonium-ammonia equilibrium in the ammonium chloride solution would cause some ammonia to be present in the vapour phase which in turn would lead to the equilibrium in equation 4.10 being shifted to the left. In this work[78] the actual presence of an appreciable vapour pressure of ammonia was detected by the fact that aquated transition metal ion exchanged mordenites picked up ammonia on equilibration over saturated ammonium chloride solution.

A second and possibly no less important reason for loss of ammonia was the thermal drying procedure used in this work (section 2.4.3.).

4.1.4. Analysis of $Pd(NH_3)_4$ and $Pt(NH_3)_4$ — X, Y and Mordenite.

As explained previously (section 4.1.) the compositions of the

hydrated platinum and palladium exchanged zeolites are given in terms of the dehydrated forms. An assumption that no dealumination had occurred on exchange was made in order to determine these zeolite compositions.

Table 4.13. Analyses of Platinum Exchanged Zeolites

| Exchanged form | $Pt(NH_3)_4$ X | | $Pt(NH_3)_4$ Y | | $Pt(NH_3)_4$ MOR | |
|---|---|---|---|---|---|---|
| Component | % w/w | mol/100g | % w/w | mol/100g | % w/w | mol/100g |
| $SiO_2$ | 36.88 | 0.6146 | 48.79 | 0.8132 | 70.31 | 1.1718 |
| $Al_2O_3$ | 24.78 | 0.2439 | 19.69 | 0.1930 | 10.80 | 0.1058 |
| $Fe_2O_3$ | 0.00 | 0.00 | 0.08 | $5.12 \times 10^{-4}$ | 0.08 | $5.12 \times 10^{-4}$ |
| PtO | 22.38 | 0.1056 | 19.39 | 0.0914 | 12.24 | 0.0577 |
| $NH_3$ | 7.36 | 0.4329 | 6.03 | 0.3529 | 3.99 | 0.2347 |
| $Na_2O$ | 8.33 | 0.4627 | 6.194 | 0.0998 | 2.66 | 0.0429 |
| Total | 99.73 % | | 100.08 % | | 100.08 % | |

Analytical results for palladium exchanged zeolites obtained by the three different methods described in section 2.4.2.11 gave results that were inconsistent with each other (Table 4.14).

The general conclusion is that the maximum level of exchange for $Pd(NH_3)_4^{2+}$ in all three zeolites is in the region of 0.62 $\pm$ 0.05. It is therefore not possible to accurately determine the number of ammonia molecules coordinated to each palladium(II) ion within the zeolite. Method 2 would indicate that exchange of $Pd(NH_3)_4$ had proceeded to a level which was consistent with previous work involving Pd-MOR morden-

denite[25].

Table 4.14 Analyses of Palladium Exchanged Zeolites

| | Pd-X $A_c$(max) | Pd-Y $A_c$(max) | Pd-MOR $A_c$(max) |
|---|---|---|---|
| Method 1 | 0.64 | 0.66 | 0.56 |
| Method 2 | 0.54 | 0.63 | 0.68 |
| Method 3 | 0.68 | 0.57 | 0.63 |

## 4.2. THE ION EXCHANGE ISOTHERMS.

Experimental isotherms are shown in figures 4.1 to 4.25 inclusive. The equilibria are represented in terms of the equivalent fraction of the ingoing ion in the zeolite $M_c$ being plotted on the abscissae and the equivalent fraction of the same in solution $M_s$ along the ordinates. In all cases the zeolites showed a preference for the ingoing ion; values of selectivity coefficient $\alpha$ are shown in figures 4.30 to 4.43.

In the cases of 1st row transition metal ion exchange into $NH_4$/Na-X, ternary exchange was exhibited. The resulting isotherms are depicted in such a way as to show this by plotting along the abscissae both the transition metal and sodium contents of the crystal phase ($M_c$ + $Na_c$) for a given $M_s$ value. From these data the equivalent fraction of ammonium may be inferred, since it must be true that for any given value of $M_s$,

$$(NH_4)_c = 1 - (M_c + Na_c)$$

For the ternary exchange equilibria the value of the selectivity coefficients was re-defined as $\alpha^N_t$.

$$\alpha^N_t = \frac{A_c(1-A_s)\times T_N/Z_A}{(1-A_c)\times m_A}$$

Where the fraction (1 - As) x $T_N/Z_A$ replaces the value of $M_B$ in equation 1.190 and represents the total molarity of the outgoing ions in solution.

For systems where the value of $\Delta G^\ominus$ was not calculated (due either to the occurrence of ternary exchange or because insufficient activity coefficient data were available) plots of a normalised mass action quotient ($K^N_M$) were constructed. For the case of uni-univalent exchange

$$K^N_m = \alpha^N$$

whereas for uni-divalent exchange

$$K^N_m = (\alpha^N)^2 . m_A / A_c$$

Full tables of data are found in Appendix II

These include:

(1) Isotherm Data

(2) Kielland plot data

(3) Values of crystal phase activity coefficients

(4) Selectivity coefficients

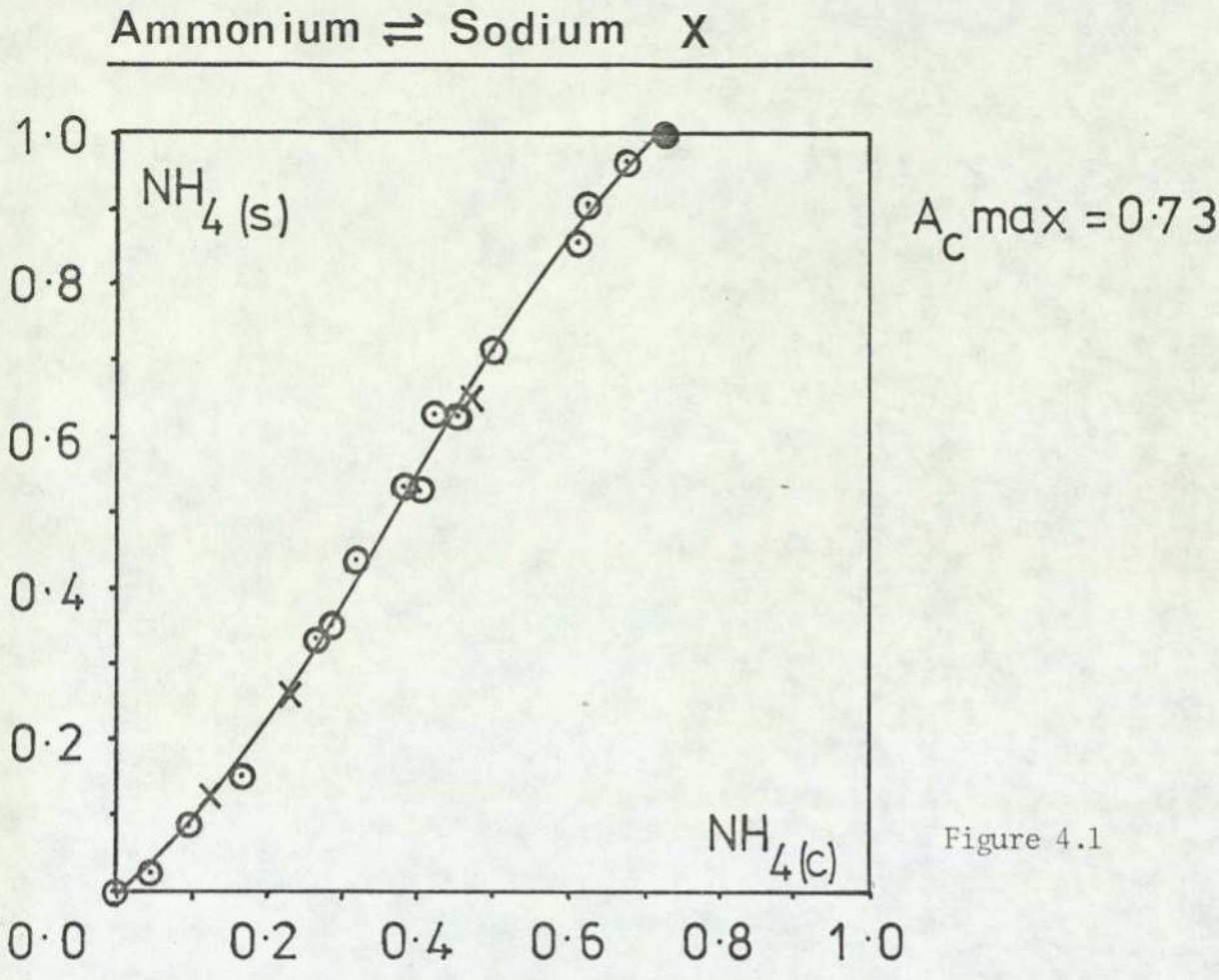


Figure 4.1

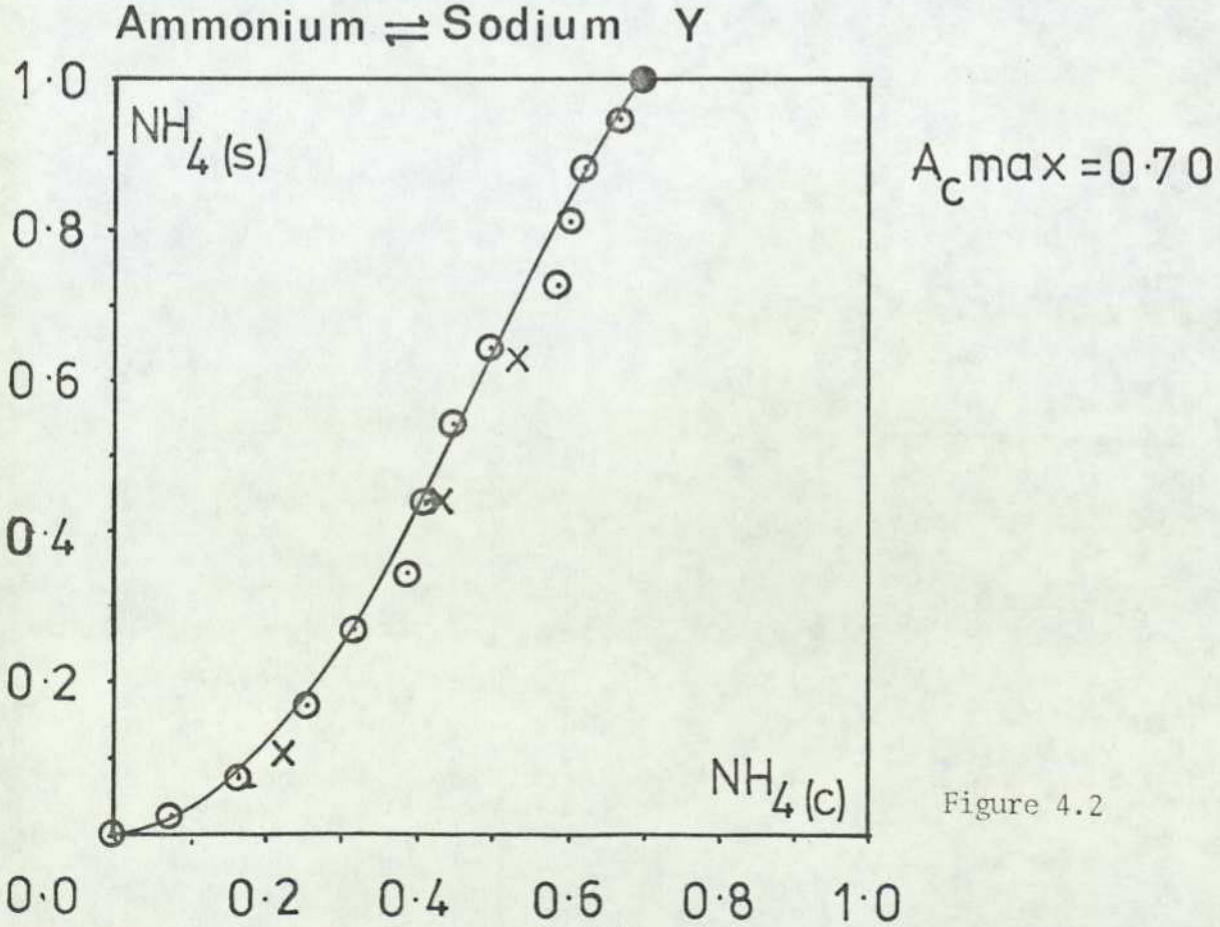


Figure 4.2

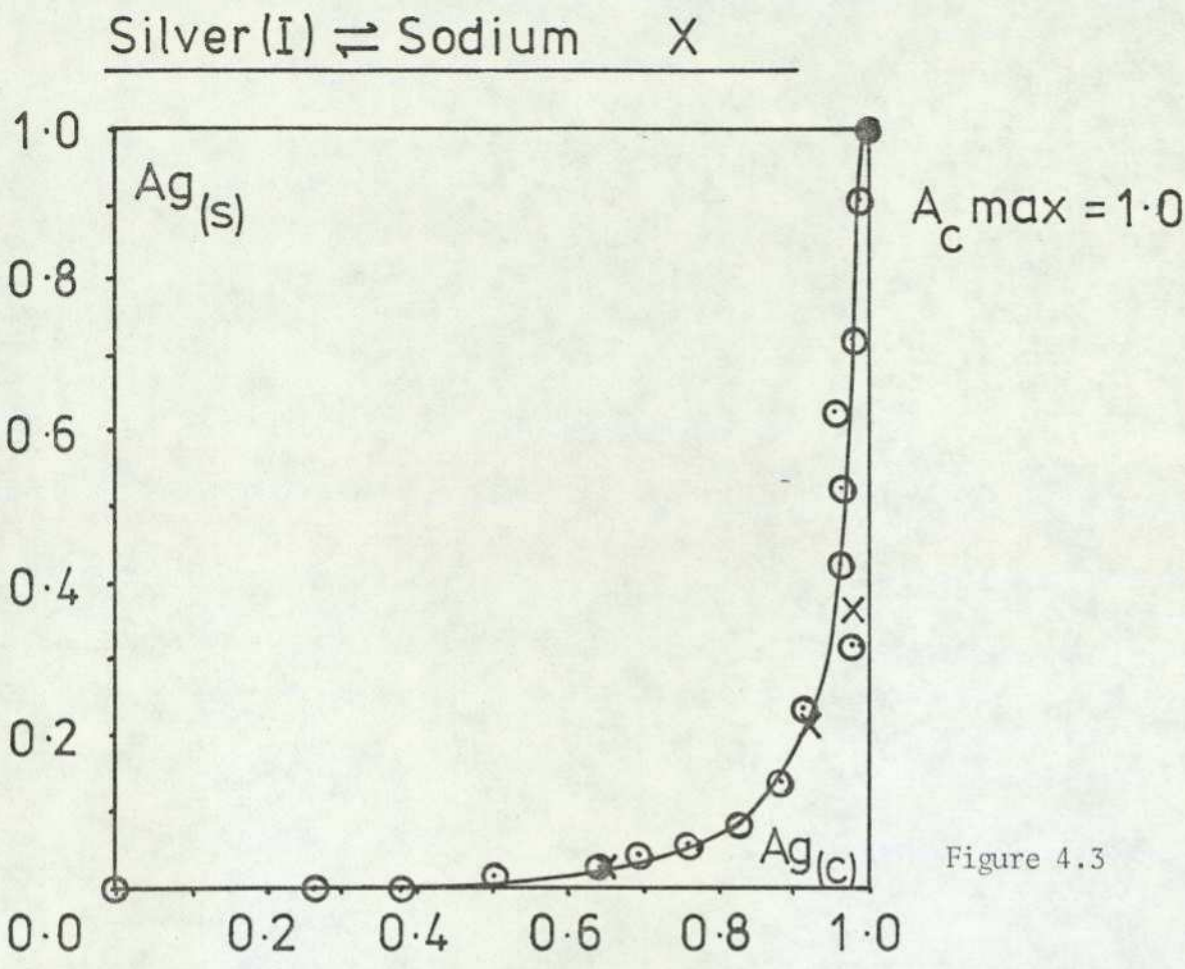


Figure 4.3

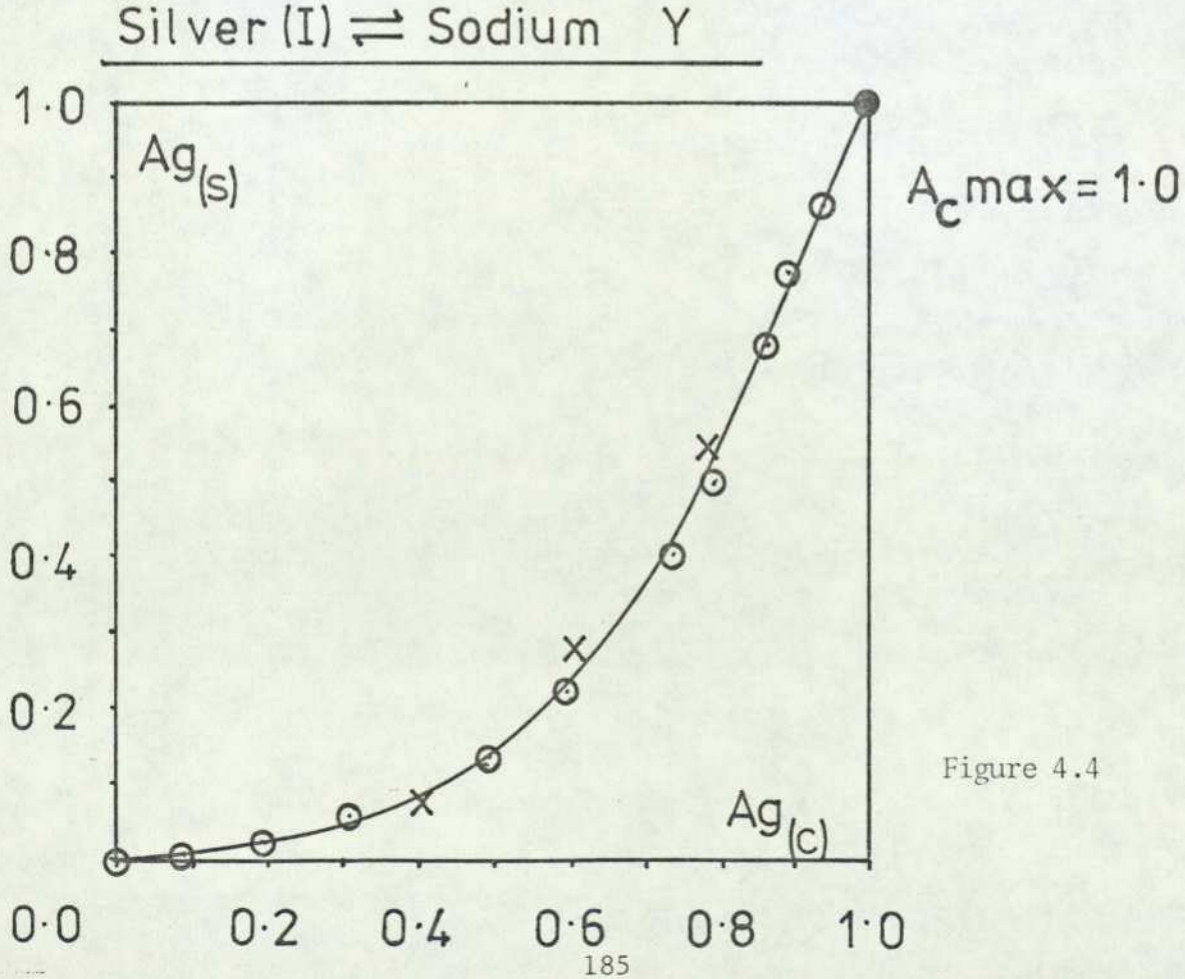


Figure 4.4

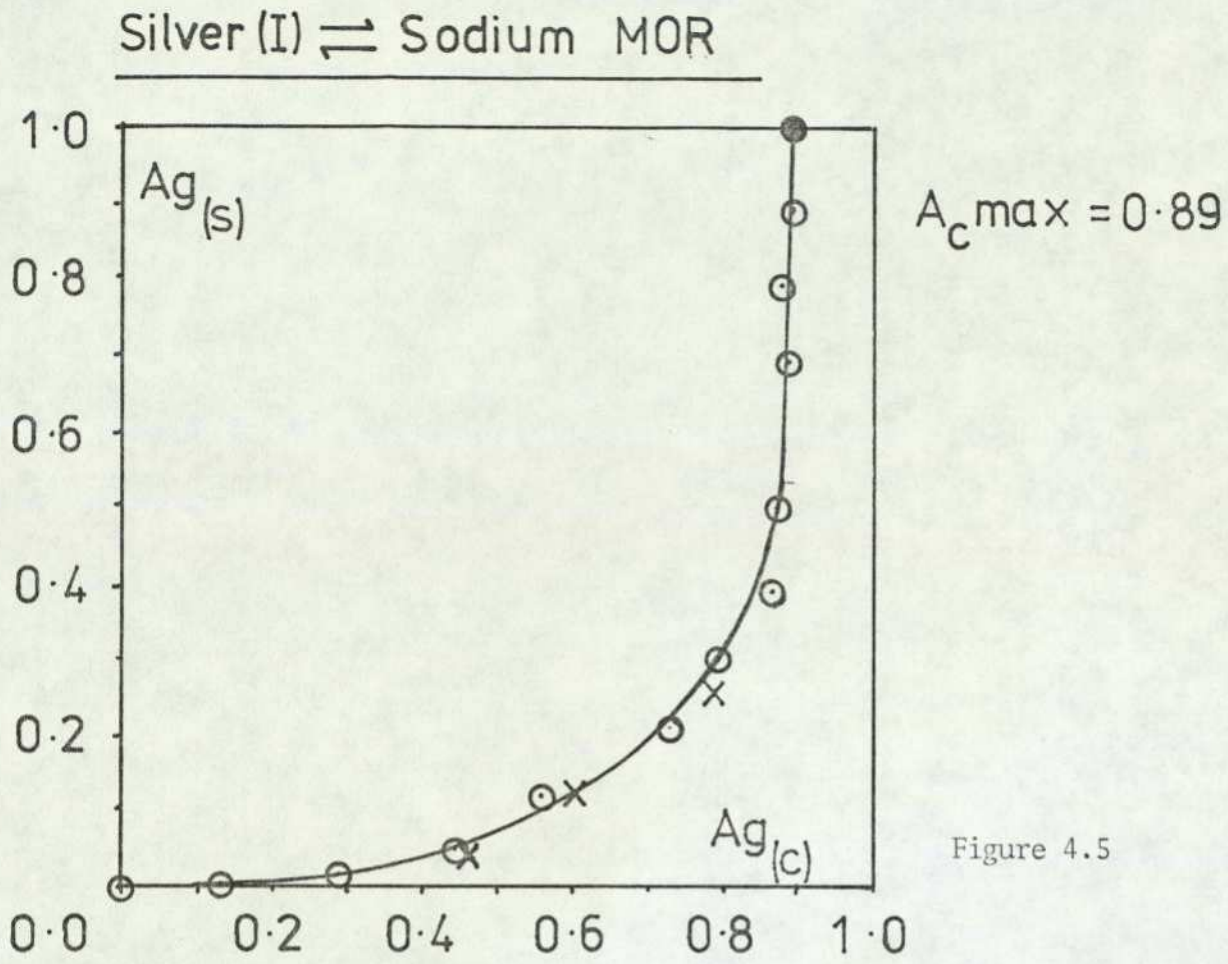


Figure 4.5

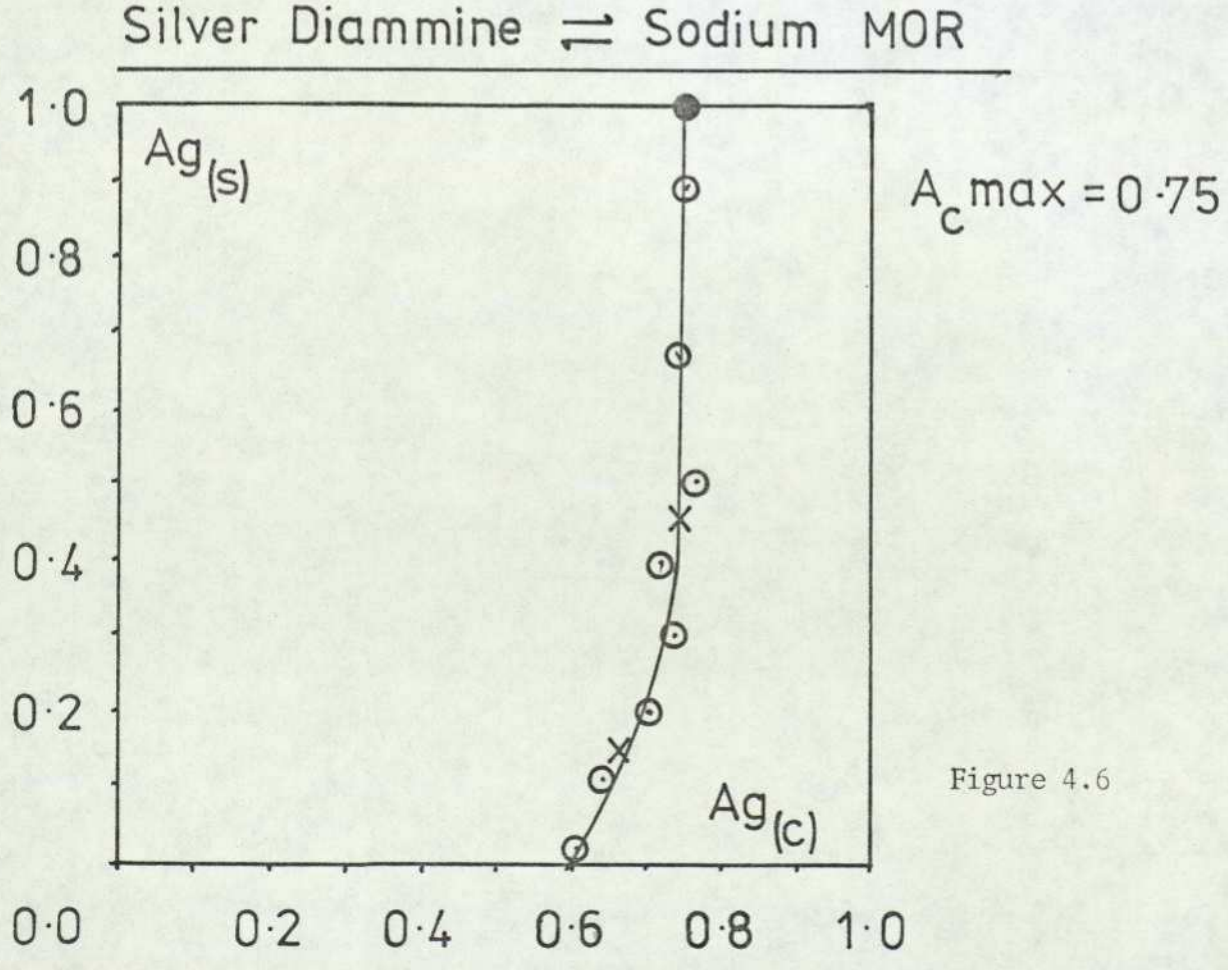


Figure 4.6

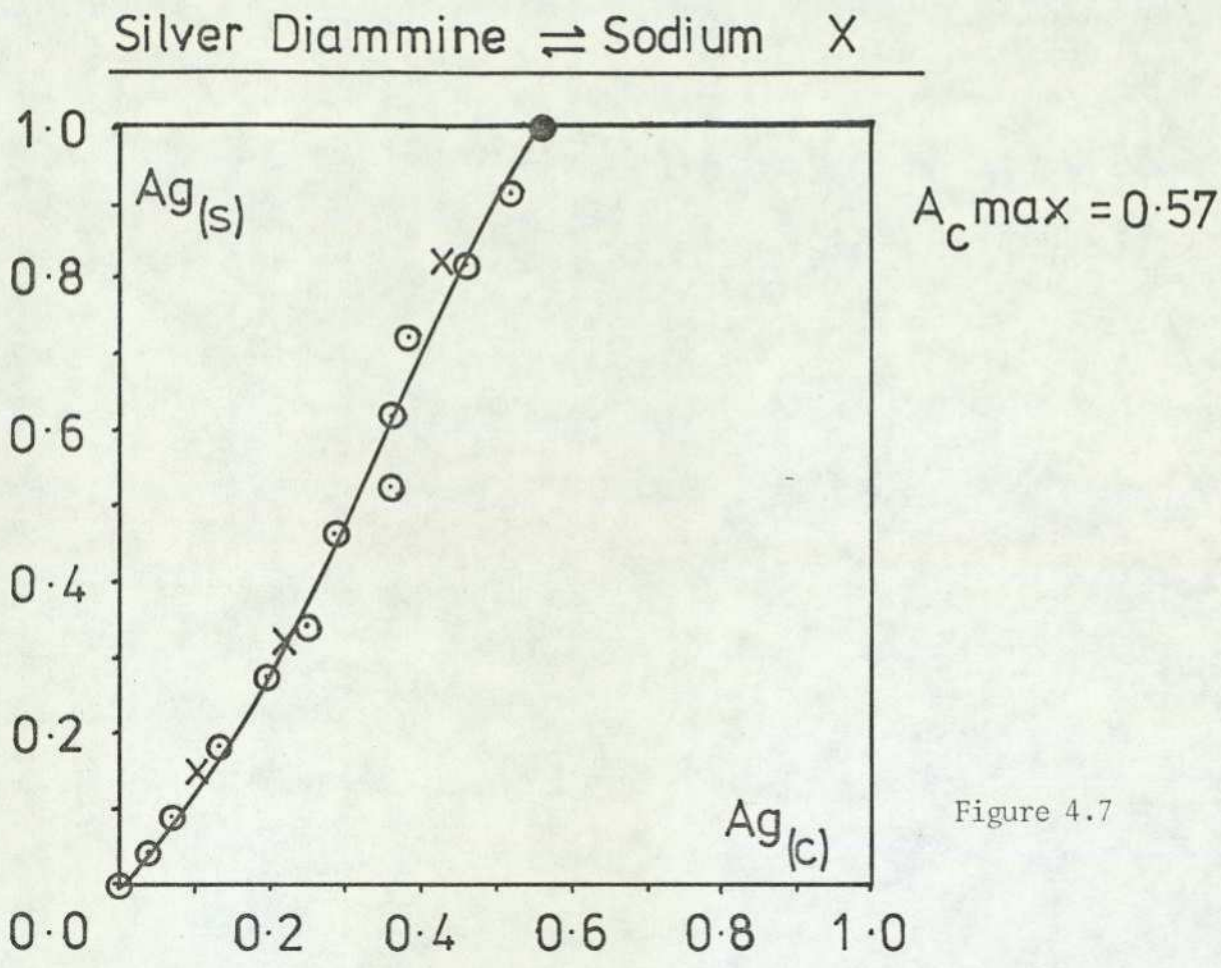


Figure 4.7

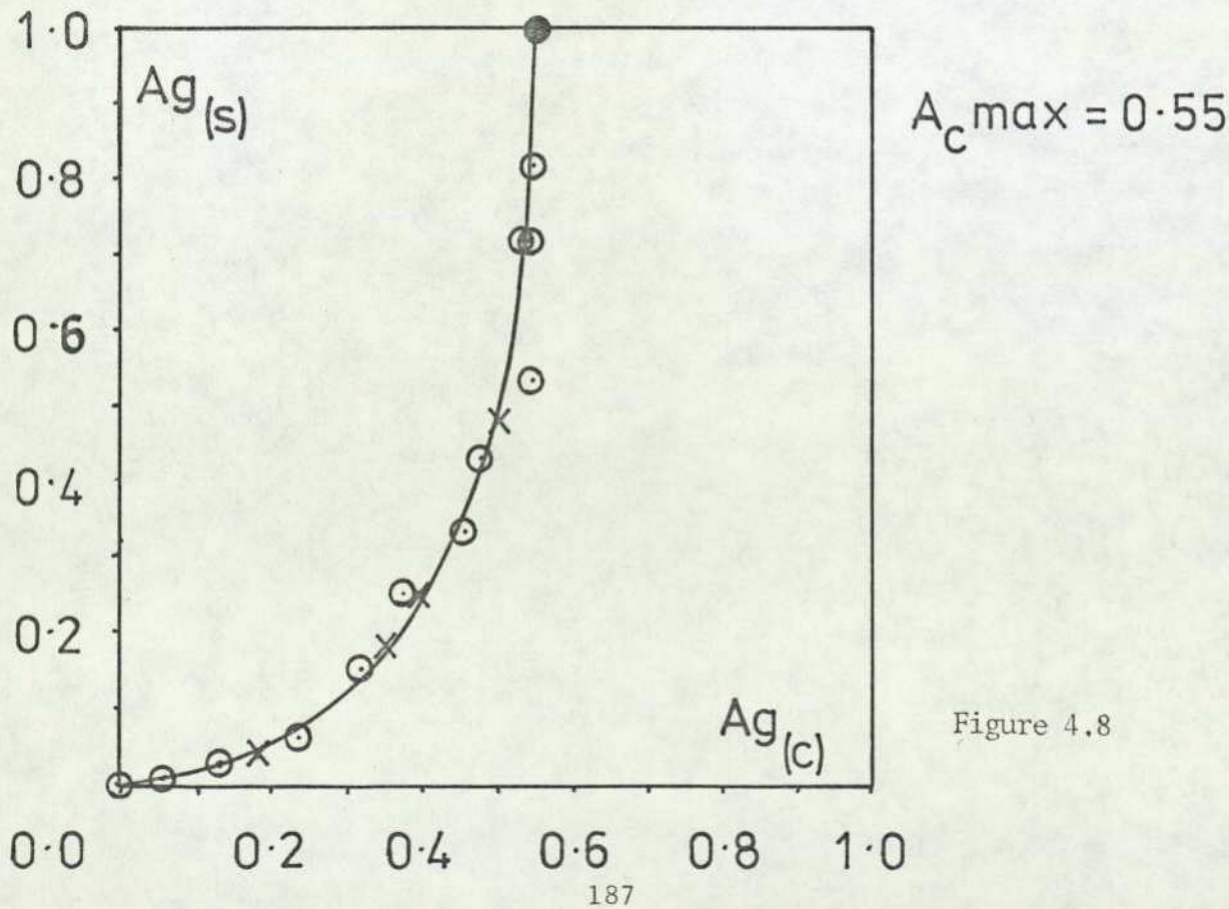


Figure 4.8

Silver Diammine ⇌ Ammonium MOR

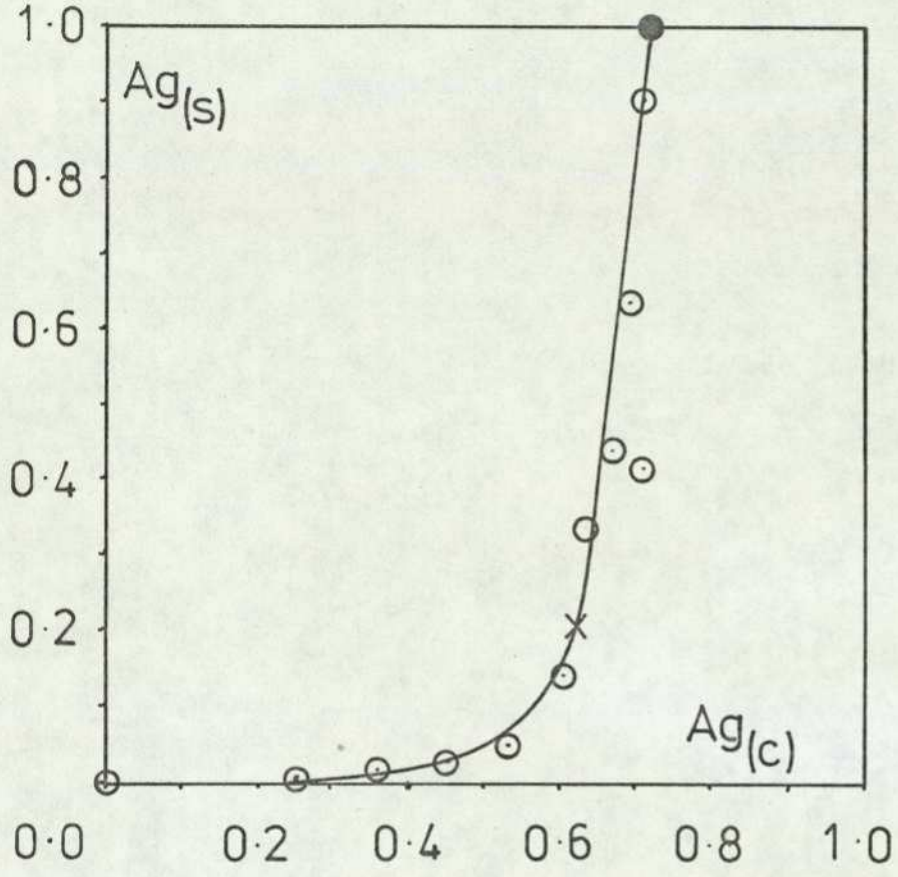


$A_c max = 0·72$

Figure 4.9

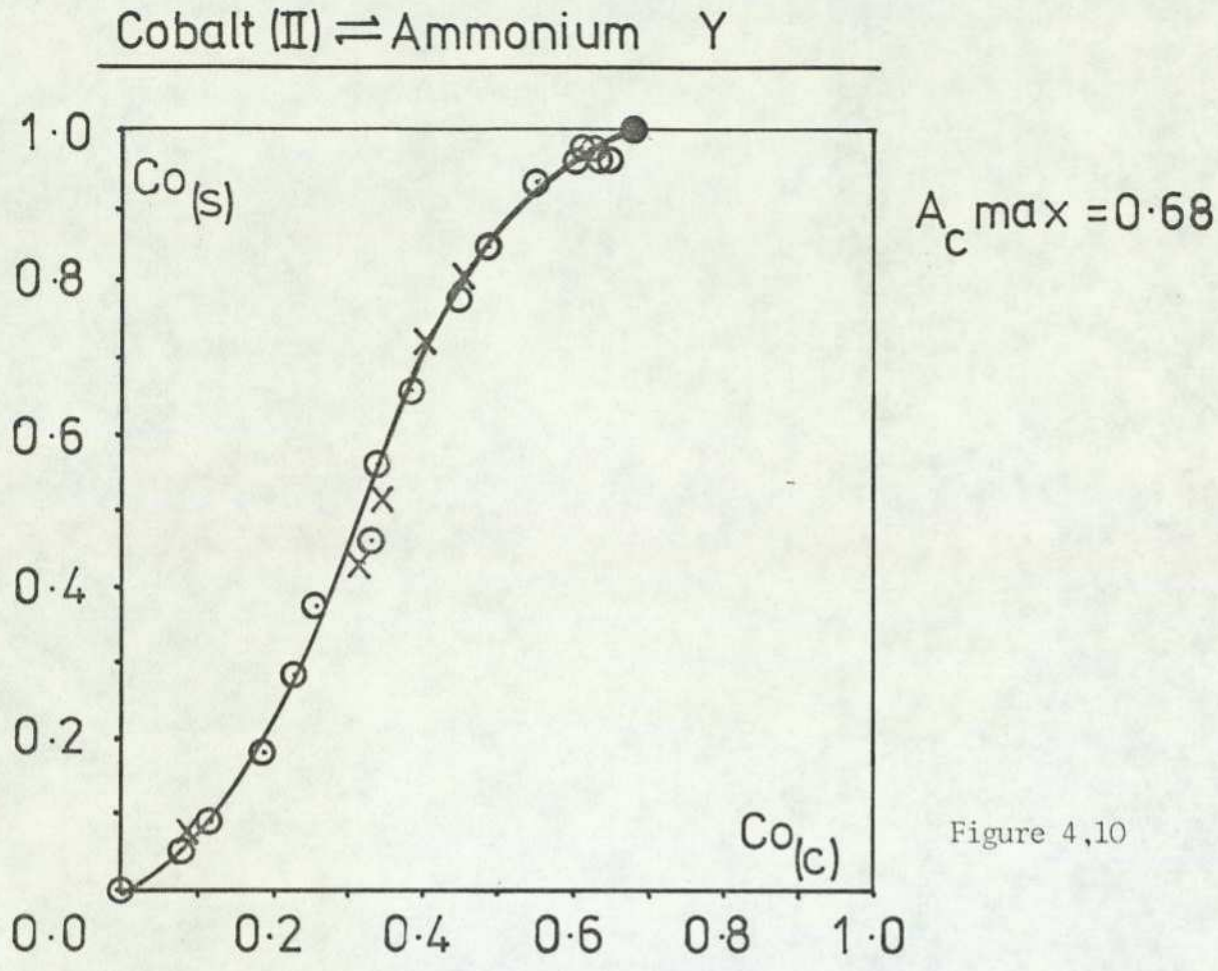


Figure 4,10

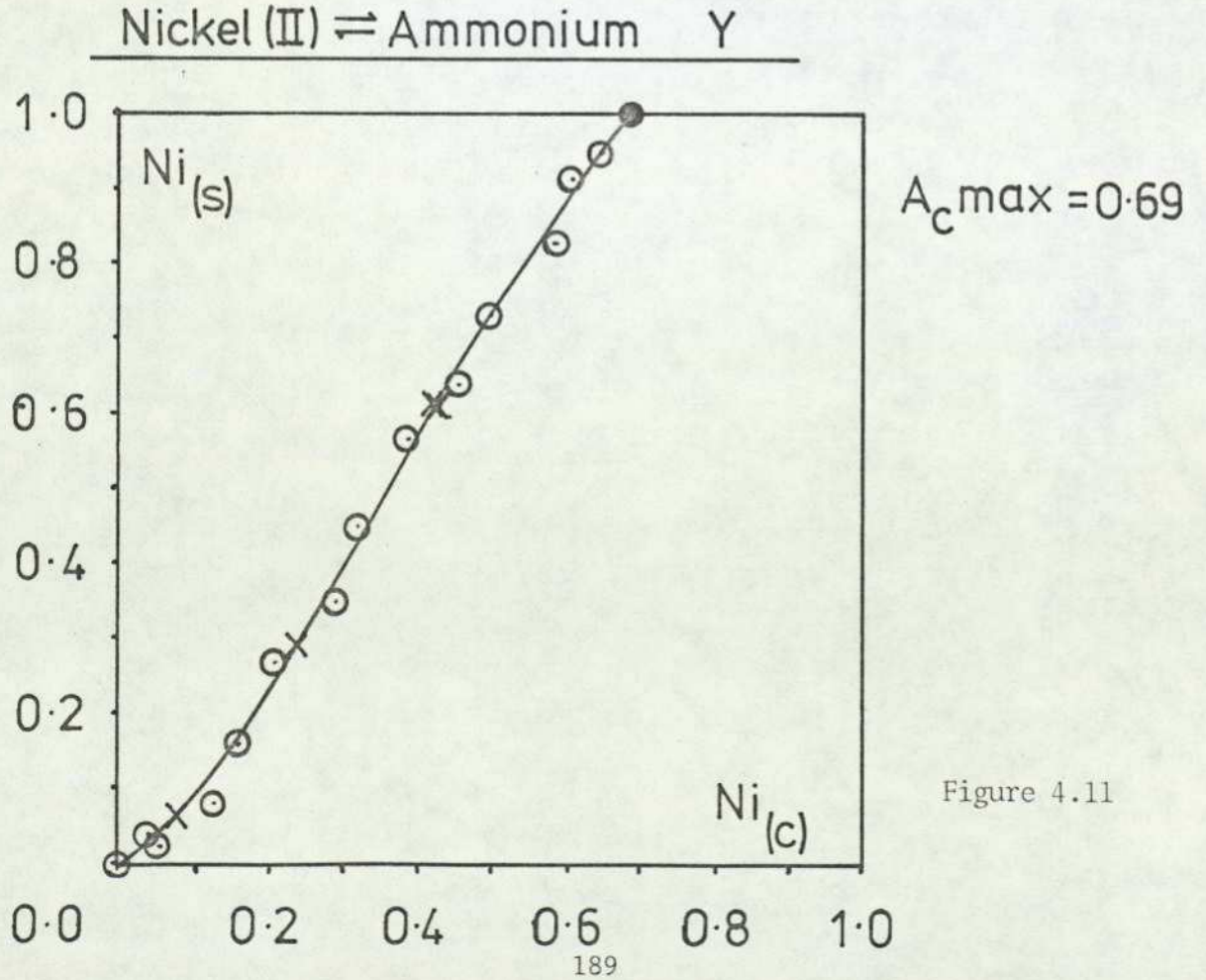


Figure 4.11

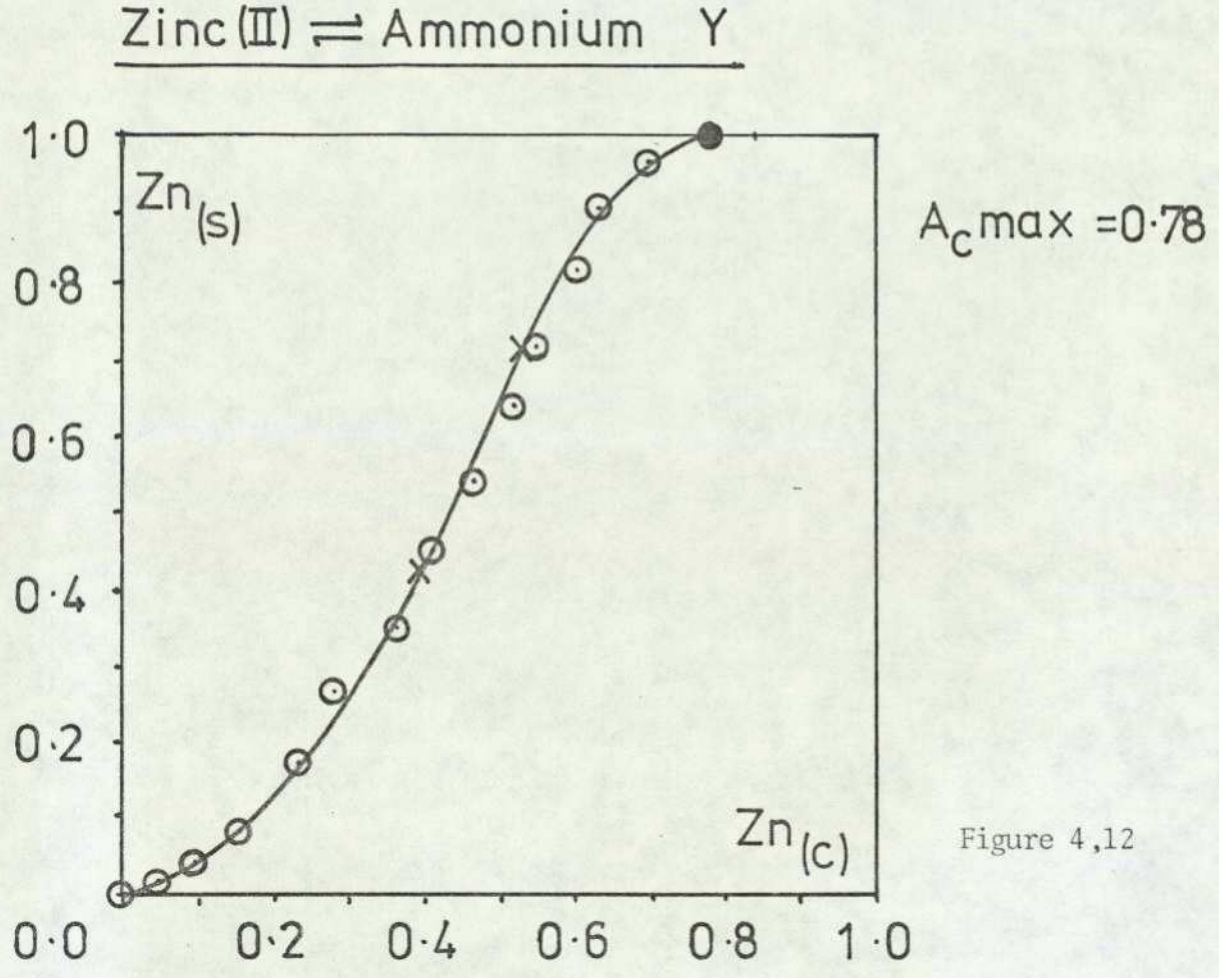


Figure 4,12

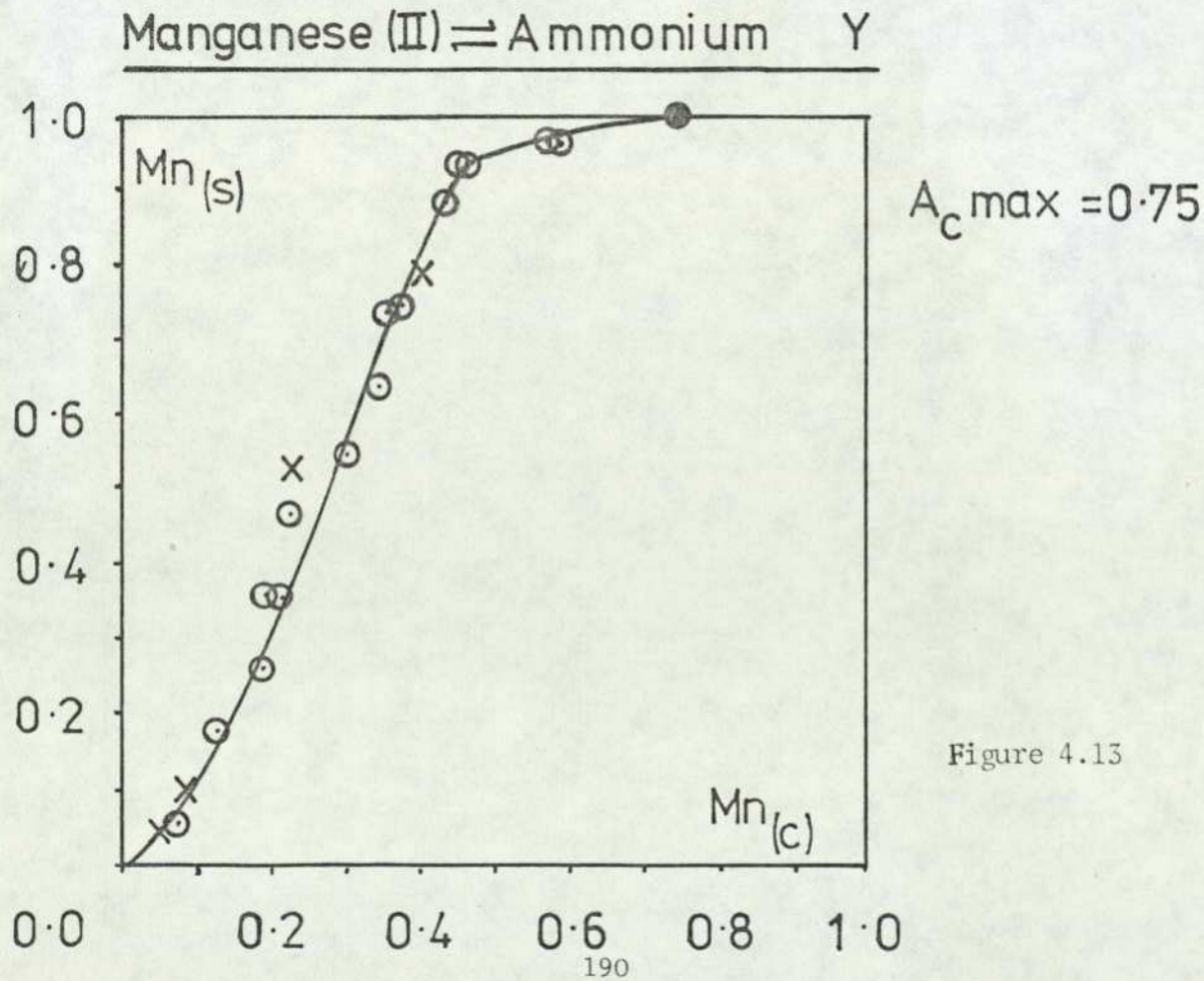


Figure 4.13

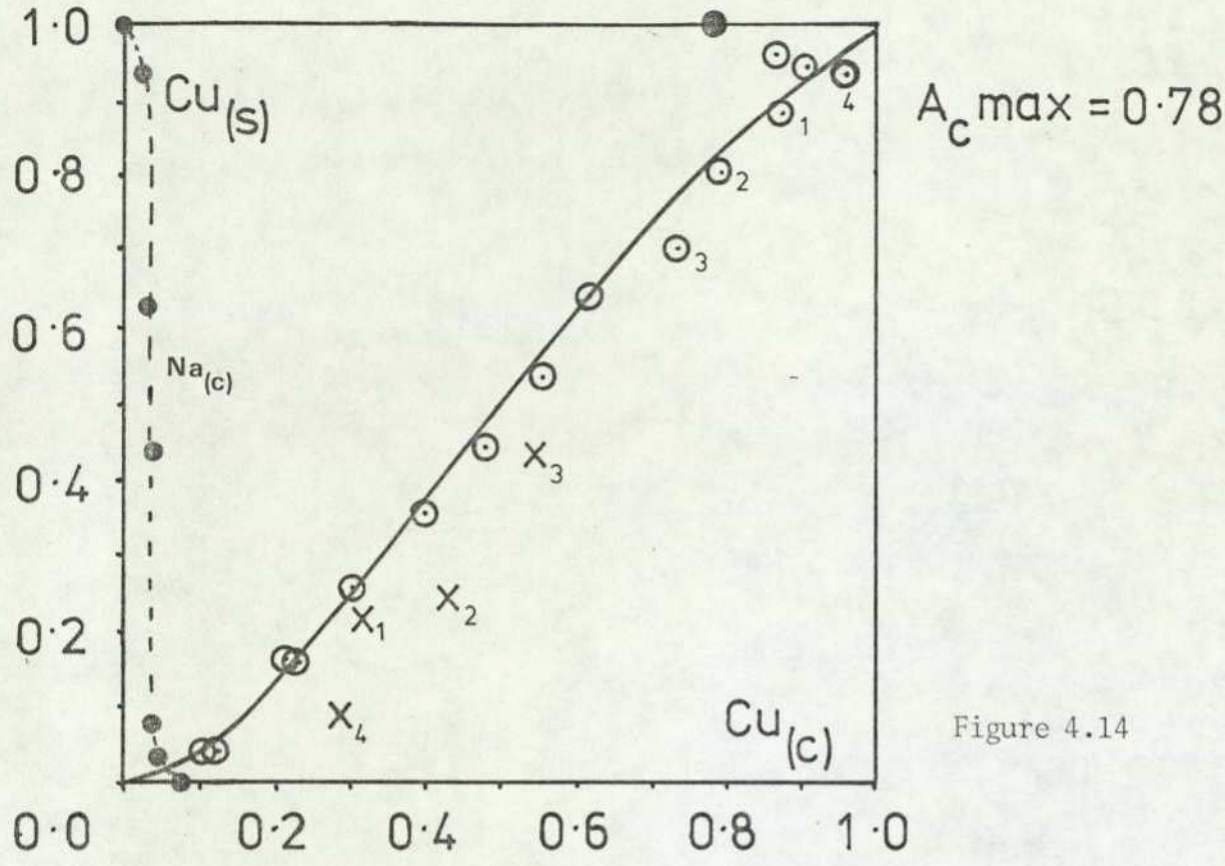


Figure 4.14

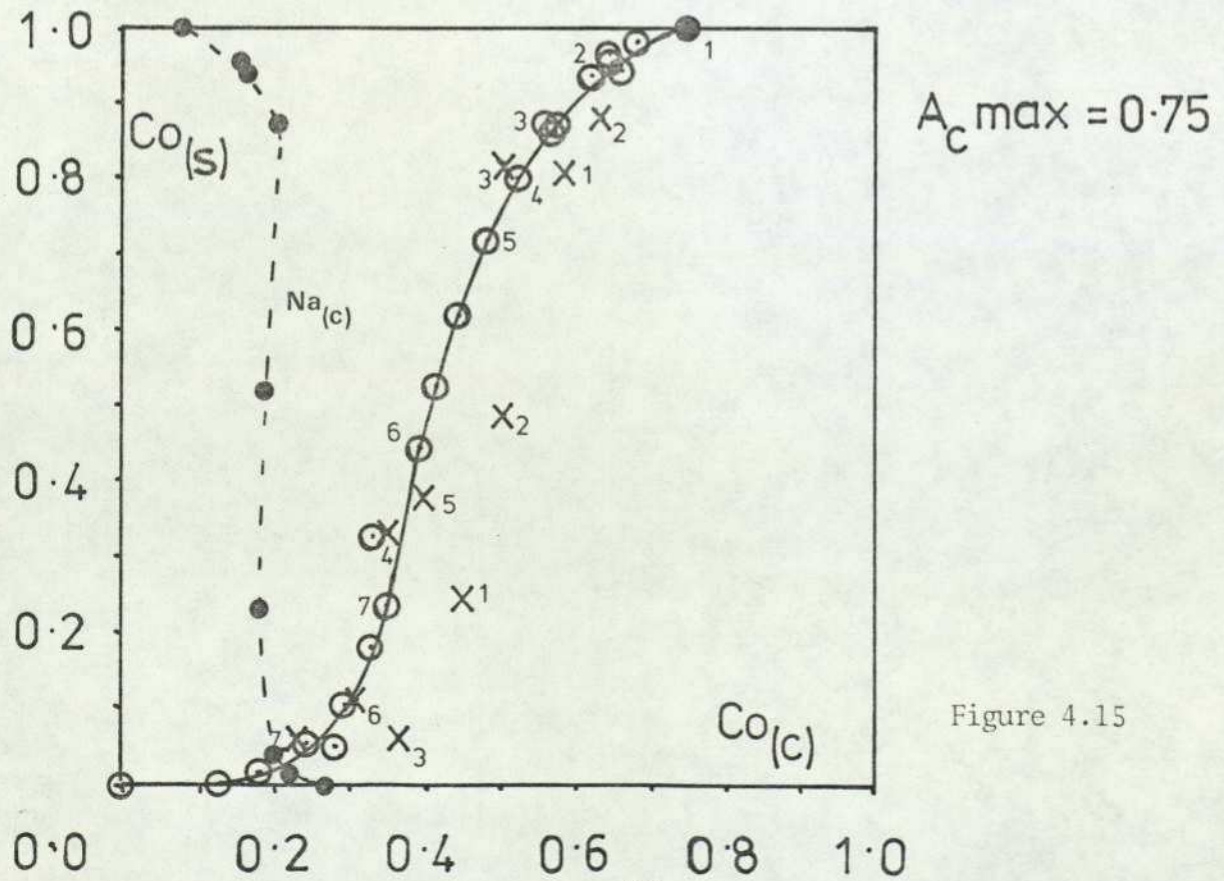


Figure 4.15

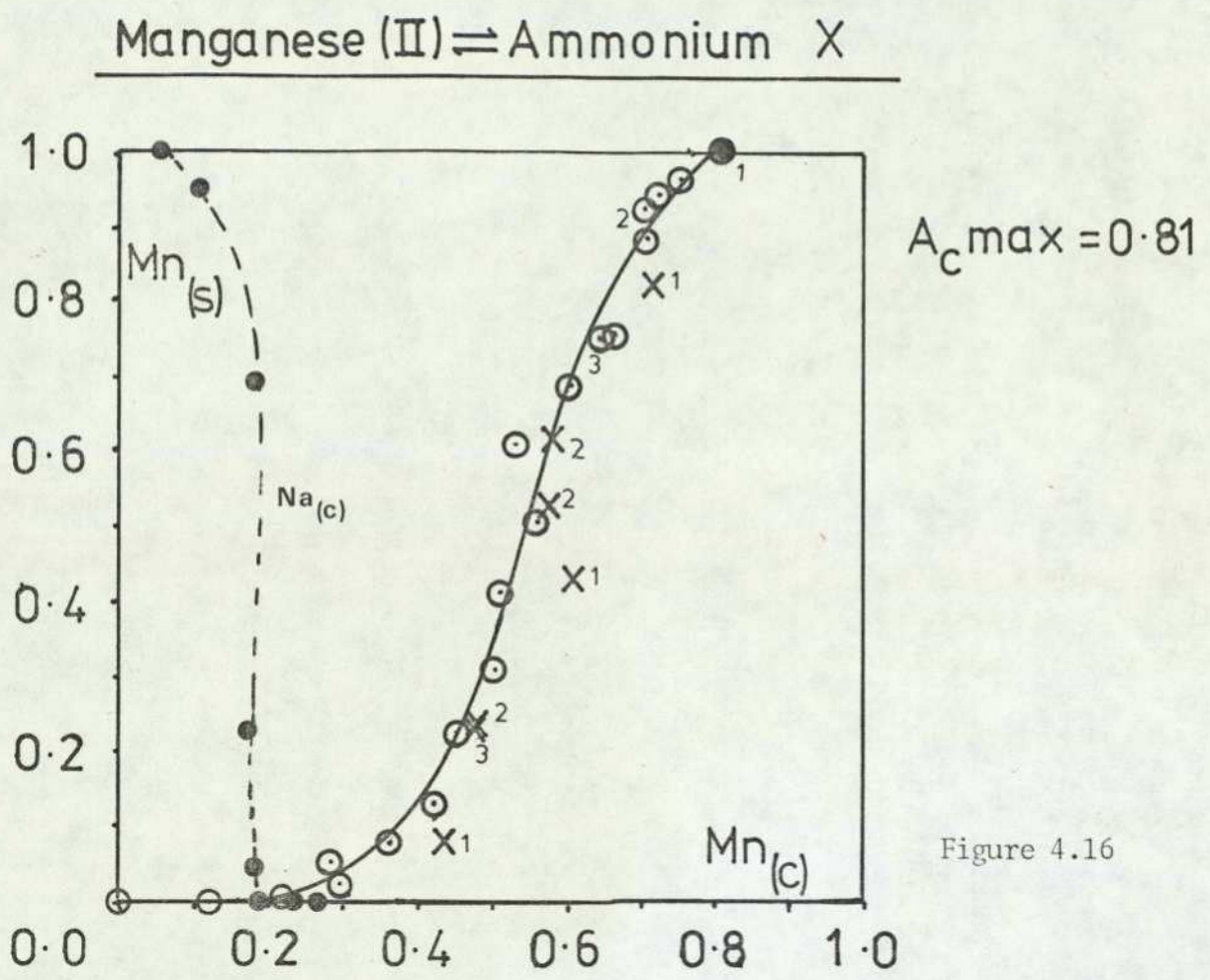


Figure 4.16

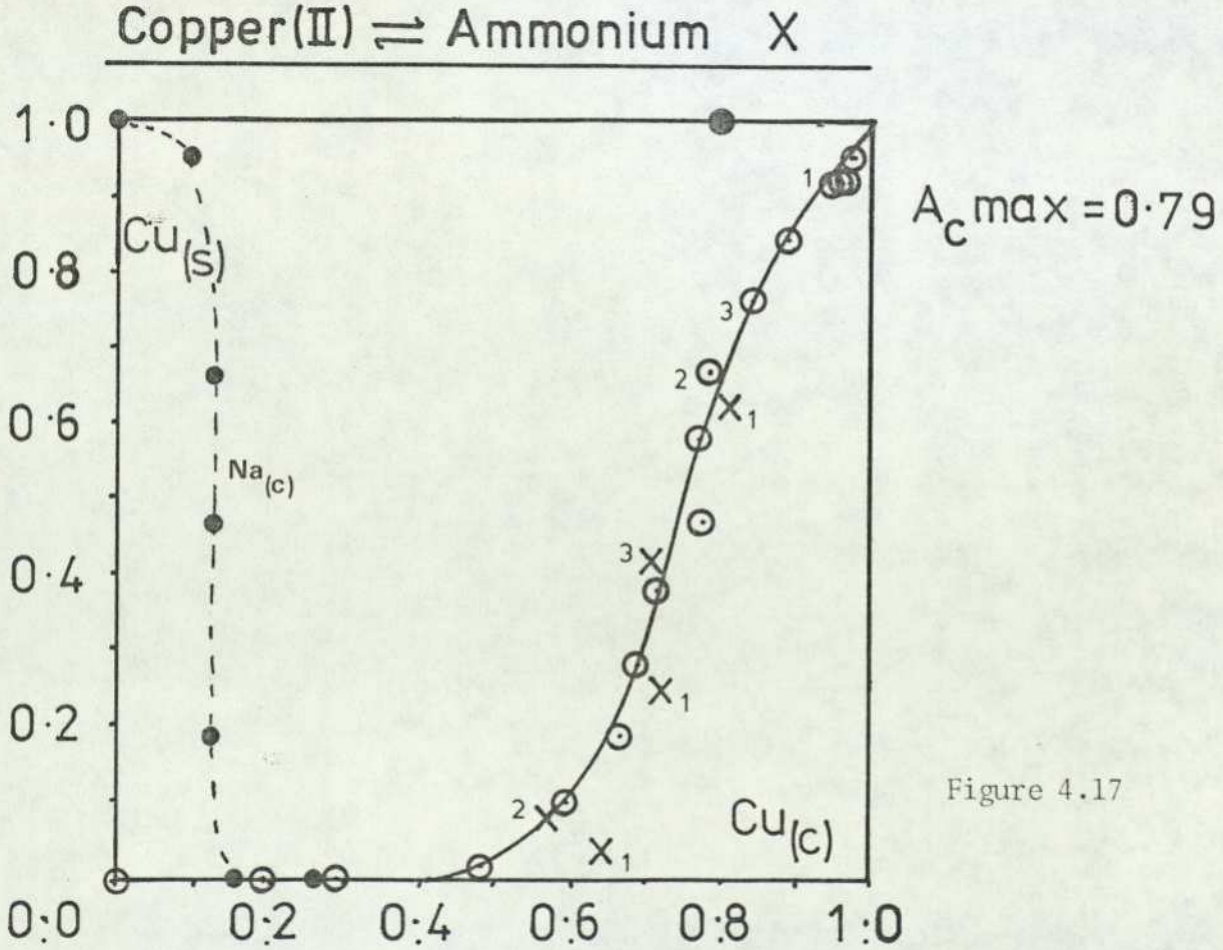


Figure 4.17

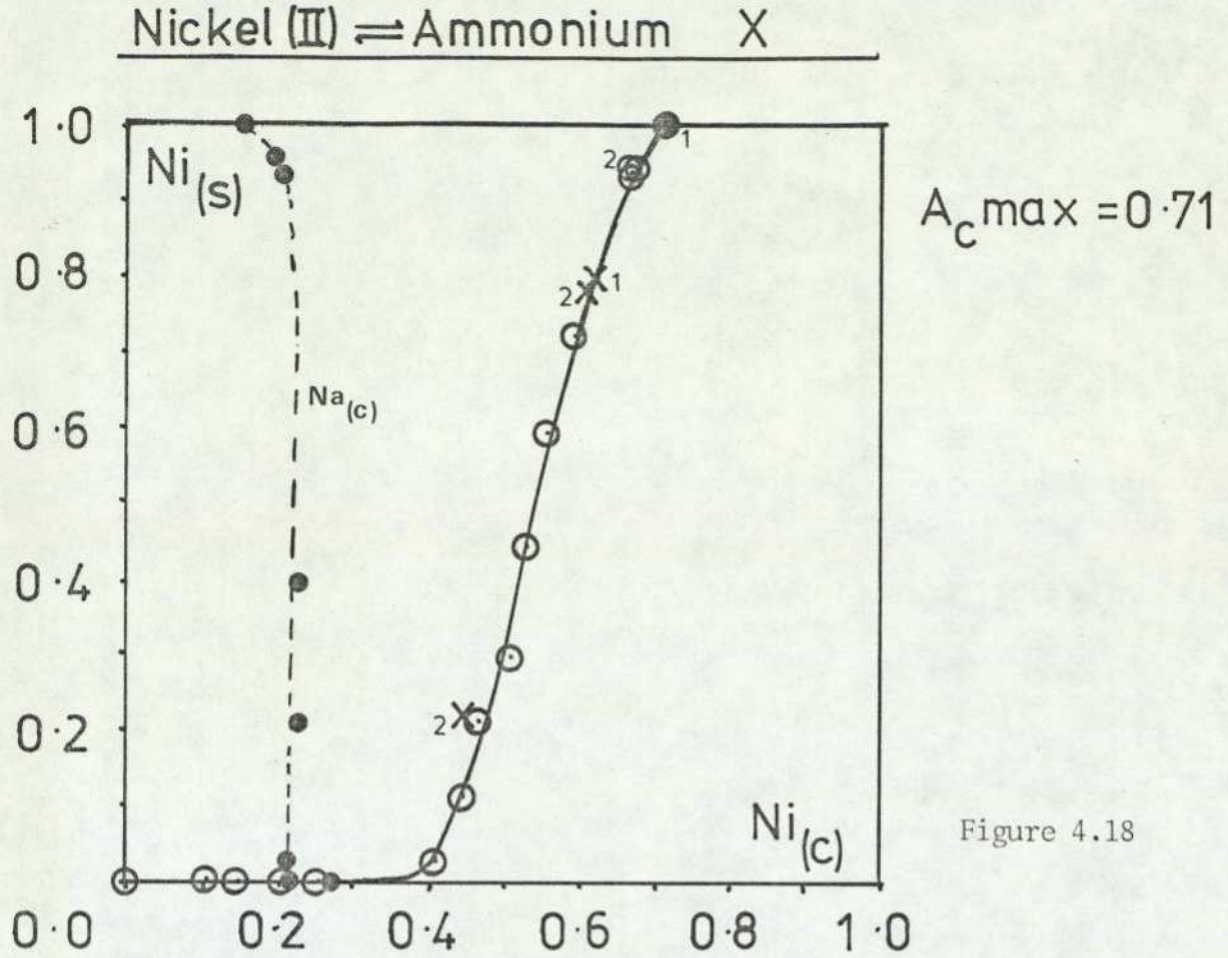


$A_c max = 0·71$

Figure 4.18

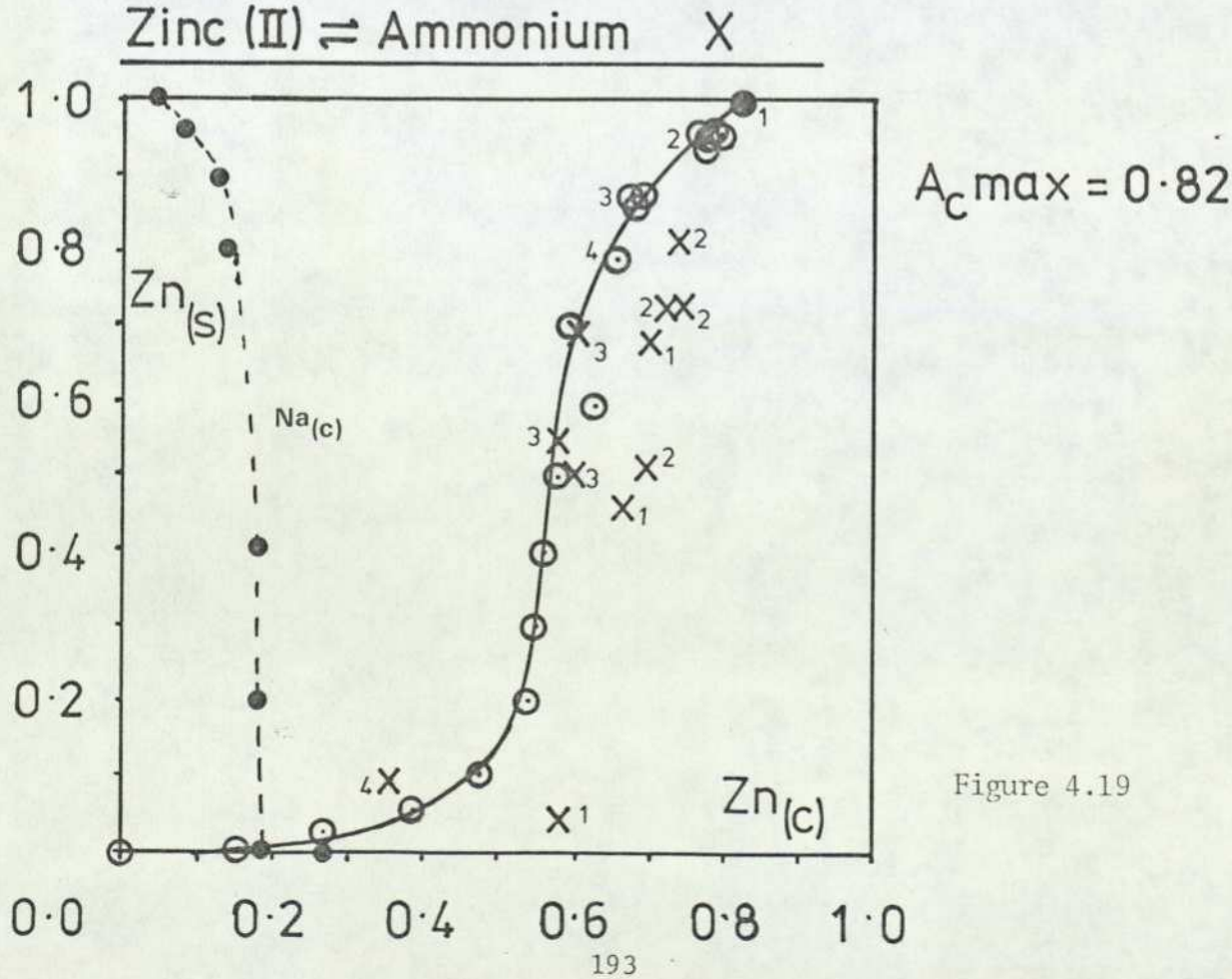


$A_c max = 0·82$

Figure 4.19

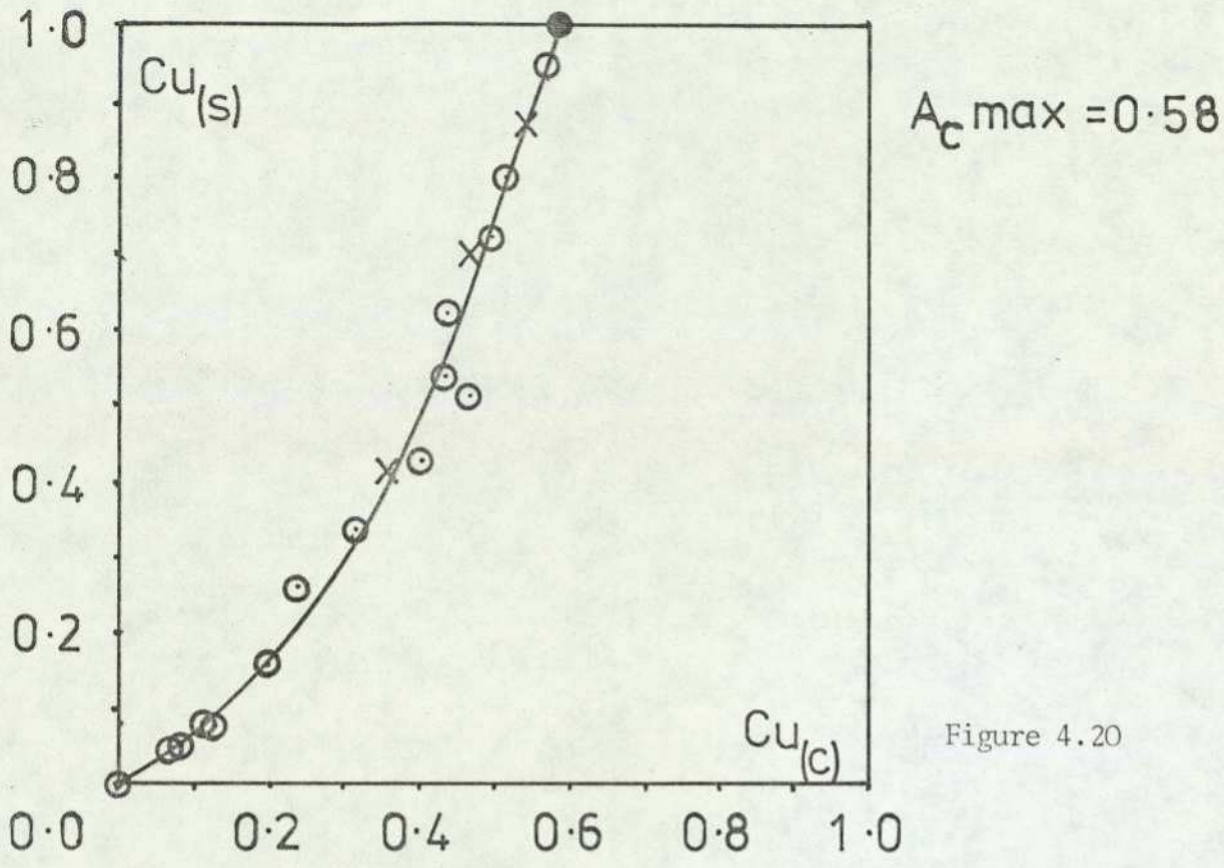


Figure 4.20

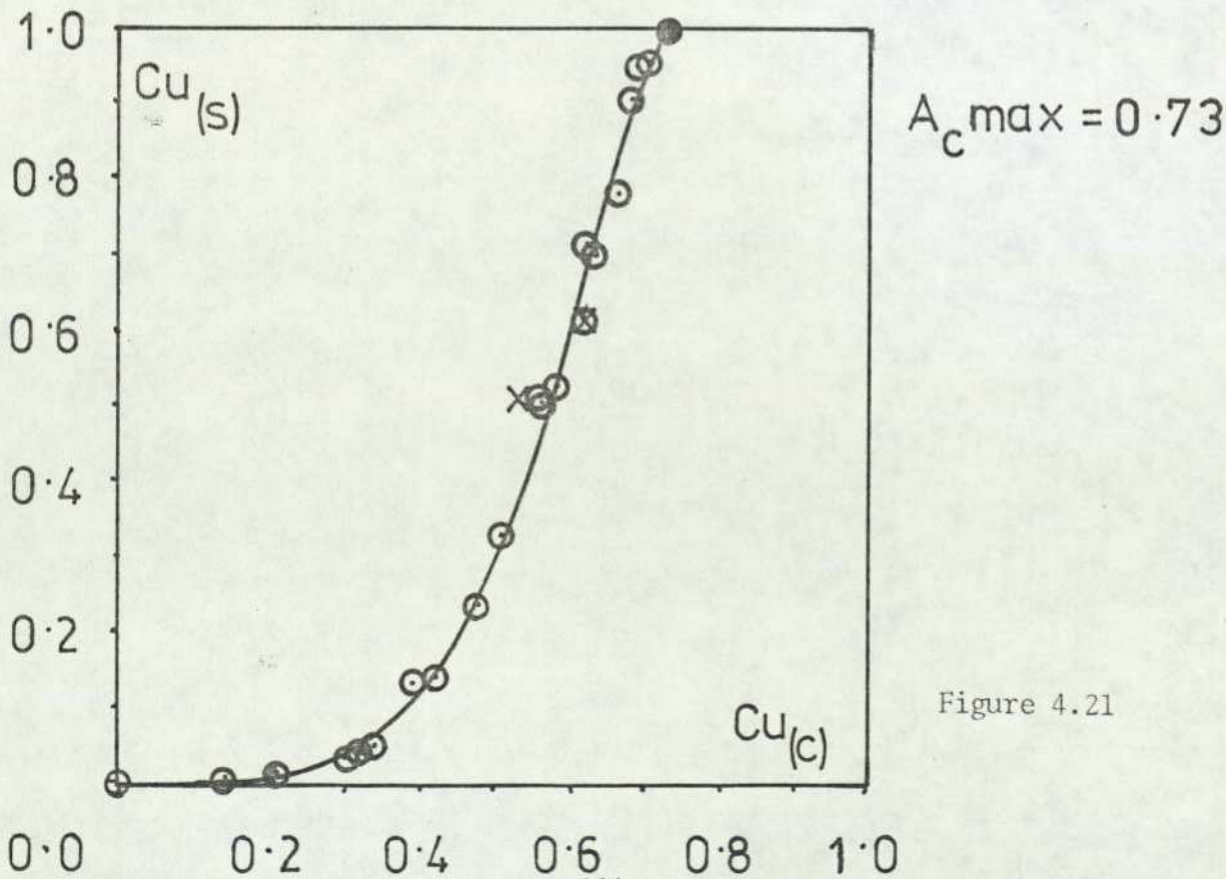


Figure 4.21

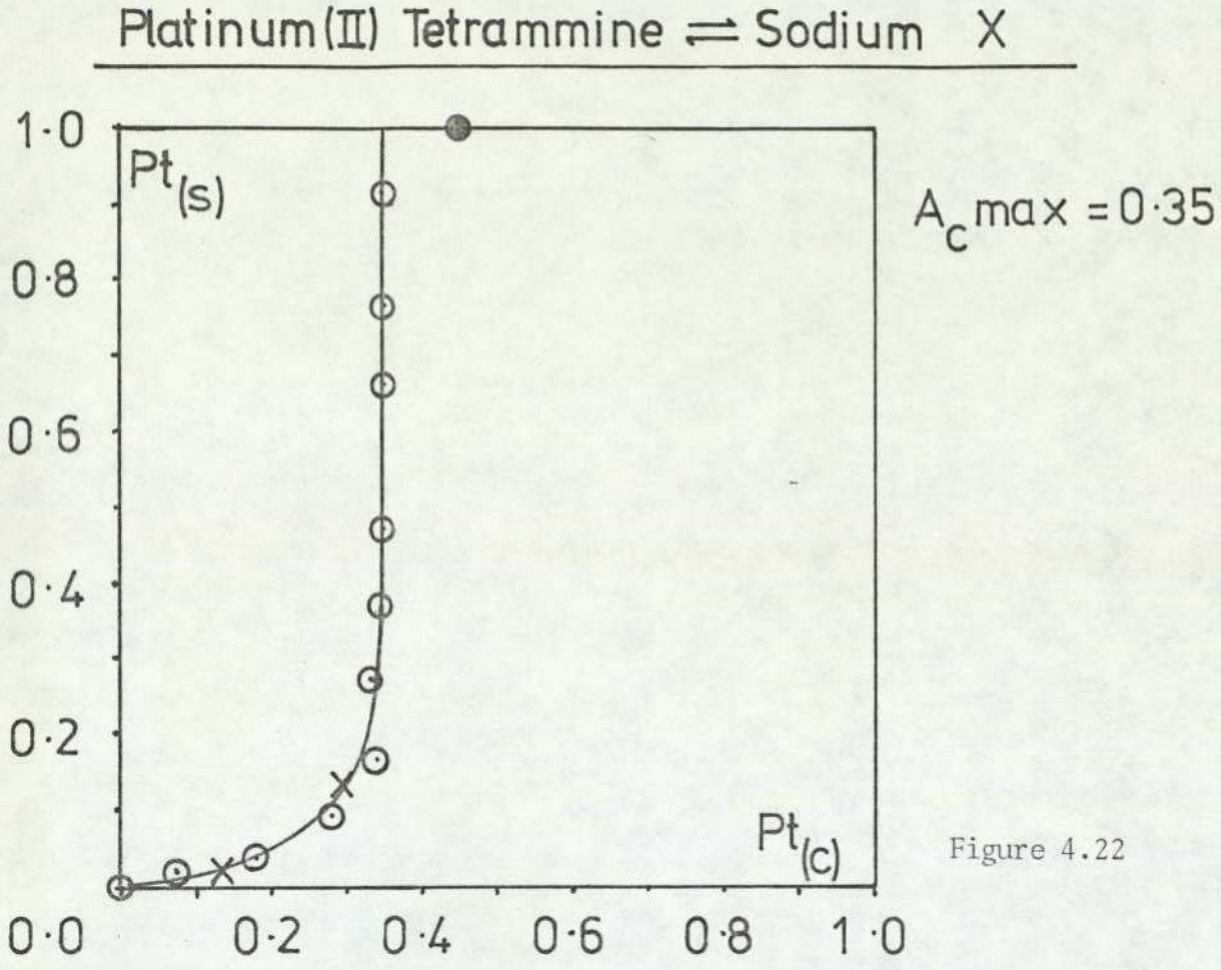


Figure 4.22

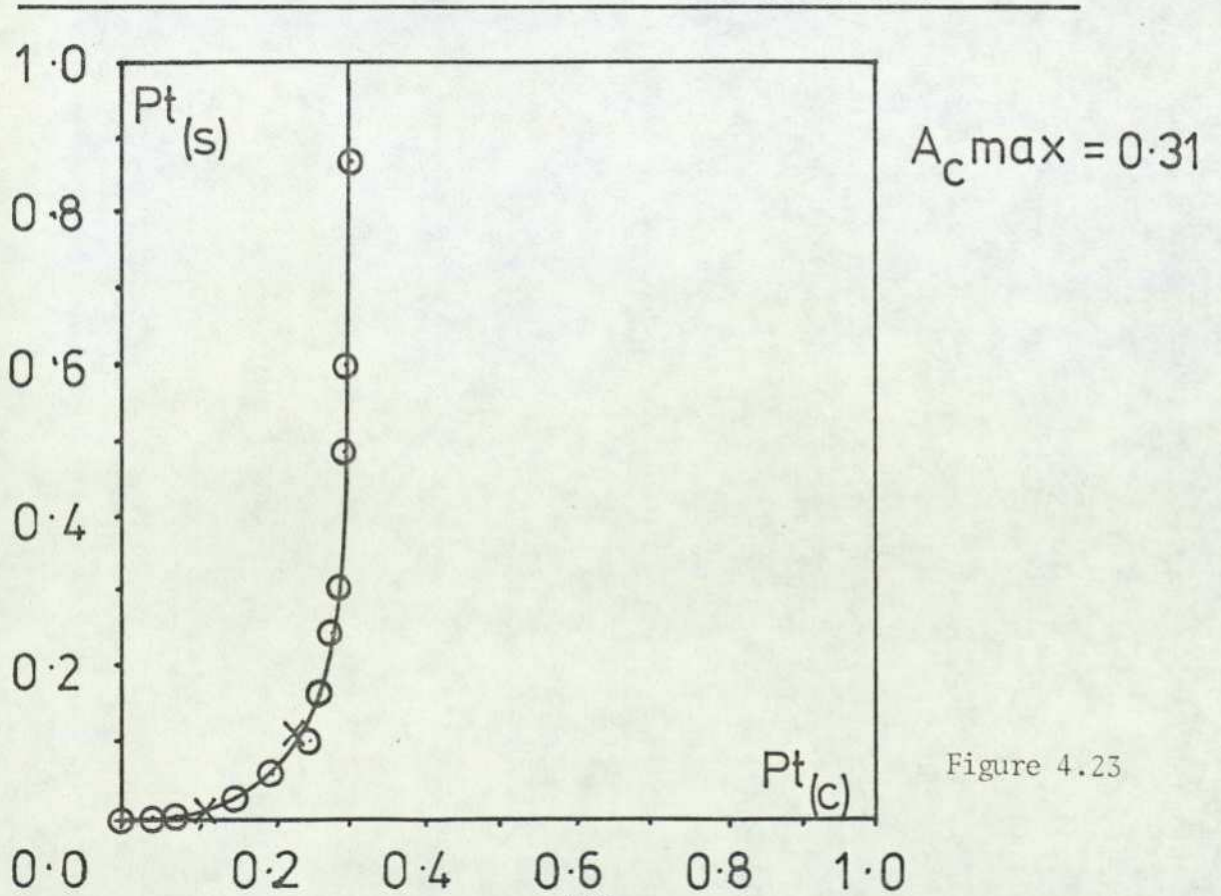


Figure 4.23

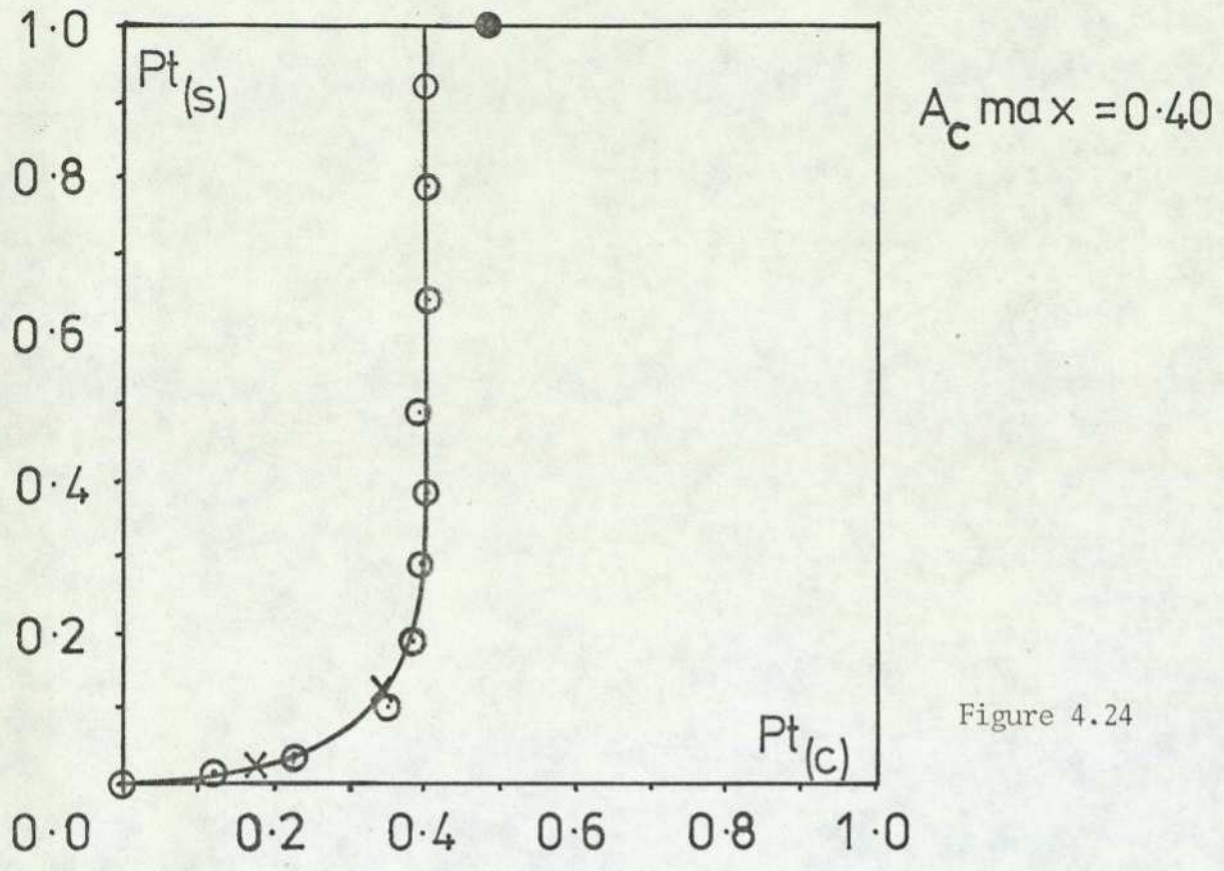


Figure 4.24

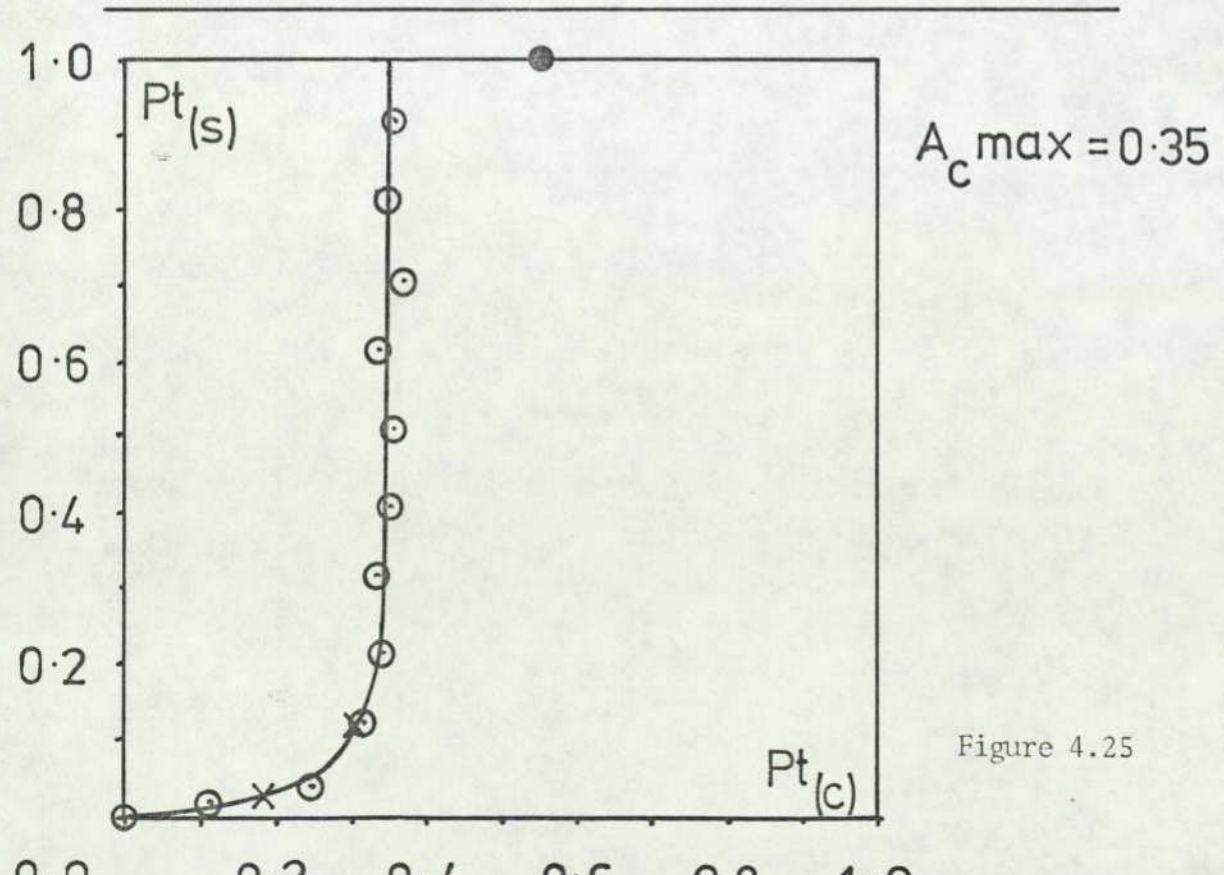


Figure 4.25

## Palladium (II) Tetrammine ⇌ Sodium MOR

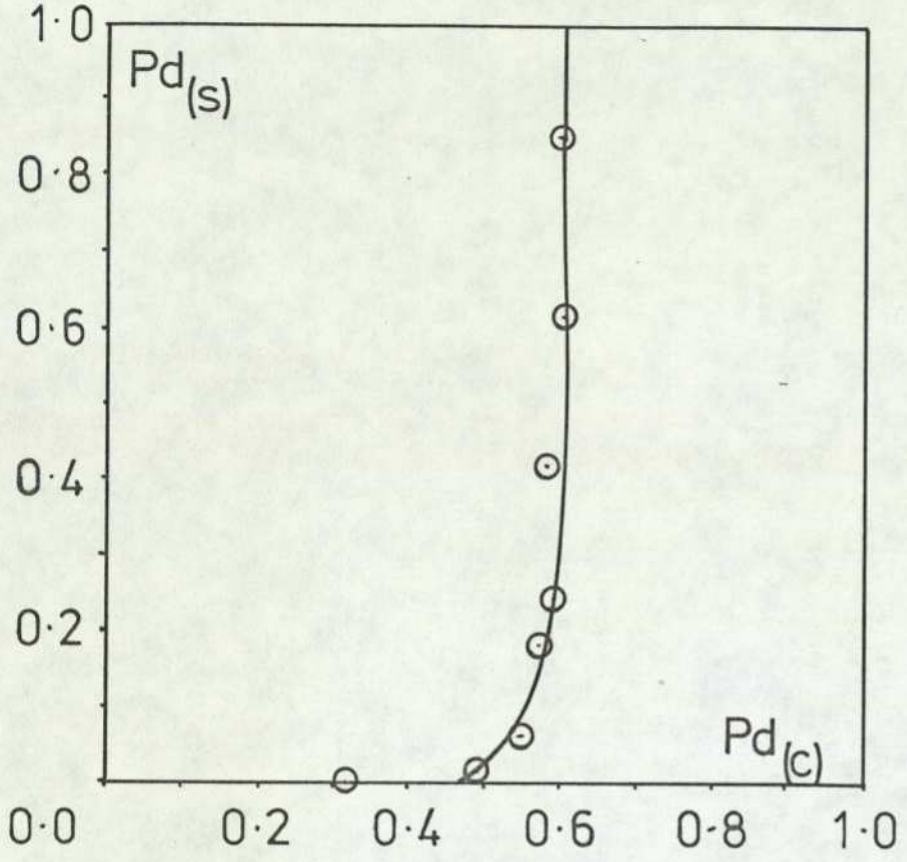


Figure 4.26

## Palladium (II) Tetrammine ⇌ Sodium Y

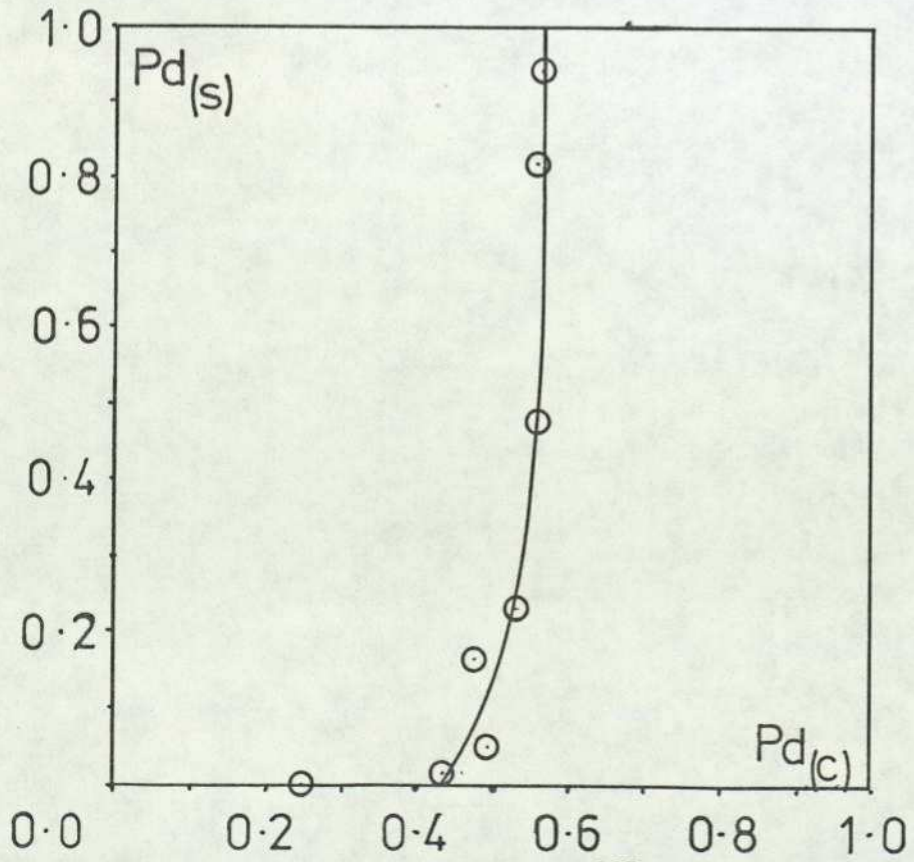


Figure 4.27

Palladium (II) Tetrammine Sodium X

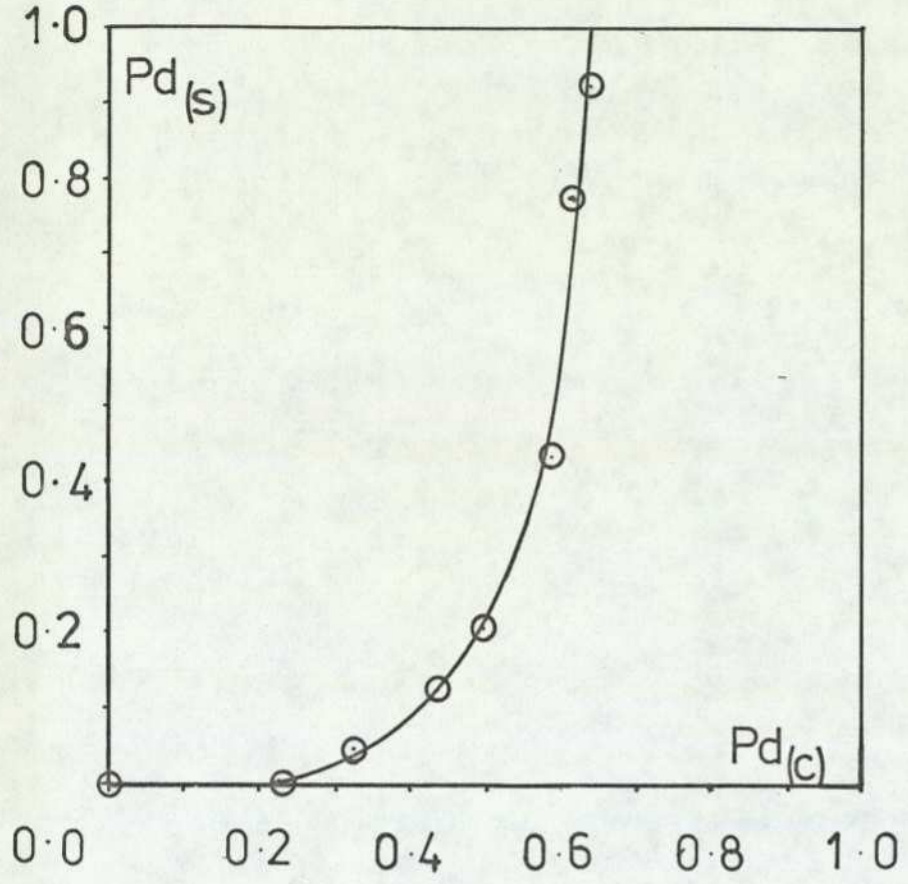


Figure 4.28

COPPER (II) [Chloride] ⇌ AMMONIUM X

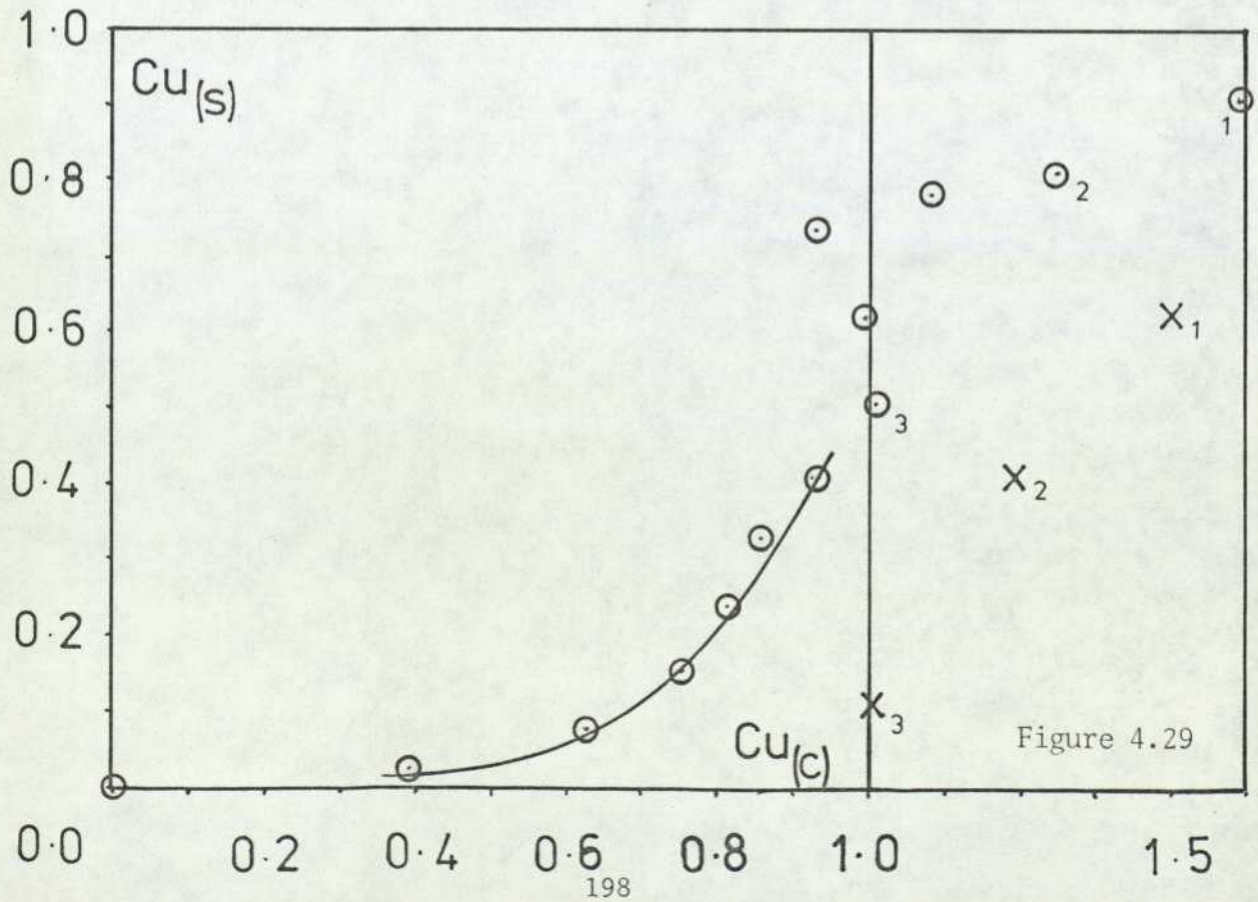


Figure 4.29

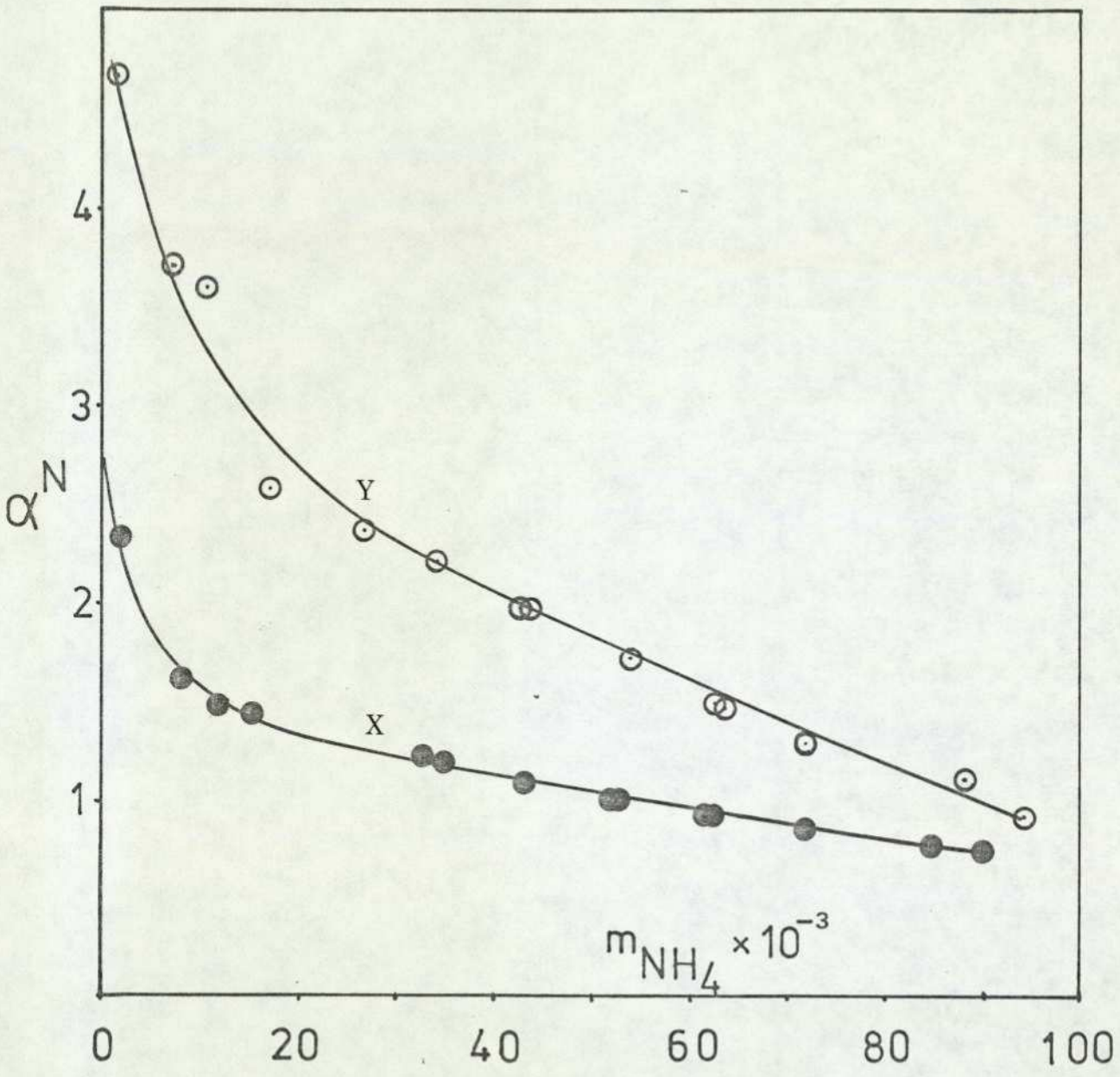


Plots of selectivity quotient $\alpha^N$ versus molarity of ammonium ion in solution for the $NH_4 \rightleftarrows Na$ equilibria. Figure 4.30

Plots of selectivity quotient $\alpha^N$ versus molarity of silver ion in solution for the Ag $\rightleftharpoons$ Na equilibria.

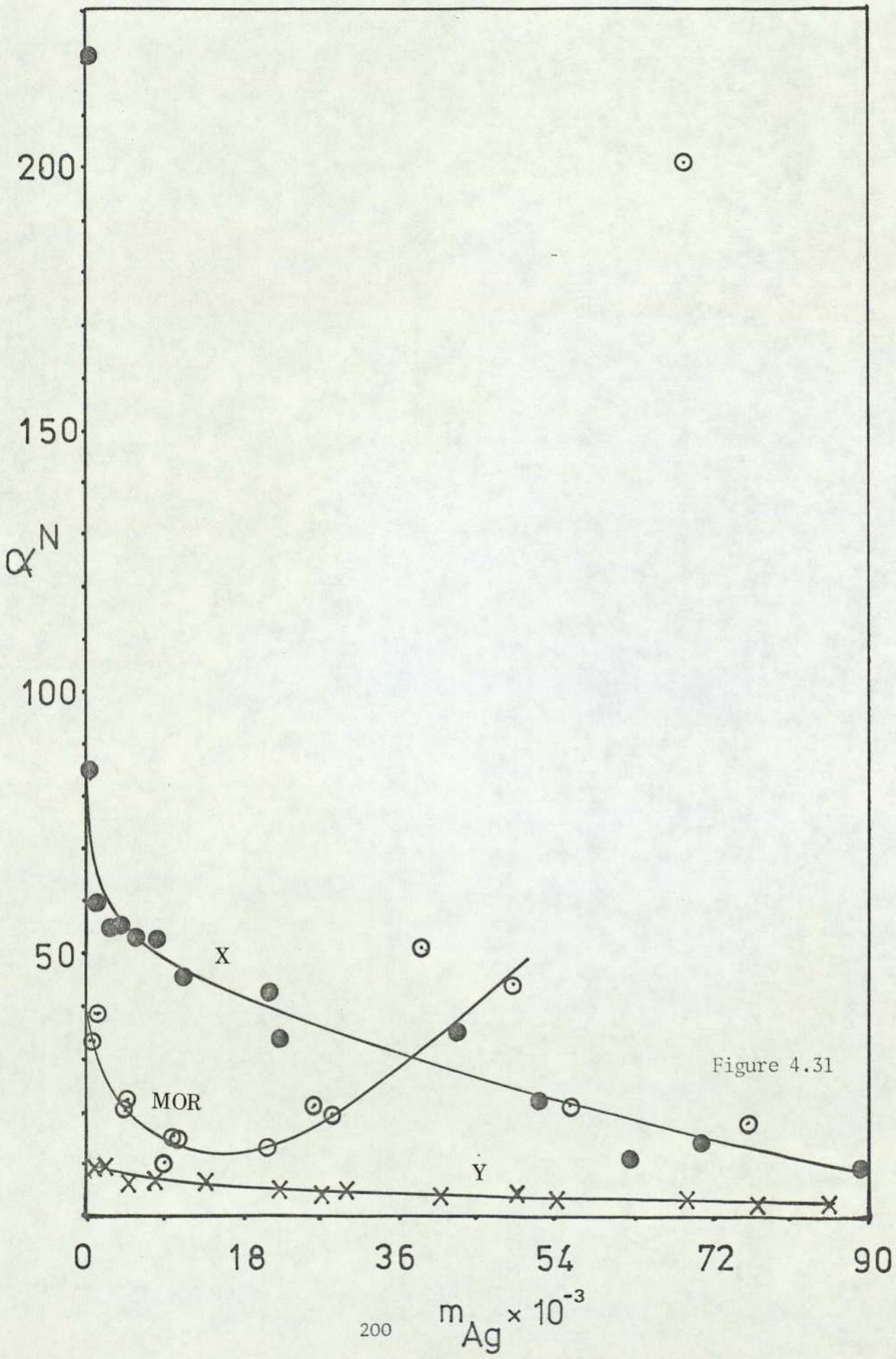


Figure 4.31

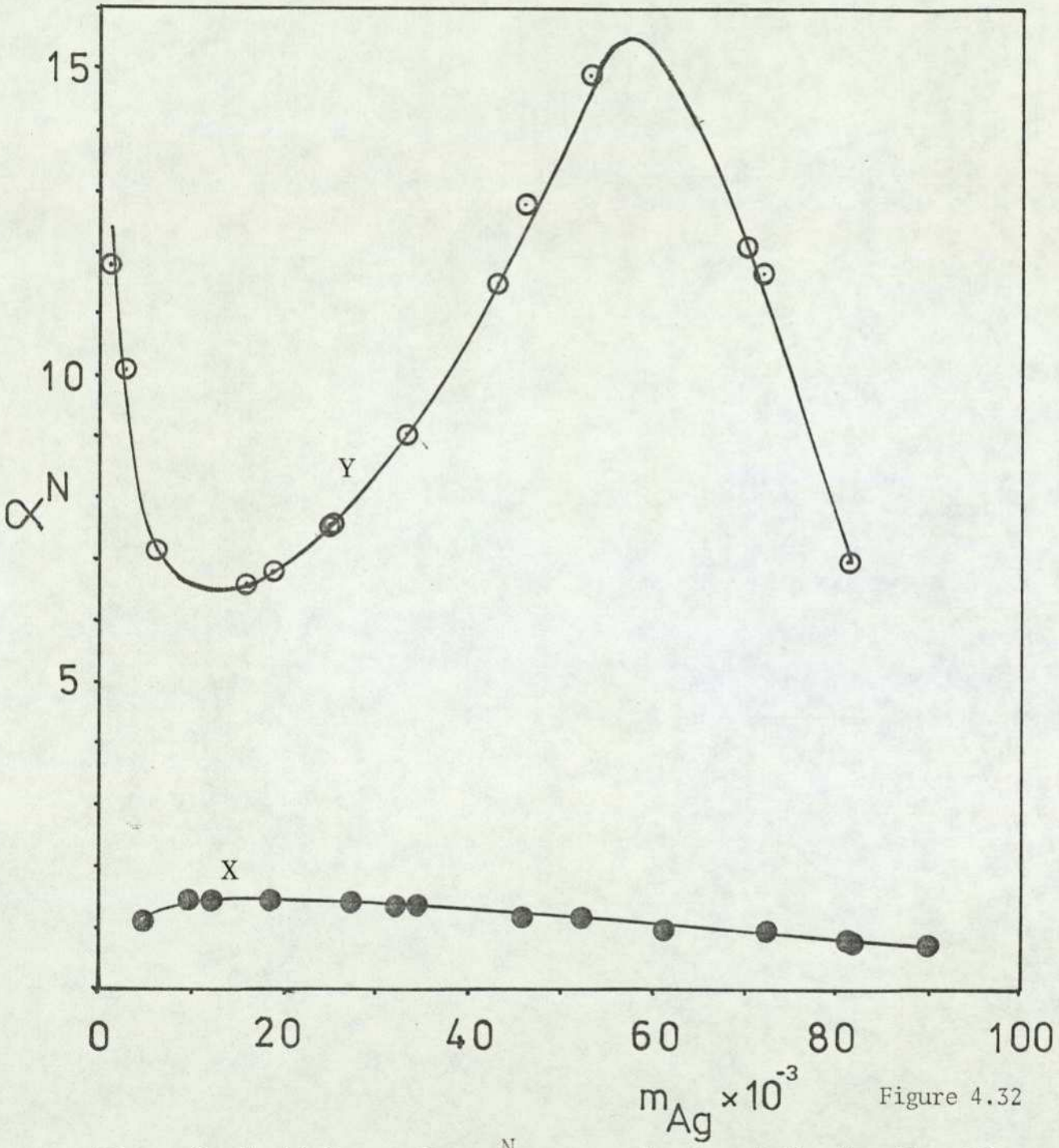


Figure 4.32

Plots of selectivity quotient $\alpha^N$ versus molarity of diamminesilver(I) in solution for the $Ag(NH_3)_2 \rightleftharpoons Na$ equlibria.

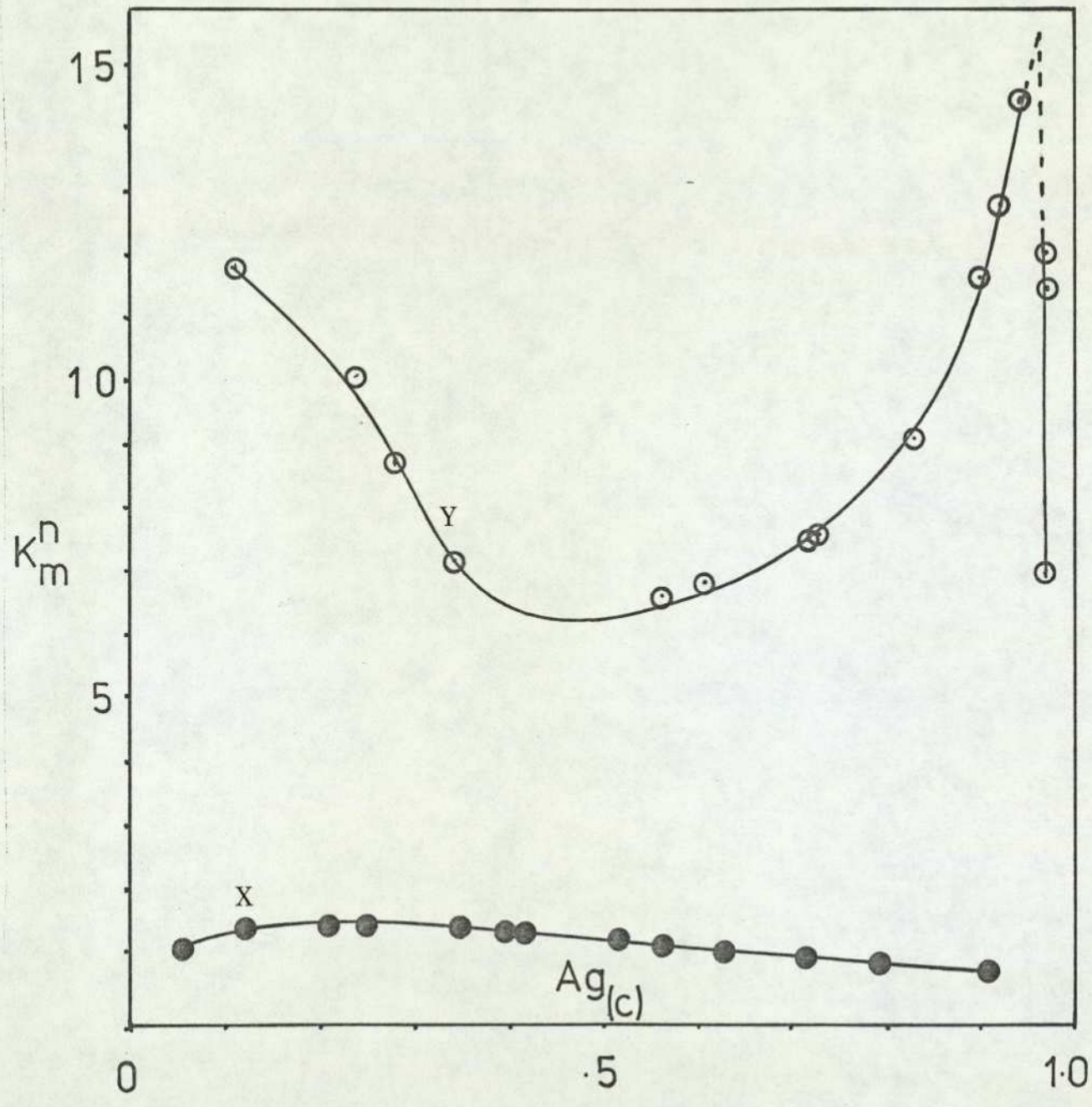


Figure 4.33

Plot of the normalised mass action quotient $K_m^N$ versus equivalent fraction of diamminesilver(I) in the zeolite phase for the $Ag(NH_3)_2 \rightleftharpoons Na$ equlibria.

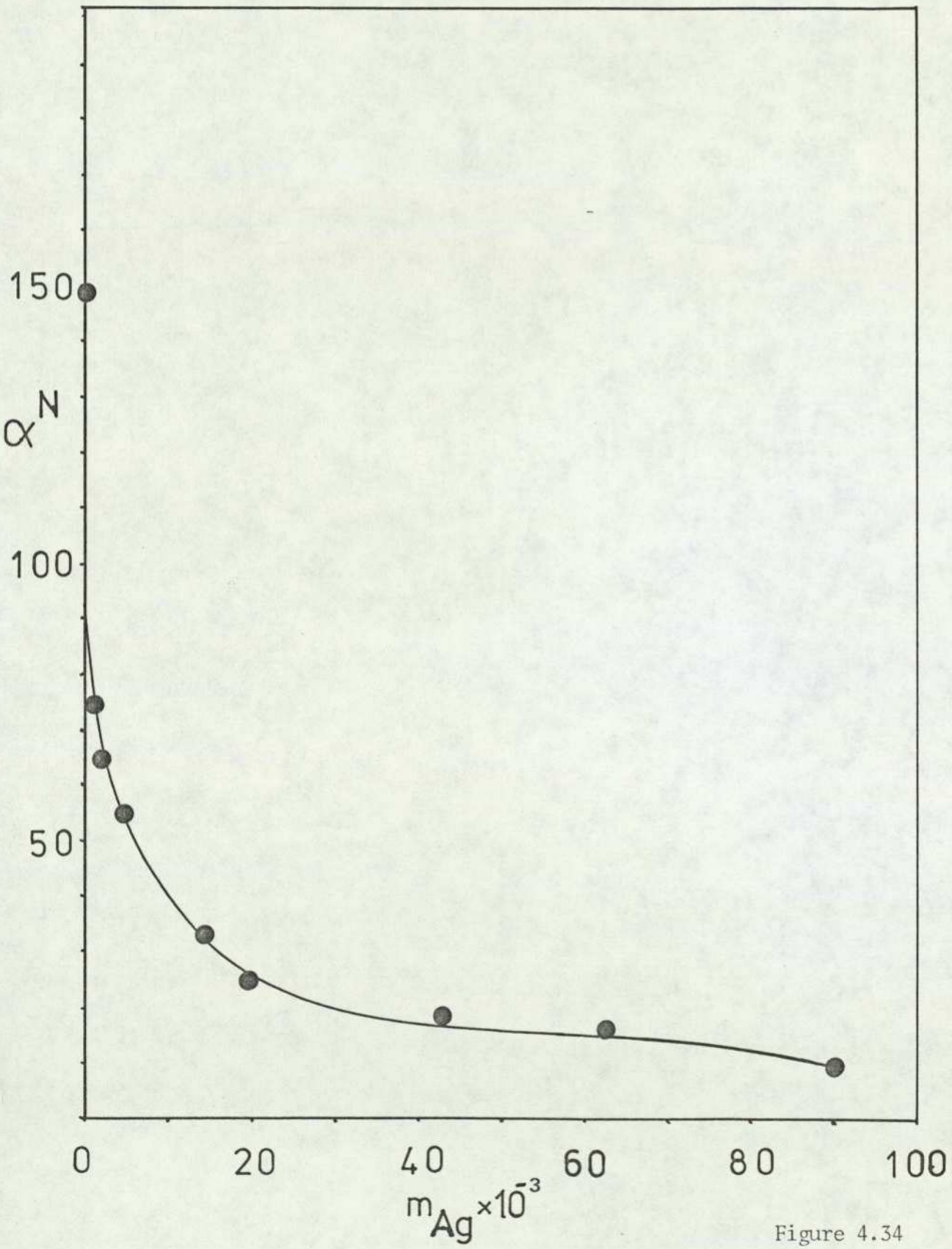


Figure 4.34

Plot of selectivity quotient $\alpha^N$ versus molarity of diamminesilver(I) in solution for the $Ag(NH_3)_2 \rightleftharpoons NH_4$ equilibria in mordenite.

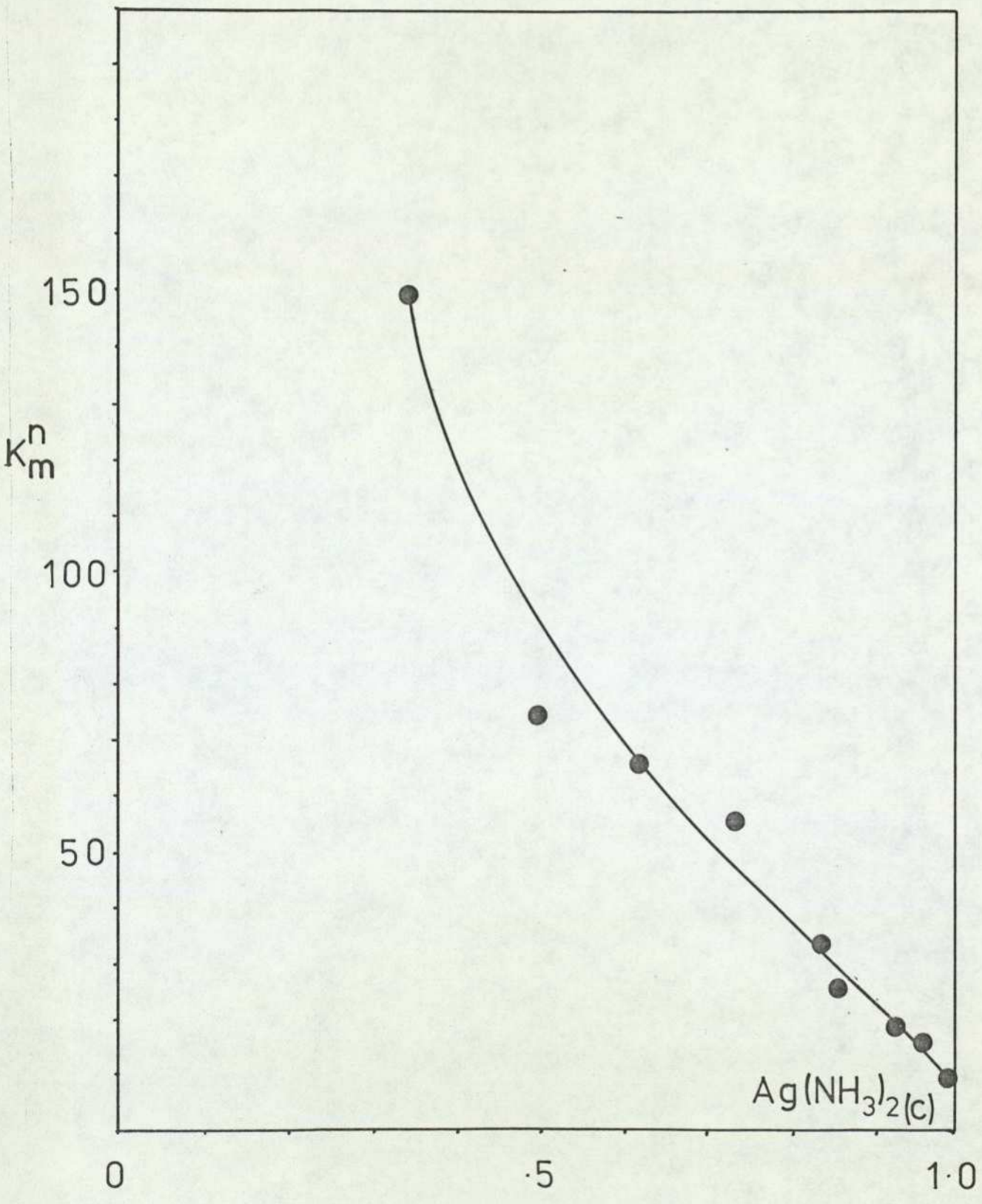


Figure 4.35

Plot of normalised mass action quotient $K_m^N$ versus equivalent fraction of diamminesilver(I) in the zeolite phase for the $Ag(NH_3)_2 \rightleftharpoons NH_4$ equlibria in mordenite.

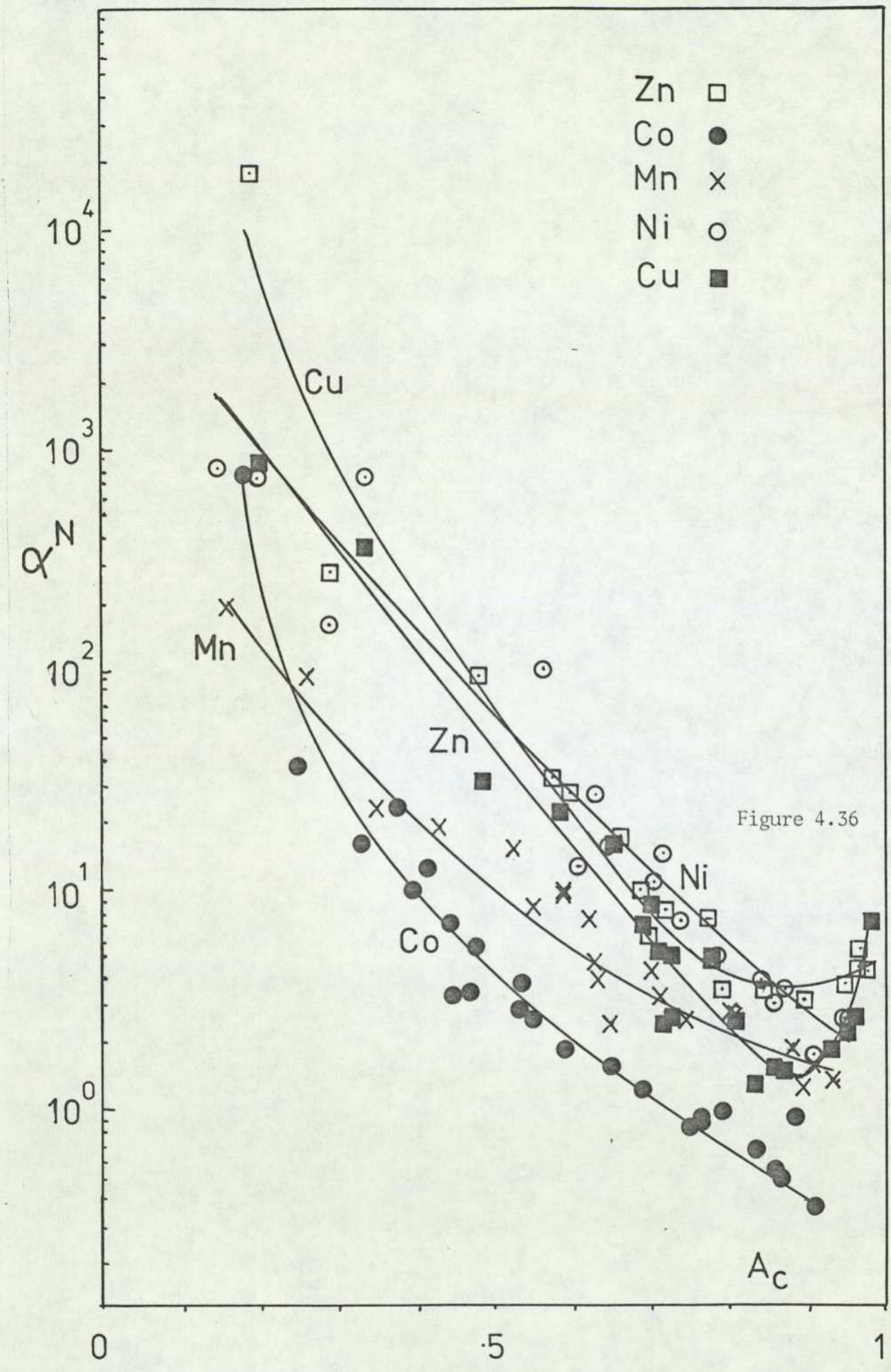


Figure 4.36

Plots of $\alpha^N$ versus $M_c$ for the first row transition metals in zeolite X

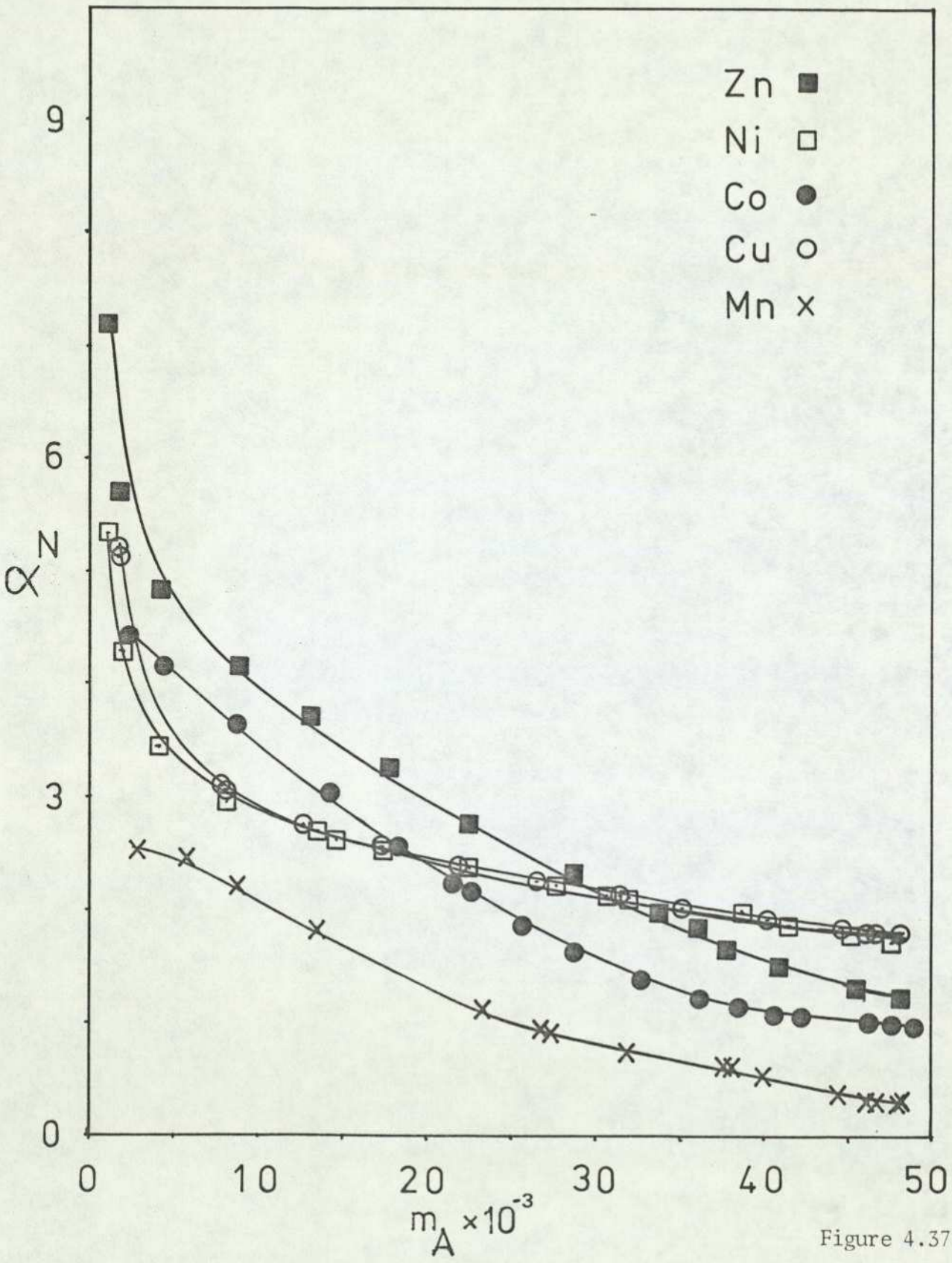


Figure 4.37

Plots of $\alpha^N$ versus molarity of transition metal ion in solution for the first row transition metal equilibria in ammonium Y

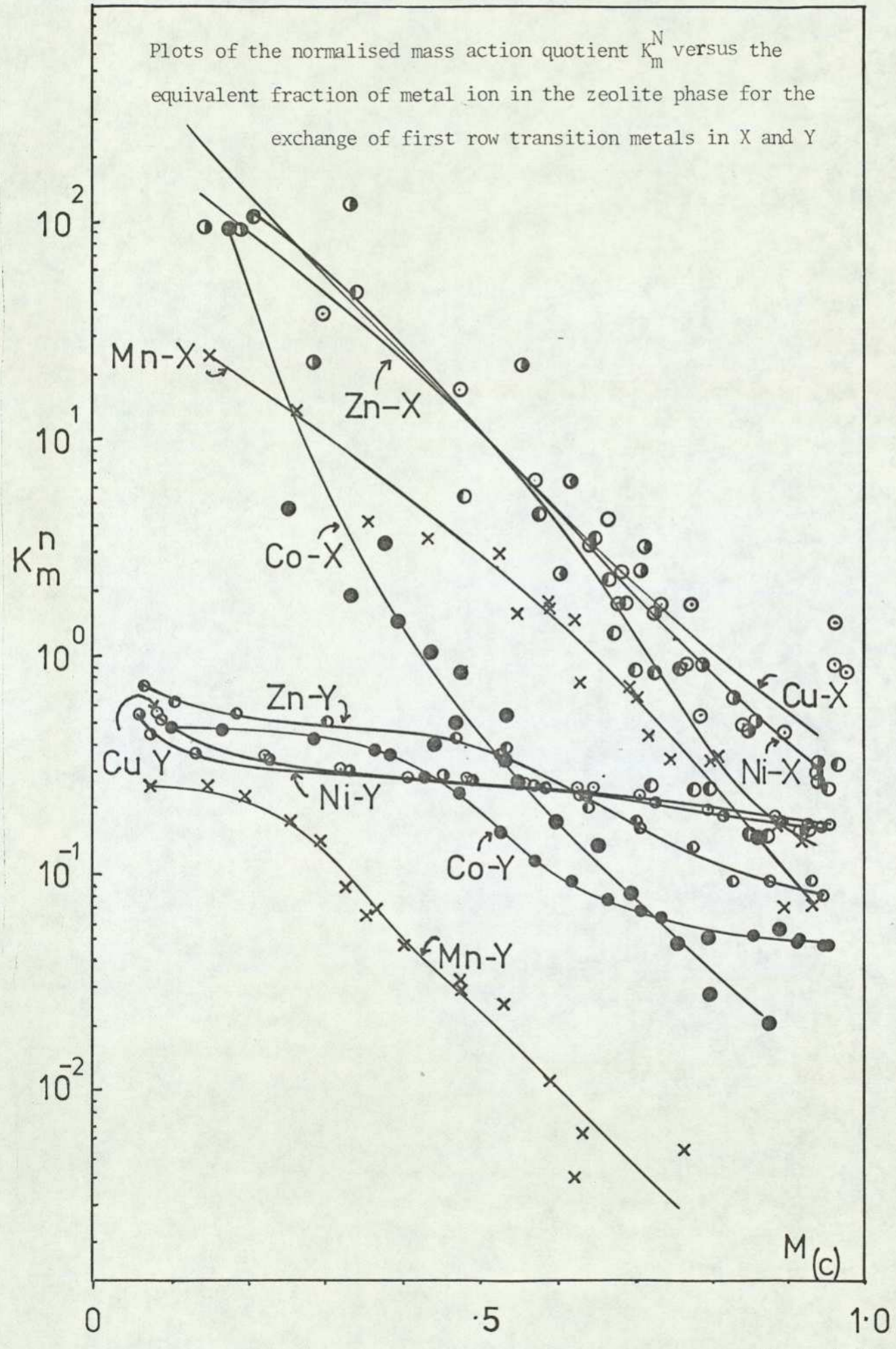
Plots of the normalised mass action quotient $K_m^N$ versus the equivalent fraction of metal ion in the zeolite phase for the exchange of first row transition metals in X and Y
$10^2$
$10^1$
$10^0$
$10^{-1}$
$10^{-2}$
$K_m^n$
Mn-X
Zn-X
Co-X
Cu-X
Ni-X
Zn-Y
Cu Y
Ni-Y
Co-Y
Mn-Y
$M_{(c)}$
0
·5
1·0

Figure 4.38

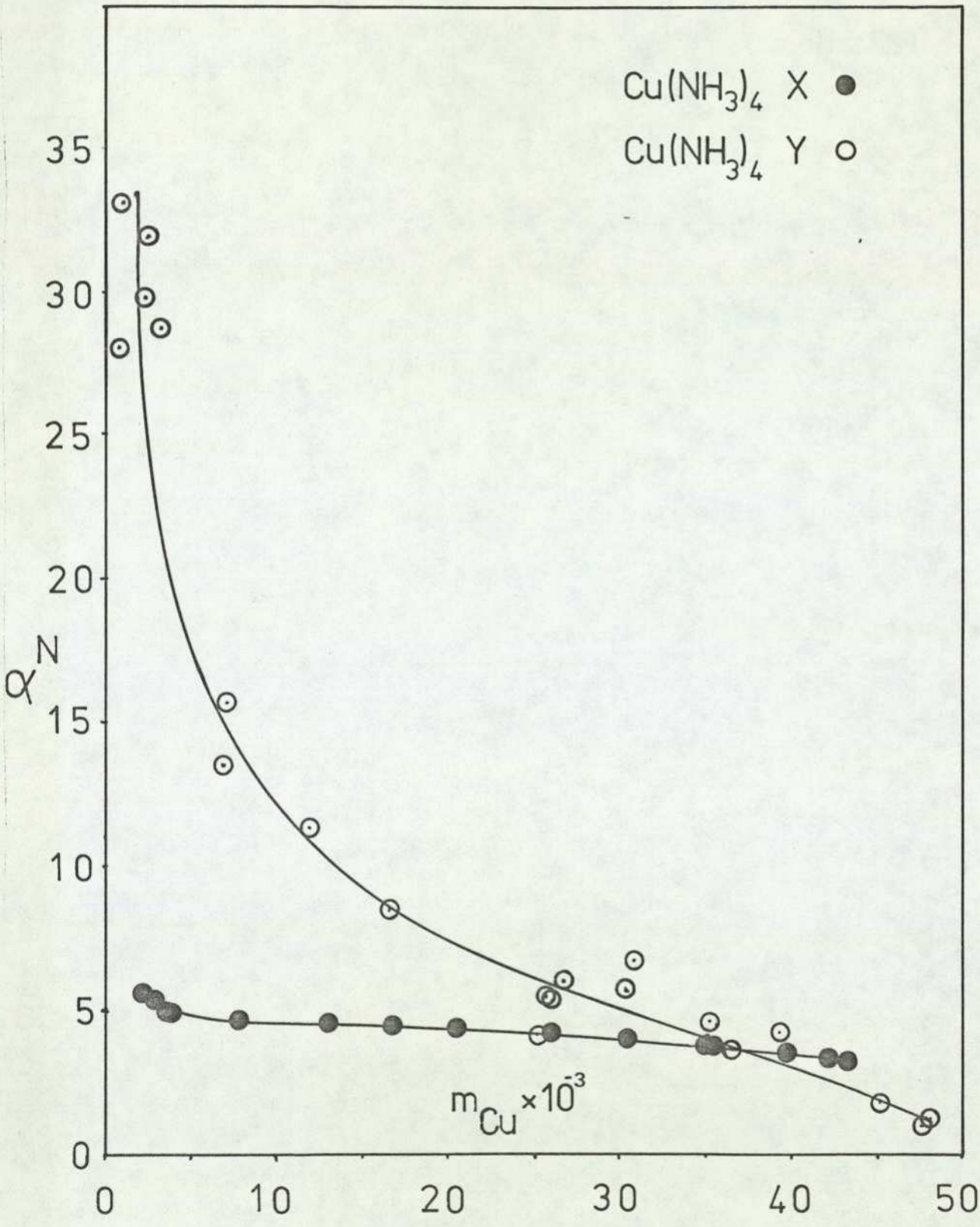


Figure 4.39

Plots of $\alpha^N$ versus molarity of tetramminecopper(II) in solution for the $Cu(NH_3)_4 \rightleftharpoons NH_4$ equlibria in X and Y.

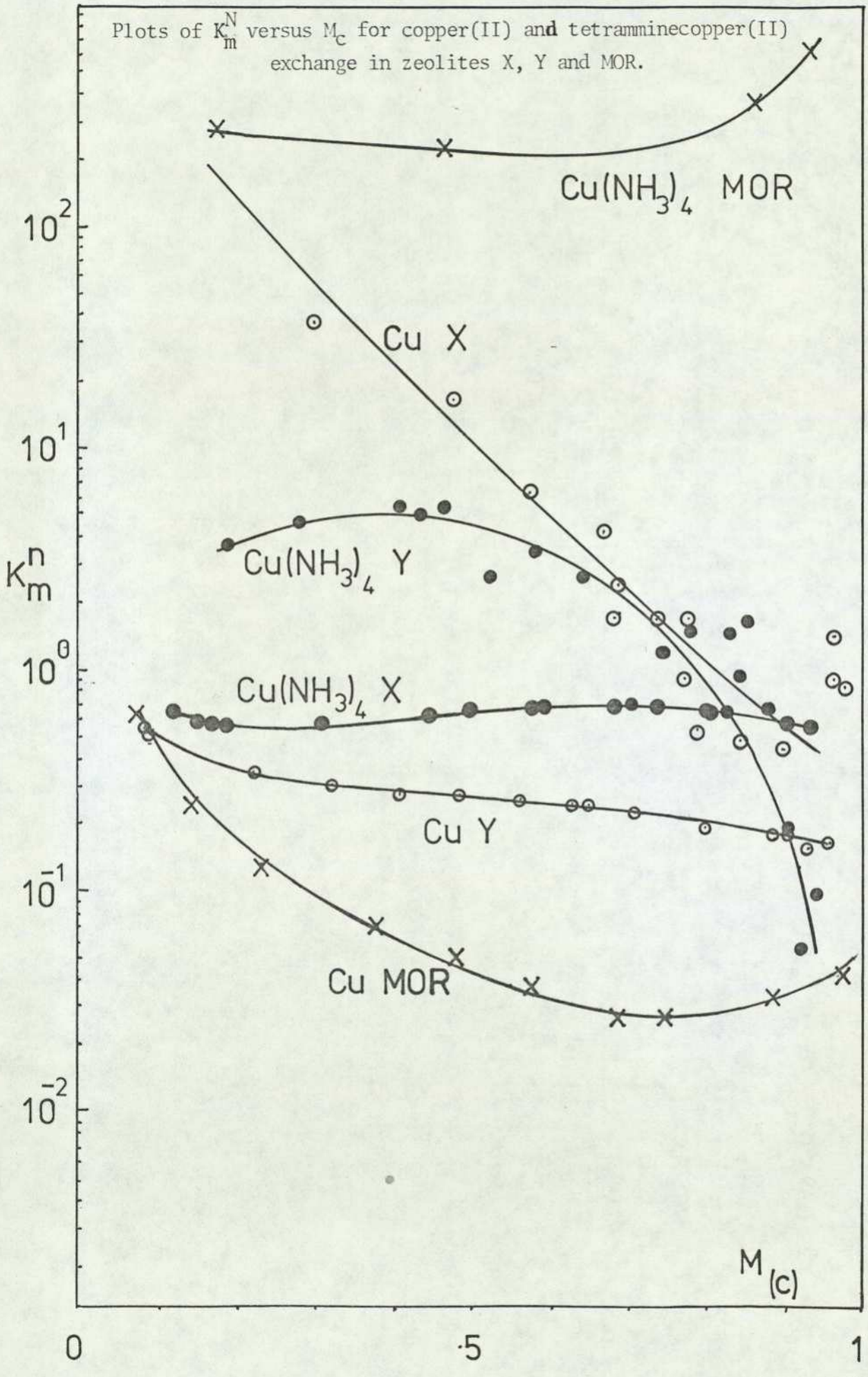
Plots of $K_m^N$ versus $M_c$ for copper(II) and tetramminecopper(II) exchange in zeolites X, Y and MOR.
$Cu(NH_3)_4$ MOR
Cu X
$Cu(NH_3)_4$ Y
$Cu(NH_3)_4$ X
Cu Y
Cu MOR
$K_m^n$
$10^2$
$10^1$
$10^0$
$10^{-1}$
$10^{-2}$
$M_{(c)}$
0
·5
1

Figure 4.40

Plots of $\alpha^N$ versus molarity of tetrammineplatinium(II) in solution for the $Pt(NH_3)_4 \rightleftharpoons$ Na or $NH_4$ equilibria .

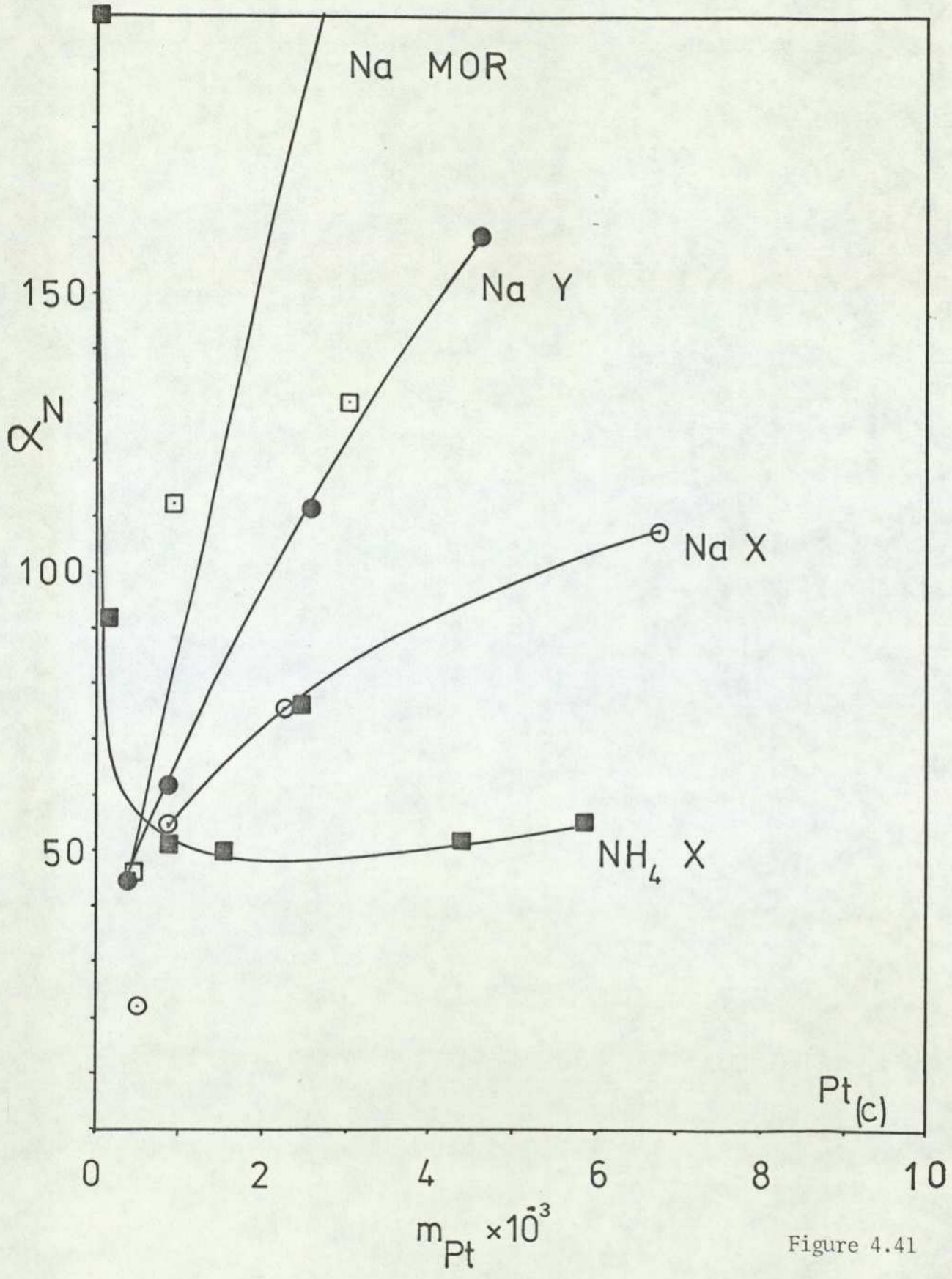


Figure 4.41

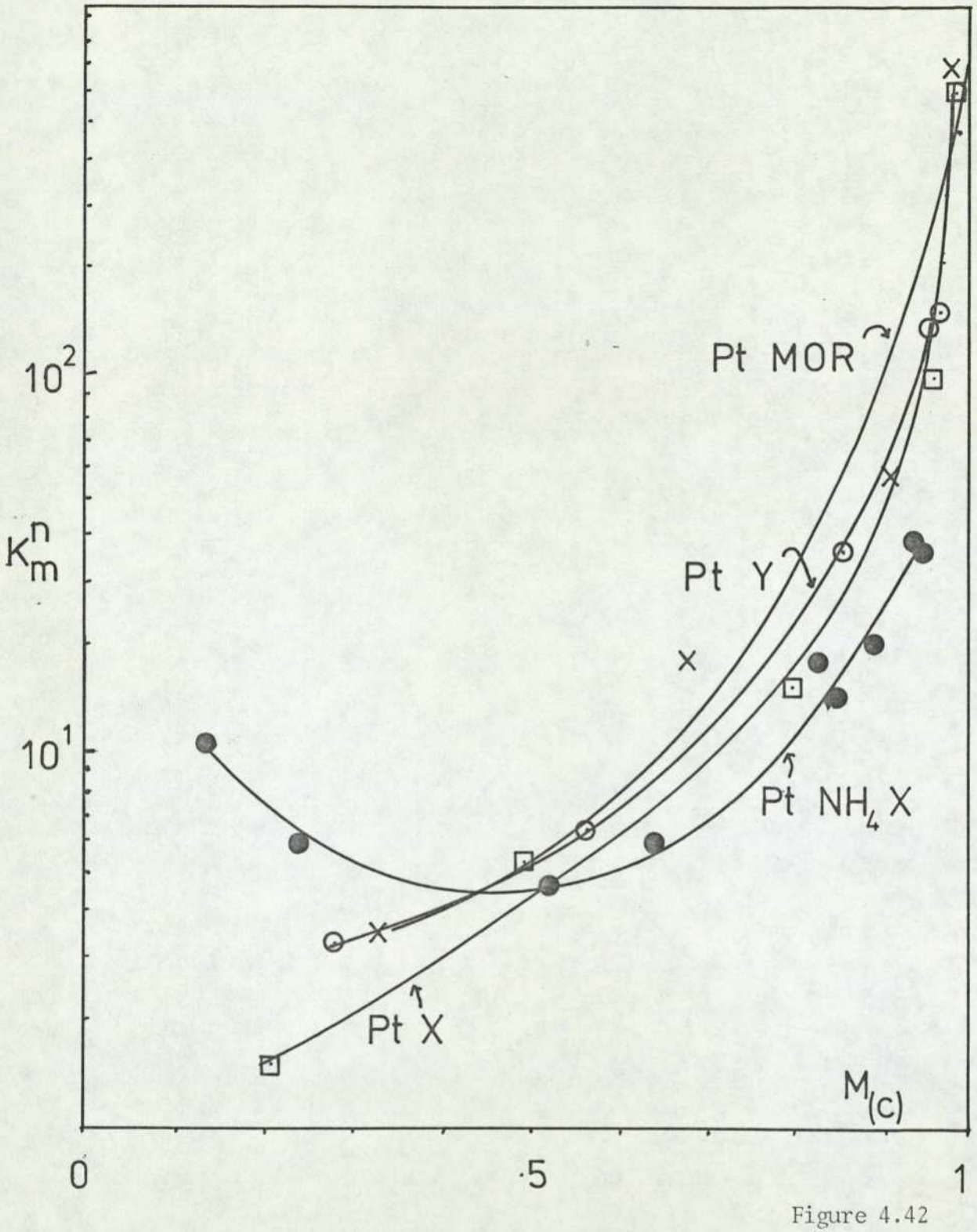


Figure 4.42

Plots of $K_m^N$ versus the equivalent fraction of tetrammineplatinum(II) in the zeolite phase foe the $Pt(NH_3)_4 \rightleftarrows$ Na or $NH_4$ equilibria.

The experimental error observed for the values of $K_m^N$ for the $Co \rightleftharpoons NH_4$ Equilibria in both X and Y.

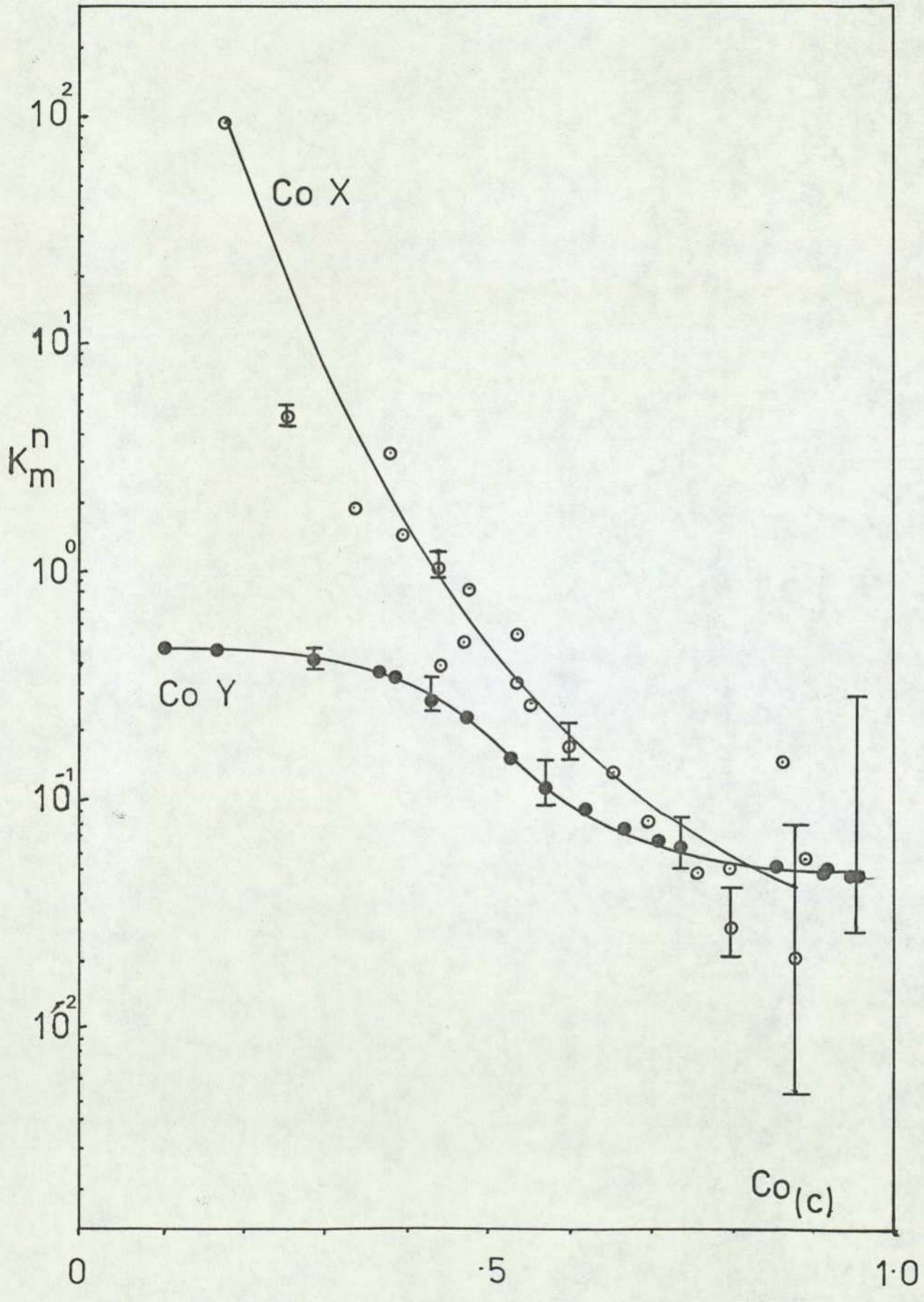


Figure 4.43

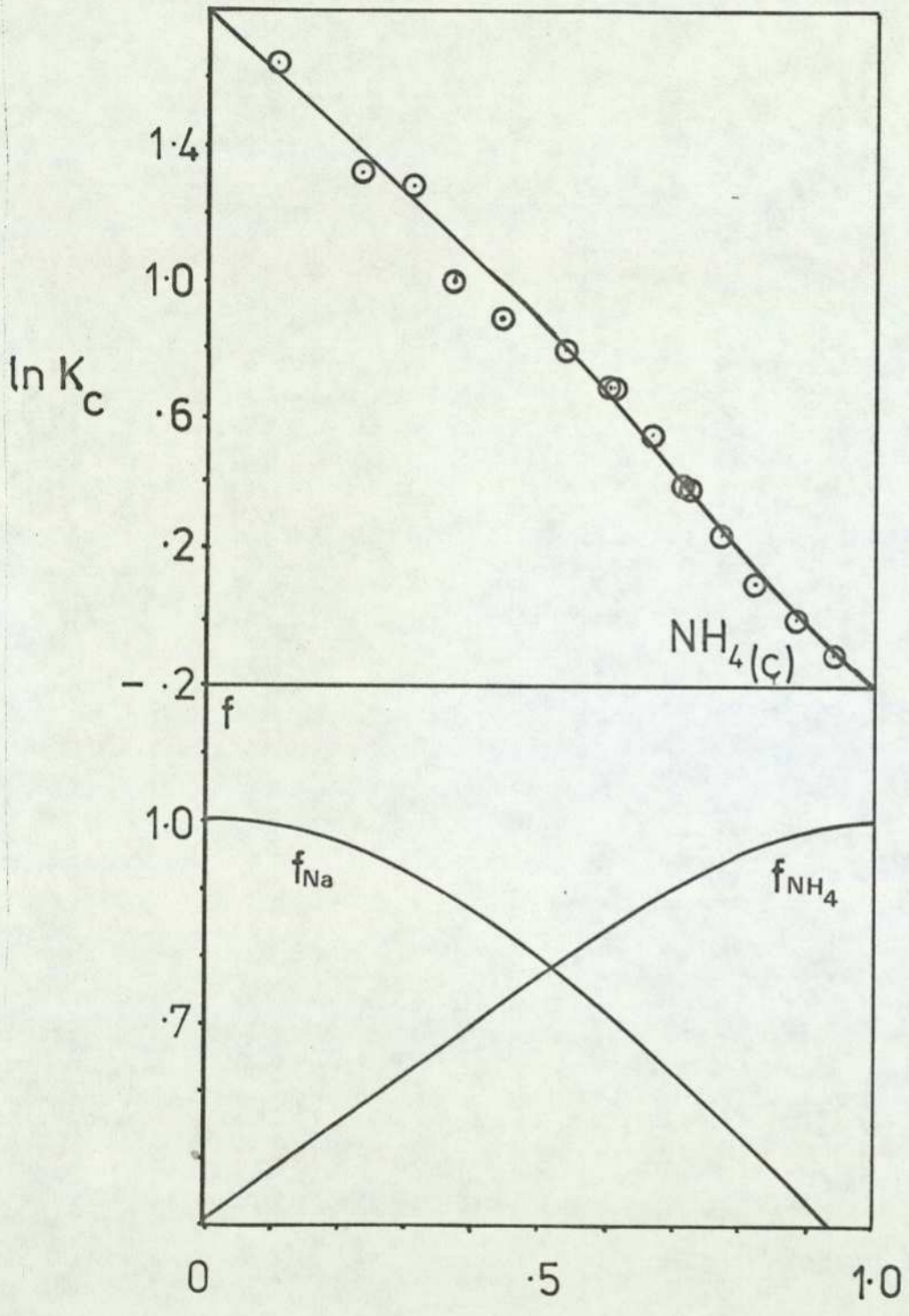


Figure 4.44

Kielland plot and plots of zeolite phase activity coefficients versus $NH_{4(c)}$ for the $NH_4 \rightleftharpoons$ Na equilibria in X.

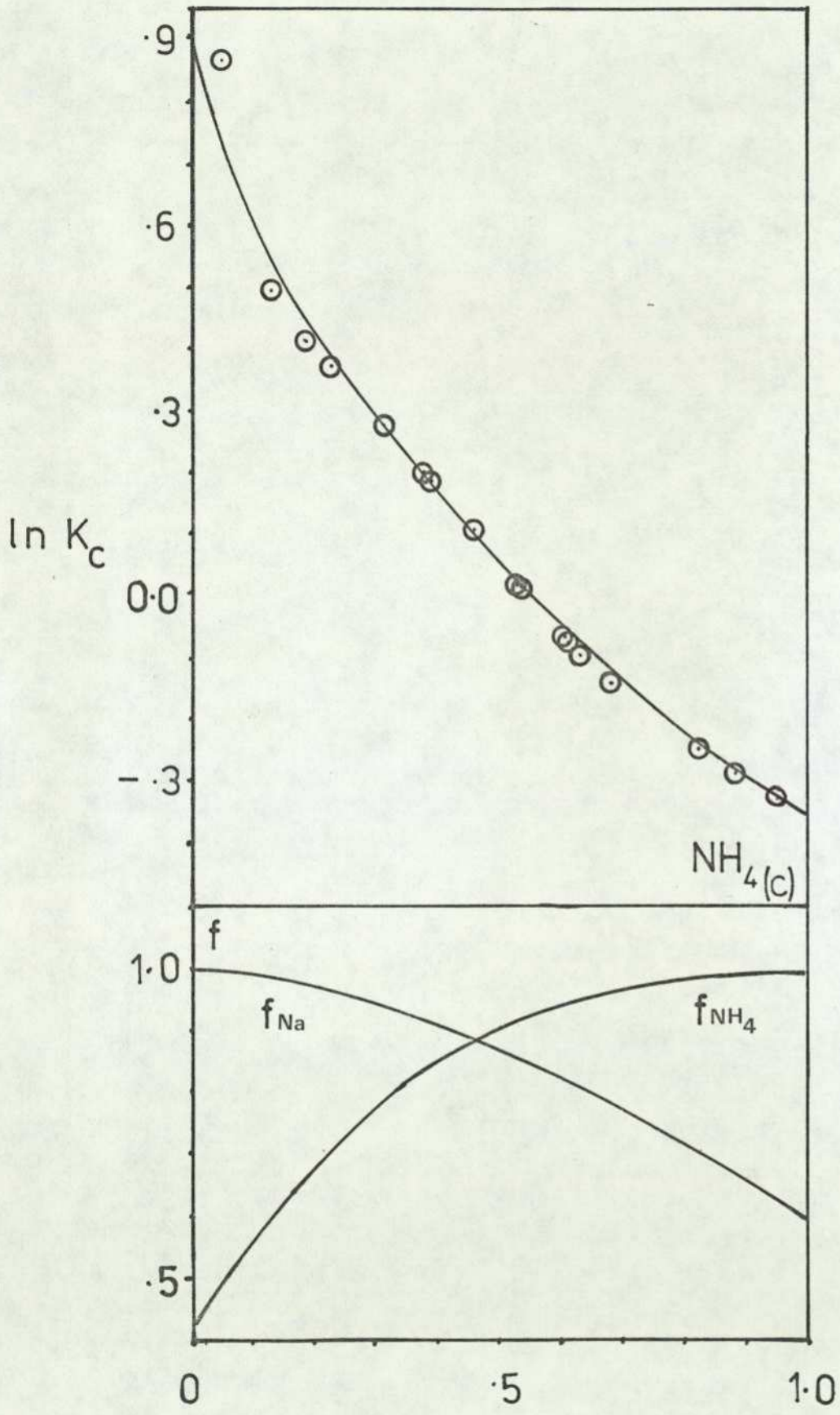


Figure 4,45

Kielland plot and plots of zeolite phase activity coefficients versus $NH_{4(c)}$ for the $NH_4 \rightleftarrows$ Na equilibria in Y.

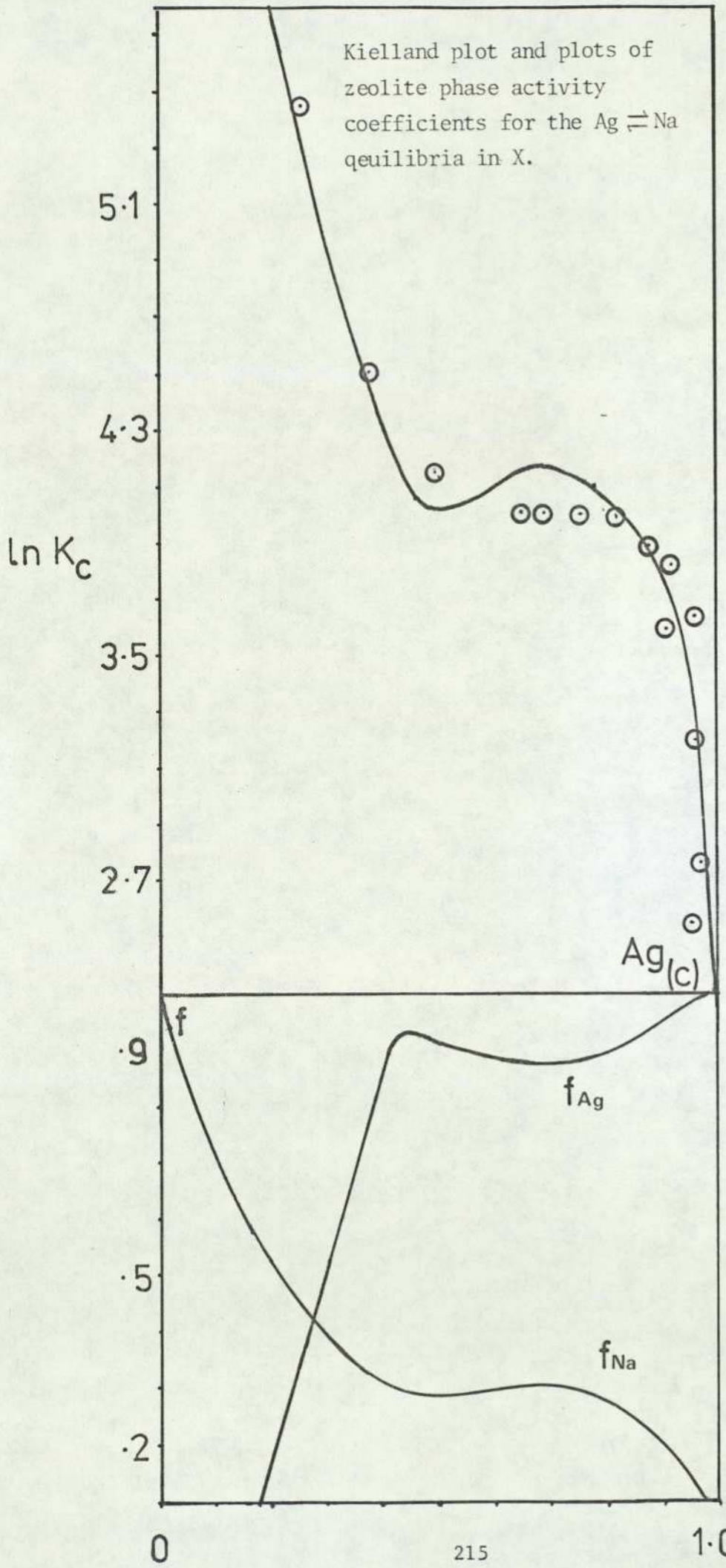
Kielland plot and plots of zeolite phase activity coefficients for the Ag ⇌ Na qeuilibria in X.
5·1
4·3
3·5
2·7
ln $K_c$
$Ag_{(c)}$
f
·9
·5
·2
$f_{Ag}$
$f_{Na}$
0
1·0

Figure 4.46

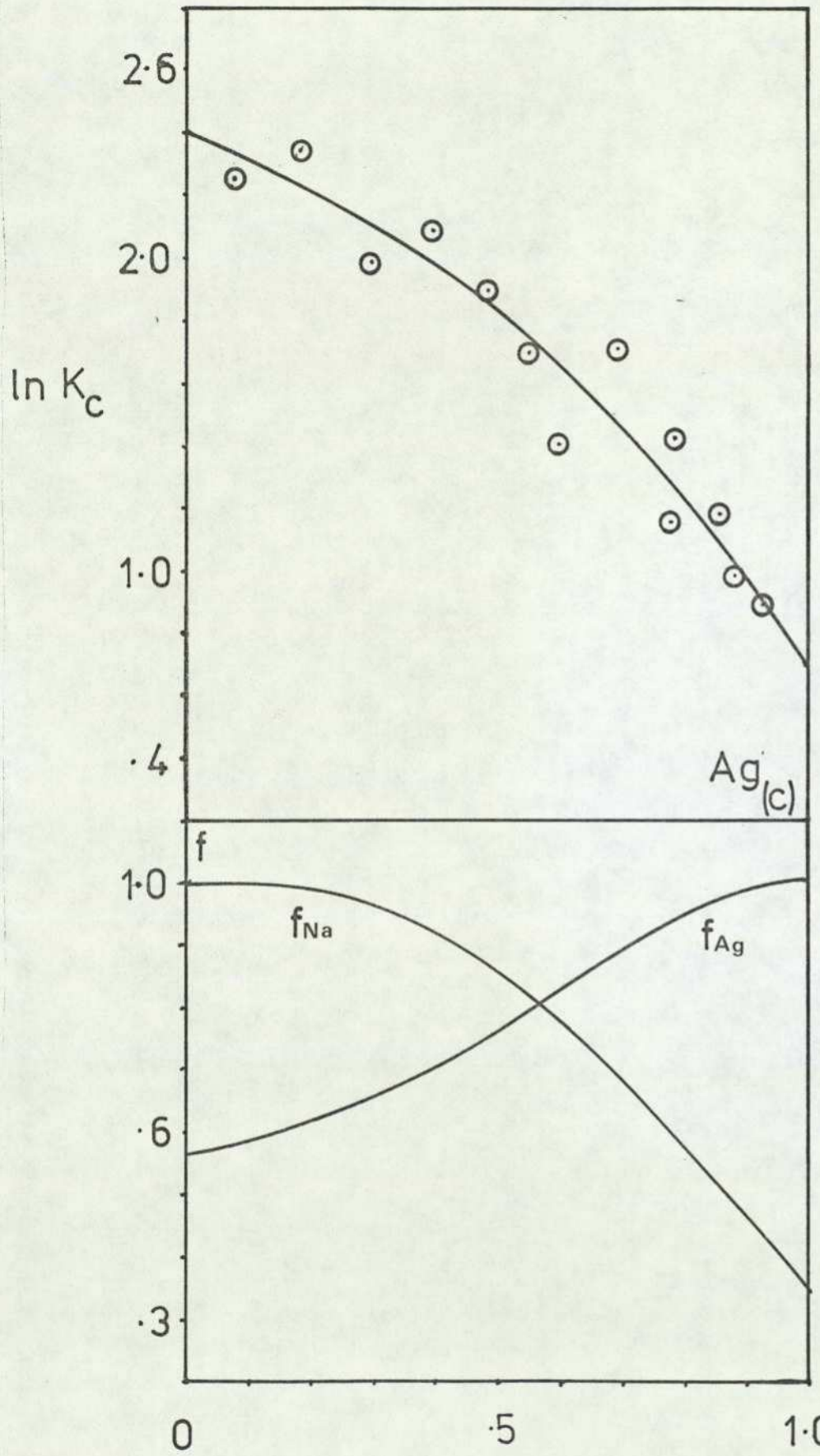


Figure 4.47

Kielland plot and plots of zeolite phase activity coefficients versus $Ag_{(c)}$ for the $Ag \rightleftharpoons Na$ equilibria in Y.

Kielland plot and plots of zeolite phase activity coefficients versus $Ag_{(c)}$ for the $Ag \rightleftharpoons Na$ equilibria in MOR.

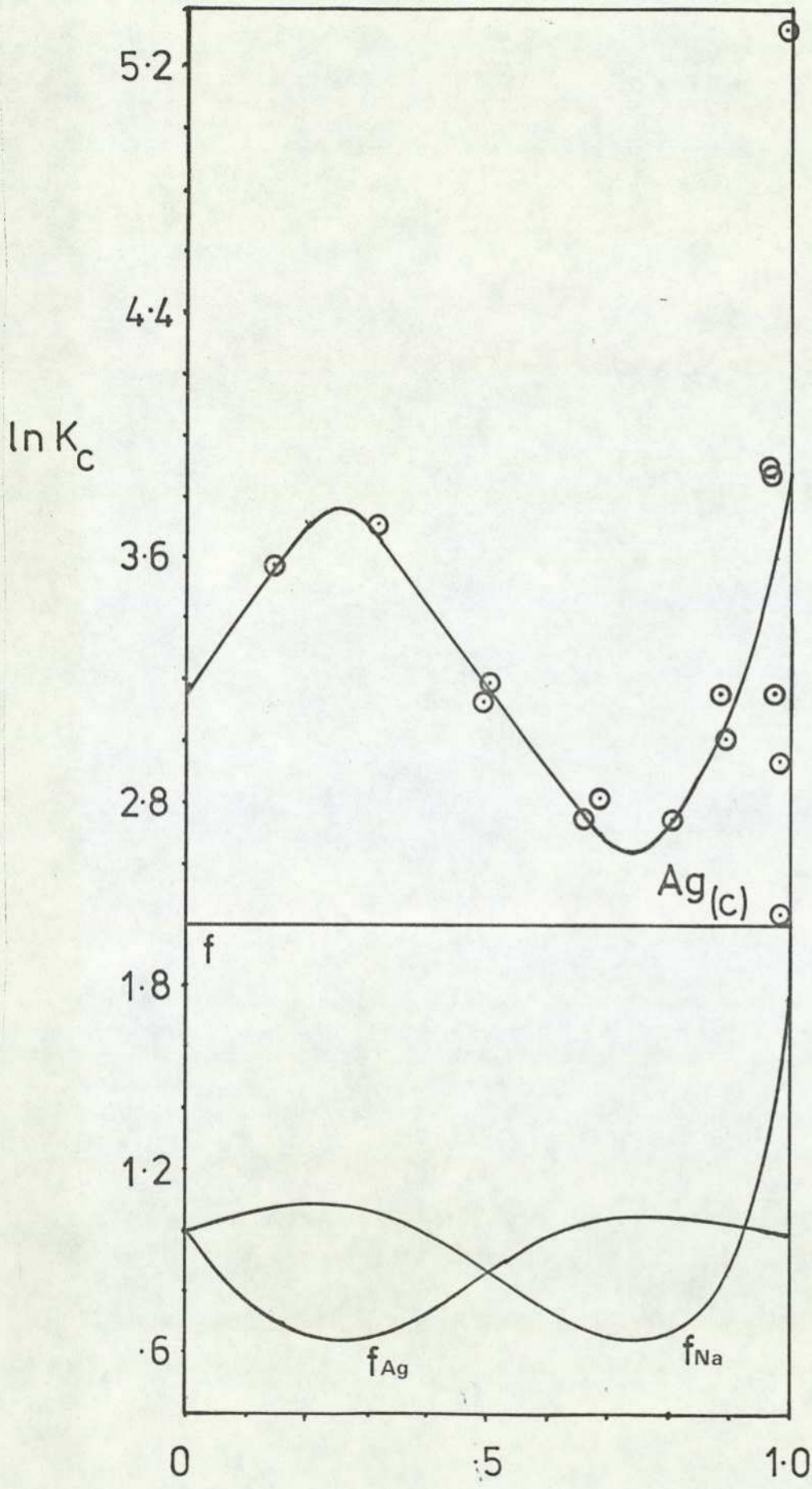


Figure 4.48

Kielland plot and plots of zeolite phase activity coefficients as in Figure 4.48 but with points $Ag_{(c)} \rightarrow 1$ removed.

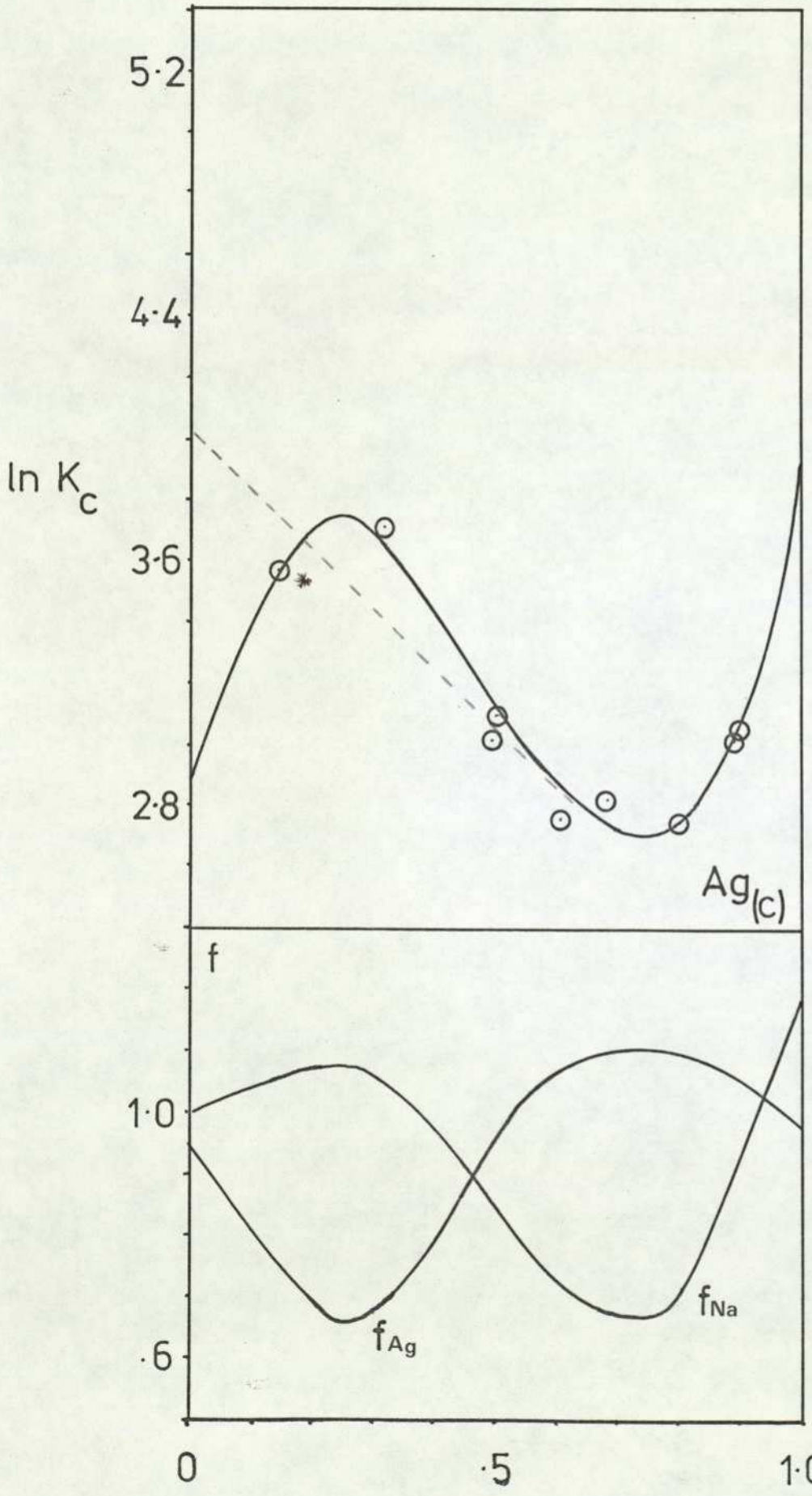


Figure 4.49

Kielland plot and plots of zeolite phase activity coefficients versus $Zn_{(c)}$ for the $Zn \rightleftharpoons NH_4$ equilibria in Y.

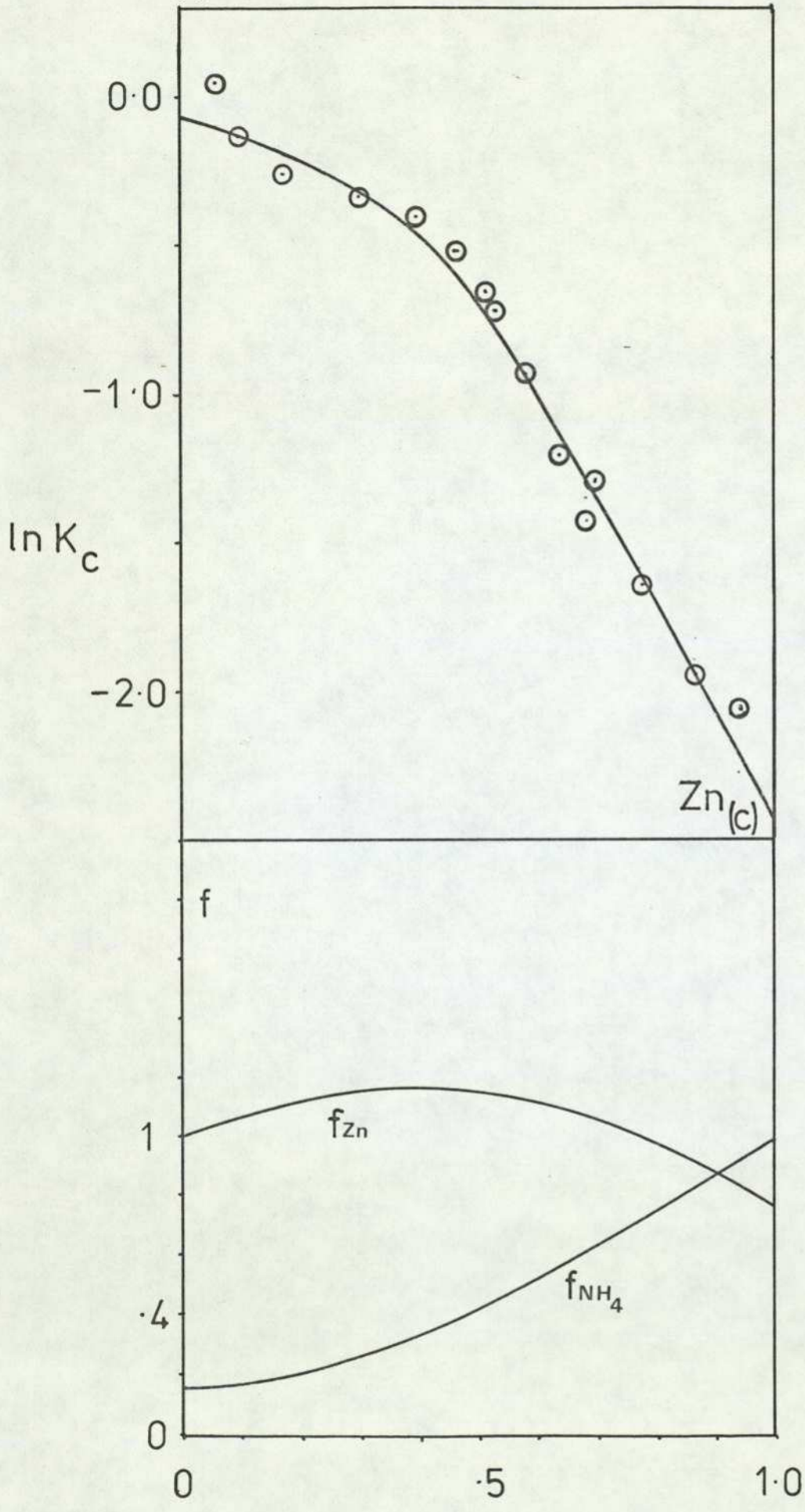


Figure 4.50

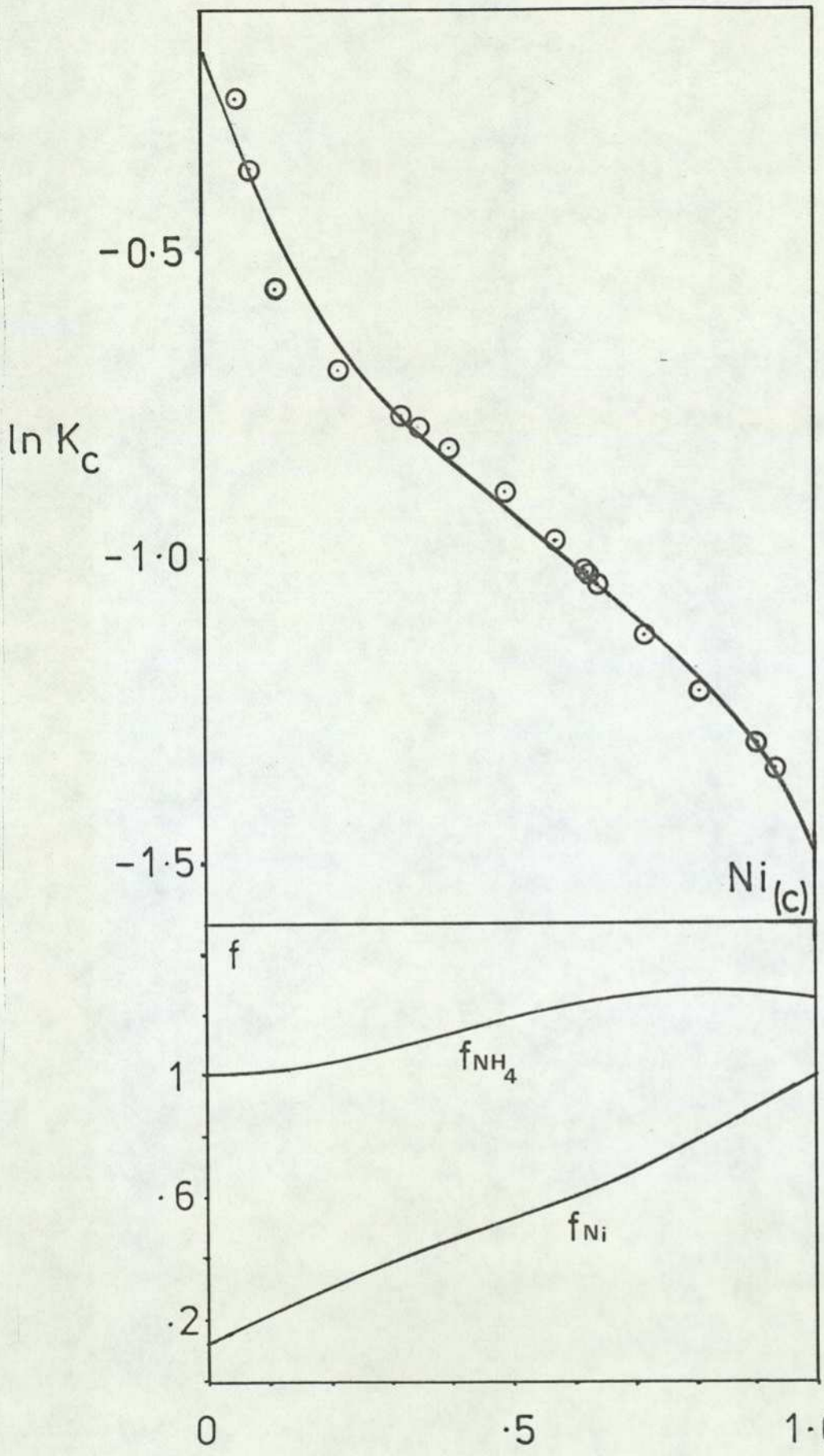


Figure 4.51

Kielland plot and plots of zeolite phase activuty coefficients versus $Ni_{(c)}$ for the $Ni \rightleftharpoons NH_4$ equilibria in Y.

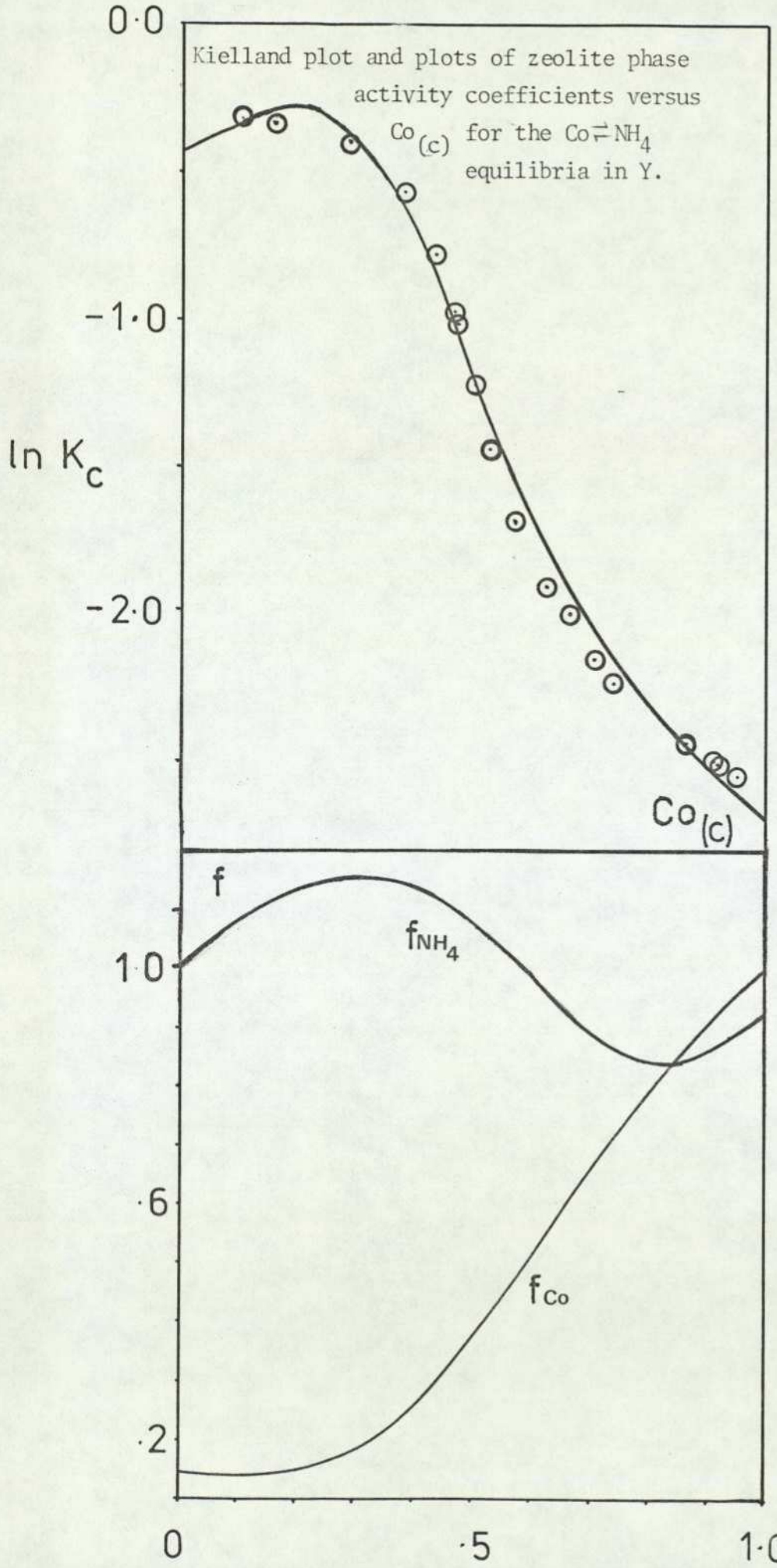
0·0
Kielland plot and plots of zeolite phase activity coefficients versus $Co_{(c)}$ for the $Co \rightleftharpoons NH_4$ equilibria in Y.
-1·0
ln $K_c$
-2·0
$Co_{(c)}$
f
$f_{NH_4}$
1·0
·6
$f_{Co}$
·2
0
·5
1·0

Figure 4.52

## 4.3. ION EXCHANGE ISOTHERMS AND DERIVED DATA.

This section is detailed under two headings dealing with uni-univalent exchange and uni-divalent exchange respectively.

### 4.3.1. Uni-Univalent Exchange.

Exchange isotherms for the ammonium / sodium exchange in zeolites Na-X and Na-Y (figures 4.1. and 4.2.) show no definite preference for either of the exchanging ions, in the case of X, whereas a slight preference for ammonium over sodium is shown by zeolite Y. The plots of selectivity versus solution concentration (figure 4.30) indicate again the greater preference for the ammonium ion in zeolite Y. Both selectivity plots show that the selectivity increases as the molarity of the ingoing ion in solution is lowered.

In both zeolites ion exchange at low exchange levels of ingoing cation is likely to involve primarily the sodium ions in sites IV and V, which can be considered to be almost completely hydrated species. In this situation the zeolite would be expected to prefer the ion with the lower hydration energy, which on the grounds of charge density is the ammonium ion.

The Kielland plots for both systems (figures 4.44 and 4.45) show trends closely reflecting the selectivity curves; in both cases the plots approach linearity. The zeolite phase activity coefficients show marked deviations from ideality.

Equilibrium studies for the silver$_{(aquo)} \rightleftharpoons$ sodium systems in zeolites

X, Y and MOR (figures 4.3.,4.4. and 4.5.) indicate a preference for silver ions over the sodium ions. 100% replacement of sodium by silver can be effected in zeolites X and Y, whereas 90% removal of sodium ions only was obtained in sodium mordenite. This figure agrees with the previously reported value for Ag-MOR[25]. The plots of selectivity (figure 4.31) show in the case of zeolite Y that monotonic increases in selectivity occur with both decreasing level of silver exchange or with concentration of silver ions in solution. The trend is not so clear in the case of mordenite; very high selectivity values are seen at low levels of ion exchange, followed by a plateau in the region Ac = 0.5 to Ac = 0.8. At higher values of $A_c$ a constant decrease in selectivity occurs as the level of ion exchange tends to 100%.

The selectivity plot for Na-X (figure 4.31) compares well with the earlier work of Sherry[29], but the earlier work did not however show values for selectivity at low levels of ion exchange. It is tempting to interpret the exchange behaviour in terms of ion exchange into three distinct site sets as was done in previous work[29]. The high selectivity in the region below 40% exchange would then be attributed to a preference for the ion of lowest free energy of hydration (in this case silver[87]) and selectivity at higher regions of exchange would be interpreted in the same manner as Sherry[29]. If the interpretation is as simple as this model suggests then we should observe similarly high selectivities for the silver ion in sodium Y at low levels of silver exchange, but this is not observed. A further point is that recent X-ray data[46] indicate that 32 sodium ions in the supercages of zeolite are associated with site III' and therefore cannot justifiably be considered to be purely hydrated species. Thus any interpretation must involve consideration of interactions between ions, intracrystalline water mol-

ecules and the zeolite framework oxygens.

The Kielland plots for the silver $\rightleftharpoons$ sodium equilibria in X, Y and MOR broadly reflect, as would be expected, the shape of the selectivity coefficients. The Kielland plot for Ag-MOR (figure 4.48) shows considerable experimental scatter in the region $Ac \rightarrow 1$. A second Kielland plot for this system was constructed by omitting these ambiguous points (figure 4.49). The best-fitting polynomial equation used to represent these data is hardly different to the polynomial used for the original data which included the ambiguous data points. A very significant data point is however, in the region $Ac \rightarrow 0$ marked *. This point causes the best-fitted polynomial equation to show decreasing values of $\ln K_c$ as $A_c \rightarrow 0$. An alternative extrapolation marked ------- would increase the area under the curve between $A_c = 0$ and $A_c = 1$. It is estimated that this would only increase the value by approximately 3%, causing an insignificant increase in the value of $\Delta G^{\ominus}$.

The zeolite phase activity coefficient values for zeolite X show a dramatic decrease as $Ag_c$ tends to zero. The high selectivity for silver ions in this region and consequently the increased experimental error throw some doubt on the validity of these points, but an assessment of experimental error indicates that the general trend is correct.

The ion exchange isotherms involving the silver(I) diammine ion show that mordenite is highly selective for the complexed silver ion (figure 4.6.) with a maximal level of exchange for silver of $\sim 75\%$. Zeolites X and Y (figures 4.7. and 4.8.) show a much lower preference for the complexed silver ion than in mordenite, with a maximum level of exchange of about 55% in both cases. An ion sieving effect is possible

in these cases, which prevents the $Ag(NH_3)_2^+$ ions from entering the sodalite cages, accompanied by incomplete removal of the supercage sodium ions. Selectivity plots for the diamminesilver(II) $\rightleftharpoons$ sodium equilibria (figures 4.32. and 4.33.) indicate a smooth increase in selectivity with decreasing $Ag_c$ values in zeolite X, whereas the comparable selectivity plot in Y (figure 4.33) shows a distinct change in trend at about 50% exchange (based on the normalised isotherm). The dramatic drop in selectivity as Ac $\rightarrow$0 is most likely due to experimental error in the estimation of the equivalent fraction of sodium ions in the zeolite phase.

Interpretation of these isotherms in terms of exchange with sodium ions into various sites would imply that the exchange in zeolite Y involved at least two distinct ion sites within the supercages. However, the present X-ray data for Na-Y[47] indicate that only one crystallographic site in the supercages is populated with sodium ions. This indicates that simple analyses in terms of sodium site populations are not necessarily applicable without suitable prior knowledge of ion site populations over a range of equilibrium positions throughout the isotherm.

### 4.3.2. Uni-Divalent Exchange.

The most characteristic feature of the isotherms constructed for the exchange of hydrated transition metal ions in X and Y is the sigmoidal shape (figures 4.10 to 4.19). Barrer and Klinowski [60] have shown that sigmoidal isotherms are characteristic of uni-divalent ion exchange and are not open to interpretation simply in terms of ion exchange into discrete sites.

Partial irreversibility was observed with the first-row transition

Table 4.15. Selectivity Trends

| Equilibria | Selectivity Trend |
|---|---|
| $Cu(NH_3)_4 \rightleftharpoons NH_4$ | MOR† >> Y > X |
| $Ag(NH_3)_2 \rightleftharpoons Na$ | MOR >> Y > X |
| $Pt(NH_3)_4 \rightleftharpoons Na$ | MOR > Y > X |
| $Pd(NH_3) \rightleftharpoons Na$ | MOR > Y > X |
| $Ag \rightleftharpoons Na$ | X>> MOR > Y |
| $Cu \rightleftharpoons NH_4$ | X > Y > MOR† |
| $Co \rightleftharpoons NH_4$ | X > Y > MOR† |
| $Mn \rightleftharpoons NH_4$ | X > Y > MOR† |
| $Ni \rightleftharpoons NH_4$ | X > Y > MOR† |
| $Zn \rightleftharpoons NH_4$ | X > Y > MOR† |

† Data from a source other than this study

Table 4.16. $\Delta G^{\ominus}$ and $K_a$ for $Ag \rightleftharpoons Na$ equilibria.

| Zeolite | Ka | $\Delta G^{\ominus}$/kJ(g.equiv.)$^{-1}$ |
|---|---|---|
| X | 95.87 | -11.27 |
| Y | 5.75 | -4.32 |
| MOR | 24.99 | -7.95 (-7.98*) |

Table 4.17. $\Delta G^{\ominus}$ and $K_a$ values for $NH_4 \rightleftharpoons Na$ equilibria

| Zeolite | Ka | $\Delta G^{\ominus}$/kJ(g.equiv.)$^{-1}$ |
|---|---|---|
| X | 1.10 | -0.24 |
| Y | 2.25 | -1.99 |

Table 4.18. $\Delta G^{\ominus}$ and $K_a$ values for 1st row transition metal equilibria with ammonium in zeolite Y.

| Metal | $K_a$ | $\Delta G^{\ominus}$/kJ(g.equiv.)$^{-1}$ |
|---|---|---|
| Co | 0.0956 | 2.89 |
| Ni | 0.151 | 2.33 |
| Zn | 0.151 | 2.33 |
| Mn | 0.0156 | 5.14 |

Table 4.19. Affinity sequence for transition metal ions

| Zeolite | Affinity sequence |
|---|---|
| X* | $Ag >> NH_4$ |
| Y* | $Ag > NH_4 > Mn > Ni > Zn > Co$ |
| Y* | $Mn > Ni > Zn > Co$ |

* With respect to the sodium form of X and Y having values of $\Delta G^{\ominus}$ for the first row transition metals calculated via the triangle rule.

* With respect to the ammonium zeolite.

Table 4.20. Selectivity sequence for transition metal ions

| Zeolite | Selectivity sequence |
|---|---|
| $X(NH_4)$ | $Cu > Ni > Zn > Mn > Co > Cu(NH_3)_4$ |
| X(Na) | $Pt > Ag > Ag(NH_3)_2 > NH_4$ |
| $Y(NH_4)$ | $Cu(NH_3)_4 > Zn > Ni > Cu > Co > Mn$ |
| Y(Na) | $Pt > Ag(NH_3)_2 > Ag > NH_4$ |
| MOR(Na) | $Ag(NH_3)_2 > Pt > Ag$ |

metals in X. This irreversibility was particularly noticeable at high transition metal ion loadings. (NB. The subscripted numbers on points in the isotherm plots (figures 4.10 to 4.19) enable the reverse points to be linked to their corresponding forward points).

A significant change is observed in the shape of the isotherm and the maximum level of ion exchange upon complexing the aquated copper ion with ammonia. Ion exchange isotherms (figures 4.20 and 4.21) for exchange of $Cu(NH_3)_4^{2+}$ in $NH_4$-X and -Y show that in the case of X ammination has reduced both selectivity values and the maximum level of ion exchange. In the case of Y, selectivity values are higher for all values of $Cu_c$ than those observed with the hydrated ion (figure 4.42), but the maximum level of ion exchange is lower. Both isotherms appear to be reversible within the limits of experimental error.

Selectivity trends and derived thermodynamic data are shown in tables 4.15 to 4.20. inclusive.

## 4.4. FURTHER REVERSIBILITY TESTS ON TRANSITION METAL EXCHANGED X AND Y

Samples of both ammonium X and Y were exhaustively exchanged with transition metals, and then re-exchanged with the ammonium ion. The degree of removal of metal ion was assessed and then a further re-exchange with sodium ions was performed (section 2.11).

These data are shown in Table 4.21 and confirm previous observations[96] that in the cases of Cu-X, Cu-Y, Co-X and Ni-X some transition metal ions are irreversibly "locked" in certain sites within the zeolite framework. Insignificant irreversibility is observed with Co-Y, Ni-Y and Zn-Y.

Table 4.21 Analyses of Exhaustively Reverse Exchanged Samples *

| | Co-X | Ni-X | Cu-X | Co-Y | Ni-Y | Cu-Y |
|---|---|---|---|---|---|---|
| Maximum level of exchange | 0.75 | 0.71 | | 0.68 | 0.69 | |
| Equivalent fraction removed with $NH_4$ | 0.61 | 0.52 | 0.296 | 0.671 | 0.683 | 0.521 |
| Equivalent fraction removed with Na | 0.087 | 0.095 | 0.199 | 0.008 | 0.006 | 0.193 |
| Equivalent fraction locked in sites | 0.045 | 0.101 | 0.213 | 0.0009 | 0.0014 | 0.028 |

*Total removal of transition metal was obtained with Zinc(II) and Manganese(II) zeolites using sodium solutions.

One reason for the irreversibility observed here could be due to the preparation method employed in making the starting materials $NH_4$-X and $NH_4$-Y (section 2.5.). Exchanging at higher temperatures caused ammonium ions to exchange into X and Y which could not be exchanged at 25°C. Other reasons for the observed irreversibilities are either partial precipitation of basic transition metal salts in the alkaline zeolite environment or, (as shown by Lai and Rees [80] ) irreversible exchange of transition metal species due to a partial breakdown of the zeolite structure. In this previous work [80] breakdown was the result of thermal decomposition of the faujasite lattice, but it is probable that the aqueous transition metal ion solutions used in this work were acidic enough to partially decompose the zeolite and thus create a similar irreversibility. If dealumination has occurred, the aluminium leached out has remained within the framework, a phenomenon observed previously with mordenite.[109]

## 4.5. ION SITE REDISTRIBUTION.

It is known[65] that thermal treatment can lead to a re-distribution of the transition metal ions in the zeolite phase. In order to determine whether or not a vacuum-drying process could have a similar effect, the following test was applied to a sample of sodium X.

1g of sodium X was exhaustively exchanged with a solution containing 0.1g equiv. $dm^{-3}$ of cobalt(II) chloride until no further uptake of Co(II) could be detected. The resulting zeolite was then washed once with 50 $cm^3$ of distilled water and placed in a vacuum desiccator, under conditions of continuous evacuation for 10 hours (i.e. until completely dry). The sample was analysed for both cobalt (section 2.4.2.8.) and water content (section 2.4.2.3.). Next, a 0.2 g sample of this zeolite was further equilibrated with 50 $cm^3$ of 0.1g equiv. $dm^{-3}$ cobalt(II) solution. After separation the solution was analysed for its sodium content. A second and similar 0.2g sample was equilibrated in a desiccator over a saturated solution of sodium chloride for 15 days prior to analysis for water content.

It was observed that the original maximum level of cobalt(II) exchange was 82.8%. A fully hydrated sample of this zeolite contained 28.95% water. Vacuum drying reduced this water content to 25.38%. Re-exchanging the dried sample with Co(II) solution gave rise to a further cobalt uptake of 8.43% with respect to the total exchangeable component.

This confirms, in accord with theory [53], that the presence of guest molecules within the framework is an important factor, strongly influencing the observable ion exchange characteristics.

## 4.6 X-RAY DATA.

The X-ray powder photographs of all the transition metal exchanged faujasites except those involving copper(II) were identical to those of the original sodium or ammonium zeolites. This indicated that suspected precipitation of basic salts of the transition metals, especially in the cases of Ni-X and Co-X, or breakdown of the crystal lattice, were either negligible or not detectable using X-ray powder techniques.

The powder photographs for Cu-X and Cu-Y, prepared using aqueous cupric chloride solutions, showed the unchanged characteristic pattern for the zeolite framework structure, plus additional diffraction lines. These additional lines were identical to those exhibited by a sample of basic copper chloride, indicating the presence of this compound on and within the zeolite.

A sample of Cu-Y, prepared using aqueous copper nitrate solution, was identical to its $NH_4$-Y precursor, but a similarly prepared Cu-X sample showed the presence of extra lines which could be attributed to the presence of the basic copper nitrate salt precipitate.

Table 4.22 Maximum Levels of Ion Exchange

| Ingoing Ion | Outgoing Ion | Zeolite | Ac Max |
|---|---|---|---|
| $NH_4$ | Na | X | 0.73 |
| $NH_4$ | Na | Y | 0.70 |
| Ag | Na | MDR | 0.89 |
| Ag | Na | X | 1.00 |
| Ag | Na | Y | 1.00 |
| $Ag(NH_3)_2$ | Na | MDR | 0.75 |
| $Ag(NH_3)_2$ | Na | X | 0.57 |
| $Ag(NH_3)_2$ | Na | Y | 0.55 |
| $Ag(NH_3)_2$ | $NH_4$ | MDR | 0.72 |
| Co | $NH_4$ | Y | 0.68 |
| Ni | $NH_4$ | Y | 0.69 |
| Zn | $NH_4$ | Y | 0.78 |
| Mn | $NH_4$ | Y | 0.75 |
| Cu | $NH_4$ | Y | 0.78 |
| Co | $NH_4$ | X | 0.75 |
| Ni | $NH_4$ | X | 0.71 |
| Zn | $NH_4$ | X | 0.82 |
| Mn | $NH_4$ | X | 0.81 |
| Cu | $NH_4$ | X | 0.79 |
| $Cu(NH_3)_4$ | $NH_4$ | X | 0.58 |
| $Cu(NH_3)_4$ | $NH_4$ | Y | 0.73 |
| $Pt(NH_3)_4$ | Na | X | 0.35 |
| $Pt(NH_3)_4$ | Na | Y | 0.40 |
| $Pt(NH_3)_4$ | Na | MDR | 0.35 |
| $Pt(NH_3)_4$ | $NH_4$ | X | 0.31 |

CHAPTER FIVE DISCUSSION

5.1. THE SODIUM AMMONIUM EXCHANGE IN X AND Y

5.1.1. Application of Dielectric Theory

5.1.1.1. The Influence of Ionic Radii on Exchange Characteristics

5.1.1.2. The Influence of Framework Charge Density on Ion Exchange Characteristics

5.2. ION EXCHANGE OF SILVER AND SILVER AMMINE IN ZEOLITES

5.2.1. The Selectivity of Silver(aquo) Exchange Rationalised by Dielectric Theory

5.2.2. The Selectivity of Amminated Silver Exchange Rationalised by Dielectric Theory

5.3. THE EXCHANGE OF HYDRATED FIRST ROW TRANSITION METALS IN $NH_4$/Na X AND Y

5.3.1. The Isotherms for Transition Metal Exchange

5.3.1.1. Hydrated Ions in X

5.3.1.2. Hydrated Ions in Y

5.3.2. Maximum Levels of Exchange

5.3.3. Selectivity and Affinity in X and Y

5.3.3.1. Selectivity Trend in X

5.3.3.2. Selectivity Trend and Affinity Sequence in Y

5.3.3.3. Comparison of Selectivity Trends in X and Y

5.3.3.4. The Effect of Experimental Error on $K_m^N$

5.3.3.5. Comparisons of Standard Free Energy Values in Y

5.4. ION EXCHANGE OF AMMINATED COPPER(II) IN X AND Y

5.4.1. Comparison of Selectivities

5.5. ION EXCHANGE OF $Pt(NH_3)_4^{2+}$ AND $Pd(NH_3)_4^{2+}$ IN SODIUM ZEOLITES

5.5.1. Maximum Exchange Levels

5.5.2. The Ion Exchange Isotherms

## 5.1. THE SODIUM-AMMONIUM EXCHANGE IN X AND Y.

The observed maximum level of ion exchange of ammonium in zeolite X can be interpreted by considering only exchange within the 26-hedra type II cages which comprise the main channels, assuming that for steric reasons exchange must be confined to these cavities. However, the maximum level of exchange is below the limit expected for complete removal of sodium ions from these large sites and also below the limit imposed by the volume requirements for the particular ions[66]. In the case of ammonium exchange in Y, confinement of the large ammonium ions within the large channels is again indicated, but in contrast to X complete removal of sodium ions in the 26-hedra type II cages appears to occur.

The assumption that a maximum exchange level of about 68% ∿ 70% in zeolite Y indicates complete exchange of ions in the large cages has been made previously[70] and is based on the fact that all the sodium ions resident within the large cages predominantly occupy S(III) positions[100,46]. Thus it appears that ion exchange of ammonium with sodium in Y involves only one set of sites. In sodium X the exchange appears to involve sodium ions resident in sites III, IV and V and also to some small extent those sodiums resident in site II. This can again be deduced by analogy with previous work[91], which describes the cation site population of an ammonium exchanged potassium Y.

It must be emphasised that interpretations of ion exchange isotherms cannot be made without adequate knowledge of the cation site distributions at any equilibrium position and consequently all interpretations based on isotherm shapes and maximum levels of ion exchange alone must

be speculative to some extent. If we are to assume that the previous analogy with the ammonium/potassium Y is correct then we must assume that there is some controlling factor which prevents complete removal of the sodium ions from site (II). This controlling factor need not be steric in nature. For example, the thermodynamic equilibrium constant $K_a$ may be expressed in terms of a product of the equilibrium constants between ions in solution and those in each site set within the crystal lattice. Then the equilibrium constant involving site II may be small, thus preventing major re-population of these sites with the ingoing ion. It is interesting to note that Barrer and Klinowski[90] in a study of the statistical mechanics of ion exchange considered this situation, and showed that partial ion exchange may arise in this manner not because the controlling factor is steric but purely as an intrinsic function of the ratio of total number of sites to the lattice charge. Their conclusions have been summarised by Townsend[149].

### 5.1.1. Application of Dielectric Theory to Ammonium-Sodium Exchanges

The selectivity plots in figure 4.30 show that zeolite Y is more selective for the ammonium ion than is zeolite X. This trend is consistently reflected in both the Kielland plots (figures 4.43 and 4.44.) and in the plots of selectivity versus ammonium solution concentration. The values of standard free energy also show that both zeolites prefer the larger ammonium ion over the sodium, with zeolite Y having a higher affinity for ammonium than zeolite X. These observed trends can be rationalised by simple dielectric theory previously developed[74,75,76].

#### 5.1.1.1. The Influence of Ionic Radii

Considering $\Delta G^{\ominus}$ for ammonium ions in sodium mordenite the exchange

reaction is

$$NH_4^+{}_{(s)} + Na^+{}_{(c)} \rightleftharpoons NH_4^+{}_{(c)} + Na^+{}_{(s)}$$

if $\varepsilon_{NH_4}(S)$ and $\varepsilon_{Na}(S)$ are the permittivities of the aqueous solutions containing $NH_4^+$ and $Na^+$ ions respectively and $\varepsilon_{NH_4}(C)$ and $\varepsilon_{Na}(C)$ are the permittivities of $NH_4$- and Na-MOR respectively, then from equation 1.620 the standard free energy of exchange is

$$\Delta G^\theta = \frac{Le^2}{8\pi}\left[\frac{1}{r_{Na}}\left(\frac{1}{\varepsilon_{Na}(S)} - \frac{1}{\varepsilon_{Na}(C)}\right) + \frac{1}{r_{NH_4}}\left(\frac{1}{\varepsilon_{NH_4}(C)} - \frac{1}{\varepsilon_{NH_4}(S)}\right)\right] \qquad 5.100$$

If we then assume[74,75] that

$$\varepsilon_{NH_4}(S) \sim \varepsilon_{Na}(S) = \quad \text{and} \quad \varepsilon_{NH_4}(C) \sim \varepsilon_{Na}(C) = \varepsilon_s$$

equation 5.100 simplifies to

$$\Delta G^\theta = \frac{Le^2}{8\pi}\left[\left(\frac{1}{r_{NH_4}} - \frac{1}{r_{Na}}\right)\left(\frac{1}{\varepsilon_c} - \frac{1}{\varepsilon_s}\right)\right] \qquad 5.100$$

Since

$$\varepsilon_s > \varepsilon_c \quad \text{then} \quad \left(\frac{1}{\varepsilon_c} - \frac{1}{\varepsilon_s}\right) > 0$$

and for the situation where $r_{NH_4} > r_{Na}$ i.e.

$$\left(\frac{1}{r_{NH_4}} - \frac{1}{r_{Na}}\right) < 0$$

then $\Delta G^\theta$ must be less than zero. Consequently we would expect that any exchange involving ammonium as the ingoing ion and sodium as the outgoing ion would be accompanied by a negative standard free energy. This is observed both in this work and in earlier work involving X and Y[66] and mordenite[85].

5.1.1.2. The Influence of Framework Charge Density on Ion Exchange Characteristics.

Equation 1.620 can be simplified (section 1.8.1) to

$$\Delta G^{\theta} = \frac{Le^2}{8\pi}\left(\frac{Z_A}{r_A} - \frac{Z_B}{r_B}\right)\left(\frac{1}{\varepsilon_c} - \frac{1}{\varepsilon_s}\right) \qquad 5.120$$

This equation can be applied also to the experimentally determined values of $\Delta G^{\ominus}$ (table 4.17), in order to explain the observed affinity sequence for the ammonium sodium exchange reaction through a series of zeolites. From equation 5.120

$$\Delta G^{\theta}_{(lc)} = \frac{Le^2}{8\pi}\left(\frac{Z_A}{r_A} - \frac{Z_B}{r_B}\right)\left(\frac{1}{\varepsilon_c(lc)} - \frac{1}{\varepsilon_s}\right) \qquad 5.130$$

$$\Delta G^{\theta}_{(hc)} = \frac{Le^2}{8\pi}\left(\frac{Z_A}{r_A} - \frac{Z_B}{r_B}\right)\left(\frac{1}{\varepsilon_c(hc)} - \frac{1}{\varepsilon_s}\right) \qquad 5.140$$

where (hc) and (lc) refer to zeolites having higher charge density and lower charge density respectively. $\varepsilon_c(lc)$ and $\varepsilon_c(hc)$ refer to the relative permittivities of the crystal phases for these two situations. A and B refer conventionally to the ingoing cations and outgoing cations respectively. Implicit in this application is the assumption that[75] $\varepsilon_c < \varepsilon_s$ consequently $\frac{1}{\varepsilon_c} - \frac{1}{\varepsilon_s}$ is always positive. The sum of the quotients

$$\frac{Z_A}{r_A} - \frac{Z_B}{r_B}$$

is the function that determines the sign of the value of $\Delta G^{\ominus}$ and as shown before (section 1.8.1) for the case of uni-univalent exchange where $r_A > r_B$, the quotient must be negative. If we consider the sums of the quotients

$$\frac{1}{\varepsilon_c(1c)} - \frac{1}{\varepsilon_s}$$

and

$$\frac{1}{\varepsilon_c(hc)} - \frac{1}{\varepsilon_s}$$

in equations 5.130 and 5.140 respectively, and assume that the Permittivity of the higher charge zeolite will be greater than that found in the lower charge zeolites[75], then

$$\frac{1}{\varepsilon_c(hc)} < \frac{1}{\varepsilon_c(1c)}$$

consequently

$$\left(\frac{1}{\varepsilon_c(hc)} - \frac{1}{\varepsilon_s}\right) < \left(\frac{1}{\varepsilon_c(1c)} - \frac{1}{\varepsilon_s}\right)$$

Thus for a zeolite having a high charge density, the sum of these quotients will be positive but less than the value found for the lower charge density zeolite. Consequently the modulus of the standard free energy of exchange will be less for a zeolite of high framework charge density than for a zeolite of lower framework charge density. Thus, if the sign of the standard free energy, as determined by $\frac{Z_A}{r_A} - \frac{Z_B}{r_B}$ is positive the $\Delta G^{\ominus}$ will be less positive for the zeolite of higher framework charge. In contrast, if the sign of the standard free energy is negative, then $\Delta G^{\ominus}_{(hc)}$ will be less negative than $\Delta G^{\ominus}_{(1c)}$ which is the opposite situation to that preceeding.

Thermodynamic affinities have been reported for the ammonium sodium exchange in X, Y and mordenite in this work and elsewhere[85,66]. These zeolites are not all isostructural but they do have markedly different framework charge densities (table 5.1.). From the data in table 5.1., we would predict the trends shown in table 5.2.

Table 5.1 Zeolite Framework Charge Densities*

| Zeolite | Na-X | Na-Y | Na-MOR |
|---|---|---|---|
| Charge Density/$_{C\ m}$-3 | $8.97 \times 10^8$ | $6.5 \times 10^8$ | $4.23 \times 10^8$ |

*Calculated from data by Meier [159]

Table 5.2 Predicted Affinity Sequences

| Sign of $\Delta G^{\ominus}$ | Affinity Sequence |
|---|---|
| + | X > Y > MOR |
| - | MOR > Y > X |

This gives an adequate explanation for the observed affinity sequence in both this work (table 4.17 ) and in work by Barrer and Klinowski[85] who reported a value of $\Delta G^{o}$ for the $NH_4$-Na exchange in mordenite of -3.2. The thermodynamic affinity for ammonium ion in mordenite has a greater affinity than in either X or Y which conforms to the predictions of simple dielectric theory.

## 5.2. ION EXCHANGE OF SILVER AND DIAMMINESILVER(I) IN SODIUM X, Y AND MORDENITE.

### Maximum Levels of Exchange.

The maximum levels of exchange observed for the Ag/Na-X and Ag/Na-Y

exchanges show that total removal of sodium ions from the respective framework was effected in agreement with Sherry's observations[70]. This implies the presence of silver ions in the sodalite cages and even in the hexagonal prizms. Recent X-ray data for hydrated silver Y confirms this conclusion[146]. Assuming the presence of $Ag^+$ ion in the small cages one may conclude that the diameter of the six-oxygen windows between the 26-hedra type II and the sodalite cages must be at least 0.25 nm, (since the ionic radius of $Ag^+$ is $\sim$0.125 nm) and that the hydration shell around the silver ion does not hinder passage through this channel.

The maximum level of exchange of silver ions into sodium mordenite is 90%. On the basis of reported site distributions within this zeolite[85], both site sets appear to be involved in the exchange. It would be expected from a knowledge of the ionic radius of $Ag^+$(aquo), that penetration into the side pockets of mordenite via the 8-oxygen windows could easily occur.

The maximum levels of exchange for the $Ag(NH_3)_2$/Na-X and Y systems indicate the ion sieve effect that would be expected on consideration of the size of the silver ammine ion. The silver ammine ion is linear in structure having a minimum diameter at right angles to the major axis which approximate to the diameter of the ammonia ligand. This is in the region of 0.28 nm, which is somewhat greater than the free diameter of the 6-oxygen windows. The level of ion exchange of about 55% for both Na-X and Na-Y suggests that some of the sodium ions resident within the supercages of the zeolite have not been replaced with $Ag(NH_3)_2^+$ ions at 25°C. In contrast, the exchange limit for $Ag(NH_3)_2$ in mordenite appears to involve ions from within the side pockets.

In ion exchange involving large ingoing ions[66,151], the extent of

exchange may be limited by the available intracrystalline space of the zeolite[152,153]. Theng et al[66] concluded that for the ammonium ion and $CH_3NH_3^+$ this "volume steric effect" should not restrict exchange levels, whereas $C_2H_5\ NH_3^+$ and larger molecules should only partially exchange. Other examples of the volume steric effect can be found in the literature[150,151]. It is therefore quite conceivable that this volume steric restriction may also apply to ion exchange of the silver diammine species in zeolites X and Y especially as more recently, the volume steric effect has been observed with complexed nickel ions[150].

Space requirements are considerations which must not be overlooked; however, again it is emphasised that partial ion exchange can be an intrinsic function of ion exchange in zeolites[90], being dependent upon the interactive forces between the exchanging cations and also the number and availability of ion exchange sites. Thus it is not always necessary to interpret maximum levels of ion exchange in terms of either volume steric or ion sieve effects.

### 5.2.1. Selectivity and $\Delta G^\ominus$ for Silver(aquo) Exchange Rationalised by Dielectric Theory.

The affinity sequence for exchange of the silver ion in Na-X, -Y and -MOR is (table 4.17) X > MOR > Y. All values of $\Delta G^\ominus$ for these systems are highly negative, reflecting the very high affinities of the three zeolites for the aquated silver ion. The negative $\Delta G^\ominus$ values of these systems can be rationalised by consideration of the magnitudes of the (Pauling) ionic radii of the two exchanging cations. These radii are 0.126 nm and 0.095 nm for $Ag^+$ and $Na^+$ respectively[87].

From (section 5.1.1.1) it was shown that for a uni-univalent ion exchange process the condition for $\Delta G^{\ominus}$ to be negative was that

$$r_A > r_B$$

where $r_A$ and $r_B$ are the radii of the ingoing and outgoing cation respectively. This condition is met for the exchange of silver into sodium zeolites.

Consideration of zeolite framework charge densities (section 5.1.1.2) shows that for the situation where $\Delta G^{\ominus}$ is negative the affinity sequence for a series of zeolites with different framework charge densities should be

$$\Delta G^{\theta}_{(1c)} > \Delta G^{\theta}_{(hc)}$$

where (1c) and (hc) refer to low charge and higher charge respectively. Thus the expected affinity sequence for the Ag $\rightleftharpoons$ Na equilibrium should be

$$MOR > Y > X$$

which does not agree with experiment.

The observed affinity sequence puts the free energy of exchange for zeolite X out of position, assigning a value much higher than would be predicted by simple dielectric theory. This can be explained by considering the assumptions used in the derivation of simple dielectric theory.

The ion exchange reaction is conventionally expressed as[71]

$$Z_A B^{ZB+}_{(1)} + Z_B A^{ZA+}_{(2)} \rightleftharpoons Z_A B^{ZB+}_{(2)} + Z_B A^{ZA+}_{(1)}$$

Where $Z_A$ and $Z_B$ are the respective charges on the ions A and B in one

of the two phases (1) or (2). It follows that[71]

$$\Delta G^{\theta} = \frac{Le^2}{8\pi}\left[\frac{Z_A}{r_A}\left(\frac{1}{\varepsilon_A(1)} - \frac{1}{\varepsilon_A(2)}\right) + \frac{Z_B}{r_B}\left(\frac{1}{\varepsilon_B(2)} - \frac{1}{\varepsilon_B(1)}\right)\right] \qquad 5.145$$

Where $r_A$ and $r_B$ are the radii of ions the A and B respectively and $\varepsilon_A(1)$, $\varepsilon_A(2)$, $\varepsilon_B(1)$, $\varepsilon_B(2)$ are the permittivities of the respective media. (see also section 1.8.) The exchange reaction for the situation under consideration is

$$Ag^+_{(s)} + Na^+_{(c)} \rightleftharpoons Ag^+_{(c)} + Na^+_{(s)}$$

Thus, from (5.145)

$$\Delta G^{\theta} = \frac{Le^2}{8\pi}\left[\frac{1}{r_{Na}}\left(\frac{1}{\varepsilon_{Na}(S)} - \frac{1}{\varepsilon_{Na}(C)}\right) + \frac{1}{r_{Ag}}\left(\frac{1}{\varepsilon_{Ag}(C)} - \frac{1}{\varepsilon_{Ag}(S)}\right)\right] \qquad 5.150$$

or, rearranging

$$\Delta G^{\theta} = \frac{Le^2}{8\pi}\left[\frac{1}{r_{Na}}\left(\frac{1}{\varepsilon_{Na}(S)} - \frac{1}{\varepsilon_{Na}(C)}\right) - \frac{1}{r_{Ag}}\left(\frac{1}{\varepsilon_{Ag}(S)} - \frac{1}{\varepsilon_{Ag}(C)}\right)\right] \qquad 5.160$$

Assuming

$$\varepsilon_{Na}(S) = \varepsilon_{Ag}(S) = \varepsilon_s$$

where $\varepsilon_s$ indicates an average solution phase dielectric constant, then

$$\Delta G^{\theta} = \frac{Le^2}{8\pi}\left[\frac{1}{r_{Na}}\left(\frac{1}{\varepsilon_s} - \frac{1}{\varepsilon_{Na}(C)}\right) - \frac{1}{r_{Ag}}\left(\frac{1}{\varepsilon_s} - \frac{1}{\varepsilon_{Ag}(C)}\right)\right] \qquad 5.170$$

An original assumption made by Barrer and Klinowski[75] was that $\varepsilon_A(C) = \varepsilon_B(C)$ or in this case $\varepsilon_{Na}(C) = \varepsilon_{Ag}(C)$. If this assumption is justified then

$$\left(\frac{1}{\varepsilon_s} - \frac{1}{\varepsilon_{Na}(C)}\right) = \left(\frac{1}{\varepsilon_s} - \frac{1}{\varepsilon_{Ag}(C)}\right) \qquad 5.180$$

So that

$$\Delta G^{\theta} = \frac{Le^2}{8\pi} \left\{ \frac{1}{r_{Na}} \left[k\right] - \frac{1}{r_{Ag}} \left[k\right] \right\} \qquad 1.590$$

Since for all known values of $\varepsilon_s$ and $\varepsilon_c$, $\varepsilon_s > \varepsilon_c$ then k is always negative. Hence we have the situation that if $r_{Na} < r_{Ag}$, then

$$\left| \frac{1}{r_{Ag}} \left[k\right] \right| < \left| \frac{1}{r_{Na}} \left[k\right] \right|$$

Consequently $\Delta G^{\theta}$ in equation 1.590 is a function of a negative number minus a smaller negative number and is thus always negative if the radius of the ingoing ion is greater than the radius of the outgoing ion. This is the same condition as was derived by Barrer and Klinowski[75].

If it is assumed that $\varepsilon_{Na}(C) \neq \varepsilon_{Ag}(C)$

there are two possibilities to be considered:

(i) $\varepsilon_{Ag}(C) > \varepsilon_{Na}(C)$

Then

$$\frac{1}{\varepsilon_{Ag}(C)} < \frac{1}{\varepsilon_{Na}(C)}$$

and now

$$\left| \frac{1}{\varepsilon_s} - \frac{1}{\varepsilon_{Na}(C)} \right| > \left| \frac{1}{\varepsilon_s} - \frac{1}{\varepsilon_{Ag}(C)} \right|$$

Consequently equation 1.590 becomes for this case

$$\Delta G^{\theta'} = \frac{kLe^2}{8\pi} \left[ \frac{1}{r_{Na}} - \frac{k'}{r_{Ag}} \right] \qquad 5.191$$

where $0 < k' < 1$

Subtract $\Delta G^{\theta}$ from $\Delta G^{\theta'}$ and

$$\Delta G^{\theta'} - \Delta G^{\theta} = \frac{kLe^2}{8\pi r_{Ag}} \left[1 - k'\right] \qquad 5.192$$

since $0 < k' < 1$

then $1 - k' > 0$

and since k is negative (already proved), then

$$\Delta G^{\theta'} - \Delta G^{\theta} < 0 \qquad 5.193$$

In the case that $\varepsilon_{Na_{(c)}} = \varepsilon_{Ag_{(c)}}$ it has already been shown that in this case $\Delta G^{\ominus}$ is always negative. therefore equation 5.193 can only be satisfied by the condition that

$$\left|\Delta G^{\theta'}\right| > \left|\Delta G^{\theta}\right|$$

i.e. that the free energy of exchange when $\varepsilon_{Ag_{(c)}} > \varepsilon_{Na_{(c)}}$ is more negative than when the permittivity of the two exchanged forms are the same.

(ii) $\varepsilon_{Ag_{(c)}} < \varepsilon_{Na_{(c)}}$

In this case $\left|\frac{1}{\varepsilon_s} - \frac{1}{\varepsilon_{Na(C)}}\right| < \left|\frac{1}{\varepsilon_s} - \frac{1}{\varepsilon_{Ag(C)}}\right|$

and consequently the free energy of exchange would be predicted to be less negative than in the case where $\varepsilon_{Na_{(c)}} = \varepsilon_{Ag_{(c)}}$.

Case (i) could be the situation occurring in the exchange reaction $Na \rightleftharpoons Ag$ in zeolite X, i.e. that the relative permittivity of the silver zeolite is greater than the relative permittivity of the sodium zeolite giving rise to a higher value of $\Delta G^{\ominus}$ than would be expected. This apparent increase in relative permittivity of the silver zeolite compared with the sodium zeolite is explicable by considering the action

of the dielectric in a parallel plate capacitor. The capacitance of a simple capacitor it given by

$$C \sim \frac{\varepsilon A}{d} \qquad 5.195$$

where d is the distance between plates having an area of overlap A, $\varepsilon$ is the permittivity of the medium. In this situation the capacitance is known to be a function of the polarization of the dielectric under the influence of an applied electric field. It is reported[154] that capacitance (C) of a capacitor of given dimensions in increased if a medium consisting of molecules that are already polarized or of higher polarizability is introduced. This must, therefore, be quantitatively reflecting an increase in the value of the permittivity (equation 5.195). It therefore follows that, in the current context, the zeolite containing the ion of higher polarizability must exhibit a higher relative permittivity. It is reported[155] that the silver ion has a greater polarizability than the sodium ion so it would be expected that the relative permittivity of a silver zeolite would be greater than that of a sodium zeolite.

It also follows that the polarisation of a particular ion would be less under the influence of a zeolite of lower framework charge. Consequently (equation 5.195) the value of $\varepsilon$ would be smaller in this case. Hence it would be expected that only effect upon the ion exchange properties which is a function of the permittivity would be less significant in zeolites of lower framework charge density. This explains the observed enhancement of the affinity of zeolite X for the silver ion, whereas this enhancing effect is not obvious for zeolites Y or mordenite (table 4.16.).

5.2.2. Selectivity for Complexed Silver Exchange Rationalised by Dielectric Theory.

Using dielectric theory it is also possible to provide an explanation for the changes in selectivity quotient $\alpha^N$ that are observed when hydrated silver ions are complexed with ammonia.

The dielectric theory is concerned with thermodynamic affinities $\Delta G^\ominus$ whereas the data discussed here are in terms of selectivities and mass action quotients. As emphasised earlier (section 1.6.3.1.) and in previous literature[65], the two functions are quite distinct and no attempt should be made to use selectivity quotients alone to predict the value of $\Delta G^\ominus$ [60]. However, it is justifiable to conclude that provided the total solution normalities of all the exchange equilibria are kept constant, if a zeolite shows a substantially higher selectivity for one ion over another, this will be reflected qualitatively by a change in affinity in the expected direction.

The selectivity quotients $\alpha^N$ for the ion exchange equilibria $Ag(NH_3)_2^+ \rightleftharpoons Na^+$ in zeolites X, Y and mordenite show a distinct selectivity sequence throughout the whole isotherm range.

$$MOR >> Y > X$$

This trend is explained in a similar way to that outlined in section 5.1.1.2. by assuming that the radius of the ingoing $Ag(NH_3)_2^+$ ion is greater than the outgoing sodium ion, leading to a negative value of standard free energy for all the zeolites studied. Using this approach, the affinity sequence predicted on the basis of framework charge density (table 5.1.) is

$$MOR > Y > X$$

which is the selectivity sequence observed.

The sign or magnitude of the value of $\Delta G^{\ominus}$ cannot strictly be inferred from the values of selectivity quotient without prior knowledge of the values of solution and zeolite phase activity coefficients. It was shown previously (section 3.5.2.1.1.) that for any exchange (but especially where the entering ion A has a higher valency than B), the ratio of single ion activity coefficients raised to the relevant powers $\Gamma$ will increase if the value of the mean molal stoichiometric activity coefficient of the salt of the ingoing ion is lower at a given ionic strength since

$$\Gamma = \frac{1}{Z_X}\left[Z_A(Z_B + Z_X)\ln\gamma_{\pm BX}^{(AX)} - Z_B(Z_A + Z_X)\ln\gamma_{\pm AX}^{(BX)}\right] \qquad 1.330$$

Raising the value of $\Gamma$ will raise the value of lnKc at any value of $A_c$ (section 1.6.). Consequently it can be concluded that an ion exchange equilibrium in which the selectivity quotients show little or no preference for the ingoing ion may still have a highly negative standard free energy if the value of $\Gamma$ is considerably greater than unity.

No values of the mean molal stoichiometric activity coefficient of the diamminesilver(I) nitrate salt could be found in the literature. In order therefore to estimate the values of the solution phase activity coefficients for the diamminesilver(I) nitrate salt in solution we may consider four possible factors:

(i) The effect of ion-dipole interactions due to the presence of ammonia in solution.

The activity coefficients are factors introduced to correct for deviations from ideality in a multi component mixture due to interaction

between the various components that constitute that phase. For aqueous solutions of weak electrolytes the major contribution to deviations from ideality is attributed to ion-ion interaction within the aqueous medium. These interactive forces are adequately accounted for by the Debye-Huckel limiting law.

The effect of interaction between ions and the dipole present on the water molecule is much less significant than the ion-ion interactions. The dipole moment of water is calculated to be 1.85 Debye[156] whilst that of ammonia is 1.49 Debye.[156] Consequently, introduction of the ammonia molecule into an aqueous medium must serve to reduce the ion-dipole interaction and hence reduce deviation from ideality. Thus it is justifiable to assume that this change in ion-dipole interaction will be of negligible magnitude compared with ion-ion interactions and certainly would not cause a greater deviation from ideality at a given ionic strength in the case of the amminated silver salt than that seen with the hydrated salt.

(ii) The effect of complexing the silver ion.

If one considers the diamminesilver(I) species in terms of the equilibrium that must exist in solution between the ligands and the solvent, then it follows that the energy of interaction between the ammonia molecule and the silver ion constitutes an interaction between the silver ion and its immediate environment and therefore contributes to the observed deviation from ideality:

$$Ag^{+}(H_2O)_n + 2NH_3 \rightleftharpoons Ag(NH_3)_2^{+} + nH_2O$$

Since the above equilibrium is shifted strongly to the right in aqueous solution it follows that the interaction between the silver ion and

the ammonia molecule is greater than the interaction between the silver ion and the water molecule and thus the consequent deviation from ideality should be greater at a given ionic strength in the ammoniacal solution, resulting in lower values for the activity coefficient than would be observed for the hydrated silver salt.

(iii) The effect of the association of the ammonia molecule in aqueous media.

The following equilibrium exists in ammoniacal solution:

$$NH_3 + H_2O \rightleftharpoons NH_4^+ + OH^-$$

If the ammoniacal solutions are being used for ion exchange, as inevitable consequence of this equilibrium is to create a ternary system, consisting of (for example) $Ag(NH_3)_2^+$, $Na^+$ and $NH_4^+$. In previous work, involving ion exchange of $Cu(NH_3)_4^{2+}$ in ammoniacal media[78] this problem was discussed and from calculations it was concluded that the equilibrium concentrations of ammonium ion was suffuciently small for considerations of a ternary system to be excluded. However, a second effect resulting from the presence of $NH_4^+$ in addition to $Na^+$ and $Ag(NH_3)_2^+$ is the effect that this third ion may have on the solution phase activity coefficients of the others. This effect is difficult to assess: however since the concentration of $NH_4^+$ ion present must be very low, it is inferred that the effect would be small.

(iv) Consideration of known values of activity coefficients.

Known values of activity coefficients for complexed metal ions other than silver lead to the conclusion that the effect of complexation would be likely to cause a substantial lowering of the value of the

activity coefficient for silver nitrate at a given ionic strength if ammonia is added. Reported data for complexed metal ion salt solutions[130] exhibit activity coefficients in the region 0.1 ~ 0.2 for a 0.1 g mol $dm^{-3}$ solution. Thus, by analogy it is likely that the activity coefficient for a 0.1g mol $dm^{-3}$ solution of $Ag(NH_3)_2^+ NO_3^-$ would also be of a similar value.

One can therefore assume on the basis of the foregoing considerations that the value of $\Gamma$ for equilibria involving diamminesilver(I) ions is likely to be substantially above unity. Consequently, despite the fairly low values of selectivity quotient observed (figure 4.33 ) these low values are not inconsistent with the $\Delta G^{\ominus}$ values being highly negative.

The dielectric theory (section 1.8.) predicts that a zeolite should show preference for the ion of larger radii. Thus the affinity trend one would expect on the basis of theory, given that $r_{Ag(NH_3)_2} > r_{Ag}$ is $Ag(NH_3)_2^+ > Ag^+$ for exchange into any sodium zeolite. Figures 4.31 and 4.32 show selectivity quotients from which we would infer the following affinity sequences

| MOR | Y | X |
|---|---|---|
| $Ag(NH_3)_2^+ >> Ag^+$ | $Ag(NH_3)_2^+ > Ag$ | $Ag > Ag(NH_3)_2$ |

Zeolites MOR and Y conform to the pattern predicted by the dielectric theory even without considering the enhancing effect of $\Gamma$ in the case of the diamminesilver(I) ion. The trend in zeolite X is not that predicted by theory; consideration of the effect of high $\Gamma$ values, or

that $\varepsilon_{Na}(C)$ may be greater than $\varepsilon_{Na}(C)$ in this case, or a combination of both effects would bring this result into line with theory.

As a further indication of the general validity of the simple dielectric theory, figure 4.35 shows the selectivity quotients as a function of $A_c$ for the $Ag(NH_3)_2^+ \rightleftharpoons NH_4^+$ equilibrium in mordenite. Dielectric theory predicts the value of $\Delta G^\ominus$ as a fraction of the relative difference in ionic radii of the two exchanging species. From this theory, (section 1.8.) it would be concluded that exchange of $Ag(NH_3)_2$ with $NH_4^+$ in mordenite would have a negative value of standard free energy and thus show high selectivity quotients (with respect to $Ag(NH_3)_2^+$) but since the radius of the outgoing ammonium ion is greater than the radius of the sodium ion the observed selectivity quotients should be less than those observed for the $Ag(NH_3)_2^+ \rightleftharpoons Na^+$ equilibrium at any given value of equivalent fraction. Simple comparisons of the isotherms (figures 4.6. and 4.9.) suggest this is the case.

## 5.3. THE EXCHANGE OF HYDRATED FIRST ROW TRANSITION METAL IONS IN AMMONIUM X AND Y

In this section, the general characteristics of the isotherms themselves are first reviewed (section 5.3.1.) and the problem of reversibility in these systems is discussed in section 5.3.1.1. Several systems involving Y were reversible (section 5.3.1.2.). In the following sections (5.3.2. and 5.3.3.) the maximal levels of exchange are discussed, and selectivities and affinities are compared.

### 5.3.1. Ion Exchange Isotherms for Transition Metal Exchange

#### 5.3.1.1. Hydrated Ions in Zeolite X

Very careful experimentation showed that all systems involving first

row transition metals and zeolite X were at least partially irreversible, especially at high levels of transition metal loadings. Light is thrown on this phenomenon by considering the isotherm in three parts (figure 5.1)

Figure 5.1

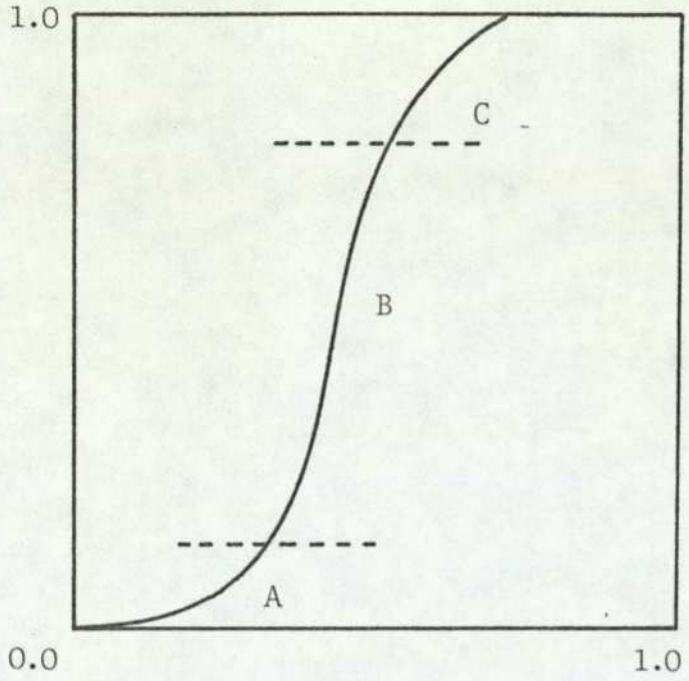


Figure 5.1., which depicts the typically sigmoid shape obtained with these systems, is divided up so that section A is confined to the region of low transition metal ion loading, section B to the central section of the isotherm, whilst section C involves that part of the isotherm beyond the point of inflexion, corresponding to high transition metal ion loadings. Irreversibility was especially associated with exchange that proceeded into section C.

The sodium content of the zeolite as a function of transiton metal ion loadings is shown both on the isotherms (Chapter 4 ) and in Appendix II. These data show that in all cases. although the quantity of sodium removed varies for the different transition metals, the behaviour

is always similar. The sodium content of the zeolite falls off sharply at low transition metal loadings (i.e. in section A (figure 5.1.)), whilst over the whole range corresponding to section B the sodium content hardly changes, indicating that ion exchange in this region involves only the ammonium ions in the zeolite. At higher transiton metal ion loadings, corresponding to section C of the isotherms, the sodium content in the equilibrated solution phase begins to increase dramatically, indicating that exchange in this region again predominantly involves sodium ions as in section A. Reverse points were constructed by a second exchange using a binary mixture of transition metal and ammonium ions only (section 2.9.1.). Since sodium was lost from the zeolite over both sections A and C of the forward isotherms, it follows that observations of irreversibility in these sections did not necessarily imply an intrinsic irreversibility in the system.

Reversibility was observed in all cases when both forward and reverse points were within the section marked B (i.e. the region in which the sodium component varies very little.)

The isotherm for nickel in X showed a slight difference from the others in that section C hardly existed (i.e. the isotherm showed only a slight sigmoidal tendency). This is in accord with earlier work[68] The sodium lost to the solution phase during exchange with nickel was lower than in all the other systems and in addition varied less markedly throughout the isotherm range. Consequently, within the limits of experimental error, the system appears reversible throughout. However, a large quantity of sodium was found in solution even with the nickel exchange when the isotherm points were restricted to section A. So the observed complete reversibility cannot be extended to low values of

transition metal ion loading (where experimental errors anyway preclude accurate analysis).

A similar conclusion can be drawn for exchange of hydrated copper(II) in zeolite X where, although the isotherm is sigmoidal, the sodium component is observed to vary only very slightly throughout most of the isotherm range. Consequently this isotherm appears to be reversible in the region $Cu_S = 0.1$ to $Cu_s = 0.95$.

A further test on reversibility was performed by exhaustive exchange of $NH_4$-X with each of the transiton metal ions individually, followed by washing and exhaustive reverse equilibrium with a solution containing ammonium ion only (section 4.4. ).

This proved that in all cases (table 4.21) transition metal ions were irreversibly exchanged into the zeolite. Even exhaustive subsequent equilibrations with sodium solutions only effected removal of the transition nickel ions in the cases of the zinc and manganese zeolites. The systems involving cobalt, nickel and copper had cobalt(II), nickel(II) and copper(II) species irreversibly 'locked' into the zeolite.

It has been noted[65] that solutions containing cobalt(II), nickel(II) or copper(II) have lower pH values than zinc(II) or manganese(II) under similar conditions and are also more prone to precipitation of the basic salts. It is therefore highly probable that in these cases precipitation or dealumination of the zeolite structure has occurred creating this irreversibility.

Detection of dealumination or precipitation by X-ray techniques is

not easy but in the case of Cu(II)-X the X-ray powder spectrum showed the presence of a line not present in the spectrum other exchanged zeolites used for comparison. This could be attributed to the presence of the basic salt.

5.3.1.2. Hydrated Ions in Zeolite Y.

Ion exchange isotherms involving cobalt and nickel in Y showed complete reversibility over the whole isotherm range (Figs 4.10 & 4.11 ). The isotherm for the reaction $Zn^{2+} \rightleftharpoons NH_4^+$ exchange in Y shows reversibility over most of the isotherm range; irreversibility occurred here when reverse points were derived from zeolite samples that had been initially exchanged to high zinc loadings. The sodium content of the zeolite (which was much lower than in X (Table 4.1 )) for the systems $Co^{2+} \rightleftharpoons NH_4^+$, $Ni^{2+} \rightleftharpoons NH_4^+$ $Zn^{2+} \rightleftharpoons NH_4^+$ and $Mn^{2+} \rightleftharpoons NH_4^+$ changed in all these cases by less than 1% of the total ion exchange capacity of the zeolite. Consequently the systems can be considered as being binary rather than ternary which was not true with X (section 5.5.1.1.) Thus the observed partial irreversibility for the zinc system cannot be attributed to sodium involvement in the equilibria.

It can be rationalised by considering the maximum level of exchange of ammonium in the zeolite sample in question at 25°C, which was 68%. The ammonium zeolite used was prepared at 60°C and the maximum level of exchange was observed to be 92%. Consequent ion exchange with zinc appears to (at high zinc loadings) involve ammonium ion in sites that were not originally accessible to incoming ammonium ions at 25°C and hence the irreversibility must be thought of in terms of irrevesibility exchanged ammonium ions rather than sodium ions. This irreversibility did not occur at low zinc loadings. As previously observed, it is not

justifiable to deduce from the shape of the isotherm which sites are involved in ion exchange and thus the extent of ion redistribution cannot be inferred until adequate X-ray techniques have been employed to determine cation sitings for any given zeolite sample.

### 5.3.2. Maximum Levels of Ion Exchange.

The analytical data (tables 4.6 to 4.9 ) indicate various exchange limits for different transition metal ions in both zeolites X and Y. The trend in exchange limits is given in table 5.3.

Table 5.3. First Row Transition Metal Exchange Limits.

| Zeolite | Exchange Limit Sequence |
|---|---|
| X | Ni < Co < Zn ∿ Mn < Cu |
| Y | Ni ∿ Co < Mn < Zn < Cu |

The position of copper(II) in these sequences is determined by extrapolations of the ion exchange isotherms to 100% replacement of the original ions, and not by the experimentally determined maximum levels of exchange on exhaustively exchanged samples, which as shown (section 4.1.3.) indicate considerable hydrolysis of the zeolites.

The sodium content of the zeolite before and after exchange with transition metal ions gives some idea as to the processes occurring in the exchange. The original ammonium zeolite X contained ∿ 27% sodium ions (table 5.4.), and it is probable that the initial exchange with ammonium ions was restricted to the main channels, leaving the sodium ions behind that reside in the sodalite units and hexagonal prisms (approximately 18% of the total exchangeable component of the zeolite) un-

changed. This assumption is not completely justifiable without adequate crystallographic data, as emphasised before in this thesis. However, previous work [91] has indicated that for $NH_4 \rightleftharpoons K$ exchange in Y the original [17] potassium ions in the SI and SII sites stay in those sites on ion exchange with ammonium and a further small proportion of $K^+$ ions in the large cages migrate to the small cage system. If this case is analogous to the exchange of ammonium into the sodium X sample used in this work, then about 9% of the exchangeable component must have consisted of sodium ions resident within the large cages, and some of these may have migrated to the SI and SII sites. If the foregoing is true, then it follows that subsequent exchange with transition metal ions caused, in all cases, the removal of more sodium than is estimated to have been resident in the large cavities in X.

Table 5.4 Percentage Sodium Contribution to Exchange in X

| Ion | Co | Ni | Zn | Mn | Cu |
|---|---|---|---|---|---|
| % sodium contribution to exchange | 18.9 | 10.7 | 21.8 | 21.1 | 27 |

This indicates that ion exchange with transition metal ions in zeolite X involves ions situated in the SI and SII sites within the network of small cavities. This can occur either by the transition metal ion passing through the 6-oxygen windows and entering the sodalite units, or by migration of the sodium ions out of these sites or by a combination of both processes.

The bare ionic radii of the transition metals are sufficiently small to allow access to the hexagonal prisms although the hydrated radii[86]

are considerably greater than the radius of the 6-oxygen windows and thus it would involve a substantial removal of the hydration shell of the transition metal ion for them to pass through. In X and Y, however, the transition metal ions, having once passed through the small 6-oxygen windows into the sodalite units, are in a comparatively open environment, in which coordination to lattice oxygens is possible The value of 100% exchange for ion exchange involving hydrated copper(II) ions observed here is consistent with previous data published on Na-X[68] and Na-Y[154]. In the case of copper exchange into Na-Y[154] copper ions situated in the sodalite units were detected by X-ray diffraction. This work, and other information[161] means that there is no reason to assume that the ionic radii or hydration energy of Co(II), Ni(II), Zn(II) and Mn(II) preclude the penetration of these ions into the sodalite units.

It is observed (figures 4.15 to 4.19) that the sodium removal from $NH_4$/NaX on exchanging with transition metal ions occurs to a constant and high degree at relatively low transition metal loading, followed by a second stage removal of sodium ions at very high transition metal loadings. This two-stage phenomenon could be due to initial exchange with sodium ions in the main channels followed by a penetration and removal of sodium ions from within the sodalite units. However, it is again important to stress the danger of interpreting exchange characteristics in terms of exchange sites within a zeolite, especially for cases other than uni-univalent exchange[60].

The relatively low exchange level obtained for nickel(II) in X, coupled with a removal of a quantity of sodium ions equivalent to those that would be expected to be resident in the main channels suggest that the exchange of Ni(II) is predominantly confined to the supercages.

Since X-ray examinations of the zeolites failed to confirm that precipitation had occurred (except in the case of copper) a different explanation for the partial irreversibility observed with Co & Ni-X (Table 4.21) appears necessary. One possible explanation is kinetic, assuming fast exchange of transition metal ions into the sodalite units but a very slow reverse exchange, effectively 'locking' the ions into these sites.

A possible explanation of maximum exchange levels involves hydration energies, and the change in hydration level that must occur when a fully hydrated ion (in the supercage) moves to some position where it is partially hydrated (in the sodalite unit). However no observable correlations exist between the standard free energies of hydration of the transition metal ions [87] and the maximum level of exchange. Similarly there is no simple correlation between the ionic radii and the exchange behaviour.

One clear trend is that the extent of sodium removed from the zeolite is directly related to extend of maximum exchange with transition metal ions. The sequence of order of sodium removal from X was

$$Ni < Co < Zn \sim Mn < Cu$$

This is the same order as the maximum level of exchange, and may reflect either the extent to which transition metal ions cause ion migration within the faujasite structure, or (if penetration to the sodalite cages and hexagonal prisms does occur) then the relative affinity of these sites for the particular ion.

Ion exchange limits for transition metal ions in zeolite Y show a similar trend to those observed in X, except that the exchange limits

for Co(II) and Ni(II) are nearly identical in Y, and are the expected levels of exchange for complete removal of ions from the large cages. Exchange of Zn(II) and Mn(II) in Y occurs to a higher level, and as in the case of X, this may indicate either exchange into the small cages or ion migration.

In summary, therefore, the factors giving rise to a given level of ion exchange are very complex. In addition to ion sieve and volume steric effects, Barrer and Klinowski [90] have shown in their recent statistical mechanical treatment of ion exchange that both the phenomenon and degree of partial exchange can be a function of the ratio of the total available sites to charges in the lattice and also to the strength of interaction between entering ions.

In addition, as discussed above, in the case of $Co^{2+}$, $Ni^{2+}$, $Zn^{2+}$, $Mn^{2+}$ and $Cu^{2+}$, exchange into the ammonium faujasite structures, especially X, further uncertainties over maximum level of exchange are seen ( Table 4.22. ) . These are due to partial irreversibility effects which arise through the sodium ions exchanging out and also because the ammonium form was heat-treated to 60°C during preparation (section 2.5) Also hydrolysis must be an important factor either because exchange may occur with the solvent to give a material partially exchanged with hydronium ions, or through dealumination, or through precipitation of basic salts within the crystal lattice. These effects would be especially important in the case of X, which is more readily hydrolysed [162] and which exhibits a higher pH in suspension than Y [162], thus encouraging precipitation of basic salts. It is therefore significant that in this present work uncertainties over both reversibility and maximum level of exchange were far more evident in X than in Y.

### 5.3.3. Selectivity and Affinity Trends in X and Y

#### 5.3.3.1. Selectivity Trends in X.

The selectivity trends in ammonium X for the series of 1st row transition metals as depicted by figures 4.36 and 4.38 show a much clearer sequence than does the corresponding selectivity plot for ammonium Y (Figure 4.37) . Inspection of figure 4.36 shows that the general selectivity sequence in X is

$$Co < Mn < Zn \lesssim Ni \sim Cu$$

except at low transition metal ion loadings, where the selectivity sequence is altered, and the values of $\alpha^N$ are significantly higher:

$$Mn < Co < Zn \sim Ni < Cu$$

The change in sequence at low exchange level (w.r.t. transition metal ion) shows the danger of inferring the relative selectivity for a given set of conditions from general selectivity trends or from thermodynamic affinities. Similar changes in selectivity sequence at lower levels of exchange were reported in previous work by Barrer and Townsend, on transition metal ion exchange in mordenite [65].

An important factor in the determination of selectivity quotients is the correct determination of the normalisation factor $f_n$. where $f_n = {}^1/A_{c(max)}$. This can significantly affect the observed value of selectivity quotient, particularly at high levels of ion exchange ( section 3.6. ). Considering the possible errors in the determination of the maximum level of exchange, particularly in the case of zeolite X, it is wrong to be dogmatic about the relative selectivity trend for Ni(II), Cu(II) and Zn(II) in X. These selectivity plots (figure 4.36) at given values of $A_c$, and the trends and magnitude of these values are sensitive to small changes in the maximum exchange limit.

The equilibrium position for a given binary mixture of ions in contact with a given number of equivalents of zeolite framework is the equilibrium position that has the lowest free energy for that combination of ions. As such it is a function of the activity of the ions in solution and consequently it is a function of the activity coefficients.

Interpretations of selectivity trends should be made after corrections have been applied for solution phase deviations from ideality (i.e. using the Kielland quotient) rather than using the experimentaly obtained $K_m^N$ values. This is clearly indicated by the work of Barrer and Townsend [65] on transition metal exchange in mordenite, where it was shown that the zeolite exhibited highest selectivity for the hydrated copper(II) ion, but the value of the standard free energy for the copper exchange was more positive than those calculated for certain other transition metal ions for which the mordenite had in fact showed a lower selectivity.

In this present study of transition metal ion exchange in zeolite X, thermodynamic affinities were not calculated, because of the irreversible nature of the isotherm (as discussed earlier (section 3.2.1.1.) this irreversibility was due, in part, to the fact that a ternary exchange was occurring, but also due to hydrolysis, dealumination and precipitation problems.) Thus it was not possible to infer the magnitude or sign of the standard free energies for these systems from the selectivity plots. Neither was it possible to justify the rationalisation of selectivity trands in terms of physical parameters such as ionic radii, energy of hydration or sodium component of the equilibria, although to some extent qualitative correlations can be made.

5.3.3.2. Selectivity Trends and Affinity Sequence in Transition Metal Exchanged Y Zeolites.

The selectivity trends (Fig. 4.37) obtained for exchange of 1st row transition metals in Y, are not easily interpreted by direct inspection. All the selectivity plots (figure 4.37 ) show an increase in selectivity as the solution becomes more dilute with respect to the ingoing cation, although manganese is an exception in this regard. Insufficient data at low transition metal loadings precludes any definite conclusions about the behaviour of the ions, but the observed trends of increasing $\alpha^N$ with decreasing molarity were predicted by Barrer and Klinowski for uni-divalent ion exchange[60] (see section 1.6.3.1. ) and has been also examined and confirmed experimentally more recently by Rees[129].

The affinity sequence obtained from these data, using the thermodynamic procedures outlined in sections ( 1.6 to 1.6.3), shows a trend which cannot be simply rationalised using dielectric theory described earlier in the chapter. On the basis of theory, the expected trend is

$$Mn > Co \sim Zn > Ni > Cu$$

yet the observed trend is (table 4.20)

$$Ni \sim Zn > Co > Mn$$

Values of $\Delta G^{\ominus}$ were not calculated for the exchange of $Cu^{2+}$ because of the irreversibility of the isotherm even in Y and also because in this case, as with exchanges involving X, there was evidence of the existence of a ternary exchange equilibrium. The selectivity plot of $K_m^N$ Vs $Cu_c$ in Y is, however, almost identical to that observed for nickel in Y and considering the close similarity in values of $\Gamma$ for the two systems $Cu^{2+} \rightleftharpoons 2NH_4^+$ and $Ni^{2+} \rightleftharpoons 2NH_4^+$ it is probable that the value of $\Delta G^{\theta}$ for copper exchange would be similar to that for nickel

exchange.

The observed isotherm for manganese in Y showed a significant irreversibility in the region $A_c > 0.4$, and also a considerable inconsistency with the shape of the rest of the isotherm (figure 4.13 ). For this reason, $\Delta G^{\theta}$ was also calculated after choosing a value for $A_c(max)$ which excluded this irreversible portion of the isotherm, since in the above trends manganese is clearly out of line with that expected by dielectric theory.

It is emphasised, however, that the Mn-Y isotherm was reproducible and the analytical data (table 4. 7. ) indicate that ion exchange of $Mn^{2+}$ was indeed stoichiometric with respect to ammonium (i.e. ion exchange must be occurring rather than precipitation). The value of $\Delta G^{\ominus}$ so calculated using only the reversible section of the isotherm, with $A_c(max)$ being determined by extrapolation of the isotherm from the region $Mn_{(s)} < 0.8$ to $Mn_{(s)} = 1.0$, alters the observed affinity drastically.

Table 5.5

Variation of Ka and $\Delta G^{\ominus}$ for the $Mn \rightleftharpoons NH_4$ equilibria in Y with variation in Ac max.

| Ac Max | Ka | $\Delta G^{\theta}$/kJ(g.equiv)$^{-1}$ |
|---|---|---|
| 0.75 | 0.0156 | 5.14 |
| 0.50 | 0.168 | 2.19 |
| 0.49 | 0.192 | 2.03 |

It is apparent that a considerable increase in the affinity of the zeolite for the manganese ion occurs on adopting this normalisation procedure, bringing the value of $\Delta G^{\theta}$ into the position in the affinity sequence that is expected by consideration of pauling ionic radii[87] i.e.

$$Mn > Ni > Zn > Co$$

In chapter 3, the effect of varying the maximum level of exchange on the calculated values of $\Delta G^{\ominus}$ was discussed. These procedures are applied here to the $Zn^{2+} \rightleftharpoons NH_4^+$ system. The value of the maximum exchange level was systematically varied through the range of $A_c(max) \pm 0.02$ and for each value of $A_c(max)$ the equilibrium constant $K_a$ and $\Delta G^{\ominus}$ were calculated

Table 5.6

Variations of $K_a$ and $\Delta G^{\ominus}$ with varying Ac max for the $Zn \rightleftharpoons NH_4$ equilibria in Y.

| Ac max | $K_a$ | $\Delta G$ /kJ(g.equiv.)$^{-1}$ |
|---|---|---|
| .76 | .202 | 1.98 |
| .77 | .175 | 2.15 |
| .78 | .151 | 2.33 |
| .79 | .136 | 2.47 |
| .80 | .124 | 2.58 |

This table shows how much the value of $\Delta G^{\ominus}$ can vary with only small change in the normalising factor. The probable experimental error in $A_c(max)$ is $\pm 0.1$; this results in a variation of approximately $\pm 0.15$ kJ (g equiv)$^{-1}$ in the value of $\Delta G^{\ominus}$. Table 5.7. shows the effect on $\Delta G^{\ominus}$

of a change in the curve-fitting procedure applied to the treatment of the isotherm, showing how further error may be introduced by merely changing from use of raw isotherm data to smoothed isotherm data, but still using the same value of maximum level of exchange.

Table 5.7 Variations in $K_a$ and $\Delta G^{\theta}$ with change in Curve Fitting Procedure

| Equilibria | Zeolite | Method | $K_a$ | $\Delta G^{\theta}$/kJ(g.equiv)$^{-1}$ |
|---|---|---|---|---|
| Co $NH_4$ | Y | Raw Data | 0.93 | 2.94 |
| Co $NH_4$ | Y | Smoothed Data | 0.96 | 2.98 |
| Ni $NH_4$ | Y | Raw Data | 0.169 | 2.19 |
| Ni $NH_4$ | Y | Smoothed Data | 0.151 | 2.33 |
| Co $NH_4$* | X | Raw Data | 0.432 | 1.04 |
| Co $NH_4$* | X | Smoothed Data | 0.649 | 0.53 |

*This Equilibrium is not reversible and the thermodynamic data has been calculated to be used as an example only

On the basis of error analyses such as the above, it is estimated that isotherms similar to these seen here for the first row transition metlas in ammonium Y yield values for $\Delta G^{\ominus}$, with an uncertainty of around $\pm$ .25 kJ (g equiv)$^{-1}$. The error limits increase as the isotherm shape exhibits greater selectivity for the ingoing ion. Thus, for example, for a highly rectangular isotherm (such as exhibited by the $Ag(NH_3)_2^+ \rightleftharpoons Na^+$ equilibrium in mordenite ( Figure 4.6. )) the values of selectivity quotient itself have a high degree of uncertainty.

Keeping in mind this error of $\pm$ 0.25 kJ (equiv)$^{-1}$ on the value of $\Delta G^{\ominus}$ for the first row transition metals in Y a comparison is now made with the values of $\Delta G^{\ominus}$ for those systems that would be predicted by simple dielectric theory. If it is assumed that $\frac{1}{\varepsilon_c} - \frac{1}{\varepsilon_s}^{*}$ does not vary markedly for the exchanges of ammonium mordenite with the hydrated transition metal ions, by equating this $^{*}$ to the experimental values obtained for one of these ions, values of $\Delta G^{\ominus}$ may be predicted for the others. Using the values of $\Delta G^{\ominus}$ obtained for the ions $Zn(H_2O)_6^{2+}$ and $Ni(H_2O)_6^{2+}$ the values of $\Delta G^{\ominus}$ for the series were calculated and are shown in table 5.8.

Table 5.8 Thermodynamic data calculated by the Dielectric Theory

| Exchanging Ion | Ionic Radius/nm | $\Delta G^{\theta}$/kJ(g.equiv)$^{-1}$ observed | calculated using Ni data | calculated using Zn data |
|---|---|---|---|---|
| $Ni(H_2O)$ | 0.072 | 2.33± 0.25 | 2.33 | 2.41 |
| $Co(H_2O)$ | 0.074 | 2.89 0.25 | 2.25 | 2.33 |
| $Mn(H_2O)^{*}$ | 0.08 | 2.09 0.25 | 2.02 | 2.09 |
| $Zn(H_2O)$ | 0.074 | 2.33 0.25 | 2.25 | 2.33 |

$^{*}$The value of $A_c$(max) chosen for this system was 0.49

With the exception of the cobalt ion, these data show good correlation between the predicted values of $\Delta G^{\ominus}$ and the observed values of $\Delta G^{\ominus}$.

5.3.3.3. Comparison of Selectivity Trends in X and Y

A comparison of selectivities between transition metal exchanged X and Y can be seen in figure 4.38., in terms of plots of $K_m^N$ (the mass action quotient) versus $A_c$. A greater preference for the transition metals is exhibited by zeolite X than Y.

To calculate values of $\Delta G^\ominus$ from these data for X is an incorrect procedure due firstly to the irreversibility observed in these systems an and secondly, because of the ternary nature of the equilibria. In consequence the mass action quotient $K_m^N$ values are not strictly appropriate since the equilibrium is not a binary one. It is however justifiable to assume in these cases of transiton metal exchange, that the $\Delta G^\ominus$ values for the equilibria in X would be more negative than that for zeolite Y due to the excessively large differences in the comparative $K_m$ values. This justification is made assuming that the sodium present in both zeolite and solution phase for both zeolites behaves in a manner only marginally different to the ammonium ions present. This inferred trend in $\Delta G^\ominus$ between zeolites X and Y is that expected on consideration of framework charge density of the two zeolites (section 5.1.1.2.).

5.3.3.4. The Effect of Isotherm Experimental Error on $K_m^N$

In order to estimate the experimental error in the values of $K_m^N$ calculated from experimental data, the isotherms for cobalt exchanging with ammonium (and sodium) in both X and Y were taken as an example (figures 4.15 and 4.10 ). Values of $K_m^N$ were calculated using particular isotherm points throughout the isotherm for values of $Ac \pm \theta$ (where $\theta$ was defined previously (section 3.1.). Variations in both $A_c$ and $A_c(max)$ were taken into account in these calculations with $A_c(max)$ being

varied by $\pm$ 1%. It was assumed that any variation in $m_A$ or $m_B$ would be insignificant compared with changes in $A_c$ and consequently $B_c$.

Figure 4.43. shows the maximum and minimum values obtained using the above procedure. High experimental error is observed in the region $A_c \rightarrow 0$, as would be expected (section 3.6. ). These data (figure 4.43) show the danger in interpreting trends in standard free energy or selectivity that are similar or approximately equal in magnitude.

5.3.3.5. Comparison of Standard Free Energies

In order to compare the standard free energies for the transition metal exchanges in the ammonium zeolites employed here with those previously reported for sodium zeolites, two methods are available.

(i) The Application of the Triangle Rule.

For the reactions

$$M^{2+}_{(S)} + 2NH^{+}_{4(C)} \rightleftharpoons M^{2+}_{(C)} + 2NH^{+}_{4(S)}$$

$$M^{2+}_{(S)} + 2Na^{+}_{(C)} \rightleftharpoons M^{2+}_{(C)} + 2Na^{+}_{(S)}$$

$$NH^{+}_{4(S)} + Na^{+}_{(C)} \rightleftharpoons NH^{+}_{4(C)} + Na^{+}_{(S)}$$

where M represents a divalent transition metal, the thermodynamic equilibrium constants are respectively

$$K_a^{(NH_4/M)} = \frac{a_M(C) \cdot a_{NH_4}(S)^2}{a_M(S) \cdot a_{NH_4}(C)^2} \qquad 5.200$$

$$K_a^{(Na/M)} = \frac{a_M(C) \cdot a_{Na}(S)^2}{a_M(S) \cdot a_{Na}(C)^2} \qquad 5.210$$

$$K_a^{(Na/NH_4)} = \frac{a_{NH_4}(C) \cdot a_{Na}(S)}{a_{NH_4}(S) \cdot a_{Na}(C)} \qquad 5.220$$

It is evident that

$$K_a^{(Na/M)} = K_a^{(NH_4/M)} \times \left(K_a^{(NH_4/Na)}\right)^2 \qquad 5.230$$

The values of $K_a$ for transition metal ion exchange in sodium Y can then be calculated by application of equation 5.230 using data from tables 4.19 and 4.20.

Table 5.9 Values of Thermodynamic Data Calculated by the Triangle Rule

| Equilibria | $Ka^{(NH_4/M)}$ | $Ka^{(Na/NH_4)}$ | $Ka^{(Na/M)}$ | $\Delta G^{\ominus(Na/M)}$ /kJ(g.equiv.)$^{-1}$ |
|---|---|---|---|---|
| Zn Y | 0.151 | 2.25 | 0.764 | 0.334 |
| Co Y | 0.096 | 2.25 | 0.484 | 0.899 |
| Ni Y | 0.151 | 2.25 | 0.764 | 0.334 |

(ii) Application of Dielectric Theory

The free energies of exchange have been shown to be related to the relative permittivities of the respective media by

$$\Delta G^{\theta} = \frac{Le^2}{8\pi}\left[\left(\frac{Z_A}{r_A} - \frac{Z_B}{r_B}\right)\left(\frac{1}{\varepsilon_c} - \frac{1}{\varepsilon_s}\right)\right] \qquad 5.120$$

If it is assumed that each phase permittivity does not change significantly with change in ion type; then the function

$$\left(\frac{1}{\varepsilon_c} - \frac{1}{\varepsilon_s}\right) \text{ remains constant}$$

This allows the assumption that

$$\Delta G^{\theta} = K\left[\frac{Z_A}{r_A} - \frac{Z_B}{r_B}\right] \qquad 5.240$$

where $$K = \frac{Le^2}{8\pi}\left[\frac{1}{\varepsilon_c} - \frac{1}{\varepsilon_s}\right] \qquad 5.250$$

Using values of $\Delta G^{\ominus}$, $r_A$, $r_B$, $z_A$ and $z_B$ for one exchange system it is therefore possible to calculate K and consequently predict $\Delta G^{\ominus}$ for other values of $r_A$, $z_A$, $r_B$, $z_B$, hence other exchange systems in the same zeolite.

Table 5.10 shows predicted values of $\Delta G^{\ominus}$ for the $Zn \rightleftharpoons Na$, $Co \rightleftharpoons Na$ and $Ni \rightleftharpoons Na$ systems in Y using the mean value of $\Delta G^{\ominus}$ for the $Ni \rightleftharpoons NH_4$ exchange in Y (found in table 5.8.)

Table 5.10 Thermodynamic Data Calculated Using Dielectric Theory

| Equilibria | $\Delta G^{\theta}$/kJ(g.equiv.)$^{-1}$ |
|---|---|
| $Zn \rightleftharpoons Na$ Y | 1.87 |
| $Co \rightleftharpoons Na$ Y | 1.87 |
| $Ni \rightleftharpoons Na$ Y | 1.96 |

Tables 5.9. and 5.10 show an inconsistency between the two methods of estimating the standard free energy for the transition metal equili-

ibria in sodium Y. Method (i) involves a compound error which arises when two standard free energy values both of which are themselves subject to experimental error are used to predict the $\Delta G^{\ominus}$ values in table 5.9. Method (ii) involves the assumption that the sum of the reciprocals of the respective crystal and solution phase permittivities remains constant (equation 5.250)

As has been shown (section 5.2.1. ) for exchange of aquated silver ions in X, Y and mordenite, the polarisability of the metal ions are significant and may affect the crystal phase permittivities such that the previous assumption is not valid.

A comparison of literature data for the $Zn \rightleftharpoons Na$, $Co \rightleftharpoons Na$ and $Ni \rightleftharpoons Na$ equilibria in Y (using predicted values from method (i) ) is given in table 5.11.

Table 5.11 Comparison of Standard Free Energies for Transition Metal Exchange in Sodium Y

| Equilibria | $\Delta G^{\ominus}$/kJ(g.equiv)$^{-1}$ | Reference |
|---|---|---|
| Co Na | 1.26 | Maes and Cremers[68] |
| Co Na | 0.89 | this work |
| Ni Na | -0.19 | Maes and Cremers[68] |
| Ni Na | 0.33 | This work |

From these data it is obvious that there is very little consistency between the complementary studies. This must be due in the main part to the methods used in obtaining the thermodynamic data and the errors inherent in these methods which have already been discussed here in depth (i.e. estimation of maximum level of exchange, integration of Kielland plots and experimental error at the extremities of the isotherms (see section 3.6)

## 5.4. ION EXCHANGE OF $Cu(NH_3)_4^{2+}$ IN AMMONIUM X AND Y.

A comparison of the isotherms (figures 4.20 and 4.21. ) shows that in both X and Y, the cuprammine ion exchanges did not proceed beyond 58% and 73% in X and Y respectively. This appears to be another example of the operation of the ion sieve effect[78,150], which for X and Y was first discussed in detail by Sherry[70]. Apparently, the cuprammine ions are restricted to the supercages in X and Y, with, in the case of X, incomplete removal of the ammonium ions originally resident in these sites. This observed partial exchange agrees with earlier studies[78] on the exchange of $Cu(NH_3)_4^{2+}$ in mordenite.

The absence of solution phase activity coefficients for the cuprammine ion precludes the calculation of the standard free energies for those exchange systems.

### 5.4.1. Comparison of Selectivities.

Values of both the normalised selectivity coefficients $\alpha^N$ and the normalised mass action quotients $K_m^N$ were calculated for these ion exchange systems. Values of the mass action quotients throughout the isotherms plotted against $A_c$ are shown in figure 4.40), with data for exchange of $Cu(NH_3)_4^{2+}$ in mordenite previously published[78], also plotted for

comparison) show a relative affinity of MOR>>Y > X. It is justifiable to compare the zeolites in this manner since because the solution concentrations were similar, the solution phase activity coefficient ratio would be similar for all these cases.

This trend can be rationalised by simple dielectric theory in the same manner as used before for the rationalisation of exchange of diamminesilver(I) ions in Na X, Y and MOR. (section 5.1.1) where it was shown that if the ratio of the ionic radii of the two exchanging cations causes the predicted $\Delta G^{\Theta}$ values to be negative, the affinity sequence for a series of differently charged zeolites would be that the lowest charged zeolite would be most selective, i.e.:

$$MOR > Y > X$$

The condition for exchange of $Cu(NH_3)_4^{2+}$ with an ammonium zeolite to exhibit a negative standard free energy is

$$r_{Cu(NH_3)_4} > \left( \frac{z_{Cu(NH_3)_4}}{z_{NH_4}} \right) r_{NH_4}$$

where r stands for the radii of the negative ions of charge z. This condition is assumed for the exchange equilibria exhibited here.

Dielectric theory is concerned with thermodynamic affinities rather than selectivities. However it is reasonable to conclude that in this situation trends in selectivity will be reflected by a trend in affinities in the same direction. This is observed here, in that the predicted affinity trends agree with the observed selectivity

trends as shown in figure 4.17.

The case of exchange of $Cu(NH_3)_4^{2+}$ in X can be compared with the exchange of $Ag(NH_3)_2^{+}$ in the same zeolite (section 5.2.2. ). In both cases the selectivity data show lower selectivity for the amminated species than for the simple aquo species (figure 4.40.) in contradiction to predictions of dielectric theory. The dielectric theory predicts a higher affinity for the larger amminated species. These selectivity data (Figures 4.33. & 4.40) may show the inadequacy of simple dielectric theory but they can be rationalised by assuming a significantly higher value for $\Gamma$ (section 5.2.2.) for the amminated species than the aquo species. The effect on $\Delta G^{\ominus}$ by changing $\Gamma$ is shown in section 3.5.2.1.1.

## 5.5. ION EXCHANGE OF $Pt(NH_3)_4^{2+}$ AND $Pd(NH_3)_4^{2+}$ INTO SODIUM ZEOLITES.

### 5.5.1. Maximum Levels of Exchange.

For zeolites X, Y and mordenite, the maximal levels obtained by exhaustive re-exchange with the $Pt(NH_3)_4^{2+}$ ion are 0.45, 0.48 and 0.55 respectively, and are in the cases of X and Y considerably lower than those normally obtained with transition metal ion exchange in these zeolites.

The maximum level obtained for exchange in mordenite is consistent with the 50% level of exchange obtained previously with first row transition metals[65.78]. It again appears in the case of X and Y that amminated platinum species are confined to exchange within the supercages, and that total removal of the sodium ions originally resident within those sites did not occur. For the exchange in mordenite, since it is probable

that the ion sieve effect[65,78] is in operation and the platinum ion is primarily confined to the main channels, then the level of exchange observed indicates removal of ∿50% of the original sodium ions, thought to be resident in the main channels[39], plus a small number of sodium ions from the side pockets, with possibly a partial penetration of the $Pt(NH_3)_4^{2+}$ ion into these sites.

The maximum levels of exchange for the tetramminepalladium(II) ion in the three zeolites were less easily determined but in all cases appeared to involve about 60% removal of the original sodium ion content. These results show similar effects to those observed for the platinum complex ion, except that, in the case of the palladium complex, higher levels of ion exchange occurred. In the case of mordenite it is probable that cation redistribution has taken place, with sodium ions migrating out of the sidepockets to exchange with complexed palladium ions, which then remain in the main channels.

An interesting phenomenon observed with the exchange of tetrammineplatinum(II) in all three zeolites is that the determined maximum levels of ion exchange appear to be inconsistent with the shapes of the isotherms (figures 4.22 to 4.25). This effect has been observed previously with mordenite exchanged with hexamminenickel(II) ions dissolved in triethanolammine[150]. It is interesting to note that nickel(II) has an outer electronic configuration of $d^8$, identical for those of platinum(II) and palladium(II), indicating that the maximum level of exchange may be a function of the ability of the ion coordinate to the lattice oxygens and hence be a reflection of the electonic configuration.

5.5.2. The Ion Exchange Isotherms.

All the isotherms (figures 4.22 to 4.28 ) obtained for both $Pt(NH_3)_4^{2+}$ and $Pd(NH_3)_4^{2+}$ exchange in X, Y and mordenite are highly rectangular in contrast to the characteristic sigmoidal shape observed with transition metals. Highly rectangular isotherms are frequently observed for exchange of amminated species[78,150]. The lack of data points at high levels of ion exchange, however, do not preclude the possibility of sigmoidal isotherms occurring, especially in the cases of tetrammineplatinum(II) exchange where the maximum levels of exchange do not correspond to the isotherm shapes. These data (figures 4.22 to 4.25 ) could indicate a change in selectivity at high values of $Pt(NH_3)_4$ (s)

The calculation and interpretation of selectivity data for the platinum and palladium systems are difficult because of the highly selective nature of the isotherms plus ambiguities in the determination of maximum exchange levels (see section 3.6. ). Selectivity data for the platinum systems, based on a maximum level of exchange predicted by extrapolation of the isotherm, are shown in figures 4.41. and 4.42 . These plots emphasise the difficulty in interpreting selectivity plots with very few meaningful data points (which always is the case with rectangular isotherms). Inspection of the selectivity data for $Pt(NH_3)^{2+}$ exchange (Figures 4.41 & 4.42 )indicate that exchange selectivity is lower in Na- X than in either Na-MOR or Na-Y. The general trends indicate an affinity sequence of

$$MOR > Y > X$$

for this complexed ion which is the sequence predicted by simple dielectric theory and is the same as observed for both the amminated ions of copper and silver.

In this context, it is of interest that the selectivity values for $Pt(NH_3)_4^{2+}$ in $NH_4$-X (figure 4.11) are generally lower than for Na-X. This is in accord with simple dielectric theory assuming, justifiably that the solution phase activity coefficients of the sodium ion are insignificantly different to those for the ammonium ion under similar conditions.

Values of selectivity coefficients were not calculated for the $Pd(NH_3)_4^{2+} \rightleftharpoons Na$ equilibria due to the high degree of uncertainty about the maximum levels of ion exchange (section 4.1.4.)

Inspection of the isotherms for these systems (figures 4.26 to 4.28) indicate that zeolite X shows a lower preference for the platinum(II) complex than either Y or mordenite. The mordenite isotherm (figure is highly rectangular and consequently the general selectivity sequence inferred from these data is

$$MOR \sim Y > X$$

This again conforms to the trend in $\Delta G^{\ominus}$ that would be predicted by simple dielectric theory (section 5.1.1.2.)

GENERAL CONCLUSION

This work has attempted to investigate some of the factors affecting the observed selectivity of zeolites X, Y and synthetic mordenite towards transition metal ions.

The problems inherent in exchanging the first row transition metals, such as precipitation of basic salts, hydrolysis and dealumination, were shown to be of prime importance.

Selctivity trends for the first row transition metals exchanging in ammonium X and Y were calculated but factors such as evidence of ternary exchange and irreversibility precluded the complete rationalisation of these trends. Comparison of these trends with previously reported data shows need for great caution in the interpretation of selectivity data due to the dramatic changes in the derived data caused by variation in the experimental measurement. A major source of error in determination of selectivities is inaccuracy in the determination of the maximum level of exchange. In the case of transition metal exchange this value is subject to errors due to hydrolysis or precipitation.

Affinity sequences for the exchanges $NH_4^+ \rightleftharpoons Na^+$ and $Ag^+ \rightleftharpoons Na^+$ in various zeolites were rationalised using the simple dielectric theory and, in the case of silver exchange in Na-X, a modification of this theory. Changes in selectivity for the silver(I) and copper(II) ions, upon complexation with ammonia, were rationalised using the simple dielectric theory as was the exchange of complexed platinum(II) and palladium(II) in Na-X, Na-Y and Na-MOR. These data showed the general adequacy of the dielectric theory for predicting trends in the standard free energy of exchange.

## APPENDIX I SELECTIVITY COEFFICIENTS

The mass action quotient (equation 1.210 ) and the selectivity quotient are related as follows [142]

If $$K_m = \frac{A_c^{ZB} \cdot m_B^{ZA}}{B_c^{ZA} \cdot m_A^{ZB}} \qquad \text{(i)}$$

and $$\alpha = \frac{A_c \cdot m_B}{B_c \cdot m_A} \qquad \text{(ii)}$$

Then $$K_m^{1/ZA} = \frac{m_B}{B_c} \left(\frac{A_c}{m_A}\right)^{ZB/ZA} \qquad \text{(iii)}$$

$$= \frac{A_c\, m_B}{B_c\, m_A} \left(\frac{A_c}{m_A}\right)^{\left(\frac{ZB-ZA}{ZA}\right)} \qquad \text{(iv)}$$

rearanging and substituting equation (ii)

$$\alpha = K_m^{1/ZA} \cdot \left(\frac{A_c}{m_A}\right)^{\left(\frac{ZA-ZB}{ZA}\right)} \qquad \text{(v)}$$

This relationship was derived by Barrer and Klinowski [60].

If ZA = ZB then equation (v) simplifies to $\alpha = K_m^{1/ZA}$. For the case of uni-univalent exchange, $\alpha = K_m$.

For the case of uni-divalent exchange, where the divalent ion is the ingoing species (i.e. ZA = 2, ZB = 1 ) comparison of equations (i) and (ii) show

$$K_m = \frac{\alpha^2\, m_A}{A_c} \qquad \text{(vi)}$$

# APPENDIX II EXPERIMENTAL DATA

Thid section consists of the following data:

Isotherm data

Derived thermodynamic data

Kinetic data

Sodium contribution towards exchange of first row transition metal exchange in zeolites

Isotherm Data

1st Row Transition Metals in $NH_4$/Na X

| $Cu_{(s)}$ | $Cu_{(c)}$ | $Co_{(s)}$ | $Co_{(c)}$ | $Ni_{(s)}$ | $Ni_{(c)}$ |
|---|---|---|---|---|---|
| 0.84 | 0.89 | 0.905 | 0.532 | 0.719 | 0.591 |
| 0.76 | 0.84 | 0.795 | 0.521 | 0.591 | 0.553 |
| 0.665 | 0.78 | 0.715 | 0.488 | 0.293 | 0.511 |
| 0.577 | 0.77 | 0.616 | 0.448 | 0.209 | 0.458 |
| 0.471 | 0.776 | 0.523 | 0.419 | $0.111^{-2}$ | 0.447 |
| 0.288 | 0.686 | 0.443 | 0.398 | $2.51\times10^{-2}$ | 0.40 |
| 0.188 | 0.667 | 0.329 | 0.331 | 0.005 | 0.202 |
| 0.097 | 0.596 | 0.236 | 0.355 | 0.931 | 0.669 |
| 0.01 | 0.477 | 0.181 | 0.331 | 0.304 | 0.501 |
| 0.00285 | 0.29 | 0.0518 | 0.2851 | $0.941^{-3}$ | 0.669 |
| 0.38 | 0.717 | 0.0177 | 0.188 | $1.35\times10^{-3}$ | 0.242 |
| 0.952 | 0.977 | 0.960 | 0.651 | $0.936^{-4}$ | 0.637 |
| 0.00025 | 0.1877 | 0.942 | 0.666 | $6.6\times10^{-4}$ | 0.142 |
| 0.914 | 0.9677 | $0.863^{-4}$ | 0.571 | $4.4\times10^{-4}$ | 0.107 |
| 0.915 | 0.961 | $6.04\times10^{-4}$ | 0.138 | 0.439 | 0.525 |
| 0.915 | 0.943 | 0.953 | 0.652 | 0.923 | 0.648 |
| 0.913 | 0.953 | 0.934 | 0.624 | 0.749 | 0.612* |
| 0.425 | 0.697* | 0.872 | 0.561 | 0.220 | 0.431* |
| 0.081 | 0.576* | 0.874 | 0.573 | 0.785 | 0.604* |
| 0.621 | 0.813* | 0.115 | 0.298 | | |
| | | 0.981 | 0.683 | | |
| | | 0.0642 | 0.248 | | |
| | | 0.807 | 0.507* | | |
| | | 0.331 | 0.351* | | |
| | | 0.377 | 0.404* | | |
| | | 0.11 | 0.31 * | | |
| | | 0.066 | 0.224* | | |
| | | 0.0642 | 0.368* | | |
| | | 0.481 | 0.501* | | |
| | | 0.874 | 0.631* | | |

* Reverse Points

## Isotherm Data

### 1st Row Transition Metals in $NH_4/Na$ X

| $Mn_{(s)}$ | $Mn_{(c)}$ | $Zn_{(s)}$ | $Zn_{(c)}$ |
|---|---|---|---|
| 0.686 | 0.603 | 0.870 | 0.695 |
| 0.608 | 0.529 | 0.785 | 0.658 |
| 0.504 | 0.561 | 0.697 | 0.59 |
| 0.41 | 0.51 | 0.593 | 0.637 |
| 0.305 | 0.503 | 0.494 | 0.579 |
| 0.221 | 0.449 | 0.401 | 0.561 |
| 0.124 | 0.428 | 0.296 | 0.55 |
| 0.049 | 0.285 | 0.203 | 0.539 |
| 0.931 | 0.84 | 0.114 | 0.477 |
| 0.957 | 0.754 | 0.0569 | 0.392 |
| 0.938 | 0.728 | $2.94 \times 10^{-3}$ | 0.274 |
| 0.749 | 0.649 | 0.953 | 0.809 |
| 0.764 | 0.663 | 0.874 | 0.674 |
| 0.931 | 0.748 | 0.931 | 0.758 |
| 0.883 | 0.713 | 0.861 | 0.689 |
| 0.072 | 0.352 | 0.948 | 0.781 |
| 0.00185 | 0.127 | 0.952 | 0.761 |
| 0.0075 | 0.214 | 0.951 | 0.762 |
| 0.0271 | 0.298 | 0.951 | 0.762 |
| 0.931 | 0.748 | 0.951 | 0.762 |
| 0.931 | 0.748 | 0.952 | 0.789 |
| 0.620 | 0.581* | $6 \times 10^{-4}$ | 0.167 |
| 0.238 | 0.480* | 0.691 | 0.592* |
| 0.231 | 0.481* | 0.35 | 0.57 * |
| 0.535 | 0.571* | 0.1 | 0.346* |
| 0.822 | 0.713* | 0.512 | 0.591* |
| 0.439 | 0.618* | 0.812 | 0.731* |
| 0.0821 | 0.439* | 0.726 | 0.712* |
| | | 0.728 | 0.737* |
| | | 0.514 | 0.678* |
| | | 0.0507 | 0.577* |
| | | 0.462 | 0.659* |
| | | 0.68 | 0.698* |

* Reverse Points

Isotherm Data

1st Row Transition Metals in $NH_4$/Na Y

| $Cu_{(s)}$ | $Cu_{(c)}$ | $Co_{(s)}$ | $Co_{(c)}$ | $Ni_{(s)}$ | $Ni_{(c)}$ |
|---|---|---|---|---|---|
| 0.887 | 0.874 | 0.925 | 0.548 | 0.948 | 0.648 |
| 0.801 | 0.791 | 0.842 | 0.485 | 0.901 | 0.605 |
| 0.703 | 0.738 | 0.774 | 0.450 | 0.901 | 0.605 |
| 0.628 | 0.614 | 0.653 | 0.386 | 0.824 | 0.603 |
| 0.531 | 0.554 | 0.577 | 0.339 | 0.731 | 0.497 |
| 0.440 | 0.478 | 0.455 | 0.332 | 0.639 | 0.453 |
| 0.352 | 0.397 | 0.370 | 0.256 | 0.556 | 0.387 |
| 0.254 | 0.302 | 0.286 | 0.229 | 0.456 | 0.318 |
| 0.161 | 0.218 | 0.176 | 0.189 | 0.349 | 0.291 |
| 0.0361 | 0.126 | 0.0879 | 0.119 | 0.269 | 0.206 |
| 0.935 | 0.961 | 0.048 | 0.0775 | 0.0812 | 0.137 |
| 0.964 | 0.856 | 0.954 | 0.644 | 0.0412 | 0.0396 |
| 0.938 | 0.899 | 0.974 | 0.605 | 0.025 | 0.0533 |
| 0.158 | 0.238 | 0.974 | 0.605 | 0.165 | 0.159 * |
| 0.0374 | 0.104 | 0.973 | 0.618 | 0.615 | 0.455 * |
| 0.21 | 0.32 * | 0.973 | 0.618 | 0.616 | 0.437 * |
| 0.241 | 0.433 * | 0.973 | 0.618 | 0.297 | 0.254 * |
| 0.426 | 0.546 * | 0.956 | 0.608 | 0.066 | 0.087 * |
| | | 0.954 | 0.638 | | |
| | | 0.723 | 0.417 * | | |
| | | 0.437 | 0.332 * | | |
| | | 0.0588 | 0.380 * | | |
| | | 0.811 | 0.468 * | | |
| | | 0.517 | 0.368 * | | |

* Reverse Points

Isotherm Data

1st Row Transition Metals in $NH_4/Na$ Y

| $Mn_{(s)}$ | $Mn_{(c)}$ | $Zn_{(s)}$ | $Zn_{(c)}$ |
|---|---|---|---|
| 0.935 | 0.449 | 0.91 | 0.630 |
| 0.856 | 0.426 | 0.821 | 0.603 |
| 0.741 | 0.349 | 0.720 | 0.548 |
| 0.643 | 0.340 | 0.644 | 0.520 |
| 0.465 | 0.224 | 0.543 | 0.465 |
| 0.179 | 0.129 | 0.453 | 0.411 |
| 0.364 | 0.211 | 0.349 | 0.364 |
| 0.272 | 0.171 | 0.265 | 0.280 |
| 0.062 | 0.069 | 0.172 | 0.233 |
| 0.549 | 0.291 | 0.0805 | 0.158 |
| 0.746 | 0.368 | 0.039 | 0.0956 |
| 0.274 | 0.187 | 0.965 | 0.691 |
| 0.960 | 0.575 | 0.0201 | 0.056 |
| 0.958 | 0.557 | 0.791 | 0.548* |
| 0.921 | 0.451 | 0.427 | 0.411* |
| 0.119 | 0.0917* | 0.130 | 0.328* |
| 0.798 | 0.407* | | |
| 0.531 | 0.232* | | |

* Reverse Points

Isotherm Data : Sodium X

| $NH_4$(s) | $NH_4$(c) | $Ag_{(s)}$ | $Ag_{(c)}$ | $Ag(NH_3)_2$(s) | $Ag(NH_3)_2$(c) |
|---|---|---|---|---|---|
| 0.854 | 0.612 | 1.0 | 1.0 | 0.819 | 0.451 |
| 0.711 | 0.497 | 0.016 | 0.50 | 0.722 | 0.379 |
| 0.629 | 0.423 | 0.056 | 0.762 | 0.526 | 0.353 |
| 0.534 | 0.382 | 0.138 | 0.883 | 0.343 | 0.239 |
| 0.435 | 0.319 | 0.235 | 0.915 | 0.186 | 0.129 |
| 0.350 | 0.284 | 0.321 | 0.992 | 0.088 | 0.0601 |
| 0.155 | 0.165 | 0.320 | 0.980 | 0.920 | 0.510 |
| 0.0817 | 0.0992 | 0.425 | 0.964 | 0.039 | 0.031 |
| 0.909 | 0.628 | 0.623 | 0.953 | 0.274 | 0.189 |
| 0.624 | 0.452 | 0.718 | 0.975 | 0.463 | 0.279 |
| 0.529 | 0.401 | 0.0016 | 0.264 | 0.618 | 0.355 |
| 0.022 | 0.0421 | 0.0320 | 0.650 | 0.32 | 0.226 |
| 0.334 | 0.261 | 0.007 | 0.382 | 0.151 | 0.1* |
| 0.254 | 0.230* | 0.526 | 0.963 | 0.818 | 0.423* |
| 0.128 | 0.122* | 0.081 | 0.827 | 1.0 | 0.565 |
| 0.654 | 0.475* | 0.894 | 0.989 | | |
| 1.0 | 0.731* | 0.038 | 0.692* | | |
| | | 0.215 | 0.924* | | |
| | | 0.369 | 0.98* | | |

| $Pt(NH_3)_4$(s) | $Pt(NH_3)_4$(c) | $Pd(NH_3)_4$(s) | $Pd(NH_3)_4$(c) |
|---|---|---|---|
| 1.0 | 0.348 | 1.0 | 0.64 |
| 0.765 | 0.356 | 0.772 | 0.615 |
| 0.661 | 0.350 | 0.431 | 0.589 |
| 0.601 | 0.270 | 0.205 | 0.491 |
| 0.469 | 0.346 | 0.124 | 0.431 |
| 0.368 | 0.348 | 0.049 | 0.320 |
| 0.273 | 0.335 | 0.00494 | 0.228 |
| 0.163 | 0.341 | 0.921 | 0.639 |
| 0.0938 | 0.279 | | |
| 0.0343 | 0.173 | | |
| 0.02256 | 0.0723 | | |
| 0.0249 | 0.133* | | |
| 0.124 | 0.286* | | |

*Reverse Points

Isotherm Data : Sodium Y

| $NH_4$(s) | $NH_4$(c) | Ag(s) | Ag(c) | $Ag(NH_3)_2$(s) | $Ag(NH_3)_2$(c) |
|---|---|---|---|---|---|
| 1.0 | 0.706 | 1.0 | 1.0 | 1.0 | 0.55 |
| 0.075 | 0.166 | 0.866 | 0.936 | 0.818 | 0.549 |
| 0.173 | 0.255 | 0.774 | 0.891 | 0.717 | 0.533 |
| 0.0242 | 0.0759 | 0.68 | 0.869 | 0.527 | 0.549 |
| 0.271 | 0.318 | 0.494 | 0.795 | 0.43 | 0.479 |
| 0.347 | 0.387 | 0.404 | 0.739 | 0.334 | 0.456 |
| 0.438 | 0.414 | 0.306 | 0.700 | 0.245 | 0.373 |
| 0.542 | 0.448 | 0.133 | 0.495 | 0.152 | 0.320 |
| 0.640 | 0.496 | 0.221 | 0.599 | 0.0675 | 0.239 |
| 0.727 | 0.584 | 0.0598 | 0.308 | 0.0285 | 0.136 |
| 0.884 | 0.623 | 0.0234 | 0.195 | 0.703 | 0.544 |
| 0.946 | 0.671 | 0.081 | 0.408 * | 0.0103 | 0.0586 |
| 0.111 | 0.223 * | 0.0101 | 0.085 | 0.251 | 0.389 * |
| 0.44 | 0.438 * | 0.278 | 0.604 * | 0.184 | 0.331 * |
| 0.631 | 0.536 * | 0.540 | 0.782 * | 0.038 | 0.186 * |
| | | | | 0.476 | 0.501 * |

| $Pt(NH_3)_4$(s) | $Pt(NH_3)_4$(c) | $Pd(NH_3)_4$(s) | $Pd(NH_3)_4$(c) |
|---|---|---|---|
| 1.0 | 0.401 | 1.0 | 0.62 |
| 0.784 | 0.407 | 0.479 | 0.55 |
| 0.638 | 0.409 | 0.239 | 0.528 |
| 0.620 | 0.278 | 0.165 | 0.472 |
| 0.489 | 0.390 | 0.0564 | 0.491 |
| 0.385 | 0.401 | 0.00264 | 0.346 |
| 0.185 | 0.384 | 0.821 | 0.601 |
| 0.288 | 0.392 | 0.943 | 0.612 |
| 0.102 | 0.350 | 0.019 | 0.431 |
| 0.0369 | 0.221 | | |
| 0.0171 | 0.115 | | |
| 0.0261 | 0.178* | | |
| 0.119 | 0.341* | | |

* Reverse Points

Isotherm Data : Sodium MOR

| $Ag_{(s)}$ | $Ag_{(c)}$ | $Ag(NH_3)_{2(s)}$ | $Ag(NH_3)_{2(c)}$ |
|---|---|---|---|
| 1.0 | 0.889 | 1.0 | 0.753 |
| 0.788 | 0.877 | 0.886 | 0.753 |
| 0.687 | 0.888 | 0.777 | 0.754 |
| 0.494 | 0.870 | 0.663 | 0.747 |
| 0.392 | 0.864 | 0.496 | 0.77 |
| 0.298 | 0.796 | 0.396 | 0.716 |
| 0.213 | 0.714 | 0.295 | 0.740 |
| 0.114 | 0.588 | 0.20 | 0.704 |
| 0.0435 | 0.444 | 0.111 | 0.642 |
| 0.0118 | 0.286 | 0.0247 | 0.608 |
| 0.005 | 0.131 | 0.451 | 0.693* |
| 0.899 | 0.881 | 0.148 | 0.671* |
| 0.042 | 0.451* | | |
| 0.261 | 0.791* | | |
| 0.119 | 0.605* | | |
| 0.556 | 0.861* | | |

| $Pt(NH_3)_4$ (s) | $Pt(NH_3)_4$ (c) | $Pd(NH_3)_4$ (s) | $Pd(NH_3)_4$ (c) |
|---|---|---|---|
| 1.0 | 0.356 | 1.0 | 0.61 |
| 0.831 | 0.347 | 0.85 | 0.60 |
| 0.707 | 0.367 | 0.61 | 0.607 |
| 0.509 | 0.356 | 0.418 | 0.586 |
| 0.411 | 0.354 | 0.241 | 0.598 |
| 0.318 | 0.324 | 0.178 | 0.567 |
| 0.213 | 0.343 | 0.062 | 0.558 |
| 0.124 | 0.316 | 0.0015 | 0.319 |
| 0.0387 | 0.243 | 0.020 | 0.493 |
| 0.0207 | 0.116 | | |
| 0.0241 | 0.181* | | |
| 0.120 | 0.30 * | | |

* Reverse Points

## Isotherm Data

### $Cu(NH_3)_4$ in $NH_4$/Na X and Y

| X | | Y | |
|---|---|---|---|
| $Cu(NH_3)_{4(s)}$ | $Cu(NH_3)_{4(c)}$ | $Cu(NH_3)_{4(s)}$ | $Cu(NH_3)_{4(c)}$ |
| 0.792 | 0.511 | 0.785 | 0.642 |
| 0.719 | 0.495 | 0.515 | 0.541 |
| 0.617 | 0.432 | 0.331 | 0.493 |
| 0.536 | 0.43 | 0.137 | 0.378 |
| 0.443 | 0.405 | 0.0484 | 0.314 |
| 0.336 | 0.311 | 0.0224 | 0.201 |
| 0.259 | 0.237 | -0.0169 | 0.141 |
| 0.159 | 0.196 | 0.713 | 0.598 |
| 0.0763 | 0.107 | 0.614 | 0.598 |
| 0.0722 | 0.129 | 0.528 | 0.561 |
| 0.944 | 0.568 | 0.239 | 0.467 |
| 0.0434 | 0.0674 | 0.143 | 0.413 |
| 0.0570 | 0.0834 | 0.0561 | 0.335 |
| 0.698 | 0.463* | 0.0408 | 0.295 |
| 0.412 | 0.353* | 0.952 | 0.662 |
| 0.219 | 0.307* | 0.906 | 0.658 |
| 0.869 | 0.546* | 0.953 | 0.678 |
| | | 0.702 | 0.615 |
| | | 0.508 | 0.540 |
| | | 0.615 | 0.614 * |
| | | 0.514 | 0.510 * |

### Silver and Platinum complexes in $NH_4$-X

| X | | Y | |
|---|---|---|---|
| $Pt(NH_3)_{4(s)}$ | $Pt(NH_3)_{4(c)}$ | $Ag(NH_3)_{2(s)}$ | $Ag(NH_3)_{2(c)}$ |
| 1.0 | 0.309 | 1.0 | 0.70 |
| 0.60 | 0.299 | 0.636 | 0.695 |
| 0.514 | 0.309 | 0.438 | 0.673 |
| 0.429 | 0.318 | 0.142 | 0.608 |
| 0.38 | 0.293 | 0.0036 | 0.252 |
| 0.236 | 0.277 | 0.049 | 0.534 |
| 0.164 | 0.259 | 0.416 | 0.726 |
| 0.100 | 0.251 | 0.903 | 0.712 |
| 0.0643 | 0.196 | 0.0136 | 0.365 |
| 0.0357 | 0.151 | 0.025 | 0.451* |
| 0.00665 | 0.0732 | 0.203 | 0.626* |
| 0.00143 | 0.0389 | | |
| 0.308 | 0.290 | | |
| 0.863 | 0.297 | | |
| 0.0186 | 0.116 * | | |
| 0.111 | 0.220 * | | |

* Reverse Points

Ammonium $\rightleftharpoons$ Sodium X Derived Data

| $NH_4(c)$ | $\alpha^N$ | $\alpha_{un}$ | ln $K_c$ | ln $K_c$(calc) | $f_A$ | $f_B$ | $m_A$ |
|---|---|---|---|---|---|---|---|
| 0.818 | 0.771 | 0.254 | -0.247 | -0.236 | 0.979 | 0.700 | 0.0854 |
| 0.678 | 0.857 | 0.398 | -0.141 | -0.107 | 0.948 | 0.771 | 0.0711 |
| 0.609 | 0.919 | 0.472 | -0.0712 | -0.053 | 0.929 | 0.799 | 0.0629 |
| 0.534 | 1.001 | 0.558 | 0.0145 | 0.0066 | 0.906 | 0.826 | 0.0534 |
| 0.458 | 1.098 | 0.652 | 0.1068 | 0.0731 | 0.876 | 0.854 | 0.0435 |
| 0.390 | 1.189 | 0.740 | 0.187 | 0.142 | 0.842 | 0.880 | 0.0350 |
| 0.209 | 1.444 | 0.984 | 0.381 | 0.406 | 0.698 | 0.950 | 0.0155 |
| 0.126 | 1.626 | 1.141 | 0.499 | 0.582 | 0.603 | 0.978 | 0.00817 |
| 0.881 | 0.744 | 0.181 | -0.282 | -0.310 | 0.989 | 0.657 | 0.0909 |
| 0.605 | 0.923 | 0.476 | -0.0667 | -0.0495 | 0.928 | 0.800 | 0.0624 |
| 0.530 | 1.006 | 0.563 | 0.0191 | 0.0098 | 0.905 | 0.828 | 0.0529 |
| 0.209 | 1.445 | 0.984 | 0.381 | 0.406 | 0.698 | 0.950 | 0.0115 |
| 0.050 | 2.353 | 1.694 | 0.868 | 0.784 | 0.501 | 0.996 | 0.0022 |
| 0.377 | 1.207 | 0.758 | 0.202 | 0.157 | 0.834 | 0.885 | 0.0334 |
| 0.307 | 1.303 | 0.849 | 0.278 | 0.246 | 0.787 | 0.912 | 0.0231 |
| 0.180 | 1.496 | 1.031 | 0.416 | 0.464 | 0.667 | 0.961 | 0.0128 |
| 0.629 | 0.899 | 0.449 | -0.0929 | -0.0687 | 0.935 | 0.792 | 0.0654 |

Ammonium $\rightleftharpoons$ Sodium Y Derived Data

| $NH_4(c)$ | $\alpha^N$ | $\alpha_{un}$ | ln $K_c$ | ln $K_c$(calc) | $f_A$ | $f_B$ | $m_A$ |
|---|---|---|---|---|---|---|---|
| 0.233+ | 3.738 | 2.455 | 1.332 | 1.336 | 0.566 | 0.959 | 0.00750 |
| 0.351 | 2.599 | 1.605 | 0.968 | 1.135 | 0.652 | 0.904 | 0.01720 |
| 0.104 | 4.673 | 3.227 | 1.554 | 1.535 | 0.479 | 0.992 | 0.00242 |
| 0.468 | 2.371 | 1.351 | 0.876 | 0.920 | 0.740 | 0.828 | 0.02710 |
| 0.539 | 2.200 | 1.177 | 0.802 | 0.782 | 0.793 | 0.772 | 0.03470 |
| 0.606 | 1.980 | 0.980 | 0.696 | 0.644 | 0.841 | 0.713 | 0.04380 |
| 0.669 | 1.710 | 0.773 | 0.551 | 0.512 | 0.882 | 0.655 | 0.05420 |
| 0.723 | 1.460 | 0.599 | 0.396 | 0.396 | 0.914 | 0.605 | 0.06400 |
| 0.771 | 1.296 | 0.460 | 0.251 | 0.285 | 0.940 | 0.558 | 0.07270 |
| 0.828 | 1.098 | 0.328 | 0.108 | 0.153 | 0.965 | 0.501 | 0.08150 |
| 0.882 | 0.988 | 0.223 | 0.00115 | 0.025 | 0.983 | 0.449 | 0.08840 |
| 0.940 + | 0.904 | 0.116 | -0.0867 | -0.117 | 0.995 | 0.394 | 0.09460 |
| 0.313 | 3.640 | 2.298 | 1.305 | 1.203 | 0.623 | 0.925 | 0.01110 |
| 0.608 | 1.975 | 0.975 | 0.694 | 0.642 | 0.842 | 0.713 | 0.04400 |
| 0.717 | 1.488 | 0.614 | 0.410 | 0.406 | 0.911 | 0.609 | 0.06310 |

* Reverse points
\+ Original Isotherm Data

Silver(I) $\rightleftharpoons$ Sodium X Derived Data†

| $Ag_{(c)}$ | $\alpha^N$ | ln $K_c$ | ln $K_c$(calc) | $f_A$ | $f_B$ | $m_A$ |
|---|---|---|---|---|---|---|
| 0.5 | 61.5 | 4.157 | 4.065 | 0.919 | 0.282 | 0.0016 |
| 0.762 | 53.97 | 4.027 | 4.176 | 0.880 | 0.302 | 0.0056 |
| 0.883 | 47.14 | 3.891 | 3.765 | 0.941 | 0.213 | 0.0138 |
| 0.915 | 35.04 | 3.595 | 3.531 | 0.963 | 0.173 | 0.0235 |
| 0.964 | 36.23 | 3.628 | 3.042 | 0.991 | 0.109 | 0.0425 |
| 0.953 | 12.27 | 2.546 | 3.166 | 0.986 | 0.123 | 0.0623 |
| 0.975 | 15.31 | 2.768 | 2.907 | 0.995 | 0.096 | 0.0718 |
| 0.264 | 223.82 | 5.449 | 5.518 | 0.352 | 0.462 | 0.00016 |
| 0.65 | 56.178 | 4.067 | 4.150 | 0.889 | 0.296 | 0.0032 |
| 0.382 | 87.685 | 4.512 | 4.409 | 0.753 | 0.326 | 0.0007 |
| 0.963 | 23.454 | 3.193 | 3.053 | 0.991 | 0.111 | 0.0526 |
| 0.827 | 54.236 | 4.032 | 4.037 | 0.905 | 0.269 | 0.0081 |
| 0.989 | 10.66 | 2.405 | 2.723 | 0.999 | 0.080 | 0.0894 |
| 0.692 | 56.87 | 4.079 | 4.185 | 0.879 | 0.304 | 0.0038 |
| 0.924 | 44.39 | 3.831 | 3.454 | 0.969 | 0.161 | 0.0215 |

† Original unsmoothed data used to compute thermodynamic functions

Silver(I) $\rightleftharpoons$ Sodium Y Derived Data†

| $Ag_{(c)}$ | $\alpha^N$ | ln $K_c$ | ln $K_c$(calc) | $f_A$ | $f_B$ | $m_A$ |
|---|---|---|---|---|---|---|
| 0.936 | 2.263 | 0.855 | 0.898 | 0.994 | 0.422 | 0.0866 |
| 0.891 | 2.386 | 0.985 | 1.020 | 0.983 | 0.474 | 0.0774 |
| 0.869 | 3.121 | 1.177 | 1.080 | 0.976 | 0.500 | 0.068 |
| 0.796 | 3.973 | 1.417 | 1.271 | 0.945 | 0.586 | 0.0494 |
| 0.739 | 4.177 | 1.468 | 1.404 | 0.916 | 0.649 | 0.0404 |
| 0.700 | 5.291 | 1.705 | 1.492 | 0.894 | 0.691 | 0.0306 |
| 0.495 | 6.389 | 1.893 | 1.879 | 0.767 | 0.873 | 0.0133 |
| 0.559 | 5.265 | 1.699 | 1.698 | 0.832 | 0.791 | 0.0221 |
| 0.308 | 6.997 | 1.984 | 2.125 | 0.653 | 0.965 | 0.00598 |
| 0.195 | 10.109 | 2.352 | 2.225 | 0.616 | 0.990 | 0.00234 |
| 0.408 | 7.819 | 2.095 | 2.006 | 0.715 | 0.925 | 0.0081 |
| 0.604 | 3.961 | 1.415 | 1.689 | 0.835 | 0.786 | 0.0278 |
| 0.782 | 3.056 | 1.156 | 1.303 | 0.940 | 0.601 | 0.054 |
| 0.085 | 9.501 | 3.347 | 2.283 | 0.585 | 0.999 | 0.001 |

* Reverse points

† Original unsmoothed data used to compute thermodynamic functions

Silver(I) $\rightleftharpoons$ Sodium MOR Derived Data†

| $Ag_{(c)}$ | $\alpha^N$ | $\alpha_{un}$ | ln $K_c$ | ln $K_c$(calc) | $f_A$ | $f_B$ | $m_A$ |
|---|---|---|---|---|---|---|---|
| 0.985 | 18.149 | 1.918 | 2.937 | 3.675 | 1.001 | 1.580 | 0.0788 |
| 0.998 | 202.288 | 3.612 | 5.348 | 3.792 | 1.0 | 1.774 | 0.0687 |
| 0.978 | 44.556 | 6.854 | 3.835 | 3.604 | 1.002 | 1.475 | 0.0494 |
| 0.970 | 51.541 | 9.853 | 3.980 | 3.547 | 1.004 | 1.393 | 0.0392 |
| 0.894 | 19.948 | 9.191 | 3.032 | 3.o38 | 1.037 | 0.866 | 0.0298 |
| 0.802 | 14.989 | 9.224 | 2.746 | 2.740 | 1.082 | 0.670 | 0.0213 |
| 0.660 | 15.132 | 11.0919 | 2.755 | 2.776 | 1.066 | 0.684 | 0.0114 |
| 0.494 | 21.889 | 17.559 | 3.124 | 3.212 | 0.885 | 0.879 | 0.00436 |
| 0.321 | 39.65 | 33.454 | 3.719 | 3.679 | 0.675 | 1.069 | 0.00118 |
| 0.147 | 34.346 | 29.998 | 3.579 | 3.581 | 0.736 | 1.057 | 0.0005 |
| 0.989 | 10.997 | 0.832 | 2.436 | 3.761 | 1.0 | 1.646 | 0.00899 |
| 0.506 | 23.433 | 18.737 | 3.193 | 3.188 | 0.896 | 0.868 | 0.0042 |
| 0.888 | 22.623 | 10.716 | 3.157 | 3.011 | 1.040 | 0.845 | 0.0261 |
| 0.684 | 16.045 | 11.531 | 2.814 | 2.738 | 1.079 | 0.668 | 0.0119 |
| 0.967 | 22.765 | 4.749 | 3.164 | 3.519 | 1.004 | 1.356 | 0.0566 |

† Original unsmoothed data used to compute thermodynamic functions

Silver Diammine $\rightleftharpoons$ Ammonium MOR Derived Data†

| $Ag(NH_3)_{2(c)}$ | $\alpha^N$ | $\alpha_{un}$ | $m_A$ |
|---|---|---|---|
| 0.965 | 15.91 | 1.30 | 0.0636 |
| 0.935 | 18.37 | 2.64 | 0.0438 |
| 0.845 | 33.15 | 9.41 | 0.0142 |
| 0.350 | 149.03 | 93.25 | 0.00036 |
| 0.741 | 55.72 | 22.24 | 0.0049 |
| 0.988 | 9.56 | 0.265 | 0.0903 |
| 0.507 | 74.57 | 41.69 | 0.00136 |
| 0.626 | 65.39 | 32.04 | 0.0025 |
| 0.865 | 25.22 | 6.49 | 0.0203 |

† Original unsmoothed data used to compute thermodynamic functions

Silver Diammine $\rightleftharpoons$ Sodium Y Derived Data

| $Ag(NH_3)_{2(c)}$ | $\alpha^N$ | $\alpha_{un}$ | $m_A$ |
|---|---|---|---|
| 0.968 | 6.925 | 0.260 | 0.0818 |
| 0.966 | 11.449 | 0.459 | 0.0717 |
| 0.942 | 14.499 | 0.987 | 0.0527 |
| 0.898 | 11.646 | 1.322 | 0.043 |
| 0.820 | 9.08 | 1.673 | 0.0334 |
| 0.709 | 7.495 | 2.00 | 0.0245 |
| 0.543 | 6.622 | 2.413 | 0.0152 |
| 0.340 | 7.134 | 3.228 | 0.00675 |
| 0.228 | 10.109 | 4.969 | 0.00285 |
| 0.966 | 12.116 | 0.491 | 0.0703 |
| 0.717 | 7.579 | 1.982 | 0.0251 |
| 0.606 | 6.824 | 2.256 | 0.0184 |
| 0.257 | 8.761 | 2.225 | 0.0038 |
| 0.918 | 12.794 | 1.191 | 0.0467 |
| 0.105 | 11.73 | 5.98 | 0.00103 |

Silver Diammine $\rightleftharpoons$ Sodium X Derived Data

| $Ag(NH_3)_{2(c)}$ | $\alpha^N$ | $\alpha_{un}$ | $m_A$ |
|---|---|---|---|
| 0.798 | 0.872 | 0.178 | 0.0819 |
| 0.713 | 0.956 | 0.255 | 0.0722 |
| 0.562 | 1.159 | 0.413 | 0.0526 |
| 0.414 | 1.355 | 0.576 | 0.0343 |
| 0.250 | 1.464 | 0.713 | 0.0186 |
| 0.120 | 1.419 | 0.748 | 0.0088 |
| 0.902 | 0.8 | 0.088 | 0.092 |
| 0.046 | 1.164 | 0.637 | 0.00394 |
| 0.348 | 1.415 | 0.639 | 0.0274 |
| 0.515 | 1.229 | 0.468 | 0.0463 |
| 0.632 | 1.060 | 0.337 | 0.0618 |
| 0.393* | 1.376 | 0.598 | 0.032 |
| 0.209* | 1.468 | 0.736 | 0.0151 |
| 0.797* | 0.874 | 0.179 | 0.0818 |

Nickel(II) $\rightleftharpoons$ Ammonium X Derived Data

| $Ni_{(c)}$ | $\alpha^N$ | $K_m^N$ | $m_A$ |
|---|---|---|---|
| 0.832 | 3.88 | 0.649 | 0.0359 |
| 0.779 | 4.875 | 0.899 | 0.0295 |
| 0.719 | 12.349 | 3.09 | 0.0146 |
| 0.645 | 13.757 | 3.08 | 0.0105 |
| 0.629 | 27.224 | 6.481 | 0.0055 |
| 0.563 | 100.234 | 22.49 | 0.00126 |
| 0.284 | 158.3 | 22.05 | 0.00025 |
| 0.942 | 2.412 | 0.2872 | 0.0465 |
| 0.706 | 10.976 | 2.594 | 0.0152 |
| 0.942 | 2.046 | 0.2088 | 0.0470 |
| 0.339 | 760.2 | 115.94 | 0.000068 |
| 0.948 | 2.487 | 0.3053 | 0.0468 |
| 0.199 | 755.1 | 94.5 | 0.000033 |
| 0.151 | 808.9 | 95.12 | 0.000022 |
| 0.739 | 7.253 | 1.56 | 0.0219 |
| 0.912 | 1.744 | 0.154 | 0.0462 |
| 0.869 | 3.443 | 0.542 | 0.0397 |
| 0.607 | 10.954 | 2.17 | 0.0110 |
| 0.851 | 3.121 | 0.450 | 0.0393 |

Manganese(II) $\rightleftharpoons$ Ammonium X Derived Data

| $Mn_{(c)}$ | $\alpha^N$ | $K_m^N$ | $m_A$ |
|---|---|---|---|
| 0.744 | 2.667 | 0.3279 | 0.0343 |
| 0.653 | 2.426 | 0.274 | 0.0304 |
| 0.692 | 4.424 | 0.713 | 0.0252 |
| 0.629 | 4.893 | 0.780 | 0.0205 |
| 0.620 | 7.447 | 1.368 | 0.0153 |
| 0.555 | 8.794 | 1.547 | 0.0111 |
| 0.529 | 15.861 | 2.948 | 0.0062 |
| 0.351 | 21.037 | 3.152 | 0.0025 |
| 0.931 | 1.201 | 0.0741 | 0.0479 |
| 0.898 | 1.165 | 0.0708 | 0.0469 |
| 0.801 | 2.701 | 0.3415 | 0.0375 |
| 0.819 | 2.786 | 0.362 | 0.0382 |
| 0.917 | 1.644 | 0.1374 | 0.0466 |
| 0.880 | 1.948 | 0.1904 | 0.0442 |
| 0.435 | 19.881 | 3.248 | 0.0036 |
| 0.157 | 200.649 | 23.848 | 0.000093 |
| 0.264 | 95.031 | 12.998 | 0.00038 |
| 0.717 | 3.110 | 0.418 | 0.031 |
| 0.593 | 9.314 | 1.741 | 0.0119 |
| 0.594 | 9.734 | 1.850 | 0.0116 |
| 0.704 | 4.153 | 0.6565 | 0.0268 |

Cobalt(II)$\rightleftharpoons$Ammonium X Derived Data

| $Co_{(c)}$ | $\alpha^N$ | $K_m^N$ | $m_A$ |
|---|---|---|---|
| 0.695 | 1.179 | 0.0818 | 0.0397 |
| 0.651 | 1.487 | 0.1215 | 0.0358 |
| 0.597 | 1.850 | 0.1759 | 0.0307 |
| 0.558 | 2.309 | 0.249 | 0.0261 |
| 0.530 | 2.850 | 0.339 | 0.0221 |
| 0.442 | 3.221 | 0.387 | 0.0165 |
| 0.472 | 5.809 | 0.8436 | 0.0118 |
| 0.442 | 7.145 | 1.051 | 0.0091 |
| 0.380 | 22.469 | 3.452 | 0.0026 |
| 0.250 | 37.151 | 4.858 | 0.00088 |
| 0.867 | 0.541 | 0.162 | 0.0480 |
| 0.888 | 0.982 | 0.0511 | 0.0471 |
| 0.761 | 1.013 | 0.0582 | 0.0432 |
| 0.184 | 746.205 | 91.08 | 0.00003 |
| 0.869 | 0.656 | 0.0236 | 0.0477 |
| 0.832 | 0.699 | 0.0274 | 0.0467 |
| 0.748 | 0.869 | 0.044 | 0.0436 |
| 0.764 | 0.933 | 0.0498 | 0.0437 |
| 0.397 | 10.147 | 1.478 | 0.0057 |
| 0.911 | 0.394 | 0.0084 | 0.0491 |
| 0.330 | 14.358 | 1.9 | 0.00321 |
| 0.468 | 3.556 | 0.448 | 0.0166 |
| 0.538 | 3.859 | 0.523 | 0.0189 |
| 0.413 | 11.401 | 1.731 | 0.0055 |

Zinc(II) $\rightleftharpoons$ Ammonium X Derived Data

| $Zn_{(c)}$ | $\alpha^{N}$ | $K_m^N$ | $m_A$ |
|---|---|---|---|
| 0.874 | 1.662 | 0.1374 | 0.0435 |
| 0.802 | 2.225 | 0.2421 | 0.0393 |
| 0.719 | 2.230 | 0.2407 | 0.0348 |
| 0.706 | 4.922 | 0.8745 | 0.0247 |
| 0.684 | 6.471 | 1.231 | 0.0201 |
| 0.671 | 9.689 | 2.069 | 0.0148 |
| 0.657 | 15.062 | 3.522 | 0.0102 |
| 0.776 | 4.778 | 0.871 | 0.0296 |
| 0.581 | 21.616 | 4.584 | 0.0057 |
| 0.478 | 30.361 | 5.399 | 0.0028 |
| 0.334 | 340.4 | 48.563 | 0.00014 |
| 0.986 | 7.254 | 2.540 | 0.0476 |
| 0.821 | 1.331 | 0.094 | 0.0437 |
| 0.924 | 1.812 | 0.1668 | 0.0465 |
| 0.840 | 1.698 | 0.151 | 0.0440 |
| 0.952 | 2.196 | 0.240 | 0.0474 |
| 0.928 | 1.300 | 0.0866 | 0.0476 |
| 0.929 | 1.354 | 0.0939 | 0.0476 |
| 0.962 | 2.566 | 0.3257 | 0.0476 |
| 0.204 | 815.9 | 106.7 | 0.00003 |
| 0.722 | 2.322 | 0.258 | 0.0346 |
| 0.695 | 8.468 | 1.805 | 0.0175 |
| 0.721 | 4.919 | 0.859 | 0.0256 |

Copper(II) $\rightleftharpoons$ Ammonium X Derived Data

| $Cu_{(c)}$ | $\alpha^N$ | $K_m^N$ | $m_A$ |
|---|---|---|---|
| 0.891 | 3.082 | 0.447 | 0.0420 |
| 0.840 | 3.316 | 0.497 | 0.0380 |
| 0.78 | 3.572 | 0.552 | 0.0333 |
| 0.77 | 4.909 | 0.904 | 0.0289 |
| 0.776 | 7.782 | 1.842 | 0.0236 |
| 0.686 | 10.802 | 2.447 | 0.0144 |
| 0.669 | 17.303 | 4.207 | 0.0094 |
| 0.596 | 27.498 | 6.153 | 0.00485 |
| 0.477 | 91.719 | 17.283 | 0.00098 |
| 0.29 | 285.816 | 40.28 | 0.000143 |
| 0.187 | 18485.3 | 0.827 | 0.000001 |
| 0.977 | 4.255 | 0.882 | 0.0476 |
| 0.968 | 5.624 | 1.493 | 0.0457 |
| 0.961 | 4.578 | 0.999 | 0.0458 |
| 0.717 | 8.284 | 1.818 | 0.0190 |
| 0.943 | 3.086 | 0.462 | 0.0457 |
| 0.953 | 3.864 | 0.714 | 0.0456 |
| 0.969 | 6.213 | 0.849 | 0.0213 |
| 0.576 | 30.847 | 6.61 | 0.004 |

Zinc(II) $\rightleftharpoons$ Ammonium Y Derived Data

| $Zn_{(c)}$ | $\alpha^{Z}$ | $K_m^{Z}$ | ln $K_c$ | ln $K_c$(calc) | $f_A$ | $f_B$ | $m_A$ |
|---|---|---|---|---|---|---|---|
| 0.871 | 1.331 | 0.0925 | -1.945 | -1.903 | 0.855 | 0.917 | 0.0455 |
| 0.779 | 1.54 | 0.1250 | -1.654 | -1.595 | 0.739 | 0.995 | 0.0411 |
| 0.708 | 1.888 | 0.1780 | -1.292 | -1.357 | 0.647 | 1.049 | 0.036 |
| 0.641 | 1.974 | 0.1957 | -1.223 | -1.136 | 0.564 | 1.093 | 0.0322 |
| 0.584 | 2.369 | 0.2614 | -0.946 | -0.959 | 0.498 | 1.121 | 0.0272 |
| 0.535 | 2.782 | 0.3935 | -0.728 | -0.812 | 0.444 | 1.14 | 0.0226 |
| 0.469 | 3.297 | 0.4032 | -0.529 | -0.629 | 0.379 | 1.155 | 0.0174 |
| 0.401 | 3.716 | 0.4579 | -0.419 | -0.462 | 0.323 | 1.158 | 0.0133 |
| 0.303 | 4.179 | 0.4956 | -0.345 | -0.266 | 0.258 | 1.141 | 0.0086 |
| 0.174 | 4.821 | 0.5346 | -0.278 | -0.116 | 0.202 | 1.09 | 0.004 |
| 0.103 | 5.695 | 0.6140 | -0.154 | -0.0932 | 0.185 | 1.054 | 0.00195 |
| 0.946 | 1.259 | 0.0804 | -2.075 | -2.147 | 0.943 | 0.851 | 0.048 |
| 0.0685 | 7.174 | 0.7513 | 0.0552 | -0.0999 | 0.179 | 1.036 | 0.001 |
| 0.689 | 1.736 | 0.1570 | -1.435 | -1.294 | 0.624 | 1.062 | 0.0359 |
| 0.520 | 2.908 | 0.348 | -0.673 | -0.769 | 0.428 | 1.145 | 0.0214 |

Cobalt(II) $\rightleftharpoons$ Ammonium Y Derived Data

| $Co_{(c)}$ | $\alpha^N$ | $K_m^N$ | ln $K_c$ | ln $K_c$(calc) | $f_A$ | $f_B$ | $m_A$ |
|---|---|---|---|---|---|---|---|
| 0.858 | 0.979 | 0.0517 | -2.439 | -2.547 | 0.873 | 0.845 | 0.0463 |
| 0.738 | 1.056 | 0.0636 | -2.239 | -2.286 | 0.731 | 0.881 | 0.0421 |
| 0.663 | 1.149 | 0.0771 | -2.053 | -1.997 | 0.623 | 0.939 | 0.0387 |
| 0.569 | 1.409 | 0.1141 | -1.677 | -1.559 | 0.479 | 1.026 | 0.0327 |
| 0.529 | 1.645 | 0.1473 | -1.423 | -1.355 | 0.419 | 1.063 | 0.0288 |
| 0.473 | 2.152 | 0.222 | -1.023 | -1.084 | 0.346 | 1.107 | 0.0227 |
| 0.431 | 2.586 | 0.287 | -0.779 | -0.890 | 0.299 | 1.132 | 0.0185 |
| 0.379 | 3.049 | 0.351 | -0.586 | -0.669 | 0.248 | 1.154 | 0.0143 |
| 0.280 | 3.645 | 0.417 | -0.424 | -0.358 | 0.183 | 1.157 | 0.0088 |
| 0.165 | 4.117 | 0.4519 | -0.358 | -0.263 | 0.152 | 1.106 | 0.0044 |
| 0.101 | 4.433 | 0.4669 | -0.320 | -0.380 | 0.158 | 1.062 | 0.0024 |
| 0.909 | 0.961 | 0.0477 | -2.502 | -2.552 | 0.918 | 0.865 | 0.0477 |
| 0.947 | 0.950 | 0.0464 | -2.543 | -2.505 | 0.951 | 0.901 | 0.0487 |
| 0.945 | 0.951 | 0.0466 | -2.541 | -2.509 | 0.949 | 0.898 | 0.0487 |
| 0.913 | 0.960 | 0.049 | -2.506 | -2.549 | 0.922 | 0.867 | 0.0486 |
| 0.909 | 0.961 | 0.044 | -2.502 | -2.552 | 0.918 | 0.865 | 0.0477 |
| 0.618 | 1.243 | 0.0905 | -1.901 | -1.795 | 0.553 | 0.981 | 0.0362 |
| 0.464 | 2.241 | 0.2359 | -0.967 | -1.044 | 0.336 | 1.113 | 0.0218 |
| 0.702 | 1.095 | 0.0691 | -2.157 | -2.154 | 0.680 | 0.907 | 0.0405 |
| 0.501 | 1.875 | 0.181 | -1.222 | -1.218 | 0.381 | 1.086 | 0.0258 |

Manganese(II) $\rightleftharpoons$ Ammonium Y Derived Data

| $Mn_{(c)}$ | $\alpha^N$ | $K_m^N$ | ln $K_c$ | ln $K_c$(calc) | $f_A$ | $f_B$ | $m_A$ |
|---|---|---|---|---|---|---|---|
| 0.621 | 0.229 | 0.00394 | -4.997 | -3.992 | 0.439 | 0.722 | 0.0467 |
| 0.590 | 0.373 | 0.0104 | -4.033 | -3.797 | 0.395 | 0.754 | 0.0443 |
| 0.471 | 0.624 | 0.0306 | -2.969 | -3.03 | 0.244 | 0.871 | 0.037 |
| 0.400 | 0.745 | 0.0445 | -2.606 | -2.565 | 0.175 | 0.930 | 0.0321 |
| 0.327 | 1.12 | 0.0888 | -1.927 | -2.075 | 0.119 | 0.981 | 0.0233 |
| 0.195 | 2.217 | 0.2266 | -1.026 | -1.182 | 0.054 | 1.032 | 0.00899 |
| 0.293 | 1.455 | 0.1315 | -1.552 | -1.848 | 0.098 | 0.999 | 0.0182 |
| 0.254 | 1.823 | 0.1779 | -1.255 | -1.582 | 0.078 | 1.016 | 0.0136 |
| 0.077 | 2.527 | 0.2571 | -0.911 | -0.362 | 0.023 | 1.029 | 0.0031 |
| 0.356 | 0.911 | 0.0638 | -2.252 | -2.272 | 0.139 | 0.963 | 0.0274 |
| 0.476 | 0.619 | 0.0300 | -2.988 | -3.059 | 0.249 | 0.867 | 0.0373 |
| 0.255 | 1.815 | 0.1769 | -1.261 | -1.589 | 0.078 | 1.016 | 0.0137 |
| 0.796 | 0.325 | $6.309 \times 10^{-5}$ | -4.519 | -5.082 | 0.719 | 0.539 | 0.0480 |
| 0.771 | 0.295 | 0.0054 | -4.687 | -4.926 | 0.677 | 0.562 | 0.0479 |
| 0.629 | 0.291 | 0.0062 | -4.549 | -4.043 | 0.451 | 0.713 | 0.0461 |
| 0.141 | 2.445 | 0.2514 | -0.928 | -0.808 | 0.038 | 1.036 | 0.00593 |
| 0.528 | 0.568 | 0.0244 | -3.193 | -3.401 | 0.311 | 0.817 | 0.0399 |
| 0.349 | 0.951 | 0.0689 | -2.183 | -2.226 | 0.134 | 0.967 | 0.0266 |

Nickel(II) $\rightleftharpoons$ Ammonium Y Derived Data

| $Ni_{(c)}$ | $\alpha^N$ | $K_m^N$ | ln $K_c$ | ln $K_c$(calc) | $f_A$ | $f_B$ | $m_A$ |
|---|---|---|---|---|---|---|---|
| 0.941 | 1.746 | 0.1536 | -1.348 | -1.383 | 0.939 | 1.247 | 0.0474 |
| 0.891 | 1.788 | 0.1618 | -1.301 | -1.295 | 0.887 | 1.266 | 0.0451 |
| 0.814 | 1.864 | 0.1758 | -1.223 | -1.188 | 0.808 | 1.275 | 0.0412 |
| 0.728 | 1.966 | 0.1943 | -1.132 | -1.099 | 0.726 | 1.264 | 0.0366 |
| 0.648 | 2.081 | 0.2132 | -1.047 | -1.036 | 0.658 | 1.241 | 0.0319 |
| 0.579 | 2.193 | 0.2309 | -0.975 | -0.989 | 0.603 | 1.217 | 0.0278 |
| 0.49 | 2.351 | 0.2461 | -0.892 | -0.929 | 0.534 | 1.183 | 0.0225 |
| 0.403 | 2.519 | 0.2755 | -0.822 | -0.861 | 0.474 | 1.149 | 0.0175 |
| 0.329 | 2.673 | 0.2932 | -0.771 | -0.787 | 0.419 | 1.124 | 0.0135 |
| 0.132 | 3.450 | 0.366 | -0.565 | -0.454 | 0.266 | 1.056 | 0.00406 |
| 0.084 | 4.278 | 0.4488 | -0.366 | -0.332 | 0.227 | 1.037 | 0.00206 |
| 0.064 | 5.33 | 0.5549 | -0.153 | -0.275 | 0.211 | 1.029 | 0.00125 |
| 0.226 | 2.948 | 0.3172 | -0.695 | -0.640 | 0.340 | 1.088 | 0.00825 |
| 0.628 | 2.112 | 0.2187 | -1.025 | -1.022 | 0.642 | 1.235 | 0.0308 |
| 0.629 | 2.111 | 0.2187 | -1.026 | -1.023 | 0.642 | 1.235 | 0.0308 |
| 0.356 | 2.616 | 0.2864 | -0.789 | -0.816 | 0.439 | 1.133 | 0.0149 |

Copper(II)$\rightleftharpoons$Ammonium Y Derived Data

| $Cu_{(c)}$ | $\alpha^N$ | $K_m^N$ | $m_A$ |
|---|---|---|---|
| 0.878 | 1.837 | 0.171 | 0.0444 |
| 0.794 | 1.921 | 0.186 | 0.0401 |
| 0.706 | 2.029 | 0.205 | 0.0351 |
| 0.642 | 2.121 | 0.220 | 0.0314 |
| 0.561 | 2.252 | 0.240 | 0.0265 |
| 0.484 | 2.389 | 0.259 | 0.0220 |
| 0.408 | 2.542 | 0.279 | 0.0176 |
| 0.319 | 2.753 | 0.302 | 0.0127 |
| 0.227 | 3.065 | 0.335 | 0.0081 |
| 0.0886 | 5.196 | 0.549 | 0.0018 |
| 0.928 | 1.795 | 0.162 | 0.0468 |
| 0.959 | 1.771 | 0.158 | 0.0482 |
| 0.931 | 1.793 | 0.162 | 0.0469 |
| 0.224 | 3.079 | 0.334 | 0.0079 |
| 0.090 | 5.105 | 0.541 | 0.00187 |

Copper(II) Tetrammine $\rightleftharpoons$ Ammonium Y Derived Data

| $Cu_{(c)}$ | $\alpha^N$ | $K_m^N$ | $m_A$ |
|---|---|---|---|
| 0.883 | 4.157 | 0.767 | 0.0392 |
| 0.846 | 4.677 | 0.908 | 0.0351 |
| 0.744 | 5.486 | 1.044 | 0.0258 |
| 0.678 | 8.517 | 1.776 | 0.0166 |
| 0.520 | 13.643 | 2.459 | 0.00687 |
| 0.431 | 29.882 | 4.972 | 0.0024 |
| 0.275 | 33.191 | 4.407 | 0.0011 |
| 0.195 | 28.129 | 3.449 | 0.00085 |
| 0.823 | 3.731 | 0.604 | 0.0357 |
| 0.823 | 5.827 | 1.266 | 0.0307 |
| 0.772 | 6.060 | 1.256 | 0.0264 |
| 0.642 | 11.439 | 2.425 | 0.0119 |
| 0.568 | 15.799 | 3.120 | 0.0071 |
| 0.460 | 28.773 | 5.039 | 0.0028 |
| 0.405 | 32.045 | 5.172 | 0.00204 |
| 0.911 | 1.036 | 0.0561 | 0.0476 |
| 0.904 | 1.968 | 0.194 | 0.0453 |
| 0.932 | 1.362 | 0.095 | 0.0477 |
| 0.743 | 5.601 | 1.072 | 0.0254 |
| 0.845 | 6.856 | 1.708 | 0.0307 |
| 0.706 | 4.613 | 0.769 | 0.0255 |

Copper(II) Tetrammine $\rightleftharpoons$ Ammonium X Derived Data

| $Cu_{(c)}$ | $\alpha^{N}$ | $K_{m}^{N}$ | $m_{A}$ |
|---|---|---|---|
| 0.837 | 3.607 | 0.616 | 0.0396 |
| 0.831 | 3.824 | 0.632 | 0.0359 |
| 0.767 | 4.098 | 0.676 | 0.0309 |
| 0.712 | 4.276 | 0.688 | 0.0268 |
| 0.620 | 4.462 | 0.678 | 0.0211 |
| 0.535 | 4.562 | 0.654 | 0.0168 |
| 0.448 | 4.635 | 0.619 | 0.0129 |
| 0.311 | 4.769 | 0.581 | 0.00795 |
| 0.176 | 5.159 | 0.578 | 0.00382 |
| 0.168 | 5.204 | 0.582 | 0.00361 |
| 0.903 | 3.442 | 0.554 | 0.0422 |
| 0.118 | 5.742 | 0.620 | 0.00222 |
| 0.141 | 5.431 | 0.596 | 0.00285 |
| 0.818 | 3.885 | 0.644 | 0.0349 |
| 0.611 | 4.476 | 0.675 | 0.0206 |
| 0.917 | 3.364 | 0.537 | 0.0435 |

Platinum(II) Tetrammine $\rightleftharpoons$ Sodium MOR Derived Data

| $Pt(NH_3)_{4(c)}$ | $\alpha^N$ | $K_m^N$ | $m_A$ |
|---|---|---|---|
| 0.991 | 53.209 | 57.97 | 0.0203 |
| 0.942 | 20.571 | 6.918 | 0.0154 |
| 0.925 | 53.451 | 24.34 | 0.0079 |
| 0.980 | 362.093 | 709.1 | 0.0053 |
| 0.902 | 131.317 | 58.97 | 0.0031 |
| 0.694 | 112.824 | 17.79 | 0.00097 |
| 0.331 | 46.904 | 3.45 | 0.00052 |

Platinum(II) Tetrammine $\rightleftharpoons$ Ammonium X Derived Data

| $Pt(NH_3)_{4(c)}$ | $\alpha^N$ | $K_m^N$ | $m_A$ |
|---|---|---|---|
| 0.967 | 39.86 | 24.65 | 0.0150 |
| 0.948 | 59.76 | 35.78 | 0.0095 |
| 0.896 | 56.045 | 20.65 | 0.0059 |
| 0.838 | 52.811 | 13.7 | 0.0041 |
| 0.812 | 77.896 | 18.5 | 0.0025 |
| 0.634 | 50.482 | 6.439 | 0.0016 |
| 0.488 | 51.629 | 4.872 | 0.000891 |
| 0.237 | 92.742 | 5.81 | 0.000166 |
| 0.126 | 201.139 | 11.58 | 0.000036 |
| 0.939 | 68.585 | 38.69 | 0.0077 |
| 0.961 | 7.858 | 1.349 | 0.0216 |

Platinum(II) Tetrammine $\rightleftharpoons$ Sodium X Derived Data

| $Pt(NH_3)_{4(c)}$ | $\alpha^N$ | $K_m^N$ | $m_A$ |
|---|---|---|---|
| 0.77 | 4.481 | 3.912 | 0.0150 |
| 0.989 | 195.869 | 454.0 | 0.0117 |
| 0.994 | 597.65 | 3305.3 | 0.0092 |
| 0.957 | 118.947 | 100.5 | 0.0068 |
| 0.974 | 389.117 | 636.9 | 0.0041 |
| 0.797 | 75.927 | 16.63 | 0.0023 |
| 0.494 | 55.036 | 5.273 | 0.00086 |
| 0.206 | 22.560 | 1.41 | 0.00056 |

Platinum(II) Tetrammine $\rightleftharpoons$ Sodium Y Derived Data

| $Pt(NH_3)_{4(c)}$ | $\alpha^N$ | $K_m^N$ | $m_A$ |
|---|---|---|---|
| 0.686 | 2.638 | 0.157 | 0.0155 |
| 0.962 | 54.339 | 37.43 | 0.0122 |
| 0.990 | 320.279 | 994.7 | 0.0096 |
| 0.948 | 161.112 | 125.95 | 0.0046 |
| 0.967 | 149.094 | 165.3 | 0.0072 |
| 0.864 | 112.049 | 37.75 | 0.0026 |
| 0.545 | 62.697 | 6.63 | 0.00092 |
| 0.284 | 45.809 | 3.188 | 0.00043 |

## Kinetic Plots

### First row transition metals : X

| Time /min | Cu/ mequiv.$g^{-1}$ | Co/ mequiv.$g^{-1}$ | Ni/ mequiv.$g^{-1}$ | Zn/ mequiv.$g^{-1}$ | Mn/ mequiv.$g^{-1}$ |
|---|---|---|---|---|---|
| 5 | 3.73 | 2.23 | 2.15 | 2.35 | 2.31 |
| 10 | | 2.45 | 2.40 | 2.60 | 2.64 |
| 12 | 4.42 | | | | |
| 15 | | 2.62 | 2.58 | 2.95 | 2.86 |
| 20 | 4.31 | 2.64 | 2.61 | 2.95 | 2.98 |
| 30 | 4.31 | | | | |
| 40 | | 2.68 | | 3.33 | |
| 60 | 4.40 | 2.71 | 2.71 | 3.37 | 3.48 |
| 240 | 4.40 | | 2.74 | 3.37 | 3.51 |
| 480 | 4.38 | | | | |
| 1440 | 4.42 | 2.71 | 2.72 | 3.35 | 3.64 |
| 7200 | 4.38 | 2.82 | 2.74 | 3.37 | 3.60 |

### First row transition metals : Y

| Time /min | Cu/ mequiv.$g^{-1}$ | Co/ mequiv.$g^{-1}$ | Ni/ mequiv.$g^{-1}$ | Zn/ mequiv. $g^{-1}$ | Mn/ mequiv. $g^{-1}$ |
|---|---|---|---|---|---|
| 5 | 1.43 | 0.9 | 0.95 | 1.14 | 1.05 |
| 10 | 2.07 | 1.31 | 1.37 | 1.59 | 1.47 |
| 15 | 2.61 | 1.64 | 1.77 | 2.01 | 1.94 |
| 20 | 2.71 | 1.73 | 1.864 | 2.17 | 2.06 |
| 30 | 2.87 | 1.82 | 1.91 | 2.29 | 2.14 |
| 60 | 3.01 | 1.93 | 2.06 | 2.39 | 2.21 |
| 240 | 3.09 | 1.99 | 2.11 | 2.41 | 2.23 |
| 1440 | 3.18 | 2.04 | 2.10 | 2.45 | 2.25 |
| 7200 | 3.18 | 2.01 | 2.13 | 2.47 | 2.22 |

## Kinetic Plots

The Kinetic data shows the uptake of transition metals, in m equiv $g^{-1}$, at the respective time.

### Silver Diammine : X and Y

| Time /min | X/ mequiv. $g^{-1}$ | Y/ mequiv. $g^{-1}$ |
|---|---|---|
| 5 | 0.91 | 0.72 |
| 10 | 1.31 | 1.01 |
| 15 | 1.72 | 1.29 |
| 20 | 1.81 | 1.36 |
| 30 | 1.91 | 1.45 |
| 60 | 2.01 | 1.53 |
| 240 | 2.03 | 1.57 |
| 1440 | 2.15 | 1.63 |

### Copper Tetrammine : X and Y

| Time /min | X/ mequiv. $g^{-1}$ | Y/ mequiv. $g^{-1}$ |
|---|---|---|
| 5 | 0.95 | 0.79 |
| 10 | 1.29 | 1.11 |
| 15 | 1.81 | 1.34 |
| 20 | 1.83 | 1.39 |
| 30 | 1.94 | 1.51 |
| 60 | 2.17 | 1.57 |
| 240 | 2.19 | 1.62 |
| 1440 | 2.24 | 1.79 |
| 7200 | 2.23 | 1.80 |

Kinetic plots in mordenite

| Time/ hours | $Pt(NH_3)_4$/ mequiv. $g^{-1}$ | $Pd(NH_3)_4$/ mequiv. $g^{-1}$ | Ag/ mequiv. $g^{-1}$ | $Ag(NH_3)_4$/ mequiv. $g^{-1}$ |
|---|---|---|---|---|
| 4 | 0.16 | 0.229 | 0.396 | 0.302 |
| 8 | 0.371 | 0.584 | 1.039 | 0.779 |
| 24 | 0.448 | 0.699 | 1.219 | 0.943 |
| 48 | 0.468 | 0.757 | 1.275 | 0.99 |
| 72 | 0.503 | 0.793 | 1.394 | 1.078 |
| 96 | 0.513 | 0.791 | 1.390 | 1.075 |
| 120 | 0.508 | 0.798 | 1.399 | 1.103 |
| 240 | 0.501 | 0.808 | 1.40 | 1.079 |
| 480 | 0.507 | 0.794 | 1.391 | 1.083 |

## Kinetic Plots

Silver (aquo); Platinum and Palladium tetrammine : X and Y

| Time /min | Pt X/ mequiv. $g^{-1}$ | Pt Y/ mequiv. $g^{-1}$ | Pd X/ mequiv. $g^{-1}$ | Pd Y/ mequiv. $g^{-1}$ | Ag X/ mequiv. $g^{-1}$ | Ag Y/ mequiv. $g^{-1}$ |
|---|---|---|---|---|---|---|
| 5 | 0.31 | 0.25 | 0.52 | 0.39 | 1.8 | 1.35 |
| 10 | 0.43 | 0.36 | 0.70 | 0.54 | 2.53 | 1.89 |
| 15 | 0.62 | 0.54 | 0.98 | 0.776 | 3.21 | 2.41 |
| 20 | 0.69 | 0.56 | 1.14 | 0.91 | 3.44 | 2.67 |
| 30 | 0.84 | 0.69 | 1.36 | 1.08 | 3.63 | 2.71 |
| 60 | 1.03 | 0.86 | 1.69 | 1.28 | 3.8 | 2.84 |
| 240 | 1.1 | 0.93 | 1.84 | 1.39 | 3.85 | 2.88 |
| 1440 | 1.23 | 1.06 | 1.96 | 1.56 | 3.96 | 2.95 |
| 7200 | 1.2 | 1.02 | 1.99 | 1.58 | 3.94 | 2.95 |

Sodium Components of Ion exchange Isotherms*

| Cobalt(II) X | | Copper(II) X | | Nickel(II) X | |
|---|---|---|---|---|---|
| $Na_{(c)}$ | $Co_{(s)}$ | $Na_{(c)}$ | $Cu_{(s)}$ | $Na_{(c)}$ | $Ni_{(s)}$ |
| 0.179 | 0.523 | 0.13 | 0.665 | 0.229 | 0.209 |
| 0.179 | 0.236 | 0.13 | 0.188 | 0.229 | 0.401 |
| 0.152 | 0.953 | 0.13 | 0.471 | 0.188 | 0.95 |
| 0.208 | 0.87 | 0.156 | 0.00285 | 0.215 | 0.936 |
| 0.157 | 0.934 | 0.054 | 0.915 | 0.158 | 1.0 |
| 0.075 | 1.0 | 0.00 | 1.0 | 0.206 | 0.025 |
| 0.203 | 0.0518 | 0.108 | 0.95 | 0.211 | 0.005 |
| 0.210 | 0.0178 | | | | |

| Manganese(II) X | | Zinc(II) X | | Copper(II) X | |
|---|---|---|---|---|---|
| $Na_{(c)}$ | $Mn_{(s)}$ | $Na_{(c)}$ | $Zn_{(s)}$ | $Na_{(c)}$ | $Cu_{(s)}$ |
| 0.173 | 0.686 | 0.139 | 0.8 | 0.037 | 0.073 |
| 0.170 | 0.221 | 0.187 | 0.00294 | 0.037 | 0.440 |
| 0.232 | 0.00185 | 0.177 | 0.401 | 0.031 | 0.628 |
| 0.190 | 0.0075 | 0.124 | 0.903 | 0.043 | 0.036 |
| 0.183 | 0.049 | 0.047 | 1.0 | 0.005 | 1.0 |
| 0.111 | 0.94 | 0.083 | 0.963 | 0.027 | 0.935 |
| 0.054 | 1.0 | 0.181 | 0.21 | | |

* Expressed in equivalent fractions of exchanging cations.

# APPENDIX III COMPUTER PROGRAMS

## CABIEZ: Computer Analyses of Binary Ion Exchange in Zeolites.

This program takes a set of isotherm data points and 'best fits' a series of polynomial equations between defined limits of order. The choice of polynomial is made by comparison of residual variance of data points. A facility for statistically weighting the first and last points is available. The data must be entered with the first isotherm data point being the point (1.0, $A_c$max) and the last being (0.0, 0.0). An additional facility for exchanging any 'fitted' data point for the original data is available.

Thermodynamic parameters are calculated from the 'fitted' or 'corrected' data points. The output consists of $K_c$, the values of the normalised and un-normalised selectivity quotient, $\log_{10}K_c$, $\ln K_c$, $m_A$, $m_B$ and the ionic strength at each value of $A_c$. A plot of $A_c$ against $\ln K_c$ is made and to this a polynomial equation is fitted which is then numerically integrated between the required limits to give the parameters $f_A$, $f_B$, $K_a$ and $\Delta G^{\theta}$.

```
C     ****************************************************************
C     *                                                              *
C     *      COMPUTER ANALYSIS OF BINARY ION EXCHANGE IN ZEOLITES    *
C     *                                                              *
C     ****************************************************************


      MASTER CABIEZ
      DIMENSION NI(50)
      COMMON/AREA/X(50),Y(50),A(10),ITEMS,YMAX,YMIN,XMAX,XMIN,Z(50),K,N
      COMMON/AREA2/ACMAX
      REAL LNFA,LNFB,LNKA,KA,INTY,INTX,INTZ,K1,K2,K3,K4,K5,K6,
      REAL KC,KM,I3,LOGAM1,LOGAM2,LOGAM3,LOGAM4,LOGAMA,LOGKC,MA,MB,MAN
      REAL LOGTKC,KI


C     ****************************************************************
C     *                                                              *
C     *                    READ IN DATA                              *
C     *                                                              *
C     * 1  TITLE                                                     *
C     * 2  K = HIGHEST LIMIT OF ORDER OF POLYNOMIAL FOR ISOTHERM     *
C     * 2  N = LOWEST LIMIT OF ORDER OF POLYNOMIAL FOR ISOTHERM      *
C     * 3  ITEMS = NUMBER OF DATA POINTS IN THE ISOTHERM             *
C     * 4  X AND Y COORDINATES OF ISOTHERM                           *
C     *    X = THE VALUE OF AS                                       *
C     *    Y = THE VALUE OF AC                                       *
C     * 5  KSTAT1 = THE STATISTICAL WEIGHTING OF THE POINT  0.0,0.0  *
C     *    KSTAT2 = THE STATISTICAL WEIGHTING OF THE POINT  1.0,ACMAX*
C     *    IF ANY POINT IS GIVEN A STATISTICAL WEIGHTING 'N' THAT    *
C     *    POINT MUST BE ENTERED INTO THE DATA 'N' TIMES             *
C     * 6  TN = TOTAL SOLUTION NORMALITY                             *
C     * 7  THE DEBYE HUCKEL PARAMETERS FOR EACH SALT                 *
C     *    AA = PARAMETER A, BA = PARAMETER B FOR SALT OF INGOING ION*
C     *    DB = PARAMETER    EB = PARAMETER B FOR SALT OF OUTGOING ION*
C     * 8  ZA,ZB,ZX THE CHARGES ON THE TWO EXCHANGING CATIONS AND THE*
C     *    COMMON ANION RESPECTIVELY                                 *
C     * 9  KRECT = THE NUMBER OF DATA POINTS TO BE CORRECTED TO THE  *
C     *    ORIGINAL DATA POINTS                                      *
C     * 10 (1) IF AL THE DATA POINTS ARE TO BE CORRECTED THEN THE NEXT*
C     *    CARD IS THE VALUE OF THE MAXIMUM LEVEL OF EXCHANGE        *
C     *    (2) IF 'N' POINTS TO BE CORRECTED THEN THE NEXT CARD      *
C     *    CONTAINS THE INTEGER NUMBER OF EACH POINT TO BE CORRECTED  *
C     * 11 K = HIGHEST ORDER OF POLYNOMIAL FOR KIELLAND PLOT         *
C     *    N = LOWEST ORDER OF POLYNOMIAL FOR KIELLAND PLOT          *
C     *                                                              *
C     ****************************************************************
```

```
      K6=(0.5*ZA*ZB*ZX*(ZB-ZA)*(ZB-ZA))/(ZB+ZX)
      Y1=MA/(4*I3)
      Y2=K4*LOGAM2
      Y3=K5*LOGAM1
      Y4=K6/(1.0+(I3**(-0.5)))
      Z1=MB/(4*I3)
      Z2=K1*LOGAM1
      Z3=K2*LOGAM2
      Z4=K3/(1.0+(I3**(-0.5)))
      LOGAM3=LOGAM1-(Z1*(Z2-Z3-Z4))
      LOGAM4=LOGAM2-(Y1*(Y2-Y3-Y4))
C     CALCULATION OF GAMMA
      X1=ZA*(ZB+ZX)*LOGAM4
      X2=ZB*(ZA+ZX)*LOGAM3
      LOGAMA=(1.0/ZX*(X1-X2)
      GAMA=EXP10(LOGAMA)
      KC=KM*GAMA
      LOGTKC=ALOG10(KC)
      LOGKC=ALOG(KC)
      ALPHA=(AC*MB)/(BC*MA)
      BCU=1.0-ACU
      ALP=(ACU*MB)/(BCU*MA)
      WRITE(2,202)AC,KC,ALPHA,ALP,LOGKC,LOGTKC,MA,MB,I3,GAMA
      X(I-1-KSTAT2)=KC
      Y(I-1-KSTAT1)=LOGKC
 10   CONTINUE
      ITEMS=ITEMS-2-KSTAT1-KSTAT2
      READ(1,100)K,N
      WRITE(2,313)
      CALL SORT
      CALL POLY FIT
      WRITE(2,311)
      WRITE(2,220)
      KI=8.134*279
C     CALCULATION OF ZEOLITE PHASE ACTIVITY COEFFICIENTS
      DO 40 I=1,ITEMS
C     INTEGRATION PROCEDURE
      BC=1.0-X(I)
      K2=((A(2)*(X(I)**2))/2)+((A(3)*(X(I)**3))/3)
      K3=((A(4)*(X(I)**4))/4)+((A(5)*(X(I)**5))/5)
      K4=((A(6)*(X(I)**6))/6
      K5=A(1)*X(I)
      INTY=K5+K4+K3+K2
      INTZ=(A(1))+(A(2)/2)+(A(3)/3)+(A(4)/4)+(A(5)/5)+(A(6)/6)-INTY
      LNFA=((ZB-ZA)*BC)-Z(I)+(X(I)*Z(I))+INTZ
      LNFB=(X(I)*Z(I))-((ZB-ZA)*X(I))-INTY
      FAZB=EXP(LNFA)
      FBZA=EXP(LNFB)
      FA=FAZB**(1/ZB)
      FB=FBZA**(1/ZA)

      WRITE(2,204)FA,FB,X(I),Z(I)
 40   CONTINUE
C     INTEGRATION OF KIELAND PLOT BETWEEN LIMITS AC=1 & AC=0
```

```
      READ(1,35)
      WRITE(2,35)
      READ(1,100)K,N
      READ(1,100)ITEMS
      READ(1,120)(X(I),Y(I),I=1,ITEMS)
      READ(1,41)KSTAT1,KSTAT2
      READ(1,120)YMAX,YMIN
      READ(1,120)XMAX,XMIN
      READ(1,247)TN
      READ(1,140)AA,BB,DB,EB
      READ(1,130)ZA,ZB,ZX
      READ(1,103)KRECT
      IF(KRECT.EQ.0.0)GOTO23
      IF(KRECT.NE.ITEMS)GOTO 60
      DO 25 I=1,KRECT
 25   NI(I)=I
      GOTO 23
 60   CONTINUE
      READ(1,103)(NI(I),I=1,KRECT)
 23   CONTINUE
      KSTAT1=KSTAT1-1
      KSTAT2=KSTAT2-1
      WRITE(2,160)
      WRITE(2,150)AA,BA,DB,EB
      CALL POLY FIT
      IF(KRECT.EQ.ITEMS)READ(1,106)ACMAX
      WRITE(2,314)ACMAX
      WRITE(2,311)
      WRITE(2,312)
      WRITE(2,300)
      IF(KRECT.EQ.0.0)GOTO 32
      DO 24 I=1,KRECT
 24   Z(NI(I))=Y(NI(I))
 32   CONTINUE
      MAN=TN/ZX
C     COMPUTE THE THERMODYNAMIC PARAMETERS
      DO 10 I=1,2+KSTAT2,ITEMS-KSTAT1
      ACU=Z(I)
      AS=X(I)
      BS=1.0-AS
      MB=(BS*TN)/ZB
      MA=(AS*TN)/ZA
      AC=ACU/ACMAX
      BC=1.0-AC
      KM=((AC**ZB)*(MB**ZA))/((BC**ZA)*(MA**ZB))
C     DEBYE HUCKEL MODEL
      I3=(0.5)*((MA*ZA*ZA)+(MB*ZB*ZB)+(MAN*ZX*ZX))
      P1=(-5.155E-1)*(ZA*ZX)*(I3**0.5)
      P2=(3.291E9)*AA*(I3**0.5)
      Q1=(-5.155E-1)*(ZB*ZX)*(I3**0.5)
      Q2=(3.291E9)*DB*(I3**0.5)
      LOGAM1=(P1/(1+P2))+(BA*I3)
      LOGAM2=(Q1/(1+Q2))+(EB*I3)
C     GLUECKAUF MODEL
      K1=ZB*(2*ZB-ZA+ZX)
      K2=(ZA*(ZB+ZX)*(ZB+ZX))/(ZA+ZX)
      K3=(0.5*ZA*ZB*ZX*(ZA-ZB)*(ZA-ZB))/(ZA+ZX)
      K4=ZA*(2*ZA-ZB+ZX)
      K5=(ZB*(ZA+ZX)+(ZA+ZX))/(ZB+ZX)
```

```
      INTX=A(1)+(A(2)/2)+(A(3)/3)+(A(4)/4)+(A(5)/5)+(A6)/6)
      LNKA=(ZB-ZA)+INTX
      KA=EXP(LNKA)
      DELTAG=((-KI/(ZA-ZB))*LNKA)/1000
      WRITE(2,300)DELTAG,KA
 35   FORMAT(1H1,51H            TITLE                                    )
 41   FORMAT(2I0)
 100  FORMAT(2I0)
 103  FORMAT(I0)
 106  FORMAT(1F0.0)
 120  FORMAT(2F0.0)
 130  FORMAT(3F0.0)
 140  FORMAT(4E12.4)
 150  FORMAT(10X,'INCOMING ION A =',E18.9,2X,' B=',E18.9,/,10X,'OUTGOI
     1NG ION A =',E18.9,2X,' B =',E18.9,///,10X,'ISOTHERM')
 160  FORMAT(1X,/,(10X,'DEBYE HUCKLE PARAMETERS',///,)
 200  FORMAT(8X,2HAC,11X,2HKC,8X,5HALPHA,6X,8HALPHA(1),4X,6HLOG KC,5X,1
     10HLOG 10 KC,5X,2HMA,11X,2HMB,10X,'I',9X,'GAMMA')
 202  FORMAT(1X,(10(2X,F10.6)))
 204  FORMAT(1X,F11.6,8X,F11.6,8X,F11.6,8X,F11.6)
 220  FORMAT(7X,2HFA,18X,2HFB,15X,2HAC,15X,4HLNKC)
 247  FORMAT(F0.0)
 257  FORMAT(I0)
 300  FORMAT(1X,/,40X,'STANDARD GIBBS FREE ENERGY =',F15.8,' KILO JOULES
     1 PER GRAM EQUIVALENT',//,40X,'EQUILIBRIUM CONSTANT (KA)  ='F15.8)
 314  FORMAT(///,10X,'MAXIMUM LEVEL OF EXCHANGE = 'F6.4)
 311  FORMAT(/////)
 312  FORMAT(1HO,10X,'THERMODYNAMIC DATA')
 313  FORMAT(1HO,10X,'KIELAND PLOT')
      STOP
      END
C     ***********************************************************************
C     *                                                                     *
C     * THIS SUBROUTINE TAKES A SET OF X & Y COORDINATES AND BEST FITS      *
C     * A SERIES OF POLYNOMIAL EQUATIONS BY THE METHOD OF LEAST             *
C     * SQUARES, THE MATRIX IS REDUCED AND SOLVED BY THE GAUSS JORDAN       *
C     * METHOD OF BACK SUBSTITUTION                                         *
C     *                                                                     *
C     ***********************************************************************

      SUBROUTINE POLY FIT
      DIMENSION SUMX(50),SUMXY(50),P(10,10),Q(10,10),R(10,10),S(10,10)
     1T(10,10),U(10,10),V(10,10),PI(10,10),QI(10,10),RI(10,10),SI(10,10
     1),TI(10,10),UI(10,10),VI(10,10),COR(7)
      COMMON/AREA/X(50),Y(50),A(10),ITEMS,YMAX,YMIN,XMAX,XMIN,Z(50),K,N
      L=1
      KS=K
C     DETERMINATION OF MATRIX DIMENSIONS
      NTERMS=7
      KT=2*(NTERMS-1)
C     SUMMATION OF DATA
      DO 4I=1,KT
      SUMXY(I)=0
      DO 5I=1,NTERMS
```

```
 5    SUMXY(I)=0
      DO 6I=1,KT
      DO 6J=1,ITEMS
 6    SUMX(I)=SUMX(I)+X(J)**I
      DO 8I=2,NTERMS
      DO 8J=1,ITEMS
 8    SUMXY(I)=SUMXY(I)+(Y(J)*(X(J)**(I-1)))
      DO 240 I=1,ITEMS
 240  SUMXY(1)=SUMXY(1)+Y(I)
C     EQUATION OF SUMMED DATA TO MATRIX P(I,J)
      DO 20 I=1,NTERMS
      DO 20 J=1,NTERMS
      IF(I+J.EQ.2)GOTO 20
      P(I,J)=SUMX(I+J-2)
 20   CONTINUE
      P(1,1)=FLOAT(ITEMS)
C     REDUCTION OF MATRIX TO LOWER TRIANGULAR ZERO MATRIX BY GAUSSIAN
C     ELIMINATION
      DO 21 I=1,NTERMS
      DO 21 J=1,NTERMS
 21   Q(I,J)=((P(I,J)*P(1,1))/P(I,1))-P(1,J)
      DO 22 I=2,NTERMS
      DO 22 J=2,NTERMS
 22   R(I,J)=((Q(I,J)*Q(2,2))/Q(I,2))-Q(2,J)
      DO 23 I=3,NTERMS
      DO 23 J=3,NTERMS
 23   S(I,J)=((R(I,J)*R(3,3))/R(I,3))-R(3,J)
      DO 24 I=4,NTERMS
      DO 24 J=4,NTERMS
 24   T(I,J)=((S(I,J)*S(4,4))/S(I,4))-S(4,J)
      DO 25 I=5,NTERMS
      DO 25 J=5,NTERMS
 25   U(I,J)=((T(I,J)*T(5,5))/T(I,5))-T(5,J)
      DO 26 I=6,NTERMS
      DO 26 J=6,NTERMS
 26   V(I,J)=((U(I,J)*U(6,6))/U(I,6))-U(6,J)
      DO 27 I=1,NTERMS
 27   PI(I,8)=SUMXY(I)
      DO 28 I=2,NTERMS
 28   QI(I,8)=((PI(I,8)*P(1,1))/P(I,1))-PI(1,8)
      DO 285 I=3,NTERMS
 285  RI(I,8)=((QI(I,8)*Q(2,2))/Q(I,2))-QI(2,8)
      DO 29 I=4,NTERMS
 29   SI(I,8)=((RI(I,8)*R(3,3))/R(I,3))-RI(3,8)
      DO 30 I=5,NTERMS
 30   TI(I,8)=((SI(I,8)*S(4,4))/S(I,4))-SI(4,8)
      DO 31 I=  NTERMS
 31   UI(I,8)=((TI(I,8)*T(5,5))/T(I,5))-TI(5,8)
      DO 32 I=7,NTERMS
 32   VI(I,8)=((UI(I,8)*U(6,6))/U(I,6))-UI(6,8)
 50   CONTINUE
      DO 81 I=1,NTERMS
 81   A(I)=0
      GOTO(96,95,94,93,92,91),K
 91   A(7)=VI(7,8)/V(7,7)
 92   A(6)=(UI(6,8)-A(7)*U(6,7))/U(6,6)
 93   A(5)=(TI(5,8)-A(7)*T(5,7)-A(6)*T(5,6))/T(5,5)
```

```
 94    A(4)=(SI(4,8)-A(7)*S(4,7)-A(6)*S(4,6)-A(5)*S(4,5))/S(4,4)
 95    A(3)=(RI(3,8)-A(7)*R(3,7)-A(6)*R(3,6)-A(5)*R(3,5)-A(4)*R(3,4))/R(3
      *,3)
 96    A(2)=(QI(2,8)-A(7)*Q(2,7)-A(6)*Q(2,6)-A(5)*Q(2,5)-A(4)*Q(2,4)-A(3)
      **Q(2,3))/Q(2,2)
       A(1)=(PI(1,8)-A(7)*P(1,7)-A(6)*P(1,6)-A(5)*P(1,5)-A(4)*P(1,4)-A(3)
      **P(1,3)-A(2)*P(1,2))/P(1,1)
       IF(L.EQ.2)WRITE(2,251)
       WRITE(2,200)K
       WRITE(2,220)(I,A(I),I=1,K+1)
C      CALCULATION OF PREDICTED Y COORDINATE USING FITTED POLYNOMIAL
       SUMD=0
       WRITE(2,322)
       DO 80I=1,ITEMS
       Z(I)=A(I)
       DO 60 J=1,NTERMS-1
 60    Z(I)=Z(I)+(A(J+1)*(X(I)**J))
C      SUMMATION OF RESIDUALS
       DD=(Z(I)-Y(I))**2
       WRITE(2.333)X(I),Y(I),Z(I)
       SUMD=SUMD+DD
       WRITE(2,300)SUMD
       IF(L.EQ.2)GOTO 444
       COR(K)=SUMD
       IF(KS.EQ.K)OWEST=COR(K)
       IF(COR(K).LE.OWEST)AST=K
       IF(COR(K).LE.OWEST)OWEST=COR(K)
       IF(K.EQ.N)GOTO 70
 988   K=K-1
       GOTO 50
 70    CONTINUE
       K=AST
       N=AST
       L=2
       GOTO 50
 444   CALL POLY PLOT
 445   RETURN
 220   FORMAT(1H1,10X,2HA(,I1,3H)= ,F18.9)
 200   FORMAT(1H1,5X,7HORDER= ,I2)
 251   FORMAT(1HO,10X,'BEST FITTING EQUATION')
 300   FORMAT(70X,5HFIT= ,F15.8)
 332   FORMAT(1H1,27X,1HX,17X,1HY,10X,12HY CALCULATED)
 333   FORMAT(1H1,15X,3(5X,F12.6))
       END

C      ****************************************************************
C      *  THIS SUBROUTINE PLOTS THE GRAPH OF A POLYNOMIAL EQUATION      *
C      *  PLUS ITS DATA POINTS BY COMPUTING THE INTEGER POSITION OF     *
C      *  EACH POINT WITHIN THE GIVEN DIMENSIONS OF THE GRAPH           *
C      ****************************************************************

       SUBROUTINE POLY PLOT
       DIMENSION XY(50),YX(50),XYP(50),YXP(50),JX(10)
       REAL LINE(150)
       COMMON/AREA/X(50),Y(50),A(10),ITEMS,YMAX,YMIN,XMAX,XMIN
```

```
      COMMON/AREA2/ACMAX
      DATA P/1H+/,BLANK/1H /,AST/1H*/
      WRITE(2,357)
      WRITE(2,250)XMAX
C     CALCULATION OF DIMENSION OF GRAPH
      STEP=(XMAX-XMIN)/FLOAT(60)
      B=XMAX
      Q=XMAX-XMIN
      D=YMAX-YMIN
      DO 80 I=1,101
 80   LINE(I)=BLANK
C     CALCULATION OF INTEGRAL POSITION OF Y COORDINATE OF POLYNOMIAL
C     AT THE GIVEN VALUE OF X DETERMINED BY THE POSITION ON THE X
C     COORDINATE
      DO 40 I=1,ITEMS
 40   XY(I)=INT(60*(X(I)-XMIN)/Q)
      L=60
      DO 2 J=1,59
      Z=A(1)+A(2)*B+A(3)*(B**2)+A(4)*(B**3)+A(5)*(B**4)+A(6)*(B**5)+A(7)
     1*(B**6)
      IF(B.EQ.XMAX)ACMAX=Z
      JX(1)=INT((100*(Z-YMIN)/D)+1)
      IF(Z.GT.YMAX)JX(1)=101
      IF(Z.LT.YMIN)JX(1)=1
      LINE(JX(1))=P
 81   M=2
C     DETERMINATION OF INTEGRAL POSITIONS OF DATA POINTS
      DO 50 I=1,ITEMS
      IF(L-XY(I).EQ.0)GOTO 70
      GOTO 50
 70   YX(I)=Y(I)-YMIN
      JX(M)=INT((100*YX(I)/D(+1)
      LINE(JX(M))=AST
      M=M+1
      IF(M.EQ.6)GOTO 71
 50   CONTINUE
      LINE(1)=AST
 71   WRITE(2,200)(LINE(I),I=1,101)
 82   DO 90 K=1,M-1
 90   LINE(JX(K))=BLANK
 92   L=L-1
 2    CONTINUE
 60   DO 10 J=1,101
 10   LINE(J)=AST
      WRITE(2,201)XMIN,(LINE(J),J=1,101)
      WRITE(2,202)YMIN,YMAX
 357  FORMAT(1H1,6HX AXIS)
 200  FORMAT(9X,101A1)
 201  FORMAT(1X,F7.4,1X,101A1)
 202  FORMAT(6X,F9.6,88X,F9.6,1X,6HY AXIS)
 250  FORMAT(1X,F9.6)
      RETURN
      END

C     ****************************************************************
C     * THIS SUBROUTINE TAKES A SET OF X & Y COORDINATES AND ARRANGES *
C     * THEM IN DECENDING ORDER OF MAGNITUDE WITH RESPECT TO X        *
C     ****************************************************************
```

```
      SUBROUTINE SORT
      DIMENSION P(50),Q(50)
      COMMON/AREA/Y(50),X(50),A(10),ITEMS,YMAX,YMIN,XMAX,XMIN,Z(50),K,N
      DO 3 J=1,ITEMS
      Q(J)=X(J)
      DO 10 J=1,ITEMS
      HIGHEST=X(I)
      KAST=1+I
      DO 5 I=1,ITEMS
      IF(HIGHEST.NE.-100000)GOTO 70
      HIGHEST=X(1+I)
 5    KAST=1+I
 70   CONTINUE
      DO 20 I=1,ITEMS
      IF(HIGHEST.LT.X(I))HIGHEST=X(I)
      P(J)=HIGHEST
 10   X(KAST)=-100000
C     CALCULATION OF DIMENSION OF GRAPH OF KIELLAND PLOT
      YMAX=P(1)+0.2
      YMIN=P(ITEMS)-0.2
      DO 30 I=1,ITEMS
 30   X(I)=Q(I)
      RETURN
      END


      FINISH
```

(ii) LSJ : DEBYE HUCKEL MODEL

This program takes a series of sets of two values of mean molal stoichiometric activity coefficients with their corresponding ionic strengths. These values are substituted into the modified Debye Huckel equation (equation 3.100) and the parameters a and b are solved by solution of the resulting simultaneous equations. The mean molal value of the parameter a (having the positive sign) and the corresponding parameter b are calculated for the series of sets of data.

```
      MASTER LSJ
      DIMENSION P(20),T(20),S(20),W(20)
      READ(1.150)K
C     K=THE NUMBER OF SYSTEMS TO BE COMPUTED
      DO 30 J=1.K
      WRITE(2,304)
C     WRITE HEADING
      READ(1,122)
      WRITE(2,122)
C     READ NUMBER OF SETS OF DATA
      READ(1.150)N
C     P=GAMMA(1), S=I(1),T=GAMMA(2),W=I(2)
C     READ DATA
      READ(1,100)(P(I),S(I),T(I),W(I),I=1,N)
C     READ CHARGES ON IONS   ZA=CATION   ZB=ANION
      READ(1.110)ZA,ZB
      SUMX=0
      SUMY=0
      DO 15 I=1,N
      WRITE(2,240)S(I),P(I),W(I),T(I)
      P(I)=ALOG10(P(I))
      T(I)=ALOG10(T(I))
      A=0.5155
      B=3.292E9
      V=B*SQRT(W(I))
      R=R*SQRT(S(I))
      Q=-A*ZA*ZB*SQRT(S(I))
      U=-A*ZA*ZB*SQRT(W(I))
      TF=(P(I)*W(I)/S(I))-T(I)
      A=R*V*TF
      B=(R*TF)+(V*TF)-Q*W(I)*V/S(I))+(R+U)
      C=TF-(Q*W(I)/S(I))+U
C     SOLVE SIMULTANEOUS EQUATIONS
      IF(B*B.LT.4*A*C)GOTO 30
      X1=(-B+SQRT(B*B-4*A*C)))/(2*A)
      X2=(-B-SQRT(B*B-4*A*C)))/(2*A)
      Y1=(P(I)+(0.5155*ZA*ZB*SQRT(S(I))/(1+(3.291E9*SQRT(S(I))*X1))))/S(
     *I)
      Y2=(P(I)+(0.5155*ZA*ZB*SQRT(S(I))/(1+(3.291E9*SQRT(S(I))*X2))))/S(
     *I)
      WRITE(2,200)
      WRITE(2,210)X1,Y1,X2,Y2
      IF(X1)10,10,20
 20   SUMX=SUMX+X1
      SUMY=SUMY+Y1
      GOTO15
 10   SUMX=SUMX+X2
      SUMY=SUMY+Y2
 15   CONTINUE
      A=SUMX/FLOAT(N)
      B=SUMY/FLOAT(N)
C     READ OUT DEBYE HUCKEL COEFFICIENTS PLUS THE ORIGINAL DATA AND
C     THE PREDICTED DATA USING THE MODEL
```

```
      WRITE(2,230)A,B
      WRITE(2,301)
      DO 6 I=1,N
      P(I)=EXP10(P(I))
      T(I)=EXP10(T(I))
      WON=((-0.5155*ZA*ZB*SQRT(S(I)))/(1+(A*3.291E9*SQRT(S(I))))+B*S(I))
      DON=((-0.5155*ZA*ZB*SQRT(W(I)))/(1+(A*3.291E9*SQRT(W(I))))+B*W(I))
      WON=EXP10(WON)
      DON=EXP10(DON)
      SON=(WON-P(I))*100/P(I)
      PON=(DON-T(I))*100/T(I)
6     WRITE(2,300)S(I),P(I),WON,SON,W(I),T(I),DON,PON
30    CONTINUE
      IF(B*B.LT.4*A*C)WRITE(2,220)
100   FORMAT(4F0.0)
110   FORMAT(2F0.0)
122   FORMAT(1H1,51H     TITLE                                                    )
210   FORMAT(10X,G18.6,5X,G18.6,/,10X,G18.6,5X,G18.6,/////)
220   FORMAT(10X,'COMPLEX ROOTS')
240   FORMAT(10X,4(F6.4,4X)))
150   FORMAT(I0)
160   FORMAT(F0.0)
300   FORMAT(2(10X,4(F8.4,7X,)/))
301   FORMAT(15X,'I',11X,'GAMMA',6X,'GAMMA PREDICTED',3X,'% ERORR')
200   FORMAT(20X,'A',20X,'B')
304   FORMAT(1X,/////)
230   FORMAT(10X,'MEAN VALUES    A= ',G18.6,'    B=',G18.6,/)
      STOP
      END


      FINISH
```

## APPENDIX IV

The data from the thermogravimetric analysis of ammonium exchanged X and Y is tabulated in table I.

In summary these data indicate that the thermal degradation of ammonium X involves one weight loss over the range of temperature 23°C to 413°C. The existence of two shoulders on the trace of weight loss versus temperature confirm to the theory that the degredation consists of three component sections. These are, intial loss of intracrystalline water, loss of ammonia and final dehydration of the structure involving further loss of water[85]. In contrast the decomposition of $NH_4$-Y involves three discrete weight losses over the temperature ranges 25°C to 206°C, 206°C to 474°C and 474°C to 800°C respectively. These correspond to the three distinct stages mentioned previously. The second weight loss (corresponding to loss of $NH_3$) is estimated at 4.8% of the total weight of the zeolite. However, overlap between the first two weight losses precludes accurate estimation of this value.

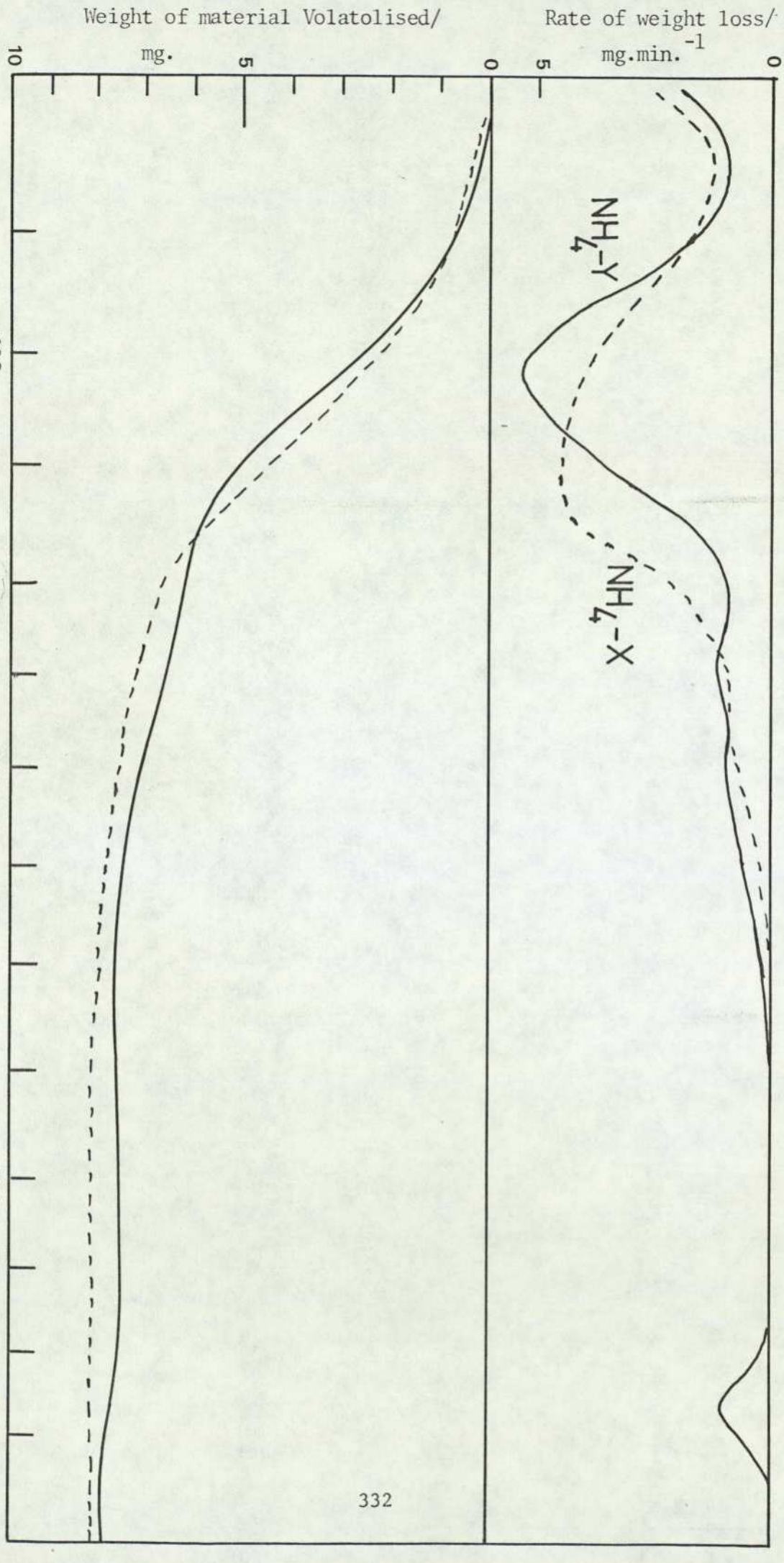
Weight of material Volatolised/
mg.
10
5
0
Rate of weight loss/
mg.min.$^{-1}$
5
0
$NH_4$-Y
$NH_4$-X
100
300
500
700
Temperature / °C

TABLE I.

The thermal decomposition of zeolites in air and nitrogen.

(a) Ammonium X and ammonium Y.

| Sample: | $NH_4Y$ (Air) | $NH_4X$ (Air) | $NH_4Y$ ($N_2$) | $NH_4X$ ($N_2$) |
|---|---|---|---|---|
| Total moisture loss. | | | | |
| Weight-fraction volatilised (%): | 21.6±0.1 | 29.2±0.2 | 21.5 | 30.4 |
| Temperature range (°C): | RT-206 | RT-413 | RT-119 | RT-720 |
| Max. rate of volatilisation (%.min$^{-1}$): | 4.3±0.3 | 2.7±0.2 | 4.3 | 2.7 |
| Temperature of max. rate (°C): | 112±2 | 155±1 | 110 | 160 |
| Max. endothermicity (cal.g$^{-1}$): a | 23.2±1.2 | 14.6±0.1 | 26.5 | 51.2 |
| Temperature of max. endothermicity(°C): | 112±2 | 155±1 | 110 | 145 |
| Second weight-loss. | | | | |
| Weight-fraction volatilised (%): | 4.8±0.1 | 1.5±0.1 | 4.9 | - |
| Temperature range (°C): | 206-474 | 413-730 | 199-498 | - |
| Max. rate of volatilisation (%.min$^{-1}$): | 3.7±0.2 | SWL | 3.7 | - |
| Temperature of max. rate (°C): | 241(305)* | - | 238(322)* | - |
| Third weight-loss. | | | | |
| Weight-fraction volatilised (%): | 1.8±0.2 | - | 1.9 | - |
| Temperature range (°C): | 474-800 | - | 498-878 | - |
| Max. rate of volatilisation (%.min$^{-1}$): | 10.3 | - | 9.4 | - |
| Temperature of max. rate (°C): | 630±1 | - | 623 | - |
| Max. endothermicity (cal.g$^{-1}$): a | 127±6 | - | 120 | - |
| Temperature of max. endothermicity(°C): | 633±5 | - | 623 | - |
| Total weight-fraction volatilised(%): | 28.0(29.5)** | 30.7±0.1 | 28.4 | 30.4 |
| Weight-fraction of residue (%): | 72.7(70.6) | 69.2±1.2 | 71.2 | 69.5 |

Key: a. endothermicity calculated by a linear correlation method rather than the more normal triangular area method.
*. this decomposition occurs either in two stages or the major DTG peak has a shoulder at temperature (T).
**. this experiment was heated isothermally at 950°C for four hours.

## REFERENCES


(1) H.S. Sherry, Adv. Chem. Ser. 1971. (Mol Sieves-I), 101, paper 28. 350-379.

(2) H.S. Sherry, Phys. Chem. Sci. Res. Rep. 1975. 1. 523.

(3) A. Cremers, Adv. Chem. Ser. 1977. 40 (mol. Sieves-2, Int. Conf. 4th) 188.

(4) R. Rudham, M.K. Sanders, J. Catalysis, 1972, 27. 287.

(5) R.M. Barrer, I.M. Galabova. Adv. Chem. Ser. 1973, 121, 357.

(6) T.A. Egerton, F.S. Stone., J.C.S. Faraday 1, 1973, 1, 22.

(7) H. Bremer, W.Morke , R. Schodel, Adv. Chem. Ser. 1973, 121, 249.

(8) D.W. Breck, et al. J. Am. Soc. 1956, 78, 5963.

(9) R.M. Barrer, G.C. Bratt, J. Phys. Chem. Solids. 1959, 12, 130.

(10) J.D. Sherman, R.J. Ross, Ger. Offen. 2, 531, 338, U.S. Appl. 488, 503, (1974).

(11) D.W. Breck, Ger. Offen. 2, 156, 471, U.S. Appl. 089 282 (1970)

(12) M.J. Schwuger. et al. Tenside Deterg. 1976, 13(6), 305.

(13) M.J. Schwuger. H.G. Smolka, A.C.S. Symp. Ser., 1977, 40, (Mol. Siev Sieves-2, Int. Conf. 4th), 696.

(14) J.B. Stamberg, D.F. Bishop, G.Kumbe. A.I.Ch.E.Symp. Ser. 1972, 68, (124), 25.

(15) P.W. Johnson, J.McN. Sieburth, Aquaculture 1974, 4 (1), 61.

(16) S.E. Joergensen. Water Res. 1976, 10(3). 213

(17) L.A. Bray, H.T. Fullam, Adv. Chem. Ser. 1971, 101, (Mol. Sieves-1), 450.

(18) B.W. Mercer, L.L.Ames, P.W. Smith, Nucl. Appl. Technol. 1970, 8(1) 62.

(19) W.L. Godfrey, D.S.Larkin, Chem. Eng. (New York) 1970, 77 (15), 56.

(20) B.W. Mercer, W.C. Schmidt, A.E.C. Accession No. 14466, Report No. RL-SA-58 (1965).

(21) K.M. Minachev , et.al. Jzr. Akad. Nauk SSR Senya Khimicheskaya, 6, 1001, 1966.

(22) J.G. Firth, Trans. Faraday. Soc. 1966, 62, 2566.

(23) J.G. Firth, H.B. Holland, Tras, Faraday. Soc., 1969, 65, 1121.

(24) J.G. Firth, H.B. Holland, Trans. Faraday Soc., 1969, 65, 1891.

(25) P. Fletcher, P.R. Lower, R.P. Townsend in "The Properties and Applications of Zeolites", ed. L.V.C. Rees and R.P. Townsend, Special Publication No. 33, Chemical Society, London 1979, in print.

(26) R.M. Barrer, J.A. Davies, L.V.C. Rees, J. Inorg. Nucl. Chem. 1968, 30, 3333.

(27) R.M. Barrer, J.A. Davies, L.V.C. Rees, J. Inorg. Nucl. Chem. 1969, 31, 2599.

(28) R.M. Barrer, L.V.C. Rees, M. Shamsuzzoha, J. Inorg. Nucl. Chem. 1966, 28, 629.

(29) H.S. Sherry, J.Phys. Chem. 1966, 70, 1158.

(30) R.M. Barrer, J. Klinowski. J.C.S. Faraday 1, 1974, 70, 2362.

(31) R.M. Barrer, R.P. Townsend, J.C.S. Farad. Trans. 1, 1976, 72, 661.

(32) D.W. Breck, "Zeolite Molecular Sieves", (Wiley Interscience 1974), p.122.

(33) L.B. Sand, "Molecular Sieves", (Soc. Chem. Ind. London 1968), p.71.

(34) D.W. Breck (Ref. 32). p.67.

(35) R.M. Barrer, "Zeolites and Clay Minerals", (Academic Press, 1978) p.23.

(36) W.M. Meier, "Molecular Sieves", Soc. Chem. Ind., London (1968) p.12

(37) R.M. Barrer (Ref. 35.) p. 44.

(38) R.M. Barrer (Ref. 35) P.40.

(39) W.M. Meier, Z. Krist., 1961, 115, 439.

(40) J.D. Sherman, M.J. Bennett, Adv. Chem. Ser., 1973, (Mol. Sieves, Int. Conf. 3rd), 121, 52.

(41) D.W. Breck, (Ref.32), p.122.

(42) L.B. Sand, "Molecular Sieves", (Soc. Chem. Ind., London, 1968), p.71.

(43) D.W. Breck, (Ref. 32.) p.95.

(44) R.M. Barrer, (Ref. 35.) p.76.

(45) J.V. Smith, "Molecular Sieve Zeolites I", (Adv. Chem. Ser. 101) Amer. Chem. Soc. 1971, 109.

(46) B. Beagley, J. Dwyer, T.K. Ibrahim, J.C.S. Chem. Comm. 1978, 12 493.

(47) J. Marti, J. Sonia, F.H. Cano, J. Colloid and Interface. Sci. 1977, 60, 82.

(48) D.W. Breck, et.al., J. Am. Chem. Soc. 1956, 78, 5963.

(49) E. Dempsey, "Molecular Sieves", Soc. Chem. Ind., London, 1968, p. 293.

(50) R.M. Barrer, G.C. Bratt, J. Phys. Chem. Solids, 1959, 12, 130.

(51) Ibid, 1969, 31, 219.

(52) J.V. Smith, Special Paper No. 1, Mineralogical Society of America, 1963.

(53) G.L. Gaines, H.C. Thomas, J. Chem. Phys. 1953, 21, 714.

(54) R.M. Barrer, A.J. Walker, Trans. Farad. Soc. 1964, 60, 171.

(55) J. Kielland, J.Soc. Chem. Ind., 1953,54, 232.

(56) R.A. Robinson, R.H. Stokes, "Electrolyte Solutions", (Butterworths London, 2nd ed. 1970), p.

(57) R.A. Robinson, R.H. Stokes, (Ref. 56) p.229.

(58) R.A. Robinson, R. H.Stokes, (Ref. 56) p.28.

(59) E. Glueckauf, Nature, 1949, 163, 414.

(60) R.M. Barrer, J. Klinowski, J.C.S. Faraday I. 1974, 70, 2080.

(61) R.M. Barrer, J. Klinowski, J.C.S. Faraday I, 1972, 68, 73.

(62) R.M. Barrer, L.V.C. Rees, M. Shamusuzzoha, J. Inorg. Nucl. Chem. 1966, 28, 629.

(63) R.M. Barrer, L.V.C. Rees, D.J. Ward. Proc. Roy. Soc. A273, 180 (1963)

(64) H.S. Sherry, J. Phys. Chem. 1966, 70, 1158.

(65) R.M. Barrer, R.P. Townsend, J.C.S. Faraday I, 1976, 72, 661.

(66) B.K. Theng, E. Vansant, J.B. Uytterhoeven, Trans. Faraday Soc., 1968, 64, 3370.

(67) L.V.C. Rees, C.J. Williams, Trans. Faraday Soc. 1965, 61, 1481.

(68) A. Maes, A. Cremers, J.C.S. Faraday 1, 1973, 71, 263.

(69) I.J. Gal, P. Radovanov, J.C.S. Faraday 1, 1975, 71, 1671.

(70) H.S. Sherry, J. Phys. Chem., 1966, 70, 1158.

(71) R.M. Barrer, J.D. Falconer, Proc. Roy. Soc. A 1956, 236, 227.

(72) R.M. Barrer, B.M. Munday, J. Chem. Soc. A 1971, 2909.

(73) R.M. Barrer, Bull, Soc. Fr. Mineral. Cristollogr. 1974, 92, 89.

(74) R.M. Barrer, L.V.C. Rees, M. Shamsuzzoha, J. Inorg. Nucl. Chem. 1966, 28, 629.

(75) R.M. Barrer, J. Klinowski, J.C.S. Faraday I, 1972, 68, -956.

(76) R.M. Barrer, J.A. Davies, L.V.C. Rees, J. Inorg. Nucl. Chem,. 1969, 31, 2599.

(77) C.J.F. Böttcher, "Theory of Electric Polarization", (Elsevier, Amsterdam 1952), p.111.

(78) R.M. Barrer, R.P. Townsend, J.C.S. Farday I, 1976, 72, 2650.

(79) R.M. Barrer, J.A. Davies, L.V.C. Rees, J. Inorg. Nucl. Chem., 1968, 30, 3333.

(80) P.P. Lai, L.V.C. Rees, J.C.S. Faraday I, 1976, 72, 1809.

(81) L. Broussard, D.P. Shoemaker, J. Am. Chem. Soc. 1960, 82, 1041.

(82) H.S. Sherry, J. Phys. Chem., 1968, 72, 4086.

(83) H.S. Sherry, J. Coll. Interface Sci. 1968, 28, 288.

(84) M.L. Costenoble, W.J. Mortier, J.B. Uytterhoeven, J.C.S. Faraday I, 1976, 72, 1877.

(85) R.M. Barrer, J. Klinowski, J.C.S. Faraday I 1974, 70, 2362.

(86) E.R. Nightingale, Sr., J. Phys. Chem., 63, 1381 (1959).

(87) D.R Rosseinsky, Chem. Rev. 1965, 65, 467

(88) I.J. Gal, et.al. Trans. Far. Soc. 1971, 67, 999.

(89) V.A. Nikashina, L.I. Zvereva, K.M. Olshanova, M.A. Potapova, J. Chromatog. 1976, 120, 153.

(90) R.M. Barrer, J. Klinowski, Phil. Tran. Roy. Soc., 1977, 285, 637.

(91) W.J. Mortier, M.L. Costenoble, J.B. Uytterhoeven, J. Phys. Chem. 1973, 77, 2880.

(92) J. Marti, J. Soria, F.H. Cano., J. Coll. Interf. Sci. 1978, 67 266.

(93) E. Gallei, D. Eisenbach, A. Ahmed, J. Catal. 1974, 33, 62.

(94) E.F. Vansant, J.B. Uytterhoeven, Trans. Faraday Sco., 1971, 67, 2961.

(95) R.M. Barrer, J. Klinowski, H.S. Sherry, J.C.S. Faraday II, 1973, 69, 1669.

(96) A. Maes, A. Cremers, Adv. Chem. Ser. 1973, 121, 230.

(97) J. Marti, J. Soria, F.H. Cano, J. Phys. Chem. 1976, 80, 1776.

(98) T. Takaishi, Y. Yatsurugi, A. Yusa, T. Kuratomi

(99) D.H. Olson, H.S. Sherry, J. Phys. Chem. 1968, 72, 4095.

(100) D.H. Olsen, J. Phys. Chem. 1970, 74, 2758.

(101) K.C. Satapathy, et.al., Indian J. Chem., 1, 402, (1963).

(102) D. Sathyanarayne , C.C. Patel, J. Inorg. Nucl. Chem., 27, 297, (1965).

(103) A.I. Vogel, "Quantative Inorganic Analysis", (Longmans, Green & Co. Limited, 1964), p.277.

(104) A.I. Vogel, "Macro and Semimacro Qualitative Inroganic Analysis" (Longmans 1954), p.42.

(105) E.J. Holmyard, "Inorganic Chemistry" (Dent & Sons Ltd., 1960) p.238.

(106) "Inorganic Syntheses", McGraw-Hill, Vol.2, p.230.

(107) (Ref. 106) p.179.

(108) D.W. Breck, (Ref. 32), p.502-505.

(109) R.M. Barrer, J. Klinowski, J.C.S. Faraday I, 1975, 71, 690.

(110) A.I. Vogel, (Ref. 103), p.433.

(111) A.I. Vogel, (Ref. 103), p.443.

(112) A.I. Vogel, (Ref. 103), p.435.

(113) A.I. Vogel, (Ref. 103), p.441.

(114) A.I. Vogel, (Ref. 103), p.445.

(115) A.I. Vogel, "Textbook of Quantitative Analysis" (Longmans 1966), p.434.

(116) A.I. Vogel, (Ref. 103), p.358.

(117) A.I. Vogel, (Ref. 103), p.260.

(118) A.I. Vogel, (Ref. 103), p.450.

(119) A. Rao, L.V.C. Rees, Trans. Faraday Soc. 1966, 62, 2505.

(120) F.D. Snell, C.T. Snell, "Colorimetric Methods of Analysis", (Van Nostrand, New York, 1959), Vol. IIA, p.317.

(121) F.D. Snell, (Ref. 120), Vol II, p.395.

(122) R.P. Townsend "Ion Exchange of Transition Metals in Zeolites" (Dept. Chem. Imperial College, London, D.I.C.Thesis, 1977), p.113.

(123) A.F. Cotton, G. Wilkinson, "Advanced Inorganic Chemistry" (Interscience Publishers 1972), p.825.

(124) G. Martini, M.F. Ottaviani, G.L. Seiravalli, J. Phys. Chem. 1975, 79, 1716.

(125) R.P. Townsend, (Ref. 122), p.105.

(126) L. Erdey, "Gravimetric Analyses Part II" (Pergamon, Oxford, 1965), p.442.

(127) J. Topping, "Errors of Observation and Their Treatment", (Chapman & Hall) 1972, p.109.

(128) R.A. Robinson, R.H. Stokes, (Ref. 56), pp 235-238.

(129) L.V.C. Rees, "The Properties and Applications of Zeolites", ed. L.V.C. Rees and R.P. Townsend, Special Publ. No. 33, Chemical Society, London 1979, in print.

(130) R.A. Robinson, R.H. Stokes, (Ref. 56) p.

(131) A.F. Cotton, G. Wilkinson, (Ref. 123) p.984.

(132) F.D. Snell, C.T. Snell, (Ref. 120) Vol.LL, p.317.

(133) C.W. Roberts, (Ref. 25) in print.

(134) I.M. Galabova, G.A. Haralampiev (Ref. 25) in print.

(135) T.J. Weeks, A.P. Bolton, J. Chem. Soc. Faraday Trans. 1 1977, 73, 1681.

(136) P.T. Wierzchoeski, S. Malinowski, S. Krzyyanowski, Chim. Ind (Milan), 1977, 59, 605.

(137) M.S. Spencer, T.V. Whittam, (Ref. 25) in print.

(138) F.O. Bravo, J. Dwyer, D.Zamboulis, (Ref. 25) in print.

(139) R.P. Townsend, (Ref.122) p 37.

(140) E.F. Vansant, J.B. Uytterhoeven, Trans. Farad. Soc. 1971, 67, 2961.

(141) R.P. Townsend, (Ref. 122) p.171.

(142) Ibid. p.28.

(143) Ibid. p.212.

(144) A.F. Cotton, G. Wilkinson,(Ref.123) p.590.

(145) R.P. Townsend, (Ref.122) p.40.

(146) M. Costenoble, A. Maes, JCS. Farad.I, 1978, 74, 131.

(147) T.H. Hseu, Ph.D Thesis, University of Washington, 1972.

(148) L.V.C. Rees, J. Klinowski,(Discussion), (Ref.25) in print.

(149) R.P. Townsend, (Ref.122) p.58.

(150) R.M. Barrer, R.P. Townsend, J. Chem. Soc. Farad. 1, 1978, 74, 745.

(151) R.M. Barrer, R. Papadopoulis, L.V.C. Rees, J. Inorg. Nucl. Chem., 1967, 29, 2047.

(152) D.J.C. Yates, J. Phys. Chem.,1966, 70, 3693.

(153) R.M. Barrer, J.W. Sutherland, Proc. Roy. Soc. A, 1956, 237, 439.

(154) I.A. Maxwell, J.J. de Boer, J. Phys Chem.,1975, 79, 1874.

(155) C.S.G. Phillips, R.J.P. Williams, "Inorganic Chemistry" (Oxford, Clarendon Press) 1965, Volume 1, p.176.

(156) Ibid. p.406.

(157) I.J. Gal, O. Jankovic, S. Malcic, P. Rdaovanov, M. Todorovic, Trans. Farad. Soc. 1971, 67(4), 999.

(158) V.A. Nikashina, L.I. Zvereva, K.M. Olshanova, M.A. Potapova, J. Chromatog, 1976, 120, 155.

(159) E.M. Meier, D.H. Olson,"Atlas of Zeolite Structure Types" (The Structure Commision of the International Zeolite Association) 1978, p.37.

(160) N.V. Sidgewick, 'The Chemical Elements and their Compounds' (Oxford, Clarendon Press)1950, Vol.II, p 1468.

(161) A. Dyer, R.P. Townsend, J. Inorg. Nucl. Chem. 1973, 35, 2995, 301.

(162) C.V. McDaniel, P.K. Maher, ACS Monograph(Zeolite Chem. Catal.) 1976 171, 285.